

THE EFFECT OF MOLECULAR STRUCTURE ON THE BIODEGRADATION OF
SELECTED SULPHONATED PHENYLAZONAPHTHOL DYES BY WHITE ROT FUNGUS

PLEUROTUS OSTREATUS

by

YIPING LU

(Under the Direction of Ian R. Hardin)

ABSTRACT

The removal of water-soluble sulphonated azo dye effluents generated by textile industries is an important issue in wastewater treatment. Microbial treatment of environmental pollutants including dyes, with white rot fungi has received wide attention as a potential alternative for conventional methods in wastewater treatment. Eight sulphonated azo dyes with similar molecular structures were selected and degraded by the white rot fungus *Pleurotus ostreatus*. The decolorization effect was measured with a UV- spectrophotometer. Due to the different molecular structures of the dyes, the decolorization efficiency ranged from 70 percent to 90 percent after a 7-days treatment. Dyes with electron withdrawing group(s) on the benzene ring degraded quickly and had relatively high decolorization. Dyes with electron donating group(s) on the benzene ring had relatively lower decolorization. Dyes without functional group(s) on the benzene ring had relatively high decolorization even though they were less affected in the first three days. The solubility of dyes as well as the difference in the solubility parameter of the molecular units that are connected to the azo bonds, affects the decolorization. The more similar the solubility of the moieties, which connected to the azo bonds, the better the

decolorization.

Chemical instrumental analysis methods such as high performance liquid chromatography (HPLC) and capillary electrophoresis combining with electrospray ionization mass spectrometry (CE-ESI-MS) were used to identify the degraded products and to develop a relationship between the chemical structures of the dyes and fungal decolorization. Fragmentation of several sulphonated dyes were investigated and fragmentation mechanisms of these breakdowns were proposed. The fragmentation supplied important information which was used to analyze the structure of the compounds. Several major degradation products were isolated and identified by HPLC and CE-ESI-MS, and the corresponding possible degradation pathways were proposed.

In addition, in order to explain the degradation pathway, enzyme assays were performed. Characteristics such as enzyme activities and concentrations were determined and related to the effectiveness of decolorization.

INDEX WORDS: *Pleurotus ostreatus*, White Rot Fungi, Decolorization, Sulphonated Phenylazonaphthol Dyes, Biodegradation, HPLC, CE-ESI-MS

THE EFFECT OF MOLECULAR STRUCTURE ON THE BIODEGRADATION OF
SELECTED SULPHONATED PHENYLAZONAPHTHOL DYES BY WHITE ROT FUNGUS
PLEUROTUS OSTREATUS

by

YIPING LU

B.E., Zhejiang Institute of Textiles, China, 1994

M.E., Nanjing University of Science & Technology, China, 1999

A Dissertation Submitted to the Graduate Faculty of the University of Georgia in Partial

Fulfillment of the Requirements for the Degree

DOCTOR OF PHILOSOPHY

ATHENS, GEORGIA

2006

© 2006

Yiping Lu

All Rights Reserved

THE EFFECT OF MOLECULAR STRUCTURE ON THE BIODEGRADATION OF
SELECTED SULPHONATED PHENYLAZONAPHTHOL DYES BY WHITE ROT FUNGUS

PLEUROTUS OSTREATUS

by

YIPING LU

Major Professor:	Ian R. Hardin
Committee:	Danny E. Akin
	Alan G. Darvill
	Helen H. Epps
	Dennis R. Phillips

Electronic Version Approved:

Maureen Grasso
Dean of the Graduate School
The University of Georgia
August 2006

To My Beloved Family

ACKNOWLEDGEMENTS

I will remain indebted to Dr. Ian Hardin, my major professor, for providing me with a great research problem and a great environment in which I could grapple with it. His guidance, encouragement and perseverance over the years have helped me grow as a scientist as well as an individual. For all this, I remain grateful.

My committee members, Dr. Alan Darvill, Dr. Danny Akin, Dr. Dennis Phillips, and Dr. Helen Epps have offered their professional wisdom, guidance, advice, and comments throughout the course of my Ph.D. program.

I am also grateful to the faculty and staff of the TMI department for helping in every possible way. Special thanks go to Susan Wilson for her help. I also thank Huantian, Xueheng, Wang, and Xiaofang for their time to help me in research discussion.

Heart felt gratitude must go to all my family members for their encouragement, support and understanding. My special gratitude also goes to my wife, Jiawei and my lovely daughter, Maggie, for their endless love, tremendous patience, and enthusiasm for life.

LIST OF CONTENTS

	Page
ACKNOWLEDGEMENTS.....	v
LIST OF TABLES.....	viii
LIST OF FIGURES... ..	ix
LIST OF SCHEMES	xv
CHAPTER	
1 INTRODUCTION.....	1
Purpose of the Study.....	4
2 REVIEW OF LITERATURE.....	5
Sulphonated Azo Dyes.....	5
Conventional Dye Wastewater Treatment Methods.....	7
Decolorization of Azo Dyes by White Rot Fungi.....	16
Analytical Techniques to Identify Dye Degradation Products.....	20
Summary of the Literature.....	25
3 MATERIALS AND METHODS	27
Materials.....	27
Methods.....	31
4 DECOLORIZATION OF SULPHONATED PHENYLAZONAPHTHOL DYES.....	40
Decolorization of Sulphonated Phenylazonaphthol Dyes.....	40

Effect of Dye Molecular Structures.....	47
Effect of Solubility Parameters of Dyes.....	53
Enzyme Assay.....	56
Conclusions of Decolorization of Sulphonated Phenylazonaphthol Dyes ...	61
5 SEPARATION AND IDENTIFICATION OF DYE DEGRADATION	
PRODUCTS.....	62
HPLC Analysis of Degradation Products.....	62
CE-ESI-MS Analysis of Degradation Products.....	74
6 CONCLUSIONS	140
REFERENCES.....	144

LIST OF TABLES

	Page
Table 1.1 Advantages and Disadvantages of the Current Methods of Dye Removal from Industry Effluents.....	12
Table 3.1 Dyes in This Research.....	36
Table 4.1 The Decolorization Effect of Dyes Degraded by <i>Pleurotus ostreatus</i> from the First Day to the Seventh.....	46
Table 4.2 The $\Delta \delta$ (cal/cm) ^{1/2} Calculation of Mordant Violet 5	54
Table 4.3 The $\Delta \delta$ (cal/cm) ^{1/2} of Sulphonated Phenylazonaphthol Dyes from the Highest to the Lowest.....	55
Table 4.4 Bio-Parameters of Culture after Seven Days Incubation	60
Table 5.1 The MS ⁿ Fragmentation of Ions from <i>m/z</i> 327 of Acid Orange 7.....	79
Table 5.2 The MS ⁿ Fragmentation of Ions from <i>m/z</i> 341 of Acid Orange 8.....	87
Table 5.3 The MS ⁿ Fragmentation of Ions from the Peak <i>m/z</i> 343 of Mordant Violet 5.....	95
Table 5.4 The MS ⁿ Fragmentation of Ions from <i>m/z</i> 329	103
Table 5.5 The MS ⁿ Fragmentation of Ions from <i>m/z</i> 327 of Acid Orange 12... ..	114
Table 5.6 The MS ⁿ Fragmentation of Ions from <i>m/z</i> 357 of Acid Red 4.....	131
Table 5.7 The Confirmation Information of Possible Degradation Products for The Phenylazonaphthol Azo Dyes.....	137

LIST OF FIGURES

	Page
Figure 2.1	A Sulphonated Azo Dye C.I. Acid Red 1.....7
Figure 2.2	Mechanism of Manganese Peroxidase Catalyzed Formation of Mn ³⁺ -oxalate Complexes.....19
Figure 2.3	Interfaces of CE-MS (Agilent® Technologies)..... 25
Figure 3.1	Structures of Dyes in This Study38
Figure 3.2	The Flow Chart of Analysis of Sulphonated Azo Dyes Degraded by the White Rot Fungus <i>Pleurotus ostreatus</i>39
Figure 4.1	Model Structure of Sulphonated Phenylazonaphthol Dyes in This Study.....40
Figure 4.2	The Decolorization of Acid Orange 7 (100 ppm) by the White Rot Fungus <i>Pleurotus ostreatus</i> with (150 rpm) and without Agitation41
Figure 4.3	The Decolorization of Acid Orange 7 by the White Rot Fungus <i>Pleurotus</i> <i>ostreatus</i> at Different Concentrations.....43
Figure 4.4	The Decolorization of Acid Orange 7 (100 ppm) by the White rot Fungus <i>Pleurotus ostreatus</i>44
Figure 4.5	The UV-Vis Spectrum of Acid Orange 7 Degraded by <i>Pleurotus ostreatus</i>45
Figure 4. 6	Comparison of Chemical Structure and Decolorization Effect for Mordant Violet 5 and Acid Orange 7...49
Figure 4. 7	Comparison of Chemical Structure and Decolorization Effect for Acid Orange 7 and Acid Orange 8.....50

Figure 4. 8	Comparison of Chemical Structure and Decolorization Effect Among Acid Orange 7, Food Yellow 3, and Acid Orange 12.....	51
Figure 4. 9	Comparison of Chemical Structure and Decolorization Effect for Acid Orange 10 and Acid Orange 12.....	52
Figure 4.10	The Structure of Compounds A and B. X and Y Stand For the Functional Groups.....	54
Figure 4.11	BSA Standard Working Curve.....	59
Figure 4.12	Protein Concentration of Culture With and Without Agitation.....	60
Figure 5.1	HPLC Analysis of the Control Sample with Supernatant Fluid.....	64
Figure 5.2	UV-Vis Spectra for Control Sample.....	65
Figure 5.3	HPLC Analysis of the Mordant Violet 5 Degradation Products after Treatment by <i>Pleurotus ostreatus</i> (First Day).....	67
Figure 5.4	The UV-Vis Spectrum of Compound at Retention Time 5.31 min – Mordant Violet 5.....	67
Figure 5.5	HPLC Analysis of the Mordant Violet 5 Degradation Products after Treatment by <i>Pleurotus ostreatus</i> (Second Day).....	68
Figure 5.6	UV-Vis Spectrum of Mordant Violet 5 Degradation Products	68
Figure 5.7	HPLC Analysis of the Acid Orange 8 Degradation Products after Treatment by <i>Pleurotus ostreatus</i> (First Day).....	69
Figure 5.8	UV-Vis Spectrum of Compound at Retention Time of 5.150 min – Acid Orange 8.....	70
Figure 5.9	HPLC Analysis of the Acid Orange 8 Degradation Products after Treatment by <i>Pleurotus ostreatus</i> (Second Day)	70

Figure 5.10	UV-Vis Spectrum of Acid Orange 7.....	71
Figure 5.11	HPLC Analysis of Acid Orange 7 Degradation Products after Treatment by <i>Pleurotus ostreatus</i> (Fifth Day).....	72
Figure 5.12	UV-Vis spectra of Acid Orange 7 Degradation Products	72
Figure 5.13	Comparing of The UV-Vis Spectrum of the Compound at Retention Time of 14.596 min from Food Yellow 3 Degraded by <i>Pleurotus ostreatus</i> (third day) with That of the Benzenesulfonic Acid Standard	73
Figure 5.14	CE-ESI-MS Base Peak Chromatogram of Control Sample with only Kirk's Medium and <i>Pleurotus ostreatus</i> (First Day)	75
Figure 5.15	Mass Spectrum of Peak with the Retention Time of 4.2 min (Control).....	75
Figure 5.16	Mass Spectrum of Peak with the Retention Time of 6.9 min (Control).....	76
Figure 5.17	Mass Spectrum of Peak with the Retention Time of 11.2 min (Control).....	76
Figure 5.18	Mass Spectrum of Acid Orange 7 in the Negative Mode of ESI-MS.....	78
Figure 5.19	The MS ² Mass Spectrum of MS Fragmentation of Peak at $m/z = 327$ of Acid Orange 7	78
Figure 5.20	CE-ESI-MS Base Peak Chromatogram (BPC) of Acid Orange 7 Treated with <i>Pleurotus ostreatus</i> (Third Day).....	82
Figure 5.21	Mass Spectrum of Peak with Retention Time of 5.6 min –Acid Orange 7... ..	83
Figure 5.22	Mass Spectrum of Peak with Retention Time of 6.8 min – Acid Orange 7.. ..	83
Figure 5.23	MS ⁿ Fragmentation Ions of Peak m/z 341- Acid Orange 8.....	86
Figure 5.24	CE-ESI-MS Base Peak Chromatogram of Acid Orange 8 Treated with <i>Pleurotus</i> <i>ostreatus</i> (Fourth Day).....	90

Figure 5.25	Mass Spectrum of Peak with Retention Time of 6.8 min -Acid Orange 8 Treated with <i>Pleurotus ostreatus</i>	91
Figure 5.26	Mass Spectrum of Peak with Retention Time of 7.5 min – Acid Orange 8 Treated with <i>Pleurotus ostreatus</i>	92
Figure 5.27	Mass Spectrum of Mordant Violet 5 in the Negative Mode of ESI-MS.....	94
Figure 5.28	MS ² Fragmentation Ions of Peak m/z 343, Mordant Violet 5.....	94
Figure 5.29	CE-ESI-MS Base Peak Chromatogram of Mordant Violet 5 Treated with <i>Pleurotus ostreatus</i> (First Day).....	98
Figure 5.30	Mass Spectrum of Peak with the Retention Time of 7.3 min of Mordant Violet 5 Treated with <i>Pleurotus ostreatus</i> (First Day).....	99
Figure 5.31	CE-ESI-MS Base Peak Chromatogram of Mordant Violet 5 Treated with <i>Pleurotus ostreatus</i> (Second Day).....	100
Figure 5.32	Mass Spectrum of Peak with Retention Time of 10.4 min- Product II.....	100
Figure 5.33	Mass Spectrum of Peak with Retention Time of 8.5 min- Product III.....	101
Figure 5.34	Mass Spectrum of Peak with Retention Time of 8.8 min- Product I.....	101
Figure 5.35	The Fragmentation Ions of Peak m/z 329.....	103
Figure 5.36	Mass Spectrum Acid Orange 12 in the Negative Mode of ESI-MS.....	112
Figure 5.37	MS ⁿ Fragmentation Ions of Peak m/z 327- Acid Orange 12.....	113
Figure 5.38	CE-ESI-MS Base Peak Chromatogram of Acid Orange 12 Treated by <i>Pleurotus ostreatus</i> (Fourth Day).....	115
Figure 5.39	Mass Spectrum of Peak with Retention Time of 25.7 min –Acid Orange 12 Treated by <i>Pleurotus ostreatus</i> (Fourth Day).....	116

Figure 5.40	Mass Spectrum of Peak with Retention Time of 14.5 min –Acid Orange 12 Treated by <i>Pleurotus ostreatus</i> (Fourth Day).....	116
Figure 5.41	ESI-MS Mass Spectrum of Food Yellow 3 in the Negative Mode.....	118
Figure 5.42	MS ⁿ Fragmentations Spectra of Food Yellow 3.....	119
Figure 5.43	CE-ESI-MS Base Peak Chromatogram of Food Yellow 3 Treated by <i>Pleurotus ostreatus</i> (First Day).....	122
Figure 5.44	Mass Spectrum of Peak with Retention Time of 11.1 min – Food Yellow 3 Treated by <i>Pleurotus ostreatus</i> (First Day)....	122
Figure 5.45	Mass Spectrum of Peak with Retention Time of 13.6 min – Food Yellow 3 Treated by <i>Pleurotus ostreatus</i> (First Day).....	123
Figure 5.46	Mass Spectrum of Peak with Retention Time of 16.1 min – Food Yellow 3 Treated by <i>Pleurotus ostreatus</i> (First Day)....	123
Figure 5.47	CE-ESI-MS Base Peak Chromatogram of Food Yellow 3 Treated by <i>Pleurotus ostreatus</i> (Third Day).....	124
Figure 5.48	Mass Spectrum of Peak with Retention Time of 14.7 min – Food Yellow 3 Treated by <i>Pleurotus ostreatus</i> (Third Day).....	124
Figure 5.49	Mass Spectrum of Acid Orange 10 in the Negative Mode of ESI-MS.....	126
Figure 5.50	MS ⁿ Fragmentation Spectra of Acid Orange 10.....	127
Figure 5.51	Mass Spectrum of Peak with Retention Time of 13.1 min –Acid Orange 10 Treated by <i>Pleurotus ostreatus</i> (Third Day).....	128
Figure 5.52	Mass Spectrum of Peak with Retention Time of 9.8 min –Acid Orange 10 Treated by <i>Pleurotus ostreatus</i> (Third Day).....	128
Figure 5.53	MS ⁿ Fragmentations of Ions from Acid Red 4.....	130

Figure 5.54	ESI-MS Mass Spectrum of Acid Red 8 in the Negative Mode.....	133
Figure 5.55	MS ⁿ Fragmentation of Ions from Acid Red 8.....	134
Figure 5.56	Mass Spectrum of Peak with the Retention Time of 11.2 min - Acid Red 8 Treated by <i>Pleurotus ostreatus</i> (Second Day).....	136

LIST OF SCHEMES

	Page
Scheme 5.1 Proposed Fragmentation Pattern for Acid Orange 7.....	80
Scheme 5.2 Proposed Mechanisms for the Degradation of Acid Orange 7 by <i>Pleurotus ostreatus</i>	84
Scheme 5.3 Proposed Fragmentation Pattern for Acid Orange 8.....	88
Scheme 5.4 Proposed Mechanisms for the Fungal Degradation of Acid Orange 8 by <i>Pleurotus ostreatus</i>	92
Scheme 5.5 Proposed Fragmentation Pattern for Mordant Violet 5.....	97
Scheme 5.6 Proposed Fragmentation Pattern for Ion at m/z 329.....	105
Scheme 5.7 The First Fungal Degradation Pathway Proposed for Mordant Violet 5 by <i>Pleurotus ostreatus</i>	107
Scheme 5.8 The Second Fungal Degradation Pathway Proposed for Mordant Violet 5 by <i>Pleurotus ostreatus</i>	108
Scheme 5.9 Proposed Fragmentation Pattern for Acid Orange 12.....	114
Scheme 5.10 Proposed Mechanism for the First Step in the Degradation of Acid Orange 12 Treated by <i>Pleurotus ostreatus</i>	117
Scheme 5.11 Proposed Fragmentation Pattern of Food Yellow 3.....	119
Scheme 5.12 Proposed Mechanism for the Degradation of Food Yellow 3 by <i>Pleurotus</i> <i>ostreatus</i>	125
Scheme 5.13 Proposed Fragmentation Pattern for Acid Red 4.....	133
Scheme 5.14 Proposed Fragmentation Pattern for Acid Red 8.....	135

CHAPTER 1

INTRODUCTION

Textile industries consume large volumes of water and chemicals for wet processing of textiles. This wastewater has a very diverse chemical composition, ranging from inorganic compounds to polymers and organic compounds (Mishra et al., 1993; Banat et al., 1996; Juang et al., 1996). Among industrial wastewaters, dye wastewater is one of the most difficult to treat. Color in wastewater is highly visible and undesirable, even if at a very low dye concentrations.

There are many structural varieties of dyes, such as acidic, basic, disperse, azo, diazo, anthroquinone based and metal complex dyes. Among these, azo dyes constitute a major class of environmental pollutants accounting for 60 to 70 percent of all dyes and pigments used. These compounds are characterized by aromatic moieties linked together with azo groups ($-N=N-$). The release of azo dyes into the environment is a concern due to the coloration of natural waters, and the toxicity, mutagenicity and carcinogenicity of these dyes and their biotransformation products. Therefore, considerable attention has been given to evaluating the fate of azo dyes during wastewater treatment and in the natural environment (Tan, 2001).

In the more developed countries, government legislation regarding the removal of dyes from industrial effluents is becoming more and more stringent. Environmental policy in the UK since September, 1995, has stated that no synthetic chemicals should be released into the marine environment. Enforcement of this law will continue to ensure that textile industries treat their dye-containing effluent to the required standard (O' Neill et al., 1999).

Their synthetic origin and complex aromatic molecular structures make dyes stable and difficult to be biodegraded. Due to the low biodegradability of dyes, conventional biological wastewater treatment systems are inefficient in treating dye wastewater. Dye wastewater is usually treated by physical or chemical treatment processes. These include physical–chemical flocculation combined with flotation, electroflotation, flocculation with Fe(II)/Ca(OH)_2 , membrane filtration, electrokinetic coagulation, electrochemical destruction, ion-exchange, irradiation, precipitation, and ozonation (Robinson et al., 2001). However, these technologies are usually inefficient in the removal of color due to high cost and little adaptability to a wide range of dye wastewaters (Banat et al., 1996).

A number of studies have focused on microorganisms which are able to degrade and absorb dyes in wastewaters in recent years. By far, white rot fungi are the most efficient single class of microorganisms which can break down synthetic dyes. This property is based on the capacity of white rot fungi to produce one or more extracellular lignin-modifying enzymes, which are able to degrade a wide range of xenobiotic compounds. Generally, decolorization by white rot fungi is a promising alternative to replace or supplement present treatment processes (Fu et al., 2001). There are many fungal strains which have the ability to decolorize dyes, such as *Phanerochaete chrysosporium*, *Pleurotus ostreatus*, and *Trametes versicolor*. There are various factors influencing the characteristics of dyes and fungal decolorization related to fungal growth. One of the most important of these factors is that dye molecules have many different and complicated structures. The relationships between dye molecule structures and fungal decolorization, and the complex mechanism involved with decolorization, need to be established.

Sulphonated azo dyes are sodium salts of organic sulphonic acids. They consist of an aromatic structure containing a chromogen and a solubilizing group(s), almost always a

sulphonic acid salt. Sulphonated azo dyes are soluble ionic compounds, where the color is contained in the anionic portion. Cao (2000) found that dyes with high solubility, such as acid dyes, are more easily decolorized by white rot fungi than dyes with low solubility, such as vat and disperse dyes.

Due to the different properties of azo dyes and their metabolites, such as solubility, volatility, and structure, a variety of spectroscopic methods, including spectrophotometry, chromatography, mass spectrometry, and capillary electrophoresis, are employed for structural identification of dyes and their breakdown fragments. In addition to ultraviolet-visible (UV/Vis) spectrophotometry and infrared (IR) spectroscopy, mass spectrometry (MS) is suitable for this purpose. Mass spectrometry with electron ionization (EI) is not suitable for nonvolatile sulphonated dyes because of the inability to thermally transfer ionic compounds to the gaseous phase, as well as excessive fragmentation. Recently, the technical maturation of soft ionization techniques (e.g. ESI) has made the analysis of nonvolatile ionic dyes possible. The sulphonic groups are strongly acidic and are therefore completely dissociated in the aqueous solution. Hence, negative ion MS is much more sensitive than positive ion MS. Negative ion ESI mass spectra have been published for some chemical compounds which contain multi-sulphonic groups, indicating that the negative ion (ESI) is probably the best method to identify nonvolatile sulphonated dyes.

High performance liquid chromatography (HPLC) has been used for analysis of various dyes in wastewater and metabolites from various degradation procedures. HPLC is a powerful analytical tool that can provide reproducible and precise analytical results. Capillary electrophoresis (CE) has been used for analysis of dyes in recent decades and can be more

suitable than HPLC for the analysis of charged dyes because of its separation principle, higher separation efficiency and simple method development.

1.1 The Purpose of This Research

The purpose of this study is to investigate the effect of molecular structure on the degradation of sulphonated azo dyes by the white rot fungus *Pleurotus ostreatus*. The influence of the structure of the dyes on the decolorization is studied. Chemical instrumental analysis methods such as HPLC and CE-MS are used to separate and identify the degraded products and to develop a relationship between the chemical constituents of dyes and fungal decolorization. Characteristics such as enzyme activities, concentrations, and molecular weights are also determined and related to the effectiveness of decolorization.

The objectives of this study are:

- (1) To study the relationship between dye molecular structures, a specific dye molecular framework used as a model, the position of substituted groups and the decolorization effect.
- (2) To use analytical methods such as CE-MS, HPLC, and UV-VIS to separate and identify the degradation products.
- (3) To establish a possible mechanism of the dye degradation pathway for the dye molecular model by *Pleurotus ostreatus*.
- (4) To investigate the extracellular ligninolytic enzymes involved in the process of dye degradation including enzyme assay and characterization such as enzyme activities and protein concentrations.

CHAPTER 2

REVIEW OF LITERATURE

The history of synthetic dyes goes back over a hundred years. William Henry Perkin, a young and talented English chemist, synthesized the first dye, Mauve, by accident in 1856 from chemicals derived from coal (Zollinger, 1987). Perkin commercialized his innovation and developed the production processes for this new dye. The brilliant hue of Mauve immediately attracted much attention and stimulated other chemists to carry out similar experiments.

2.1 Sulphonated Azo Dyes

The foundation for the production of azo dyes was laid in 1858 when P. Gries discovered the diazotization reaction, which could be used for the production of azo compounds (Zollinger 1987). The first true azo dyes were developed in 1861. Azo dyes are by far the largest (account for 60-70 percent of all dyes used) and most important group of dyes (Carliell et al. 1998), mainly due to the simple synthesis. Azo dyes are used for coloring many different materials such as textile, leather, plastics, food, and pharmaceuticals. They are also used for manufacturing paints as well.

Graebe and Liebermann were the first to observe that dye molecules contain conjugated double bonds in their structure (Zollinger, 1987). A few years later, O. N. Witt perceived that dye molecules contain certain functional groups attached to the conjugated double bonds, which he called 'chromophores'. Chromophores are functional groups that by themselves absorb

visible or near ultraviolet radiation. They are unsaturated functional groups (except for -NR_3^+) that act as electron acceptors. Examples of chromophores are the azo group (-N=N-), nitro group (-NO_2), carbonyl group (-C=O), and alky ammonium derivatives (-NR_3^+). Other functional groups attached to the conjugated double bonds, referred to as 'auxochromes', affect the absorption by usually shifting it toward longer wave lengths and increasing dye intensity. Auxochromes are saturated functional groups with nonbonding electrons on the atom attached to the conjugated system, and therefore can act as electron donors. Examples of auxochromes are the amino group (-NH_2), mono alky amino group (-NHR), dialkyl amino group (-NR_2), hydroxyl group (-OH), and ether group (-OR). The combination of all these components is the part of the molecule that is responsible for its color and is called 'chromogen'.

Currently, all dyes are organic aromatic compounds with a conjugated double bonds system, to which chromophores and auxochromes are attached. The presence of these functional groups significantly reduces the number of double bonds in the conjugation required for intense absorption of visible light.

Azo dyes are compounds containing azo groups (-N=N-) which are linked to sp^2 -hybridized carbon atoms. Due to their chemical structure, azo dyes absorb light in the visible spectrum. The azo groups are mainly bound to benzene or naphthalene rings, which can contain many different functional groups such as chloro group (-Cl), methyl group (-CH_3), nitro group (-NO_2), amino group (-NH_2), hydroxyl group (-OH) and carboxyl group (-COOH). A functional group often found in azo dyes is the sulphonic acid group ($\text{-SO}_3\text{H}$). The azo dyes containing this functional group are the so-called sulphonated azo dyes (see an example in Figure 2.1).

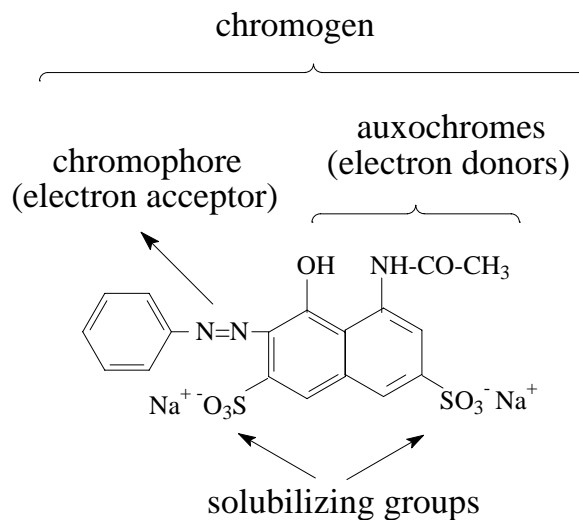


Figure 2.1 A Sulphonated Azo Dye C.I. Acid Red 1

2.2 Conventional Dye Wastewater Treatment Methods

In 1980, more than a million tons of synthetic dyes were manufactured in the United States. Russia, India, China, and Europe consumed about 600,000 tons of synthetic dyes each year (Zollinger 1987). Recent data on the world production and consumption are not available. However, it can be assumed that more dyes are produced and consumed in view of the economic prosperity and the increased production of many colored goods.

During the usage of azo dyes, an estimated amount of 10-15 percent is released into the environment after the dyeing process (Vaidya and Datye, 1982). It is likely that this figure is even higher now since the usage of reactive dyes (which include azo dyes) has increased lately and their fixation rate in dyeing processes can be as low as 50 percent (Easton, 1995). Water-

soluble azo dyes, like sulphonated azo dyes, will generally enter the environment via wastewater discharges. These sulphonated azo dyes are widely used in different industries. They have a negative aesthetic effect on the wastewater and some of these compounds and their biodegradation products are also toxic, carcinogenic and mutagenic (Grover et al., 1996). Dyes in wastewater are difficult to treat due to their complex structure and synthetic origin. The conventional dye wastewater treatment methods are chemical and physical processes which are listed below.

2.2.1 Oxidative Processes

This is the most commonly used chemical method of decolorization due to its simplicity of application. The main oxidizing agent is usually hydrogen peroxide (H_2O_2). Chemical oxidation destroys the dye from the dye-containing effluent by oxidation resulting in aromatic ring cleavage of the dye molecules (Raghavacharya, 1997).

2.2.2 H_2O_2 -Fe (II) Salts (Fenton's Reagent)

Fenton's reagent is a chemical method of treating wastewater which is resistant to biological treatment or is poisonous to live biomass (Slokar and Le Marechal, 1997). It has been shown to be effective in decolorizing both soluble and insoluble dyes (Pak and Chang, 1999). One major disadvantage of this method is sludge generation through the flocculation of the reagent and the dye molecules. The sludge which contains the concentrated impurities still requires disposal.

2.2.3 Ozonation

The use of ozone was first developed in the early 1970's. Ozone is a very good oxidizing agent due to its high instability and reactivity compared to chlorine and H_2O_2 . This method shows a preference for double-bonded dye molecules (Slokar and Le Marechal, 1997). One

major advantage is that ozone can be applied in its gaseous state and therefore does not increase the volume of wastewater and sludge. A disadvantage of ozonation is its short half-life, typically being 20 minutes. This half-life can be further shortened if dyes are present, with stability being affected by the presence of salts, pH, and temperature. Another major drawback with ozonation is cost. Continuous ozonation treatment is required due to its short half-life, thus increasing its cost (Xu and Lebrun, 1999).

2.2.4 Photochemical

This method degrades dye molecules to CO_2 and H_2O (Yang et al., 1998 ; Peralto-Zamora et al., 1999) by UV treatment in the presence of H_2O_2 . Degradation is caused by the production of high concentrations of hydroxyl radicals. UV light may be used to activate chemicals, such as H_2O_2 . The rate of dye removal is influenced by the intensity of the UV radiation, pH, dye structure and the dye bath composition (Slokar and Le Marechal, 1997). The advantages of photochemical treatment are no sludge and no foul odors.

2.2.5 Sodium Hypochlorite (NaOCl)

This method features attack at the amino group of the dye molecule by the chloride ion which can chemically reduce and cleave the azo bond. Decolorization is increased with a increase in chloride concentration. The use of chloride for dye removal is becoming less frequent due to the negative effects of releasing chloride into waterways (Slokar and Le Marechal, 1997) and the release of aromatic amines which are carcinogenic, or otherwise toxic molecules (Banat et al., 1999).

2.2.6 Cucurbituril

Cucurbituril is known to form host-guest complexes with aromatic compounds (Mock, 1995), and this may be the mechanism for reactive dye adsorption. Another proposed

mechanism is based on hydrophobic interactions or the formation of insoluble cucurbituril-dye-cation aggregates since adsorption occurs reasonably fast. Cost is a major disadvantage like many other chemical methods.

2.2.7 Electrochemical Destruction

This technique was developed in the mid 1990s. It has some significant advantages for use as an effective method for dye removal due to little or no consumption of chemicals and no sludge produced. But the relatively high flow rates cause a direct decrease in dye removal, and the cost of electricity used is also a major disadvantage of this technique.

2.2.8 Activated Carbon Adsorption

This is the most commonly used method of dye removal by adsorption (Nasser and El-Geundi, 1991) and is very effective for adsorbing cationic, mordant, and acid dyes but is slightly less effective for dispersed, direct, vat, pigment and reactive dyes (Raghavacharya, 1997; Rao et al., 1994). Activated carbon may be well suited for one particular waste system and ineffective in another. The other problems are the expensive cost of the activated carbon as well as losses that occur with the reactivation process of the carbon. Reactivation results in a 10–15 percent loss of the sorbent.

2.2.9 Membrane Filtration

This method has the ability to clarify, concentrate, and separate dye continuously from effluent (Mishra and Tripathy, 1993; Xu and Lebrun, 1999). It has some special features compared with other methods such as resistance to temperature, an adverse chemical environment, and microbial attack. The disadvantages are the concentrated residue left after separation and the high capital cost of the clogging and membrane replacement. This method of filtration is suitable for water recycling within a textile dye plant if the effluent contains a low

concentration of dyes, but it is unable to reduce the dissolved solid content, and thus it is difficult to reuse the water.

2.2.10 Ion Exchange

Wastewater is passed over the ion exchange resin until the available exchange sites are saturated. Both cationic and anionic dyes can be removed from dye-containing effluent in this way. The advantages of this method are that there is no loss of adsorbent on regeneration, reclamation of solvent after use and the removal of soluble dyes. A major disadvantage is the cost because of the expensive organic solvents involved. Ion exchange has not been widely used for the treatment of dye-containing effluents, mainly because ion exchangers cannot accommodate a wide range of dyes (Slokar and Le Marechal, 1997), and it is not very effective for disperse dyes (Mishra and Tripathy, 1993).

2.2.11 Irradiation

This is a method that requires sufficient quantities of dissolved oxygen in order for organic substances to be broken down effectively. The dissolved oxygen is consumed very rapidly and so a constant and adequate supply is required. This high consumption has an effect on cost. It has been shown that some dyes and phenolic molecules can be oxidized effectively at a laboratory scale only (Hosono et al., 1993).

2.2.12 Electrokinetic Coagulation

This is an economically feasible method of dye removal. It involves the addition of ferrous sulfate and ferric chloride, allowing excellent removal of direct dyes from wastewaters. Unfortunately, it has poor results with acid dyes. It is not a widely used method because of the high cost of the ferrous sulfate and ferric chloride and the production of large amounts of sludge resulting in high disposal costs (Gahr et al., 1994).

The advantages and disadvantages of the conventional chemical and physical treatments of dye wastewater are listed in Table 1.1. In general, the conventional dye wastewater treatment processes are expensive and can be detrimental to the environment due to the use of chemical additives.

Table 1.1 Advantages and Disadvantages of the Current Methods of Dye Removal from Industrial Effluents (Robinson et al. 2001)

Physical/chemical methods	Advantages	Disadvantages
Fenton's reagent	Effective decolorization of both soluble and insoluble dyes	Sludge generation
Ozonation	Applied in gaseous state: no alteration of volume	Short half-life (20 min)
Photochemical	No sludge production	Formation of by-products
NaOCl	Initiates and accelerates azo-bond cleavage	Release of aromatic amines
Cucurbituril	Good sorption capacity for various dyes	High cost
Electrochemical destruction	Breakdown compounds are non-hazardous	High cost of electricity
Activated carbon	Good removal of wide variety of dyes	Very expensive
Membrane filtration	Removes all dye types	Concentrated sludge production
Ion exchange	Regeneration: no adsorbent loss	Not effective for all dyes
Irradiation	Effective oxidation at lab scale	Requires a lot of dissolved O ₂
Electrokinetic coagulation	Economically feasible	High sludge production

2.2 Decolorization of Azo Dyes by White Rot Fungi

Physical and chemical methods of dye removal are effective only if the effluent volume is small. This limits the use of physio-chemical methods, such as membrane filtration and cucurbituril, to small-scale *in situ* removal. A limiting factor of these methods is cost. This is true even in lab-scale studies; therefore they are unable to be used by large-scale industry. The microbial treatment of environmental pollutants, including dyes, by the use of white rot fungi has received wide attention as a potential alternative to conventional methods in wastewater treatment. White rot fungi are able to decompose lignin extensively and simultaneously degrade all major components of wood to CO₂ and water.

In an early study (Cripps et al., 1990), several azo dyes were degraded by the white rot fungus *Phanerochaete chrysosporium*. The azo dyes that were degraded included Azure B, [3-(dimethylamino)-7-(methylamino) phenothiazin-5-ium chloride], Tropaeoline O, {4-[2,4-dihydroxyphenyl) azo] benzenesulfonic acid}, Orange II {4-[(2-hydroxy-1-naphthyl) azo] benzenesulfonic acid}, and Congo Red {3,3'-[[1,1'biphenyl]-4,4'diylbis-(azo)]bis[4-amino-1-naphthalenesulfonic acid]}. In order to understand the role of laccase in azo dye degradation, the ability of laccase to degrade 4-(4'-sulfophenylazo)-phenol derivative was examined. Among the phenol derivative dyes, only dyes with electron-donating methyl or methoxy substituents were oxidized. Unsubstituted 4-(4'-sulfophenylazo)-phenol and its 2-chloro and 2-nitro analogs were not oxidized. Cripps suggested that the phenolic ring of an azo dye has to be electron rich for oxidation by laccase.

Anthraquinone-based dyes are the most resistant to degradation due to their fused aromatic structures, and they remain colored for long periods of time in the environment. However, decolorization of three anthraquinone-based polymeric dyes, Polymeric B-411,

Polymeric R-481 and Polymeric Y-606 by *P. chrysosporium* was confirmed by Glenn and Gold (1985). Basic dyes have high brilliance and therefore high color intensity, making them difficult to decolorize. Eighteen commercial basic dyes had been reported decolorized by white rot fungi by Capalash and Sharma (1992). Only eight dyes were decolorized more than 50 percent in five days, while another 10 dyes were not decolorized at all (0 percent) in five days. The dyes which were not degradable included disperse, vat, and sulphur dyes.

Cao (2000) investigated nine white-rot fungi for their capability to decolorize dyes.

Phanerochaete chrysosporium and *Pleurotus ostreatus* were the two most effective white rot fungi. He suggested that dyes with high solubility such as acid and reactive dyes were more easily decolorized by white rot fungi than dyes with low solubility such as vat and disperse dyes because it was difficult for enzymes to attack the dyes in the form of particles. Acid dye Orange II was decolorized by 98 percent in 2 days when treated by fungal strain F29 (an unidentified basidiomycete which was isolated from a fruiting body collected from rotting willow wood) (Knapp et al., 1997).

2.2.1 The White Rot Fungus *Pleurotus ostreatus*

Although *Phanerochaete chrysosporium* has been used as an excellent organism for research into lignin degradation, the cultivation of this fungus is regulated by Japanese laws for the prevention of plant epidemics (Ha et al., 2001). In recent years, the production of ligninolytic enzymes by white rot fungi other than *P. chrysosporium* has been studied. *Pleurotus ostreatus* is an edible oyster mushroom and is found throughout the north temperate zone, almost always on dead hardwood trees. It can also be easily cultivated on a variety of substrates. This fungus grows well on liquid media and on solid media, including wood-meal and wheat-bran. It

has been found to produce manganese peroxidase (MnP) and Laccase under both liquid and solid culture conditions, without producing lignin peroxidase (LiP) (Kofujita et al., 1991).

2.2.2 The Relationship Between Chemical Structure of Textile Dyes and Biodegradation

The location of the methyl or methoxy substituent on aromatic rings appears to be important for degradation (Chivukula et al., 1995a). Spadaro and Renganathan (1994) demonstrated that Disperse Yellow 3 is oxidized to methyl-1, 2-benzoquinone and acetanilide by enzymes from white rot fungi. A detailed mechanism involving phenyldiazene and phenyl radical intermediates was proposed to explain the results. Goszcynski et al. (1994) identified 2, 6-dimethyl-1,4 benzoquinone, 4-nitrosobenzenesulfonic acid, 4-amino-benzenesulfonic acid, 2,6-dimethyl-1,4-aminophenol, 4-hydroxybenzenesulfonic acid and benzenesulfonic acid as products from the oxidation of 4-(4'-sulfophenylazo)-2,6-dimethylphenol by LiP. They proposed a mechanism involving a redox process between sulfophenyldiazene, 4-nitrosobenzenesulfonic acid, and quinone intermediates to explain the product formation. Chivukula (1995b) chose several similar chemical compounds for investigation, and found some new degradation products which were not reported in research by Goszcynski et al. (1995).

Martins et al. (2001, 2002, and 2003) studied the relationship of the chemical structures of textile dyes and the potential for their biodegradation. The dyes used in the study were derivatives of *meta*- or *para*-aminosulphonic or aminobenzoic acids and included in their structures groups such as guaiacol or syringol. The azo dye that gave the best overall decolorization performance was a *meta*-aminosulphonic acid and guaiacol derivative. GC/MS studies indicated the formation of a nitroso substituted catechol metabolite, a precursor of aromatic ring cleavage. Four novel disazo dyes were synthesized with a hydroxyl group in the *para* position of the phenolic ring in relation to the diazo bond. The decolorization of the dyes

was studied using a purified fungal laccase. Among those four diazo dyes, only one of them which had a relatively weak electron-donating carboxyl group in the *meta* position of the phenolic moiety was rapidly and totally decolorized by laccase (Soares et al., 2002). Spadaro et al. (1992) showed that aromatic rings of dyes substituted with hydroxyl, amino, acetamido or nitro groups were mineralized more effectively than those with unsubstituted rings.

There is also a clear relationship between chemical structure and potential danger of azo dyes. All azo dyes containing a nitro group were reported to be mutagenic (Chung and Cerniglia, 1992), and a high toxicity of these azo dyes was also observed for methanogenic granular sludge (Donlon et al. 1997). Furthermore, some azo dyes decay into toxic degradation products. Examples of such harmful moieties are 1,4-phenylenediamine, 1-amino-2-naphthol, benzidine and substituted benzidines, like o-tolidine (Chung et al., 1981; Reid et al., 1984; Rosenkranz and Klopman, 1989; Rosenkranz and Klopman, 1990). The benzidine moieties in azo dyes are prohibited benzidine analogue dyes.

Clear evidence exists that sulphonated azo dyes show decreased or no mutagenic effect compared to unsulfonated azo dyes due to their electric charge and low lipophilicity, which prevents uptake and metabolic activation (Chung and Cerniglia, 1992; Jung et al., 1992; Levine, 1991; Rosenkranz and Klopman, 1990). Due to the above-mentioned effects, it is clear that azo dyes should not enter the environment. An attractive method to prevent this is to apply microbial treatment methods for their mineralization.

2.3 Enzymes Produced by White Rot Fungi

Most white rot fungi are basidiomycetes. These fungi belong to a division in which the spores are born on club-shaped organs called basidia. The white rot fungi are the most potent

lignin degraders of all known microorganisms. There are several factors which affect dye degradation by white rot fungi including the concentration of nitrogen, the carbon co-substrate, oxygen tension, culture agitation, micronutrients, temperature, and pH value. In fact all these factors determine the production of extracellular ligninolytic enzymes such as LiP, MnP, and laccase.

2.3.1 Lignin Peroxidase (LiP)

The structure and reaction mechanisms of LiP have been studied extensively using enzyme preparations produced by a particular white rot fungus, *Phanerochaete chrysosporium*. Lignin peroxidase (molecular weight varies between 38 and 47 kDa due to lost transnational modification) requires hydrogen peroxide generated by other enzymes (e.g., oxidases) to be active. The enzyme comprises heme in the active site while the catalytic cycle resembles that of horseradish peroxidase (Tien et al., 1986). LiP catalyzes several oxidations in the alkyl side chains of lignin-related compounds such as C-C cleavages in the side chains of lignin subunits, oxidation of veratryl alcohols and related substances to aldehydes or ketones, intradiol cleavage of phenylglycol structures, and hydroxylation of benzylic methylene groups (Tien et al., 1983). LiP is capable of oxidizing recalcitrant non-phenolic lignin model substrates by one-electron abstraction to form reactive aryl cation radicals, which commonly decay via pathways involving C-C and C-O bond-cleaving reactions (Kersten et al., 1987). Veratryl alcohol is a fungal metabolite of low molecular mass which is oxidized by the enzyme to veratraldehyde through an aryl cation radical and has been thought to be a mediator (Kirk et al., 1987). However, the role of veratryl alcohol has been questioned since the stability of the radical (its life span) is too short to enable long-distance charge-transfer. If veratryl alcohol radicals possess mediating properties, this will only be relevant in short distance transfers when the aryl cation radical is somehow

complexed to the enzyme. Nevertheless, veratryl alcohol stimulates LiP activity, probably by protecting the sensitive enzyme from the damaging effects of excess H_2O_2 or phenolics (Akthar et al., 1997).

2.3.2 Manganese Peroxidase (MnP)

LiP has long been considered to oxidize non-phenolic, lignin-related substrates, whereas MnP oxidizes phenolic substrates. However, the two enzymes are not necessarily produced in the same fungus strain, and many *Phanerochaete chrysosporium* strains produce no detectable LiP when grown on liquid media (Hatakka, 1994). MnP has been isolated not only from *P. chrysosporium* but also from other fungi (Hofrichter et al., 1999; Lobos et al., 1994). MnP resembles LiP in that it is extracellular, glycosylated and contains heme as the reactive group (Glenn et al., 1985, Paszczynski et al., 1986). MnP is also expressed in multiple forms with molecular weights from 40 to 48 kDa. The catalytic cycle of MnP resembles that of LiP, including native ferric enzyme as well as peroxidase Compound I and Compound II (MnP I and MnP II in Figure 2.2) redox states (Wariishi et al., 1988). However, significant differences appear in the reductive reactions where Mn^{2+} is a required electron donor. Both Compound I and Compound II are reduced by Mn^{2+} while the latter is oxidized to Mn^{3+} . Mn^{3+} ions are stabilized to high redox potentials via chelation with organic acids such as oxalate, malonate, malate, tartrate, or lactate. Chelated Mn^{3+} in turn, acts as diffusible redox mediator that oxidizes phenolic lignin structures (Wariishi et al., 1992, Figure 2.2).

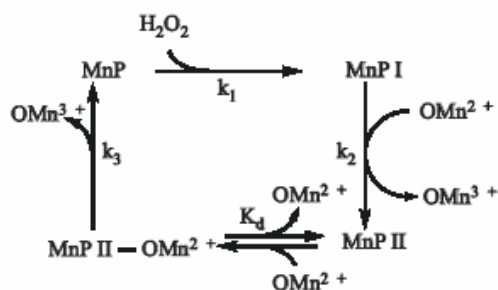


Figure 2.2. Mechanism of Manganese Peroxidase Catalyzed Formation of Mn^{3+} -oxalate Complexes. Mn-oxalate complexes Are Represented by OMn^{2+} and OMn^{3+} (adapted from Zapanta et al., 1997)

Manganese peroxidase has been shown to generate H_2O_2 in the oxidation of certain thiols (e.g., glutathione) and NAD(P)H_2 ; recently, evidence has been provided that the enzyme is even capable of acting efficiently in the absence of external H_2O_2 by oxidizing organic acids (e.g., oxalate, malonate, malate) in “oxidase-like” autocatalytic reactions involving the transient formation of several radical species (Hofrichter et al., 1998, Urzua et al., 1998). MnP has been shown to oxidize non-phenolic substrates in the presence of mediators (Wariishi et al., 1989). Due to their intense activity in oxidizing a wide variety of aromatic compounds, these enzymes have been thought to have potential for industrial use.

2.3.3 Laccase

Fungal laccase is an enzyme secreted into the medium by mycelia of *Basidiomycetes*. It occurs in several white rot fungi such as *Pleurotus ostreatus* and *Trametes versicolor*. Laccase levels are enhanced in the presence of 2, 5-xyldine. Biochemically, laccase is an enzyme which oxidizes a variety of aromatic hydrogen donors. Thus, it catalyzes the removal of an electron and a proton from phenolic hydroxyl or aromatic amino groups to form free phenoxy radicals and amino radicals, respectively. Moreover, the copper-containing laccase having four copper atoms all in the 2^+ oxidation state in the active site (i.e. blue oxidase) not only oxidizes phenolic

and methoxyphenolic acids, but also decarboxylates them (Agematu et al., 1993) and attacks their methoxyl groups through demethylation (Leonowicz et al., 1984) or demethoxylation (Potthast et al., 1995). Laccase oxidizes preferentially phenolic lignin structures to phenoxy radicals which subsequently form quinones.

2.3.4 The Other Enzymes Related to White Rot Fungi

There are also other enzymes which have been discovered in cultures of white rot fungi. A veratryl alcohol oxidase (VAO) enzyme has been reported (Sannia et al., 1991). Another type of extracellular peroxidase, D-glucose oxidase, as a generator of H_2O_2 from *Pleurotus ostreatus*, has been reported (Kang et al., 1993, Shin et al., 1997). A 3, 4-dioxygenase was isolated from *Pleurotus ostreatus*; glucose 1-oxidase, cellobiase, aryl alcohol oxidase, aryl alcohol dehydrogenase, glyoxal oxidase, and superoxide dismutase were also reported (Leonowicz et al., 2001).

The *Pleurotus ostreatus* extracellular peroxidase (PoP, 14Kda) is an H_2O_2 -dependent heme protein with iron protoporphyrin IX as a reactive group. It oxidizes a variety of organic compounds, including phenolic lignin model compounds as well as Remazol Brilliant Blue R (Shin et al., 1997, Vyas et al., 1995). PoP has substrate specificity similar to that of MnP in that it cannot oxidize non-phenolic compounds. It is not dependent on manganese for catalytic activity, in contrast to MnP.

2.4 Analytical Techniques to Identify Dye Degradation Products

The chromatographic technique was first developed by Tswett in 1906 to separate colored compounds (Reichstein, 1992) and became an indispensable tool for chemical analysis. Sulphonated azo dyes are nonvolatile and thermally unstable, so they cannot be directly be

separated by gas chromatography (GC). The polarity of sulphonated dyes requires derivatization prior to GC analysis. Methylation of sulphonic groups in dyes was done using by methyl fluorosulfate, which left the amino and hydroxyl groups unaffected (Sugiura and Whiting, 1980). Silylation is another major means to produce silyl derivatives which are more volatile and more thermally stable. The active hydrogens on the dye molecules are replaced with a trimethylsilyl (TMS) group.

High performance liquid chromatography (HPLC) is useful in analyzing dye wastewater and metabolites from various degradation procedures (Baiocchi et al., 2002; Conneely et al., 1999; Nachiyar and Rajkumar, 2003; Pielesz et al., 2002; Plum et al., 2003; Vinodgopal and Peller, 2003; Wang and Tsai, 2003). HPLC is advantageous over GC because it does not need the sample to be volatile or stable at elevated temperatures.

Reversed phase liquid chromatography (RPLC) is the most commonly used mode in HPLC and was employed in this study. Reversed phase means that the stationary phase is less polar than the mobile phase. Solute retention in RPLC is mainly driven by hydrophobic interaction between the solute and the non-polar stationary phase. Thus, compounds with different polarity elute at different retention times. Resolution is governed by three parameters: retention, column efficiency and selectivity. The most popular detector used for HPLC is the UV-VIS. Under adequate peak resolution, the UV-VIS detector can detect components in a complex mixture to ppb (parts per billion) level and quantitate them to ppm (parts per million) level.

With increasing polarity of the sulphonated azo dyes, the interaction of the analyte with the reverse-phase column becomes too weak to obtain separation, and the ion-pair RPLC becomes the method of choice (Camp and Sturrock, 1990). The most frequently used ion-pair

agents are cetyltrimethylammonium (CTMA) (Taylor and Nickless, 1979; Zerbinati et al., 1993) and tetrabutylammonium (TBA) (Reemtsma and Jekel, 1994; Lange et al., 1995; Altenbach and Giger, 1995; Jandera et al., 1983; Bear, 1986) with the symmetric TBA being favored to date.

Capillary electrophoresis (CE) is based on “differential migration of electrically charged particles in an electric field” (Righetti, 1992). CE has become an important technique for the separation of dyes due to the extraordinarily high separation efficiency, short separation times and separation in aqueous media, which makes CE especially suitable for the analysis of aqueous samples (Takeda et al., 1999). Other advantages of CE include low sample quantities and low consumption of organic solvents.

Both physical and chemical parameters that are crucial to an optimum separation have been summarized by Benedek and Guttman (2001). Physical parameters include the field strength, temperature, column length and diameter, and injection mode and size. The chemical parameters are the type and composition of electrolyte (including pH, concentration, viscosity, and additives), sample composition, and the capillary coating. Zhao (2004) investigated an optimum separation of the degradation products of several disperse dyes in terms of pH and concentration of the running buffer.

Mass spectrometers analyze mass/charge (m/z) ratios and the relative abundances of positive or negative gas phase ions formed from a sample. These data, in turn, can provide structural information and molecular weight of analytes, with the ability to quantitatively assay. The mass spectrometers which have been coupled with CE include magnetic sector, ion trap, time of flight (TOF), and Fourier transform ion cyclotron (FTICR) (Perkins and Tomer, 1994; Wey and Thormann, 2002; Verhaert et al., 2001; Marshall, 2000; Severs et al., 1996).

The ion trap mass spectrometer has been shown to be very useful for the structural elucidation and was used in this study. Because the ion trap performs functions through mass accumulation and selective mass isolation, it can supply highly sensitive and selective mass measurements. Its unique MS^n (MS^1 , MS^2 , e.g.) capability provides valuable information on compound structure. CE- MS^n is suited for the analysis of compounds at low concentrations in small amounts within complex samples.

Electrospray ionization (ESI) is conducted at atmospheric pressure and consists of four steps: formations of ions, nebulization, desolvation, and ion evaporation. The nebulizing gas and the strong electrostatic field (2-6V) in the spray chamber draw out the sample solution and break it into droplets. An electrical charge will be created on the surface of droplets by the electrostatic field and finally dispersed into a fine spray of charged droplets. The solvent in droplets along with analyte ions is evaporated by a counter flow of heated drying nitrogen. Large droplets will break into small ones with high surface-charge density through neutral molecular desolvation which results in decreasing droplet diameter and increase of Coulomb repulsion. This disintegration will continue until the charge density reaches approximately 10^8 V/cm^3 , and then ion evaporation will occur. Single ions are emitted directly from the charged droplets into the gas phase (Fenn et al., 1989).

Since its introduction in 1987 (Olivares et al., 1987), capillary electrophoresis- mass spectrometry (CE-MS) has been applied to the fields of environmental science, forensics, pharmaceuticals and life science. CE-MS combines the capillary electrophoretic concepts introduced by Mikkers and Jorgenson in the early 1980s with MS using electrospray ionization (ESI) developed concurrently by Dole and Fenn (Schmitt-Kopplin and Frommberger, 2003). Compared to ultraviolet (UV) detection, which offers little information on the structure of

unknown compounds, mass spectrometric (MS) detections reveal unambiguous information on the solute's molecular weight and possibly its structure. Although CE-MS has been used in the determination of dyes in wastewater (Riu et al., 1997), this study is the first one to use this technique to identify and quantify metabolites of dyes after fungal decolorization.

The interface of CE-MS is a critical part in the connection of these two instruments (Figure 2.3). In contrast to the widely used HPLC-MS, the amount of sample injection for CE-MS is usually in a range of nanoliters instead of microliter range used in LC-MS. Another major difference compared to LC-MS is the flow rate, which is driven by the electro-osmotic flow and is in the range of sub-microliters. Both of these characteristics have to be considered in the development of the CE-MS interface.

Smith et. al. (1988) first developed an interface using an electrospray ionization technique combined with a sheath liquid. This technique is commonly used in the CE-MS instruments for its ease of implementation and versatility (Kirby et al., 1996). The interface uses coaxial sheath-flow design. The CE capillary is in the center of the triple tubes, surrounded by the sheath liquid tube and the nebulizing gas tube. The sheath liquid electrically connects the CE outlet to the sprayer and produces the necessary flow for a stable electrospray. A gas-assisted nebulizer generates gas phase ions from the CE effluent under application of a high voltage (HV) field. The function of nebulizing gas is to combine with the applied HV and drying gas to supply efficient droplet generation.

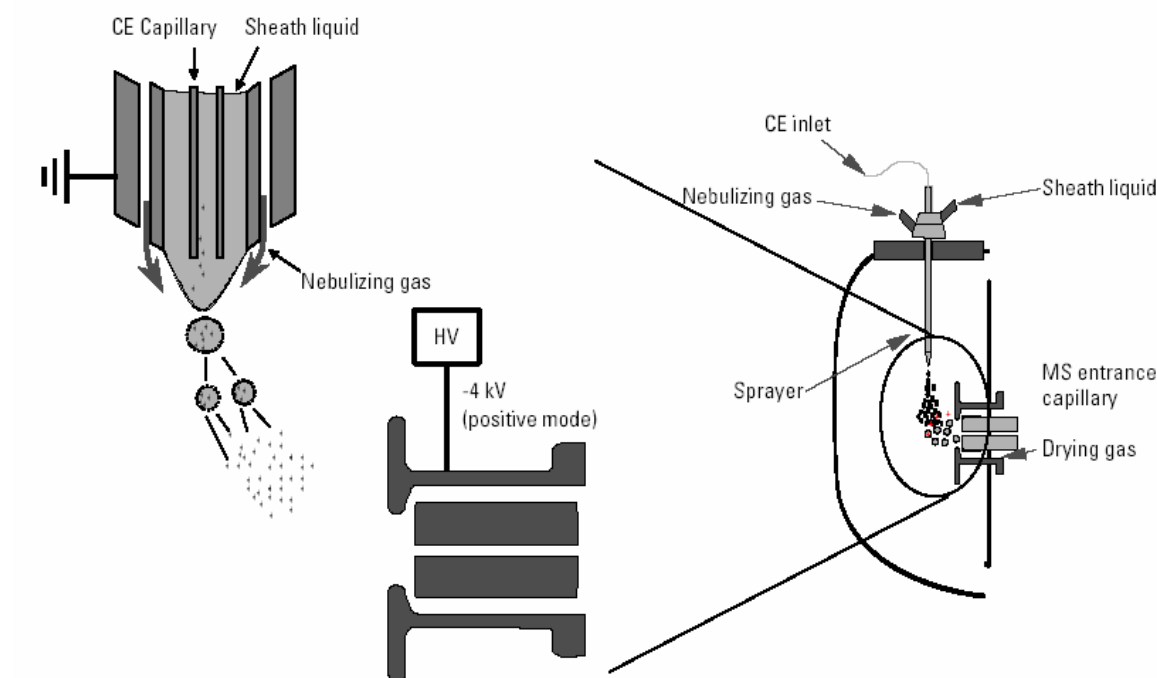


Figure 2.3 Interface of CE-MS (Agilent® Technologies)

2.5 Summary of the Literature

- (1) Dyes with high solubility such as acid and reactive dyes were more easily decolorized by white rot fungi than dyes with low solubility such as vat and disperse dyes. Orange II and the phenol derivative dyes are the acid dyes that have been investigated most often.
- (2) There is a relationship between the chemical structures of textile dyes and the potential for their degradation by white rot fungi. The position of substituted groups on aromatic rings also appears to be important for degradation.
- (3) Many white rot fungi have the ability to degrade lignin and environmental pollutants, as well as textile dyes. Among these white rot fungi, *Pleurotus ostreatus* has been studied only in recent years. The mechanism of the degradation pathway of *Pleurotus ostreatus* needs to be established.

- (4) Enzymes such as laccase, lignin peroxidase (LiP), and manganese peroxidase (MnP), are considered as the main enzymes released from white rot fungi. LiP has long been considered to oxidize non-phenolic, lignin-related substrates, whereas MnP oxidizes phenolic substrates, and laccase oxidizes a variety of aromatic hydrogen donors.
- (5) MnP and Laccase are the two major lignin-degrading enzymes released by the white rot fungus *Pleurotus ostreatus*. A 3,4-dioxygenase glucose 1-oxidase, cellobiase, aryl alcohol oxidase, aryl alcohol dehydrogenase, glyoxal oxidase, superoxide dismutase, veratryl alcohol oxidase, and *Pleurotus ostreatus* extracellular peroxidase have also been discovered in cultures of *Pleurotus ostreatus*.
- (6) HPLC, CE, and MS are the main analytical methods to separate and identify water soluble dye degradation products.

CHAPTER 3

MATERIALS AND METHODS

3.1 Materials

3.1.1 Chemicals

Eight sulphonated azo dyes were obtained from Sigma-Aldrich (St. Louis, MO, USA): 1) C.I. Mordant Violet 5; 2) C.I. Acid Orange 7; 3) C.I. Acid Orange 8; 4) C.I. Food Yellow 3; 5) C.I. Acid Orange 10; 6) C.I. Acid Orange 12; 7) C.I. Acid Red 4; and 8) C.I. Acid Red 8, are shown in Table 3.1. The structures of the dyes are shown in Figure 3.1. Compounds used as standards, benzenesulfonic acid, 4-hydroxybenesulfonic acid, veratryl alcohol, veratraldehyde, 1, 2-naphthoquinone, and other possible products were analytical reagents and obtained from Sigma-Aldrich. Unless otherwise specified, all chemicals were analytical grade.

Acetonitrile (Sigma-Aldrich) used in analysis and sample preparation was of HPLC grade. Tetrabutylammonium (TBA) was used as an ion-pair agent and was from Sigma-Aldrich. Ammonium acetate was obtained from Aldrich and ammonium hydroxide (28 percent) was purchased from J. T. Baker (Phillipsburg, NJ). All the solutions and buffers were filtered with a 0.22 μm , 13 mm, PVDF membrane (Fisherbrand).

Malt extract (Bacto®) and agar (Bacto™) were from Difco Laboratories, Detroit, MI, USA. Enzyme activity assays were done with 2, 2'-azino-di-(3-ethylbenzothiazolin-6-sulfonic acid) (ABTS), sodium acetate, veratryl alcohol, sodium tartrate, hydroxide, malonate, and manganese sulfate from Sigma-Aldrich. Bovine serum albumin (BSA) and Bradford Reagent were from Sigma-Aldrich for enzyme concentration assay.

3.1.2 Microorganism

Pleurotus ostreatus (strain Florida), was used in this work. This fungus was originally obtained from the laboratory of Dr. Karl-Erik Eriksson at the University of Georgia.

3.1.3 Culture Conditions

1. Preparation of fungi stock maintained on wood

Several small pieces of wood about one half inch were cut in length and then sterilized in a Tuttnauer Brinkmann Autoclave Steam Sterilizer (Brinkmann Inc., Westbury, NY). Then, a piece of wood or a piece of agar with white rot fungi grow on it in a 2 percent malt extract, was inoculated in an Isotemp Incubator (Fisher Scientific, USA). Several sterilized wood pieces were put into the malt extract agar plate and incubated at 30°C in the Isotemp Incubator. After three to five days incubation, white rot fungi grew on the sterilized wood pieces. Then, sterilized tweezers were used to transfer the wood pieces with white rot fungi grown on them to sterilized small plastic tubes. After transferring, the plastic tubes were stored in a freezer at -20°C. Under this circumstance the white rot fungi could be stored indefinitely. When fungi were needed, one piece of wood was taken out, inoculated in nutrient medium and incubated with fungi growing in the medium.

2. Preparation of malt extract agar plate (2 percent malt extract agar plate)

Ten grams of malt extract (Bacto®) and 7.5 g agar (Bacto™) were weighed and put into a beaker. An aliquot of 500 ml distilled water was put into the beaker and heated on a heat-stir plate with stirring until the solids dissolved in the beaker. The dissolved solution was split and poured into two 500 ml flasks with about 250 ml solution in each flask and put into the sterilizer to autoclave the solution at 121°C for 60 minutes. After one hour's sterilization, the autoclaved solution was poured into sterilized plates with about 20 ml solution in each plate

while it was still hot. The solutions were cooled down for 20 minutes to solidify before sealing with Para-film. This procedure was done inside the Sterilguard® hood (The Baker Company, Sanford, ME) with the UV light on. In order to keep the malt extract agar plates fresh, all of the plates were stored in the refrigerator.

3. Preparation of fungi stock maintained in malt extract agar plate

A piece of wood or a piece of agar with white rot fungi grown on it in 2 percent malt extract agar plate was inoculated and incubated at 30°C. After four to five days, the fungus grew over the whole plate. In this condition white rot fungus could be stored for about 4 to 8 weeks. That is, white rot fungus maintained in malt extract agar plate should be refreshed (inoculate a piece of “old” agar to a “new” malt extract agar plate). In this study, the culture was maintained on malt agar plates (malt extract 20 g/L, agar 15 g/L) at 30°C in the Isotemp Incubator with subcultures routinely made every 15 days.

4. Preparation of Kirk's medium (1 liter)

A mixture of 0.2 g KH_2PO_4 , 0.05 g $\text{MgSO}_4 \cdot 7\text{H}_2\text{O}$, 0.01 g CaCl_2 , and 0.22 g ammonium tartrate were weighed and put into a beaker. An aliquot of 1 ml mineral stock solution, 0.5 ml vitamin solution, and 0.5 ml glacial acetic acid were added to the stock solution. The formulation of mineral stock solution and vitamin solution were reported by Cao (2000). One liter of distilled water was added into the beaker. The initial pH value of the solution was 3.5. In order to adjust the pH of the solution to 5.0, which was the best for white rot fungus growth, NaOH solution (6M) was added and the pH value was measured using a pH meter. Then 10 g glucose was added to the solution, heated and stirred until all the glucose was dissolved. The solution was autoclaved at 121°C for 60 minutes.

5. Preparation of dye stock solution

The 1.25 g dyestuff was weighed using a balance and put into a clean flask. An aliquot of 100 ml DI water was poured to dissolve the dye. The solution was autoclaved for 1 hour. For calculations, suppose the concentration of dyestuff is 100%. If the concentration is X percent, then weigh $1.25 \times 100/X$ g dye. For example, if a 70 percent dye solution is desired, 1.786 g of dye would be added, $1.25 \times 100/70 = 1.786$.

After 3 days, 1 ml of the stock solution is added to 125 ml of autoclaved Kirk's medium with fungus. Then the concentration of dye is 100 ppm.

6. White rot fungi dye decolorization in liquid medium

The white rot fungus was transferred into the agar plate and incubated at 30°C for five days until the fungus colonized the entire plate. A whole piece of agar was cut with fungus grow on it and put into a flask containing 200 ml Kirk's medium. The whole medium with agar and Kirk's medium was mixed with a blender (Fisher Scientific). An aliquot of 5 ml of homogenous dispersion solution was inoculated into a flask with 120 ml of autoclaved Kirk's medium. The flask was covered with eight layers of cheesecloth to avoid dust falling in and placed in a water-bath shaker (New Brunswick Scientific, Edison, NJ, USA) at 30°C and 200 rpm. After three days of growth, 1 ml of sterilized concentrated dye solution was added to the flask. This created a 100 ppm dye solution. The rotation rate was adjusted to 150 rpm. Some water samples were periodically taken out of the flask to measure the color of the solution.

3.2 Methods

3.2.1 Color Removal Measurement—UV-Visible Spectrophotographic Analysis

An aliquot of 2 ml decolorization culture was taken out by a syringe and filtered with a 0.22 μm , 13 mm, PVDF membrane filter (Fisherbrand, USA) into a test tube. The same amount of reservoir culture (2 ml of solution contains same dye and Kirk's medium but without fungus) was added into the medium to keep a constant volume in the degradation system. An aliquot of 1 ml of the filtrate was taken into a cuvette and 1 ml of DI water was added into the cuvette. The absorbance at the wavelength maximum was measured in a spectrophotometer. The area under the absorption curve from 300 nm to 700 nm before and after treatment was measured to determine the decolorization effect. The test was replicated 5 times on a daily basis, sample had 5 replicates.

Percent color removal was calculated by the following formula:

$$\text{Percent Color Removal} = (1 - AA/AB) \times 100\%$$

Where AA = area of absorbance after treatment;

AB = area of absorbance before treatment.

3.2.2 High Performance Liquid Chromatography (HPLC) Analysis

Three milliliters of supernatant were taken from the fungal culture by pre-autoclaved pipette each day for 7 days. The same amount of liquid medium containing 100 ppm dye solution was added after each sampling to keep a constant volume in the culture flask. Five replicate flasks with the same dye concentration were used for the study and results were reported as an average of the five samples. No significant variation of dye concentration was induced by photo-degradation and no degradation products were detected in control samples

(that is, samples with no fungal culture included). The samples were filtered through a 0.22 μm , 13 mm, PVDF membrane filter prior to HPLC analysis.

Sample was analyzed using Hewlett-Packard 1100 series HPLC system (Hewlett-Packard GmbH, Germany), consisting of a model G1311A quaternary pump, G1322A degasser, and a diode array detector (Model G1315A). HP ChemStation software (version 3.1) was used for data processing and reporting.

HPLC analysis was performed under ambient conditions using a RP-C18 guard column and a stainless steel ODS column with 5 μm packing (Phenomenex, Ultracarb 150X 4.6 mm I. D.). The mobile phase was acetonitrile/water (20/80, v/v). The injection volume was 100 μl each time and the flow rate was 1 $\text{ml}/\text{min}^{-1}$. Identification of separated degradation compounds was confirmed by comparison of both the retention times and spectra with those of standard compounds.

2.2.3 Capillary Electrophoresis – Mass Spectrometry (CE-MS)

The CE equipment used was Hewlett Packard^{3D} CE (Palo Alto, CA). The capillaries for CE separation (75 μm I. D., 360 μm O. D.) were preconditioned with acetonitrile, 1 M NaOH, 0.1 M HCl, and water for 10 min each, and conditioned with running buffer for 20 min before the first run and for 3 min between runs. The running buffer was 0.1 M pH=9.0 ammonium acetate. In order to keep fresh, the running buffer was made every two weeks. Hydrodynamic injection was performed with a pressure of 50 mbar (1 mbar = 100 Pa) for 30 seconds. The voltage applied in separation was +30 kV. The mass spectrometer used was an Esquire 3000 plus ion trap equipped with an electrospray ionization (ESI) interface (Bruker Daltonics, Billerica, MA), which was operated in negative ionization mode. ESI voltage was 4.0 kV. CE and MS were connected through a commercial interface based on coaxial sheath flow (Figure

3.1). The length of the CE capillary was 80 cm. The position of the CE capillary with ESI needle was adjusted during optimization. Mass spectrometric parameters used in the analysis were listed as follows: maximum accumulation time 50 ms; scan 60-400 m/z ; average 8; compound stability 100%; scan range normal; trap drive level 100%; ion charge control activated; mass resolution 0.45 u. Sheath liquid (a mixture of 2-propanol with water 80:20 v/v) was delivered by a syringe pump at 2 $\mu\text{L}/\text{min}$ (Cole-Parmer Instrument Co., Vernon Hills, IL) using a 1000 mL syringe (Hamilton Co. Reno, NE). The standard solutions and buffers were filtered with 0.22 μm 13 mm PVDF membrane filter (FisherBrand, USA).

2.2.4 Enzyme Assay

1. Enzyme Activity

Activities of LiP, MnP and laccase were assayed spectrophotometrically. All enzyme activities are expressed in units L^{-1} (U L^{-1}), with one unit equal to 1 μmol substrate oxidized min^{-1} . Laccase activity is determined with 2, 2'-azino-di-(3-ethylbenzothiazolin-6-sulfonic acid) (ABTS) as the substrate. The reaction mixture contains 0.5 ml of 100 mM ABTS, 100 mM sodium acetate buffer (pH 4.5) and the culture filtrate. Oxidation of ABTS is monitored by an absorbance increase at 420 nm ($\epsilon_{420}=36,000 \text{ M}^{-1} \text{ cm}^{-1}$) at 30 °C.

Lignin peroxidase activity is determined by an absorbance increase at 310 nm ($\epsilon_{310}=9300 \text{ M}^{-1} \text{ cm}^{-1}$) with veratryl alcohol as the substrate. The reaction mixture contains 0.5 ml of 10 mM veratryl alcohol, 1 ml of 50 mM sodium tartrate buffer (pH 3.0), 0.54 ml of 2 mM H_2O_2 and 1 ml of culture filtrate. Reaction is started with the addition of hydrogen peroxide.

MnP activity is assayed by measuring the oxidation of manganese sulfate ($\epsilon_{270}=11,590 \text{ M}^{-1} \text{ cm}^{-1}$). The incubation conditions are 1 ml of 100 mM malonate buffer (pH 4.5), 0.5 ml of 2 mM H_2O_2 , 0.5 ml of 10 mM manganese sulfate and 1ml culture filtrate.

2. Concentration of enzymes

The Bradford method can be used to determine the concentration of proteins in solution (Bradford, 1976). It is fast, inexpensive, very sensitive, and highly specific for protein. The procedure is based on the formation of a complex between the dye, Brilliant Blue G, and proteins in solution. The protein-dye complex causes a shift in the absorption maximum of the dye from 465 to 595 nm. The amount of absorption is proportional to the protein present using dilution standards. The Bradford Reagent requires no dilution and is suitable for micro, multiwell plate, and standard assays. The linear concentration range is 0.1-1.4 mg/ ml of protein, using BSA (bovine serum albumin, Sigma-Aldrich, USA) as the standard protein. The procedure of enzyme concentration measurement by Bradford method is listed as follows:

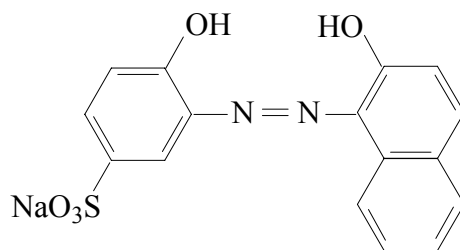
- (1). Gently mix the Bradford Reagent in the bottle and bring to room temperature.
- (2). Prepare protein standards in buffer (Gram-Pac®, pH 7.41, from Fisher Scientific, Fair Lawn, NJ) ranging from 1-10 µg/ml using a BSA standard or an equivalent protein standard.
- (3). Add 1 ml of each protein standard to separate tubes. To the tube used as the blank, add 1 ml of buffer.
- (4). Prepare the unknown sample(s) with an approximate concentration of between 1-10 µg/ml. Add 1 ml of each sample to separate tubes.
- (5). To each tube, add 1 ml of the Bradford Reagent and mix.
- (6). Let the samples incubate at room temperature for 5 to 45 minutes.
- (7). Transfer samples into cuvetts.
- (8). Measure the absorbance at 595 nm. The protein dye complex is stable up to 60 minutes. The absorbance of the samples must be recorded before the 60 minute time limit and within 10 minutes of each other.

- (9). Plot the net absorbance vs. the protein concentration of each standard.
- (10). Determine the protein concentration of the unknown sample by comparing the net 595 abs. values against the standard curve.

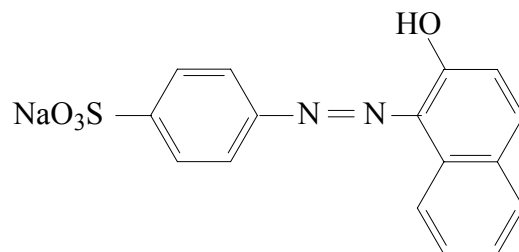
A complete flow chart of this study is shown in Figure 3.2.

Table 3.1 Dyes in This Research

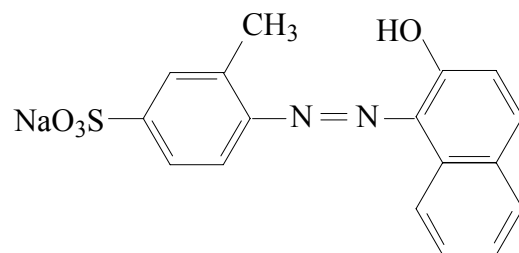
#	Name	Chemical name or molecular formulation	C.I. No.	CAS No.
1	Mordant Violet 5	$C_{16}H_{13}N_2NaO_5S$	15670	2092-55-9
2	Acid Orange 7	4-(2-Hydroxy-1-naphthylazo) benzenesulfonic acid sodium salt $C_{16}H_{11}N_2NaO_4S$	15510	633-96-5
3	Acid Orange 8	$C_{17}H_{15}N_2NaO_4S$	15575	5850-86-2
4	Food Yellow 3	$C_{16}H_{10}N_2Na_2O_7S_2$	15985	2783-94-0
5	Acid Orange 10	7-Hydroxy-8-phenylazo-1,3-naphthalenedisulfonic acid disodium salt $C_{16}H_{10}N_2Na_2O_7S_2$	16230	1936-15-8
6	Acid Orange 12	1-Phenylazo-2-naphthol-6-sulfonic acid sodium salt $C_{16}H_{11}N_2NaO_4S$	15970	1934-20-9
7	Acid Red 4	$C_{17}H_{15}N_2NaO_5S$	14710	5858-39-9
8	Acid Red 8	$C_{18}H_{14}N_2Na_2O_7S_2$	14900	4787-93-3



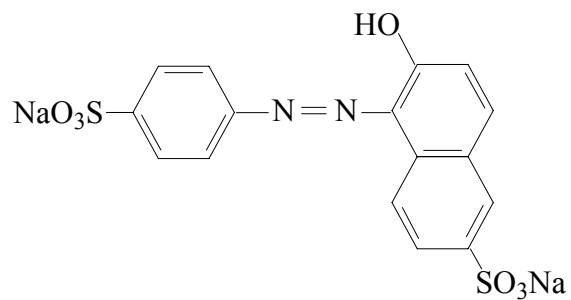
C.I. Mordant Violet 5 (peak absorption wavelength 499 nm)



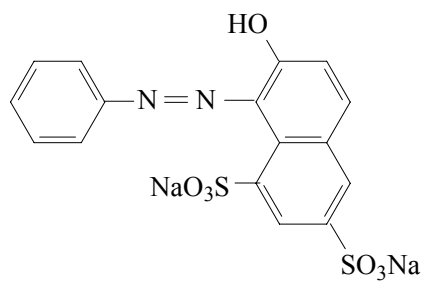
C.I. Acid Orange 7 (peak absorption wavelength 482 nm)



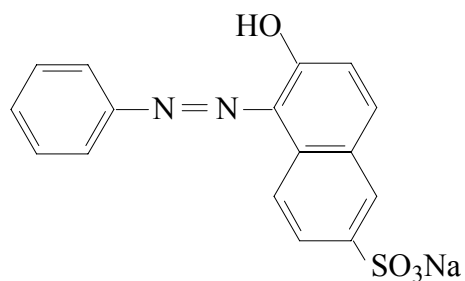
C.I. Acid Orange 8 (peak absorption wavelength 483 nm)



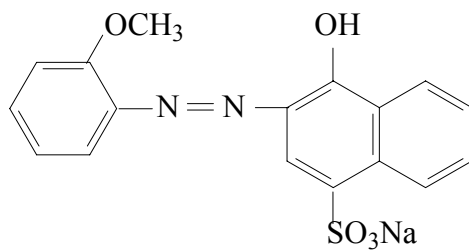
C.I. Food Yellow 3 (peak absorption wavelength 481nm)



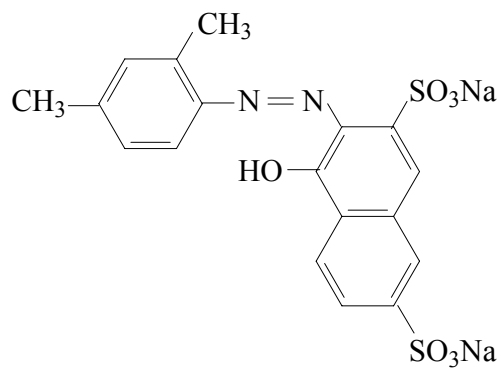
C.I. Acid Orange 10 (peak absorption wavelength 476 nm)



C.I. Acid Orange 12 (peak absorption wavelength 482 nm)



C.I. Acid Red 4 (peak absorption wavelength 506 nm)



C.I. Acid Red 8 (peak absorption wavelength 508 nm)

Figure 3.1 Structures of Dyes in This Study

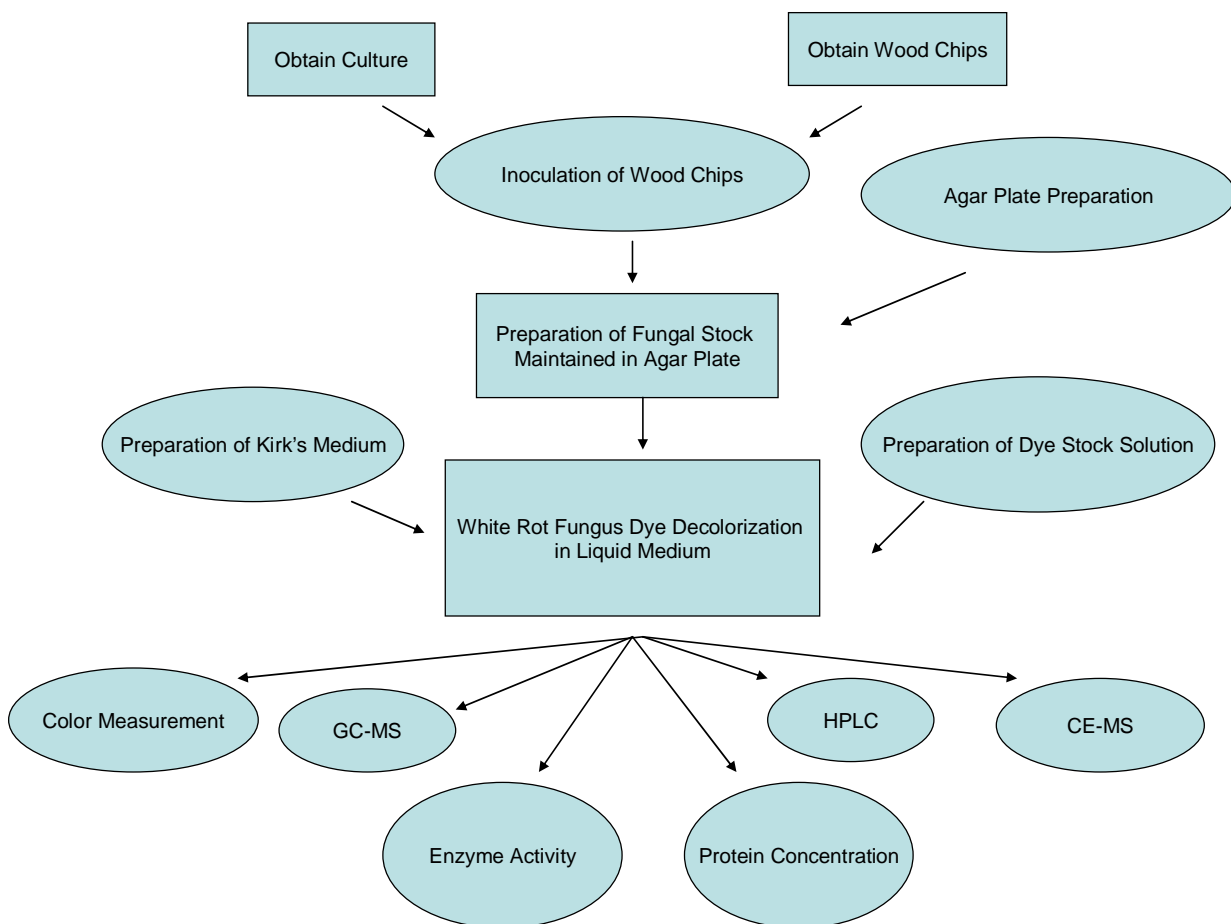


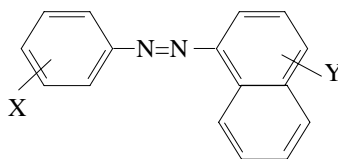
Figure 3.2 The Flow Chart of Analysis of Sulphonated Azo Dyes Degraded by the White Rot Fungus *Pleurotus ostreatus*

CHAPTER 4

DECOLORIZATION OF SULPHONATED PHENYLAZONAPHTHOL DYES

4.1 Decolorization of Sulphonated Phenylazonaphthol Dyes

Our former group member Huantian Cao investigated the treatment of twelve dyes from five classes with *Pleurotus ostreatus*. He selected the dyes with consideration of their chemical structures and prevalence in the textile industry (Cao, 2000), and he suggested that dyes with high solubility such as acid dyes and reactive dyes are easier to decolorize with white rot fungi than dyes with low solubility such as vat and disperse dyes. The temperature and pH for fungal growth and treatment were found to occur at 30°C and 4.5-5.5 respectively. In the present study, eight sulphonated azo dyes were investigated. The molecular structures of sulphonated dyes in this study were characterized by the presence of an azo group connecting a benzene ring and a naphthalene ring, as shown in Figure 4.1. X and Y stand for functional groups such as sulphonic acid groups, as others. The detailed structures were shown in Figure 3.1 and the decolorization procedures were outlined in Chapter 3.



X and Y are functional groups

Figure 4. 1 Model Structure of Sulphonated Phenylazonaphthol Dyes in This Study.

In order to investigate the effect of agitation, Acid Orange 7 was treated with *Pleurotus ostreatus* without and with agitation (150 rpm) and compared in Figure 4.2. It was clear that the

decolorization of Acid Orange 7 with agitation was significantly higher than without agitation. Previous results had indicated that agitation was essential for the decolorization of dyes due to the improved mass transfer and increased oxygen concentration in culture (Ha et al., 2001, Swamy and Ramsay, 1999). Our result confirmed that. The decolorization effect ranged from 5 percent to 9 percent over seven day's treatment without agitation. When Zhao (2004) investigated the fungus absorption of Disperse Orange 3, he found that nearly 15 percent of the dye was absorbed physically onto the fungus. He concluded that the fungus has ability to not only chemically decolorize dyes, but to also physically absorb them prior to chemical reaction. Thus, his work indicates that the decrease of color treated by *Pleurotus ostreatus* without agitation may be caused by physical absorption. Without agitation, there may be no chemical reaction involved in this system. Therefore, agitation is a requirement for decolorization and we used 150 rpm in all succeeding experiments.

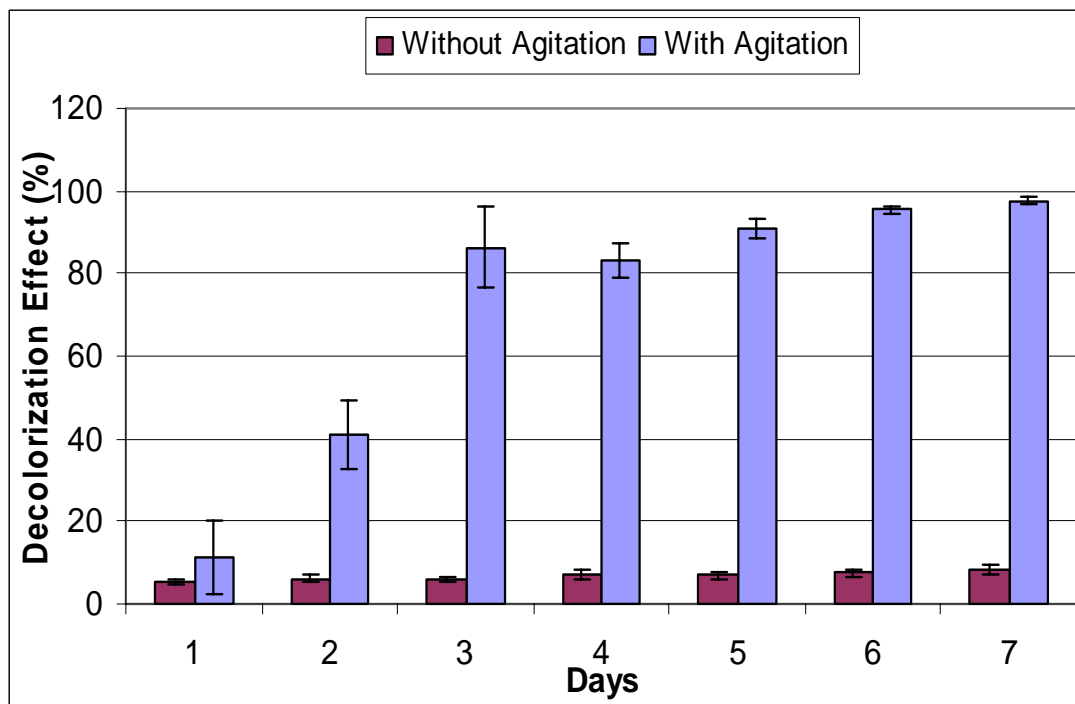


Figure 4.2 The Decolorization of Acid Orange 7 (100 ppm) by the White Rot Fungus *Pleurotus ostreatus* with (150 rpm) and without Agitation

In order to optimize the relationship of decolorization and dye concentrations, four different concentrations of 50 ppm, 100 ppm, 150 ppm, and 200 ppm of Acid Orange 7 dye solutions were treated by *Pleurotus ostreatus*. The decolorization effect was calculated based on the absorbance at the wavelength maximum for each sample. Figure 4.3 shows that the lower the concentration of dye solution, the larger the percentage decolorization effects. This is not surprising since more dye must be decolorized with increasing concentration. There was a significant difference in decolorization effects among concentration on days 2 and days 3. The standard deviation of data was also relatively higher on first three days than later. By day 7, most of the color was removed for all concentrations of dye solution and there was no significant difference among the concentrations.

The conventional concentration of dye wastewater ranges from 10 ppm to 150 ppm; therefore, 100 ppm of dye concentration was used in the following experiments.

Figure 4.4 shows typical results for Acid Orange 7 decolorized by *Pleurotus ostreatus* from day 1 to day 14. The original concentration was 100 ppm, which gave a highly visible color to the solution. After one day's treatment by *Pleurotus ostreatus*, the color of Acid Orange 7 was slightly decreased. Significant color fading was found by the third day. Most color was removed visually after seven days treatment, and the solution was almost clear after fourteen days treatment. The UV-vis spectrum of decolorized Acid Orange 7 was recorded (350 nm to 600 nm) and is shown in Figure 4. 5. The results in Figure 4.4 and Figure 4.5 are the same sample.

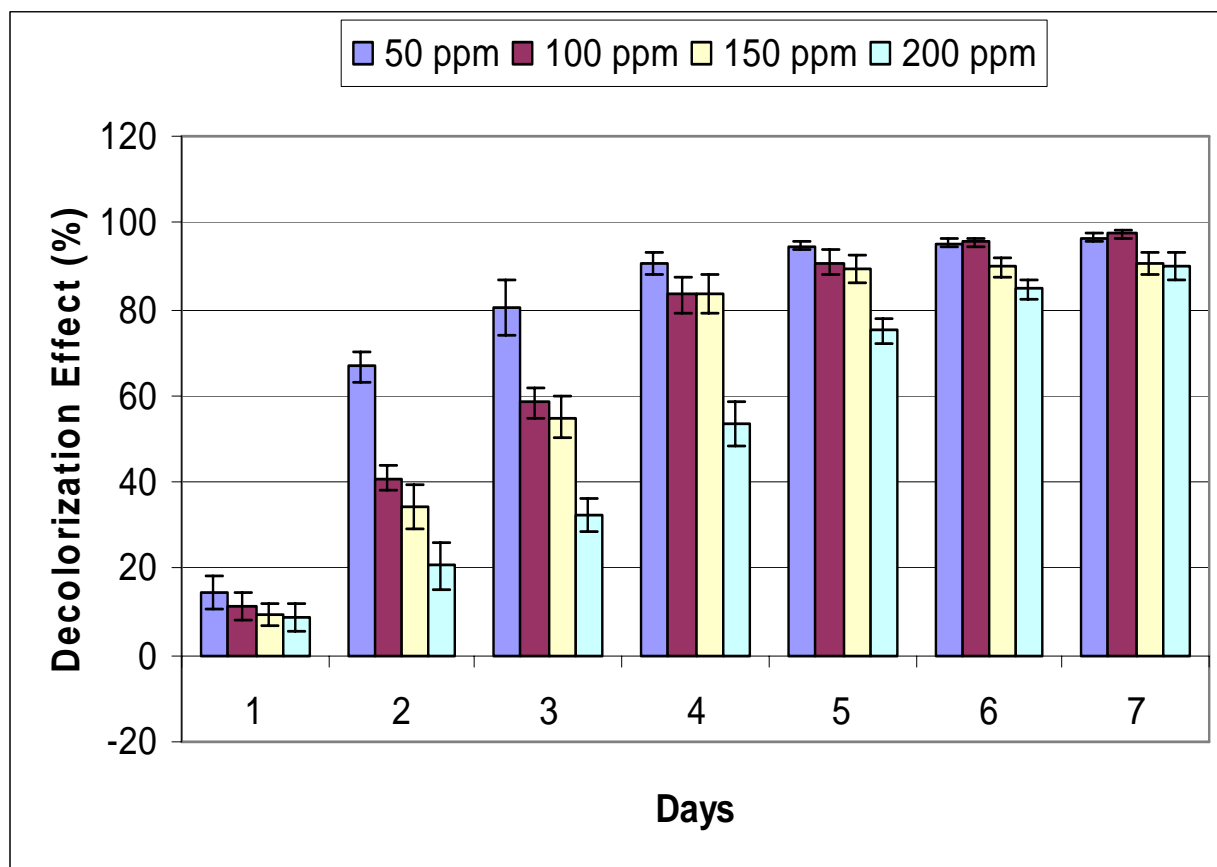


Figure 4.3 The Decolorization of Acid Orange 7 by the White Rot Fungus *Pleurotus ostreatus* at Different Concentrations

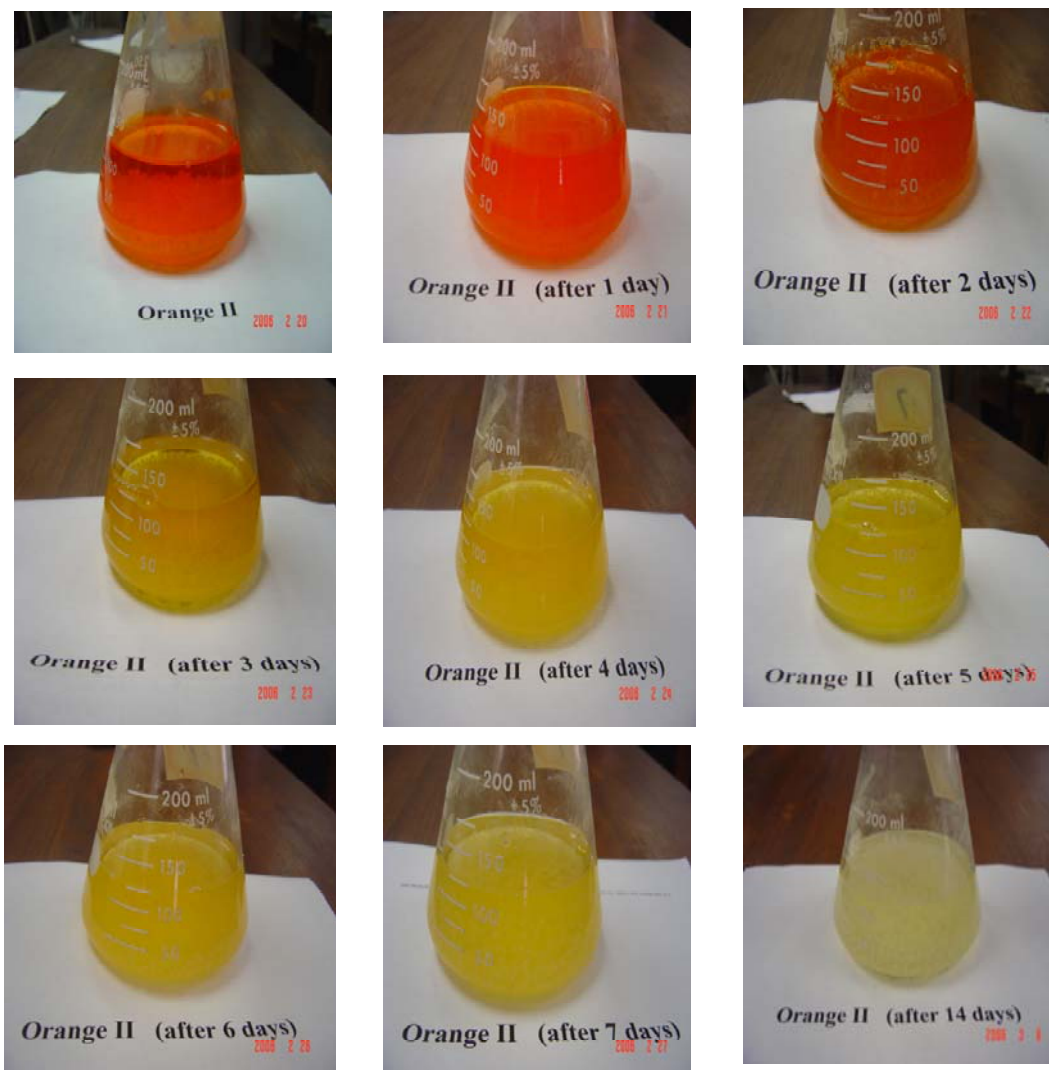


Figure 4.4 The Decolorization of Acid Orange 7 (100 ppm) by the White Rot Fungus *Pleurotus ostreatus*

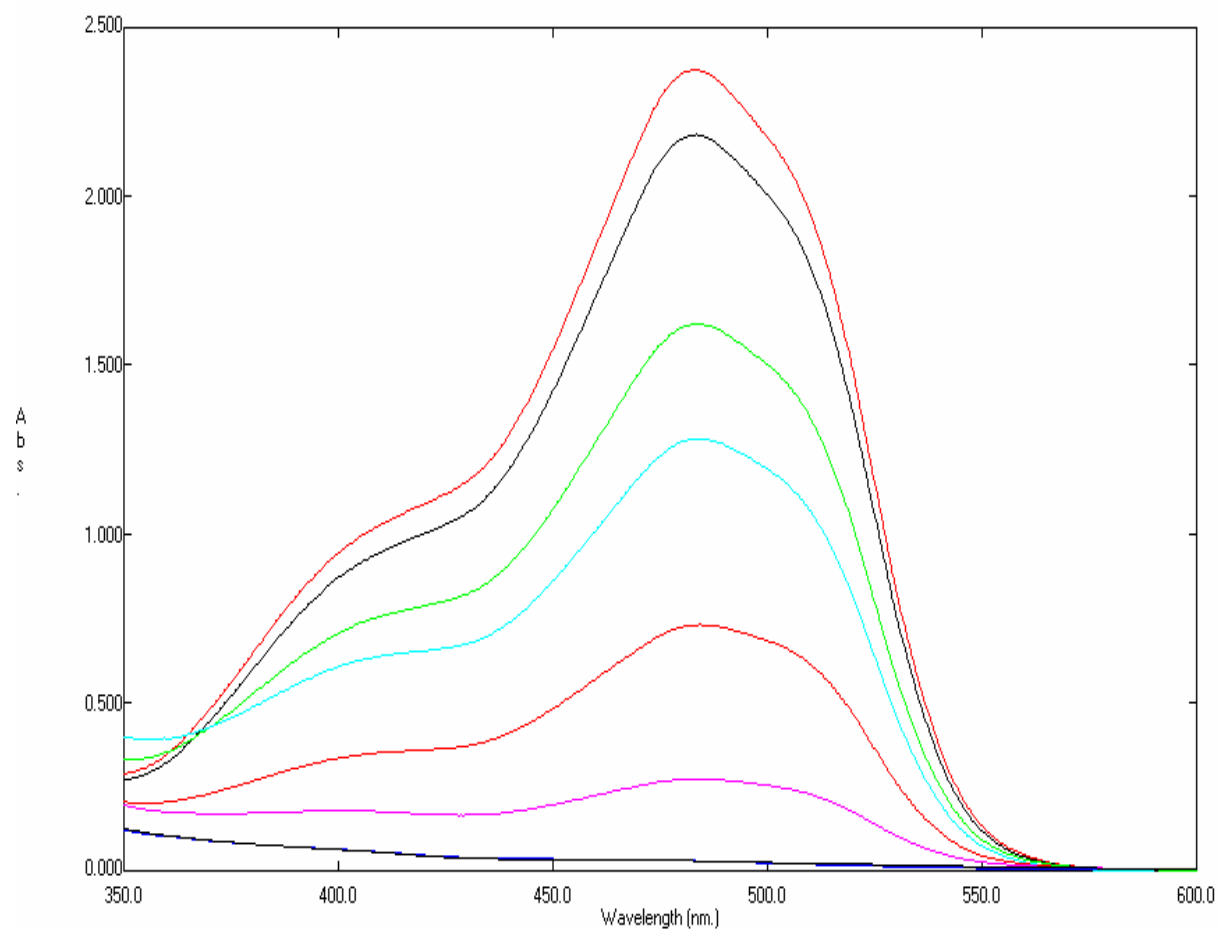


Figure 4. 5 The UV-Vis spectrum of Acid Orange 7 Degraded by *Pleurotus ostreatus*. From top to bottom are control, 1 day, 2 days, 3 days, 4 days, 5 days, 6 days, and 7 days treatment

The decolorization effect for all sulphonated dyes treated by *Pleurotus ostreatus* from the first day to the seventh is summarized in Table 4. 1. The results in Table 4.1 show that there are differences among the eight dyes investigated. In order to explain the differences in decolorization effect among the dyes, the dye molecular structures and the decolorization effect were compared.

Table 4. 1 The Decolorization Effect of Dyes Degraded by *Pleurotus ostreatus* from the First Day to the Seventh, 100 % = Total Decolorization

Day Dye	1	2	3	4	5	6	7
Mordant Violet 5	20.15 ±4.7	42.38 ±3.5	80.31 ±6.3	87.41 ±4.5	93.4 ±1.1	98.47 ±1.0	98.53 ±0.9
Acid Orange 7	11.24 ±5.0	40.96 ±4.1	58.36 ±7.6	83.29 ±4.2	90.91 ±2.6	95.6 ±0.9	97.56 ±0.9
Acid Orange 8	5.9 ±3.7	14.73 ±6.6	38.81 ±2.8	56.27 ±4.9	69.26 ±1.3	72.42 ±3.4	73.12 ±2.5
Food Yellow 3	16.34 ±4.1	50.51 ±5.8	80.36 ±6.6	88.35 ±4.2	91.47 ±1.6	96.69 ±2.4	98.82 ±1.0
Acid Orange 10	6.77 ±2.7	8.21 ±3.6	15.93 ±3.9	62.68 ±2.7	84.90 ±4.2	90.03 ±2.4	92.36 ±2.6
Acid Orange 12	10.64 ±2.1	16.26 ±2.3	33.09 ±4.0	51.92 ±4.2	82.09 ±2.1	86.25 ±1.6	87.37 ±1.4
Acid Red 4	9.21 ±3.2	12.3 ±2.9	21.07 ±4.6	50.92 ±6.4	75.94 ±3.9	81.26 ±3.4	82.74 ±2.6
Acid Red 8	8.23 ±3.0	16.98 ±2.1	21.77 ±4.1	33.69 ±2.4	63.25 ±5.9	72.38 ±5.5	77.03 ±6.4

4.2 Effect of Dye Molecular Structures

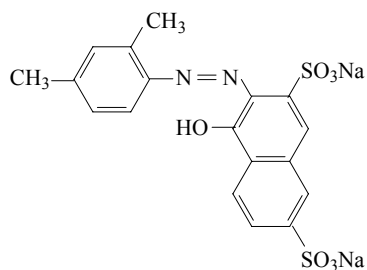
The results in Figure 4.6 show that the decolorization effects for Mordant Violet 5 and Acid Orange 7. The difference is significant at three days but not otherwise. In general, the trend of decolorization of Mordant Violet 5 is slightly higher than that of Acid Orange 7. The differences in the two dyes are the position of the sulphonic acid group and additional electron withdrawing hydroxyl group on the benzene ring for Mordant Violet 5. In Figure 4.7, the effect of an electron donating methyl group at the 2- position on the benzene ring is associated with Acid Orange 8 to being more slowly than Acid Orange 7.

Figure 4.8 compares the degradation of Acid Orange 7, Food Yellow 3, and Acid Orange 12. Food Yellow 3 has one sulphonic group on the naphthalene group whereas Acid Orange 7 has none. There is one sulphonic group on the benzene ring while acid Orange 12 has none. The trend of results shows that Food Yellow 3 has a higher decolorization effect than either Acid Orange 7 or Acid Orange 12, particular in the first three days. The decolorization difference between Acid Orange 7 and Food Yellow 3 is less than that between Food Yellow 3 and Acid Orange 12, evidently because the SO_3^- functional group on the naphthalene ring has less effect than on the benzene ring due to the benzene ring's higher aromatic property than that of the naphthalene ring.

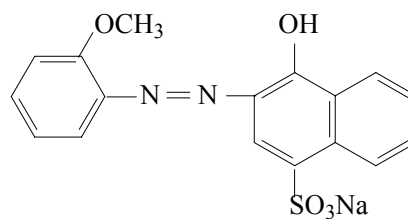
Figure 4.9 compares Acid Orange 10 and Acid Orange 12. In the first three days, Acid Orange 10 shows less decolorization than Acid Orange 12, but after that Acid Orange 10 is decolorized at a slightly higher level. This is a result for which there is no current explanation.

The comparisons above show that the functional groups on the benzene ring in these dyes play an important role during the degradation process. The electronic cloud density of the azo bond is significantly changed with the addition of functional groups. A dye with two electron

withdrawing groups, such as Mordant Violet 5, is decolorized more in the first three days, suggesting that the strong electron withdrawing effect makes the azo bond more easily attacked by the enzymes secreted by *Pleurotus ostreatus*. A dye with two methyl electron donating groups, such as Acid Red 8, has the lowest decolorization effect among the eight dyes. The electron donating groups increase the density of the electron cloud at the azo bond, decreasing its reactivity.

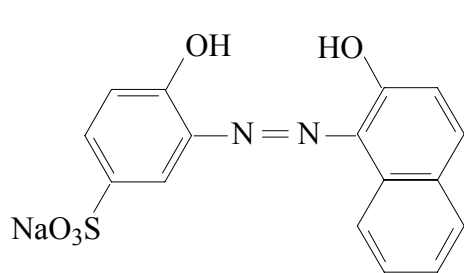
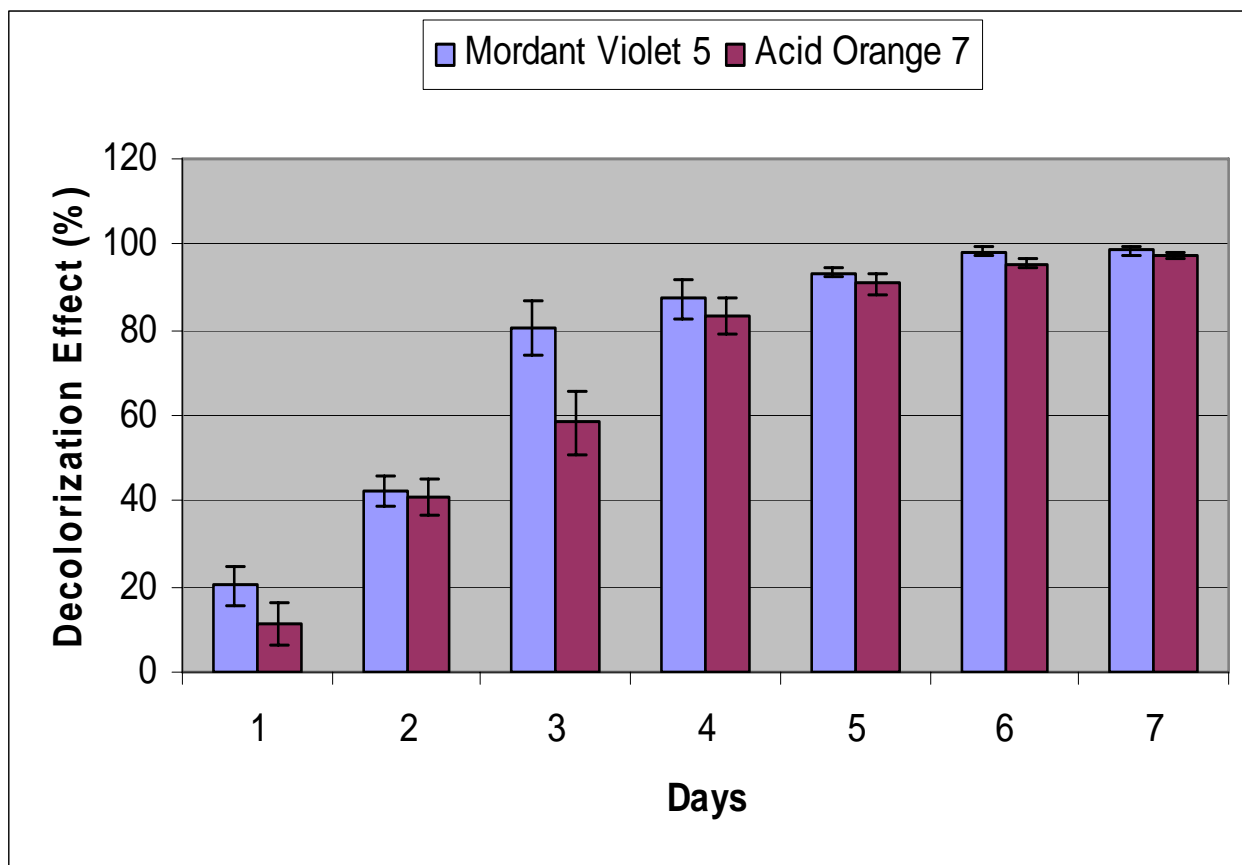


C.I. Acid Red 8

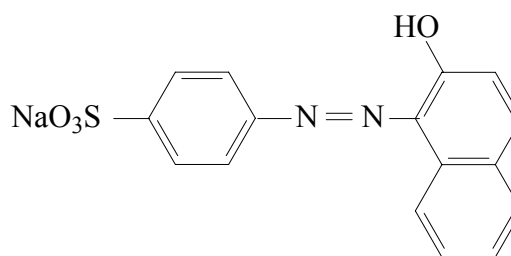


C.I. Acid Red 4

In general, the evidence shows that dyes with electron withdrawing group(s) on the benzene ring, such as Mordant Violet 5, Acid Orange 7, and Food Yellow 3, were degraded and decolorized quickly. After 4 days treatment, more than 80 percent of the dye was decolorized and after 7 days treatment more than 90 percent of color was removed. Dyes with electron donating group(s) on the benzene ring, such as Acid Orange 8 and Acid Red 4, were decolorized more slowly. Only 70 –80 percent of their color was removed after 7 days treatment. Dyes which had no functional groups on the benzene ring, such as Acid Orange 10 and Acid Orange 12, had relatively high decolorization levels, though they had less color removal in the first three days. In the first three days, less than 40 percent of their color was removed; however, more than 87 percent of color were removed after 7 days treatment.

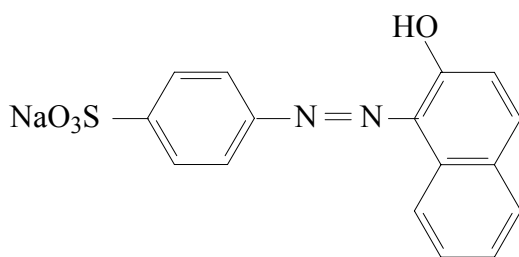
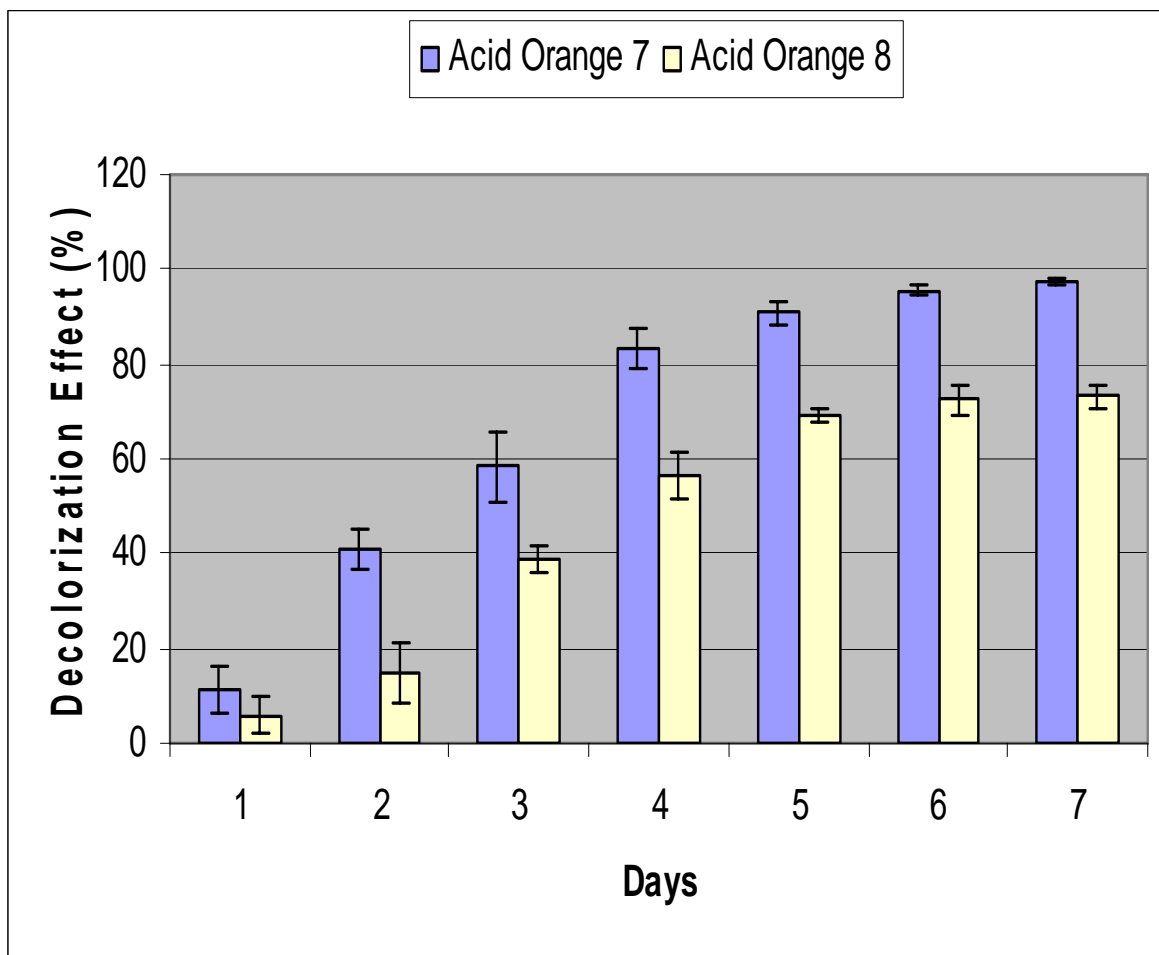


Mordant Violet 5

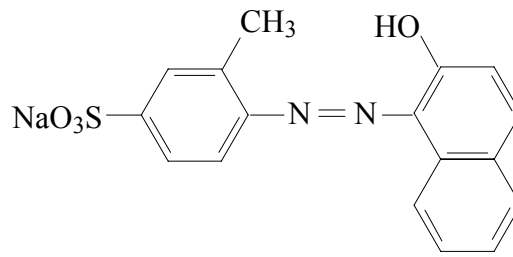


Acid Orange 7

Figure 4. 6 Comparison of Chemical Structure and Decolorization Effect for Mordant Violet 5 and Acid Orange 7

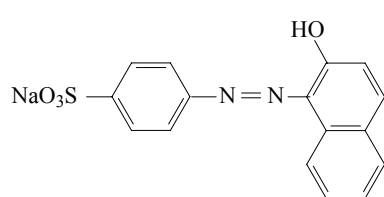
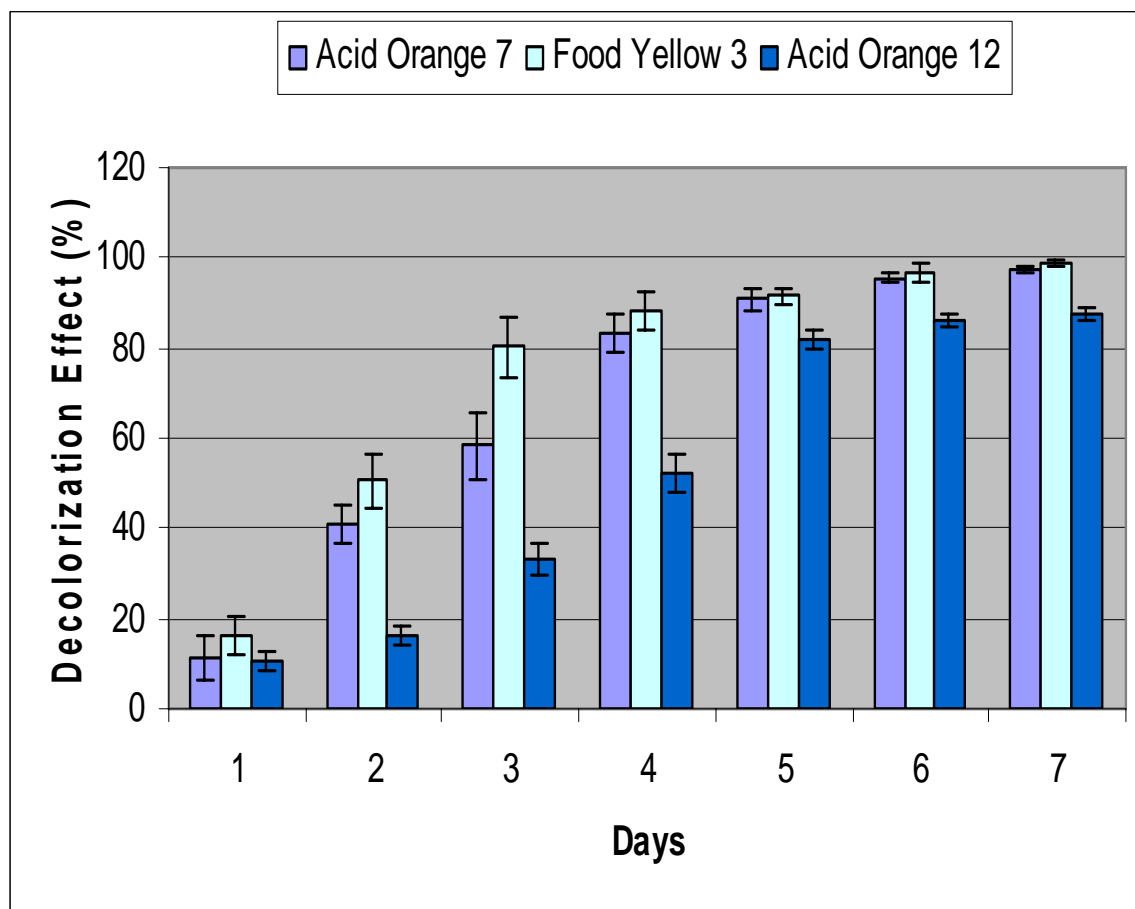


Acid Orange 7

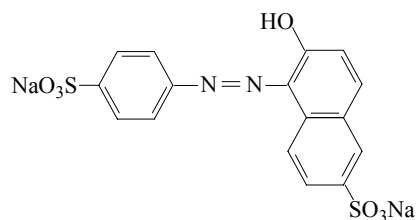


Acid Orange 8

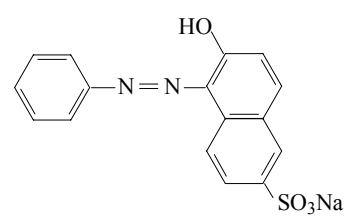
Figure 4. 7 Comparison of Chemical Structure and Decolorization Effect for Acid Orange 7 and Acid Orange 8



Acid Orange 7

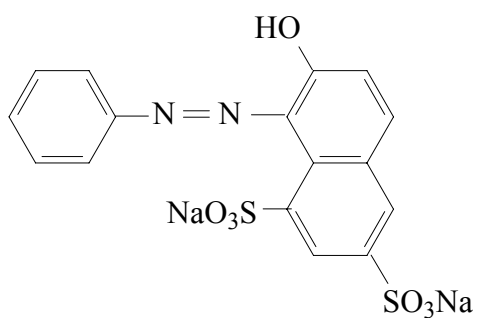
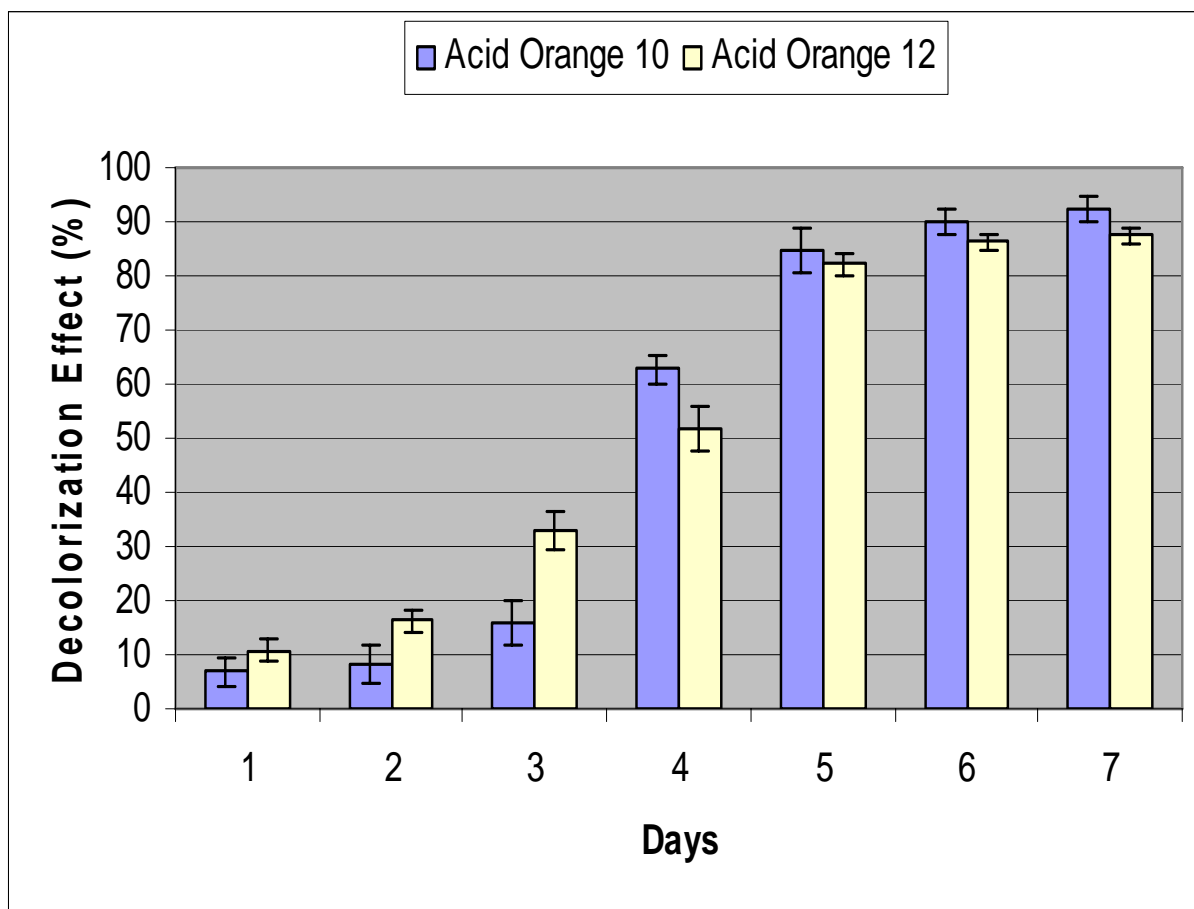


Food Yellow 3

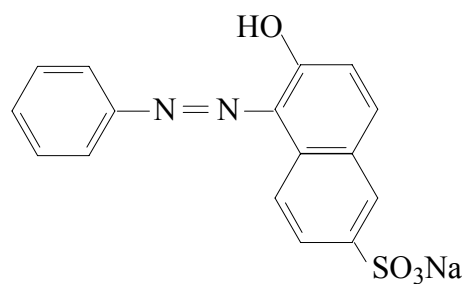


Acid Orange 12

Figure 4. 8 Comparison of Chemical Structure and Decolorization Effect Among Acid Orange 7, Food Yellow 3, and Acid Orange 12



Acid Orange 10



Acid Orange 12

Figure 4. 9 Comparison of Chemical Structure and Decolorization Effect for Acid Orange 10 and Acid Orange 12

4.3 Effect of Solubility Parameters of Dyes

The solubility of dyes affects their decolorization. Due to the existence of SO_3^- groups, acid dyes are more soluble than some other dyes. After calculating the solubility parameter of dyes by Fedors method (Fedors, 1974), we found that the factor which affects decolorization is not only the solubility parameter of dyes but the difference in solubility parameter of the molecular components connecting azo bonds. The term $\Delta \delta \text{ (cal/cm)}^{1/2}$ stands for the difference in solubility parameters of molecular components connected by azo bonds (see compound A and B in Figure 4.10). The detailed calculation of the $\Delta \delta \text{ (cal/cm)}^{1/2}$ of sulphonated azo dyes is shown in Table 4.2 with Mordant Violet 5 as an example. Based on similar calculations, all other dyes in this study are summarized in Table 4.3. It was realized that the order of decolorization effect of eight dyes in this study were almost the same as the order of $\Delta \delta$. Acid Red 8 had the highest $\Delta \delta$ (6.04) and had the lowest decolorization, whereas Mordant Violet 5 had the lowest $\Delta \delta$ (1.10) and had the highest decolorization. Food Yellow 3 ($\Delta \delta=3.35$), which had the highest decolorization, is a special case with two sulphonic groups. Basically, there is a relationship between $\Delta \delta$ and decolorization. We conclude that the more similar the solubility of the components which are connected to azo bonds, the better the decolorization because the active center of enzyme has ability to attack the azo bond completely. The hydrophilic structure of enzyme may attack the dye from two sides. The azo bond is more easily attacked if both sides are hydrophilic. Food Yellow 3 is the perfect dye which has two hydrophilic sulphonic groups on different aromatic ring thus making its relatively efficiently decolorized.

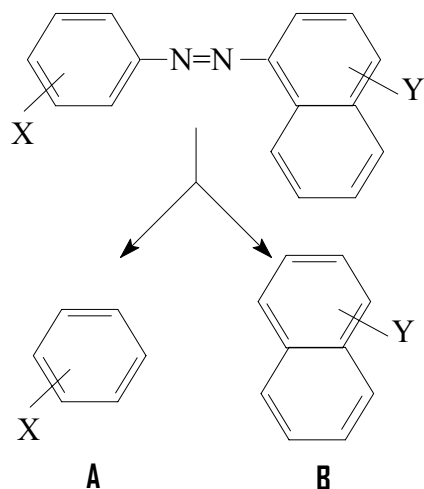


Figure 4.10 The Structure of Compounds A and B, X and Y Stand For the Functional Groups

Table 4.2 The $\Delta \delta$ (cal/cm)^{1/2} Calculation of Mordant Violet 5

<div style="display: flex; justify-content: space-around; align-items: center;"> <div style="text-align: center;"> <chem>NaO3S-c1ccc(O)cc1</chem> </div> <div style="text-align: center;"> <chem>Oc1ccc2ccccc2c1</chem> </div> </div>				
Group	Δe_i , cal/mole	Δv_i , cm/mole	Δe_i , cal/mole	Δv_i , cm/mole
-OH	7120×1	10×1	7120×1	10×1
-SO ₃ ⁻	4500×1	27.6×1		
-CH=	1030×4	13.5×4	1030×7	13.5×7
>C=	1030×2	-5.5×2	1030×3	-5.5×3
6-membered ring	250×1	16×1	250×2	16×2
Conjugated double bonds	400×3	-2.2×3	400×5	-2.2×5
Σ	19250	90	19920	109
$\delta = (\Delta e_i / \Delta v_i)^{1/2}$	14.62		13.51	
$\Delta \delta$	1.11			

Table 4.3 The $\Delta \delta \text{ (cal/cm)}^{1/2}$ of Sulphonated Phenylazonaphthol Dyes from the Highest to the Lowest

Dye	$\Delta \delta \text{ (cal/cm)}^{1/2} *$	Decolorization Ranking
Acid Red 8	6.04	8
Acid Orange 8	5.71	7
Acid Red 4	5.24	6
Acid Orange 12	5.22	5
Acid Orange 10	5.07	4
Food Yellow 3	3.35	2
Acid Orange 7	2.45	3
Mordant Violet 5	1.10	1

* The term $\Delta \delta \text{ (cal/cm)}^{1/2}$ stands for the difference in solubility parameters of the components that are connected to the azo bonds.

4.4 Enzyme Assay

The effect of agitation on dye decolorization was discussed in the beginning of Chapter 4. The results show that agitation was essential for the decolorization of dyes. The fact that decolorization with agitation was better than without agitation could be due to the improved mass transfer and increased oxygen concentration in the culture.

Ha et al. (2001) investigated the effect of agitation on growth of fungal pellets and the production of MnP and laccase. It was found that agitation was essential to produce MnP because of the need for increased oxygen concentration in the culture. However, agitation did not influence laccase production very much. Eichlerova et al. (2005) found that the effect of agitation on decolorization was dependent not only on fungal species and enzymes but also on dye types. Therefore, the effect of agitation on decolorization is not a simple one. The fungal species and target dyes also must be considered. A study on *Phanerochaete chrysosporium* indicated that during lignin degradation, the lignin had to bind to the fungal wall for effective degradation (Kirk and Farrell, 1987). If decolorization of dyes also requires such binding, agitation can likely increase such binding to give better decolorization efficiency.

In our study, the cultures were incubated and shaken at 150 rpm for 3 days to achieve the formation of uniform pellets, which was considered to be very important in *Pleurotus ostreatus* enzyme production (Ha et al., 2001). Then, an enzyme assay was conducted including enzyme concentration and enzyme activity assays.

4.4.1 Protein Concentration Assay

The protein assay, based on the method of Bradford (Bradford, 1976), a dye-binding assay in which a differential color change of a dye occurs in response to various concentrations of protein, was used to measure the concentration of enzymes. This method is a simple and accurate procedure for determining the concentration of solubilized protein. The absorbance

maximum for an acidic solution of Coomassie® Brilliant Blue G-250 dye shifts from 465 nm to 595 nm when binding to protein occurs. The blue dye binds primarily to basic and aromatic amino acid residues. Spector (Spector, 1978) found that the extinction coefficient of a dye-albumin complex solution was constant over a 10-fold concentration range. Thus, Beer's law may be applied for accurate quantitation of protein by selecting an appropriate ratio of dye volume to sample concentration. Interferences may be caused by chemical-protein and/or chemical-dye interactions. However, proteins such as bovine serum albumin and gamma globulin show little or no interference. In this study, bovine serum albumin (BSA) was used as a standard.

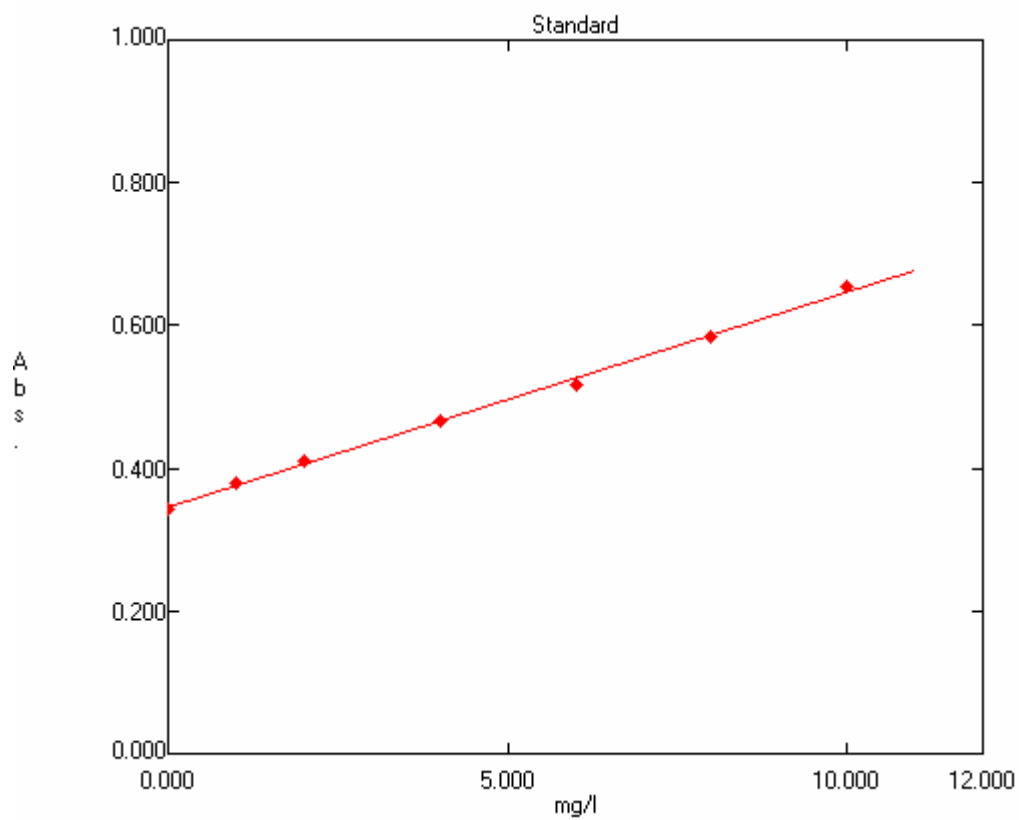
Figure 4.11 is the BSA standard working curve we used in this study. The Chi-Square value of 0.00035 means that this linear model fits the data very well. The spectrometric absorption of the culture with *Pleurotus ostreatus* was measured and the corresponding concentrations were calculated according to the working curve.

Protein concentration of culture with and without agitation was measured using Bradford method and is shown in Figure 4.12. The sampling was taken on the first, the third, and the seventh day due to limited capacity of shakers and the amount of culture aliquot. The protein concentration of the culture with agitation was constant from the first day to the seventh day with little deviation, while the protein concentration of the culture without agitation continued to increase. When we observed the growth of the fungus, we found that the viscosity of the sample with agitation was significantly less than that without agitation and that there was a mass of liquid gel on the surface of the sample without agitation. The gel may restrict or limit the consumption of oxygen. This result suggests that *Pleurotus ostreatus* may favor an anaerobic condition for protein production. This assumption will be evaluated in the future experiments.

4.4.2 Enzyme Activity

Table 4.4 shows the enzyme activity in the culture with agitation. All three ligninolytic enzymes, including LiP, MnP, and laccase, were detected. MnP and Laccase are two major enzymes in the culture of *Pleurotus ostreatus*. Since these bio-parameters were measured after seven days of decolorization, they may not reflect the actual changes of bio-parameters during the whole period.

Wesenberg et al. (2003) proved that *Pleurotus ostreatus* is not capable of producing LiP. Since both the newly discovered versatile peroxidase (VP) (Martinez et al., 1996) and veratryl alcohol oxidase (VAO) (Sannia et al., 1991) could likely take veratryl alcohol as their substrate even without hydrogen peroxide, the activity detected using the method of oxidation of veratryl alcohol does not definitely mean that LiP was produced by the culture of *Pleurotus ostreatus*. Lu (Lu, 2006) states in his dissertation that the detected LiP activity was possibly due to the existence of VP or VAO and the interference from laccase in the *Pleurotus ostreatus* cultures. He found the 16 u/l activity towards veratryl alcohol without the presence of hydrogen peroxide (Lu, 2006). The results above illustrate the complexity of ligninolytic fungal degradation systems. The ligninolytic enzymes are not the only factors involved. Many other factors, such as mediators, hydrogen peroxide, and oxygen concentration, all play very important roles in such decolorization systems. Experiments were also carried out to isolate the enzymes from the crude decolorization cultures by using fast protein liquid chromatography (FPLC) and sodium dodecyl sulfate polyacrylamide gel electrophoresis (SDS-PAGE). However, such experiments did not produce satisfactory results.



Concentration = K1 A +K0
K1=33.18
K0=-11.47
Chi-Square: 0.00035

Figure 4.11 BSA Standard Working Curve

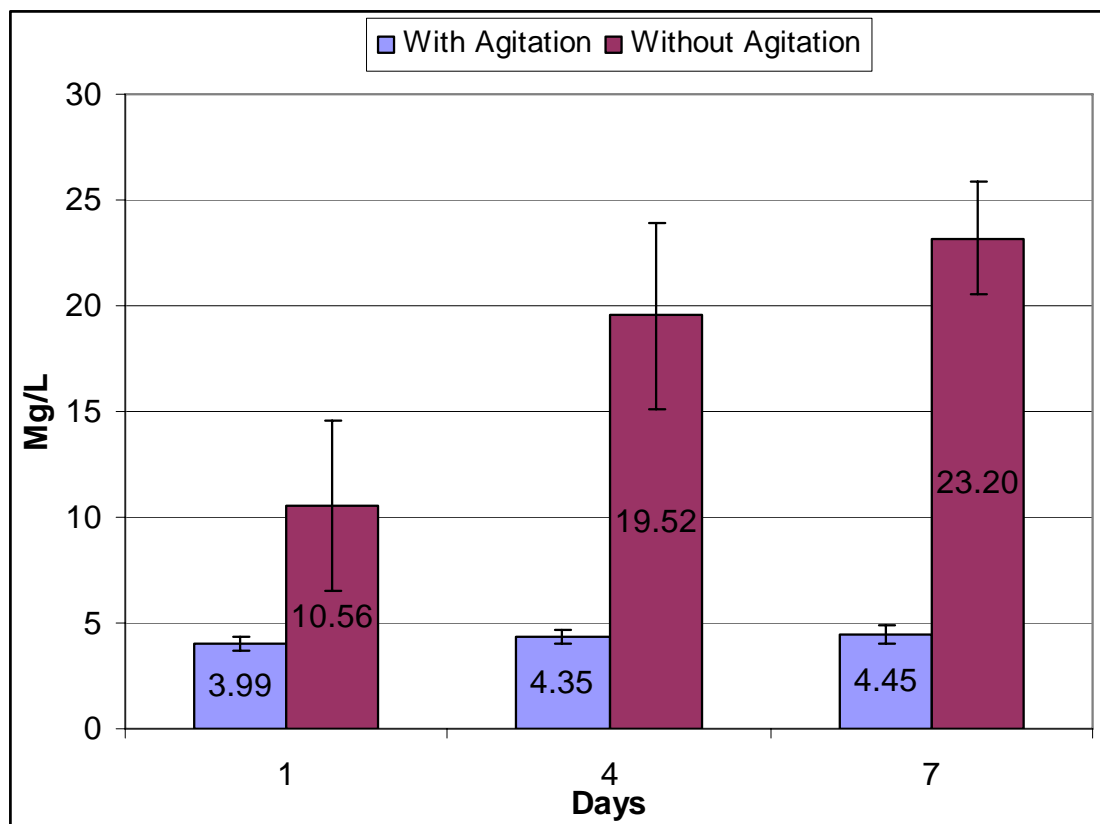


Figure 4.12 Protein Concentration of Culture With and Without Agitation

Table 4.4 Bio-Parameters of Culture after Seven Days Incubation

Bio-parameters	
Protein Concentration (mg/L)	4.45 ± 0.4
LiP Activity (U/L)	12.5 ± 0.9
MnP Activity (U/L)	47.1 ± 6.3
Laccase Activity (U/L)	50.4 ± 3.3

4.5 Conclusions about Decolorization of Sulphonated Phenylazonaphthol Dyes

Because of the different molecular structures of the dyes, the decolorization efficiency ranged from 70 percent to 90 percent after 7 days treatment. Dyes with electron withdrawing group(s) on the benzene ring degraded quickly and had relatively high decolorization. Dyes with electron donating group(s) on the benzene ring had relatively lower decolorization. Dyes without functional groups on the benzene ring had relatively high decolorization even though they were less affected in the first three days. Not only the total solubility of dyes, but also the difference in solubility parameters of molecular units connected by the azo bonds affects the decolorization. The more similar the solubility of the units connected by the azo bonds, the better the decolorization because the active center of enzyme has ability to attack the azo bond completely. Both MnP and laccase were detected in the culture system, but ligninolytic enzymes are not the only factor involved. Many other factors, such as mediators, hydrogen peroxide, and oxygen concentration all play very important roles in such decolorization system.

CHAPTER 5

SEPARATION AND IDENTIFICATION OF DYE DEGRADATION PRODUCTS

5.1 HPLC Analysis of Degradation Products

High performance liquid chromatography (HPLC) was chosen to analyze products from the commercial azo dyes in this study because of its accuracy, high separation efficiency and relatively simple sample preparation. The supernatant culture liquid sample contained background interferences such as nutrients and fungal cells but did not greatly complicate HPLC chromatography after filtration. The culture supernatant used in the HPLC analysis contains various organic compounds with different polarities. To separate the degradation products with the best resolution and highest sensitivity, the column to be used in analysis, composition of mobile phase, pH value, and running temperature were optimized (Zhao, 2004). A stainless steel Ultracarb ODS column with 5 μm packing from Phenomenex (150 \times 4.6 mm I. D.) was chosen as the analytical column and a RP-C18 guard pre-column was used to protect the analytical column. Acetonitrile was used as organic modifier for the mobile phase throughout the analysis. The HPLC separations used an isocratic gradient of 20 percent acetonitrile and 80 percent water. The detailed procedure for HPLC was given in Chapter 3.

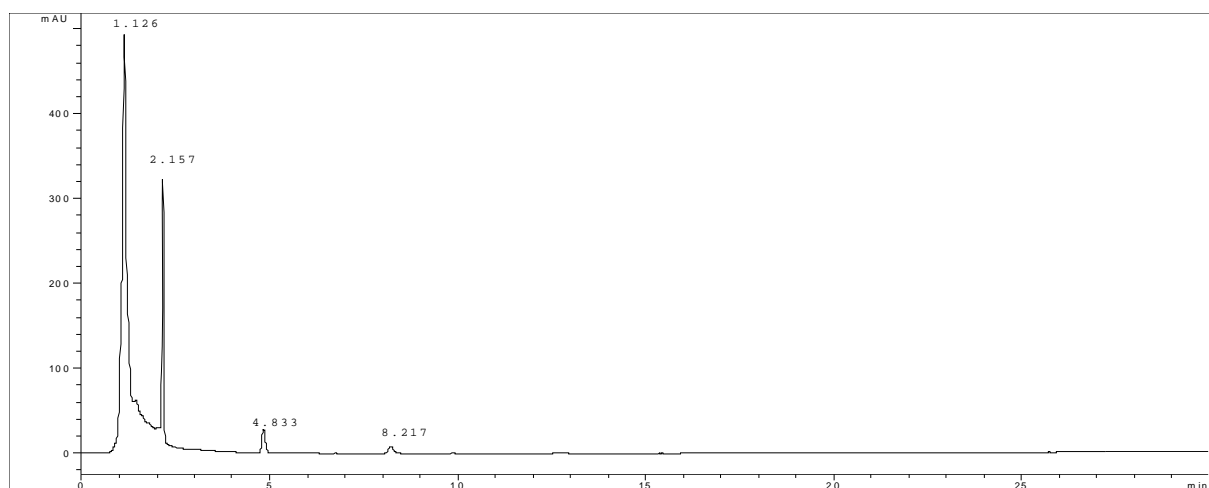
5.1.1 Identification of Products from Control Sample by HPLC

The HPLC spectra of the culture solution with Kirk's medium and *Pleurotus ostreatus* in the first day are shown in Figure 5.1 (curve A). The compounds with retention times of 1.126 min and 2.157 min are glucose and an unknown organic acid. The corresponding UV-vis spectra are

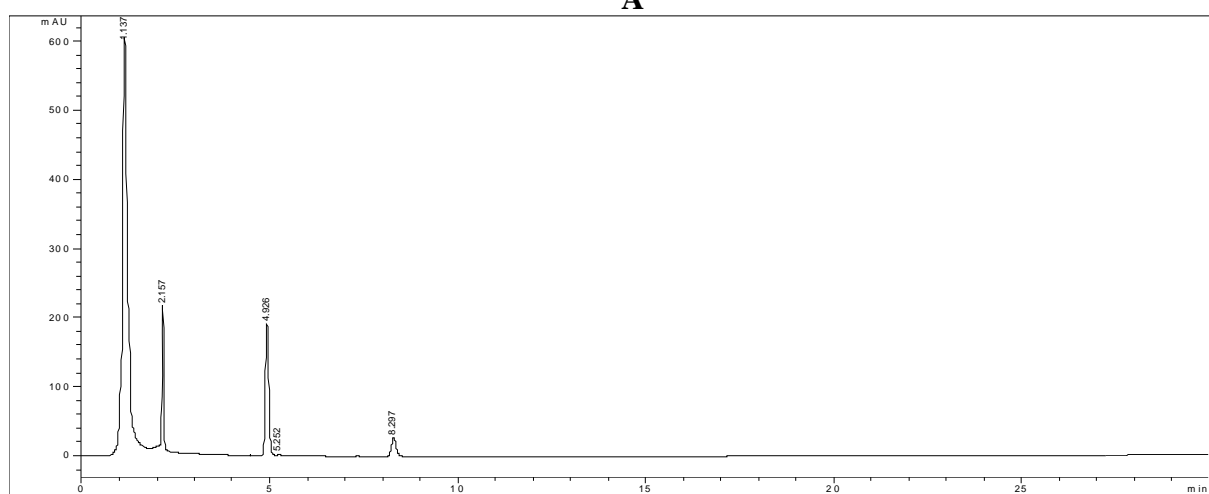
shown in Figure 5.2 (curves A and B). The compounds with retention times of 4.833 min and 8.212 min in Figure 5.1 (curve A) were identified as veratryl alcohol and veratraldehyde with their UV spectra in Figure 5.2 (curve C and D). The production of veratryl alcohol increased with incubation time while the amount of veratraldehyde stayed constant throughout incubation (Figure 5.1). In this study, the isolated compounds were compared with the retention time and UV-vis spectra with standard samples. Veratryl alcohol is crucial in the lignin peroxidase cycle during oxidations of azo dyes by helping to complete the catalytic cycle of LiP. Veratryl alcohol acts as a third substrate (with hydrogen peroxide and azo dyes) in the reaction (Paszcinski and Crawford, 1991). Veratryl alcohol can be oxidized to veratraldehyde by enzymes. Based on the identification of compounds in the control, during the investigation of dye degradation products, only the products from dye degradation solution were considered to be the possible degradation products.

5.1.2 Mechanism Study of Fungal Degradation of Mordant Violet 5

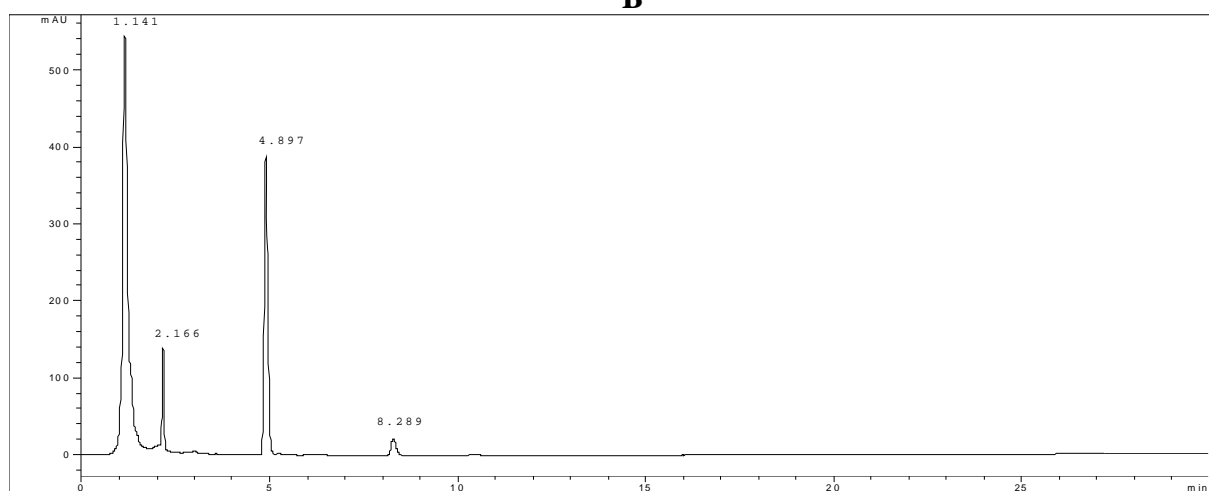
The biodegradation of aromatic pollutants is a complex process of oxidation, reduction, methylation and hydroxylation (Mester and Tien, 2000). Thus, the biodegradation of azo dyes is complicated and consists of a mixture of these reactions. Several standard samples which could be possible degradation products, including 2-naphthol, 1, 2-naphthalenediol, 1, 2-naphthoquinone, 1-amino-2-naphthol, benzenesulfonic acid, and 4-hydroxybenzenesulfonic acid, were selected based on analysis of the structure of the original azo dyes. Even though some of the degradation products have been separated and identified, there were still many unknown compounds due to lack of standards for comparison.



A



B



C

Figure 5.1 HPLC Analysis of the Control Sample with Supernatant Fluid A: the First Day; B: the Second Day; C: the Third Day.

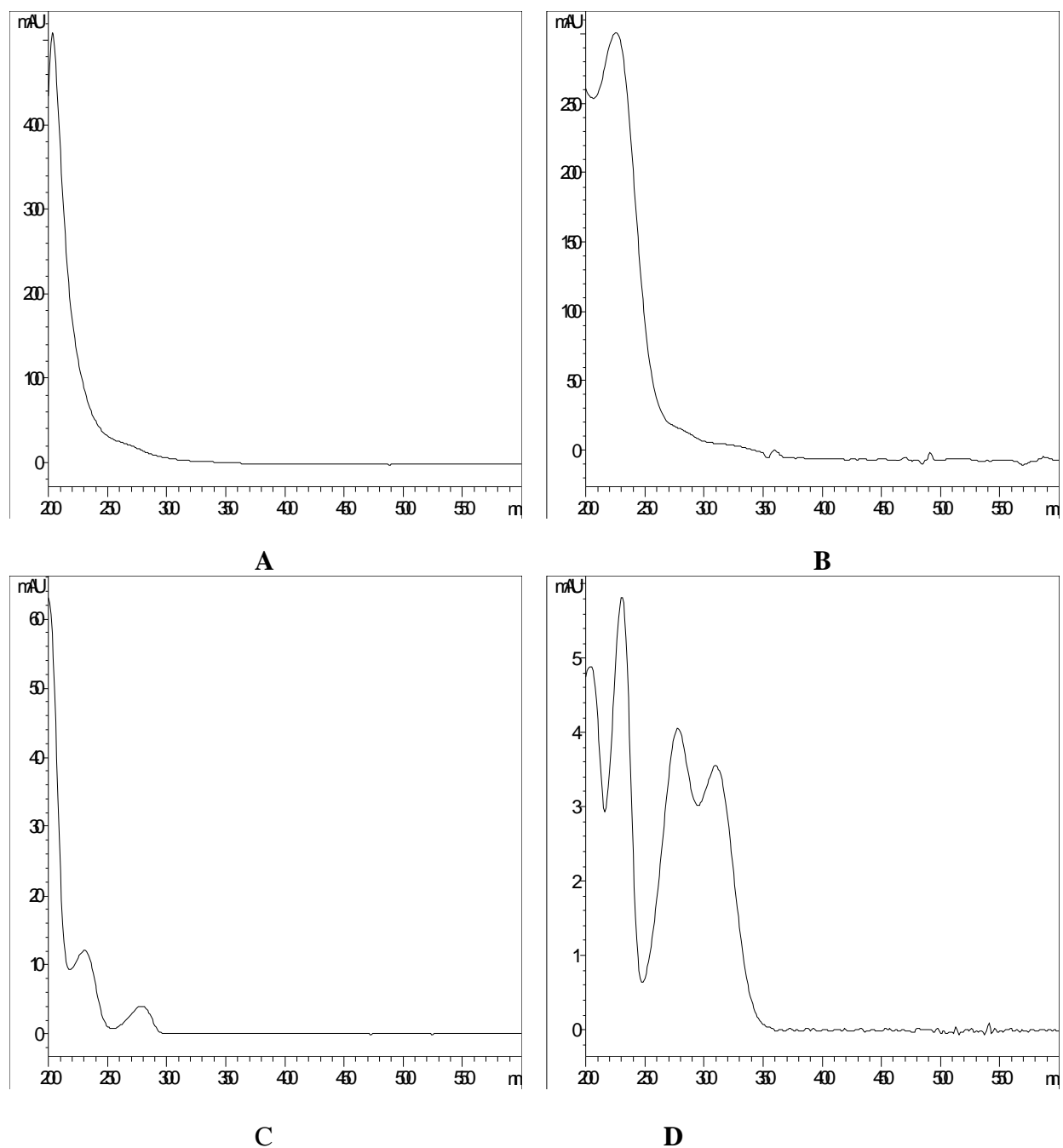


Figure 5.2 UV-Vis Spectra for Control Sample A: Compound at Retention Time 1.126 min - Glucose; B: Compound at Retention Time 2.157 min - An unknown organic acid; C: Compound at Retention Time 4.833 min - Veratryl alcohol; D: Compound at Retention Time 8.217 min - Veratraldehyde

Figure 5.3 is the HPLC spectrum of Mordant Violet 5 degraded by *Pleurotus ostreatus* in the first day. Besides the compounds which were in the control sample, there was only dye itself at the retention time of 5.31 min. There was no impurity in the dye sample. The corresponding UV-vis spectrum is shown in Figure 5.4. The strong absorption of the dye at 520 nm means the existence of a color producing structure. After one day treatment with the fungus, retention time specific by dye disappeared, and a peak appeared at the retention time of 3.916 min. The corresponding UV-vis spectrum showed there was no absorption in the visible region (Figure 5.5 and 5.6), thus suggesting that the azo bond of the dye structure was changed and a new structure was formed. In Figure 5.5, a new degradation product appeared at the retention time of 8.87 min, and was confirmed to be 1, 2-naphthoquinone (CAS#: 524-42-5) by comparing the standard compound with both the retention time and the UV-vis spectrum. The 1, 2-naphthoquinone compound disappeared in the third day's treatment, suggesting that further degradation occurred. Veratryl alcohol was after day 2 treatment and continued to be present. Moreover, the amount of veratryl alcohol was higher than any other compounds in the mixture. There was no veratraldehyde in the solution from the first day to the seventh day.

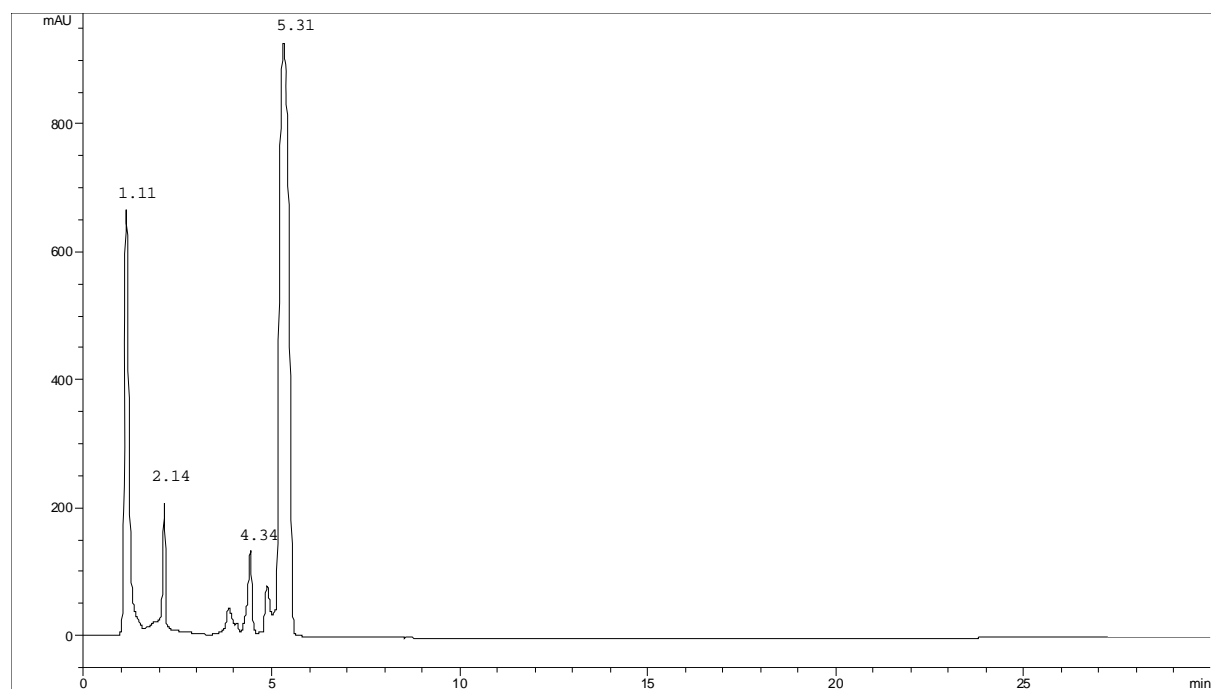


Figure 5.3 HPLC Analysis of the Mordant Violet 5 Degradation Products after Treatment by *Pleurotus ostreatus* (First Day).

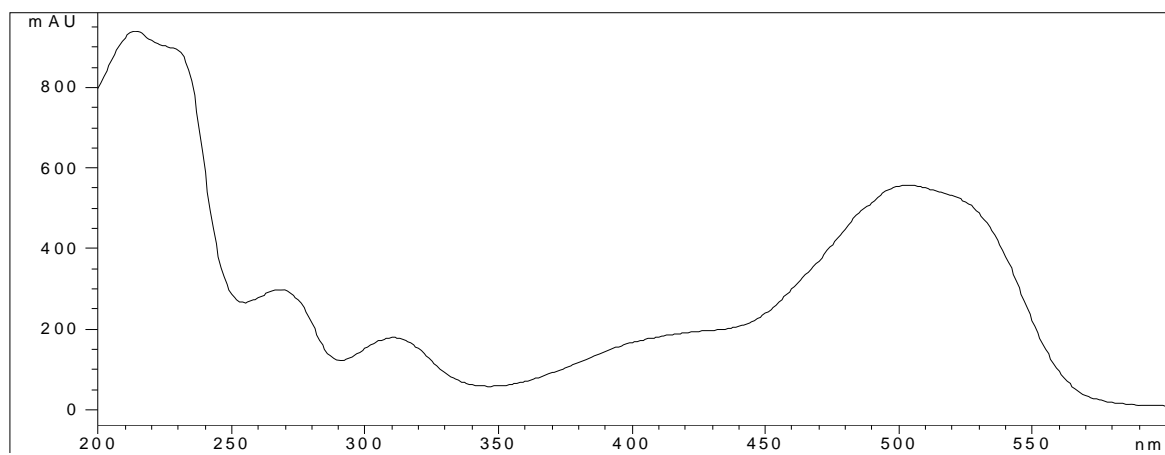


Figure 5.4 The UV-Vis Spectrum of Compound at Retention Time 5.31 min - Mordant Violet 5

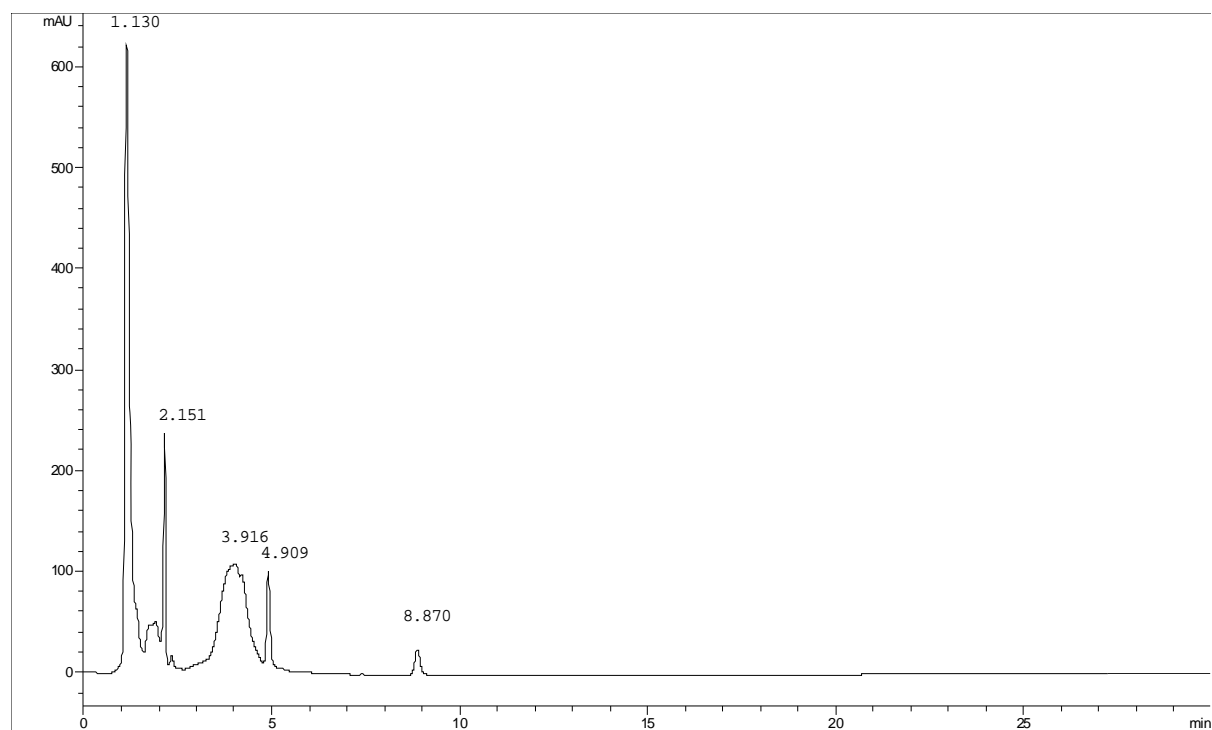


Figure 5.5 HPLC Analysis of the Mordant Violet 5 Degradation Products after Treatment by *Pleurotus ostreatus* (Second Day).

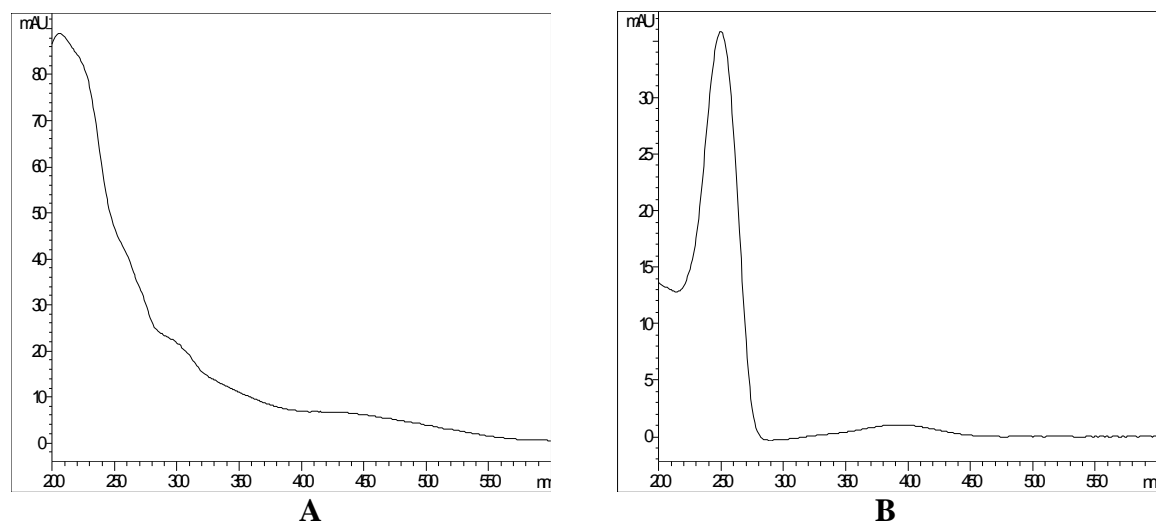


Figure 5.6 UV-Vis Spectrum of Mordant Violet 5 Degradation Products A: Compound at Retention Time 3.916 min - Unknown product; B: Compound at Retention Time 8.870 min - 1,2-naphthoquinone

5.1.3 Mechanism Study of Fungal Degradation of Acid Orange 8

Figure 5.7 is the HPLC spectrum of Acid Orange 8 degraded by *Pleurotus ostreatus* in the first day. The retention time of 5.150 min was assigned to Acid Orange 8 whose UV-vis spectrum is shown in Figure 5.8. The maximum absorption is at 552 nm. After one day treatment with fungus (as with Mordant Violet 5) 1, 2-naphthoquinone was isolated at the retention time of 8.282 min (see Figure 5.9). The 1, 2-naphthoquinone disappeared after the third day's treatment suggesting that further degradation occurred. Veratraldehyde was separated and identified in the five day's treatment sample, but at a lower amount than veratryl alcohol.

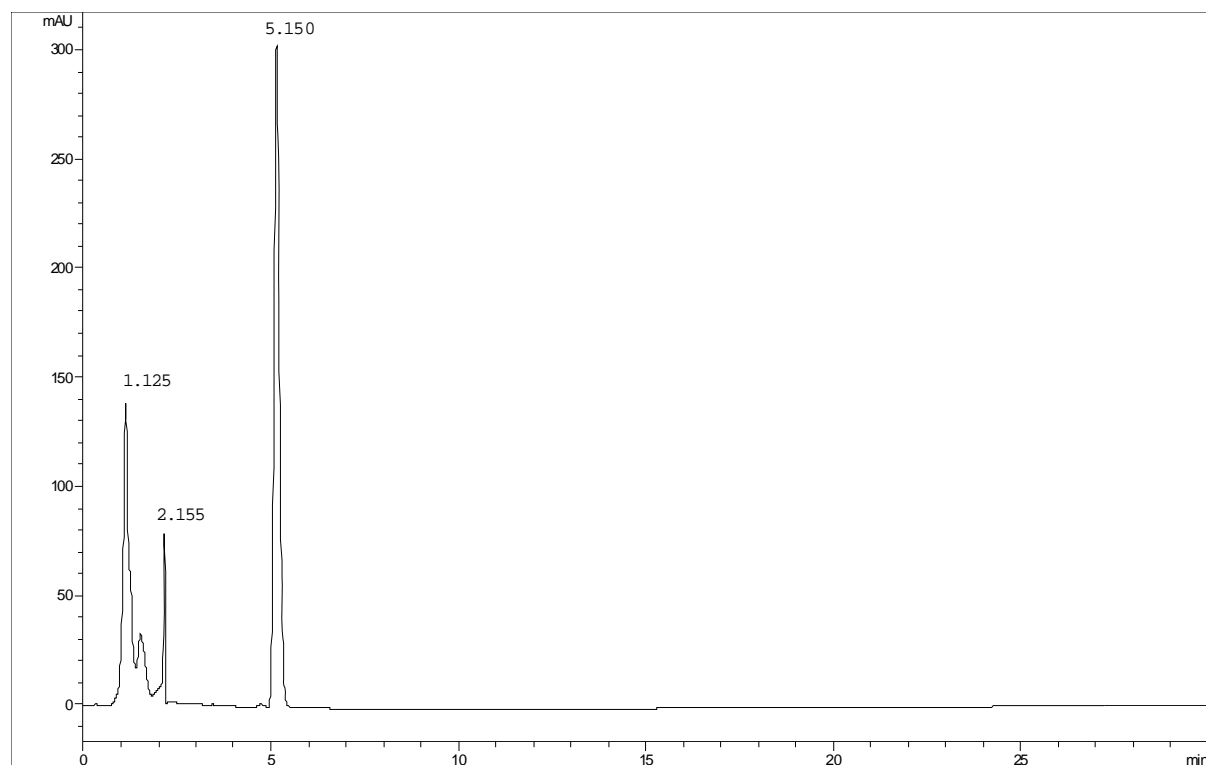


Figure 5.7 HPLC Analysis of the Acid Orange 8 Degradation Products after Treatment by *Pleurotus ostreatus* (First Day).

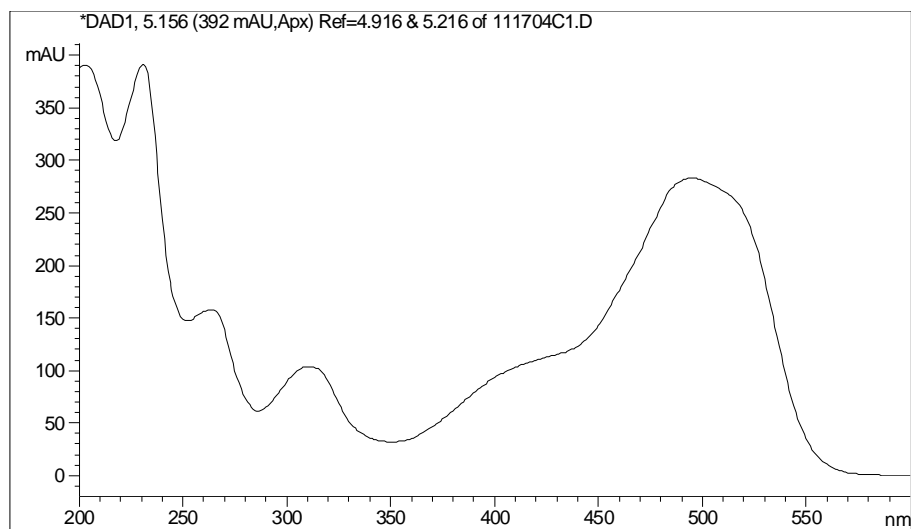


Figure 5.8 The UV-Vis Spectrum of Compound at Retention Time 5.150 min - Acid Orange 8

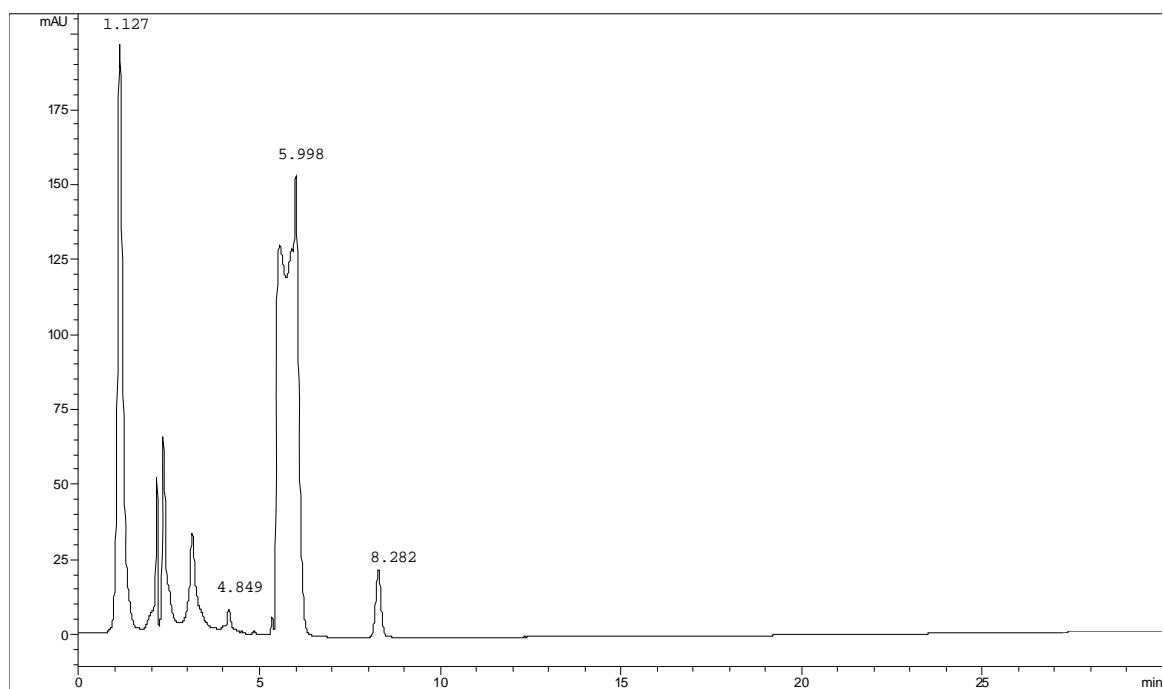


Figure 5.9 HPLC Analysis of the Acid Orange 8 Degradation Products after Treatment by *Pleurotus ostreatus* (Second Day).

5.1.4 Mechanism Study of Fungal Degradation of Acid Orange 7

The HPLC spectrum of Acid Orange 7 degraded by white rot fungus *Pleurotus ostreatus* is similar to that of Acid Orange 8. Only the dye was present in the first day sample. The UV-vis spectrum is shown in Figure 5.10. In the second days' treatment, 1, 2-naphthoquinone was isolated at the retention time of 8.280 min. Another very important compound was separated in the fifth day's treatment sample with retention time of 12.542 min (Figure 5.11) which was identified as benzenesulfonic acid (CAS#: 98-11-3) by comparing both the retention time and the UV-vis spectrum at the 99 percent probability. Benzenesulfonic acid existed in the solution from the onset of the experiment, suggesting that there was no further degradation reaction involved. In Figure 5.12, the compound at retention time of 8.127 min is veratryl alcohol, while other two peaks at retention times of 18.524 and 28.076 min were unknown compounds. There is also a tiny peak at retention time of 10.165 min. By comparing the standards, we confirmed that it is 4-hydroxybenzenesulfonic acid (CAS#: 98-67-9). The existence of benzenesulfonic acid and 4-hydroxybenzenesulfonic acid were also confirmed using the CE-MS method discussed in the following section.

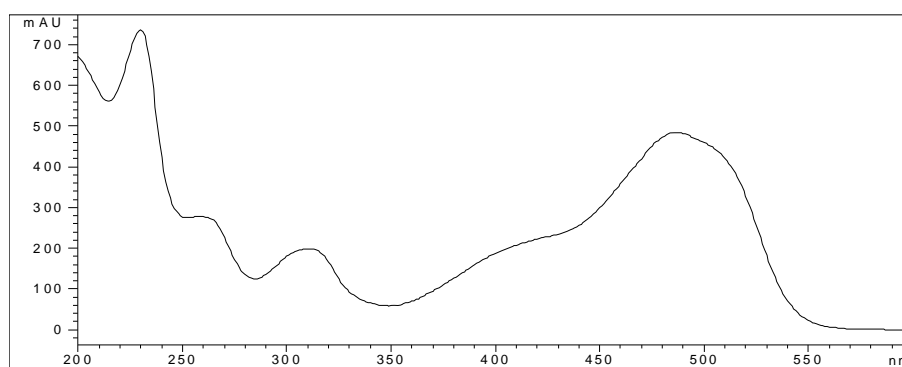


Figure 5.10 The UV-Vis Spectrum of Acid Orange 7

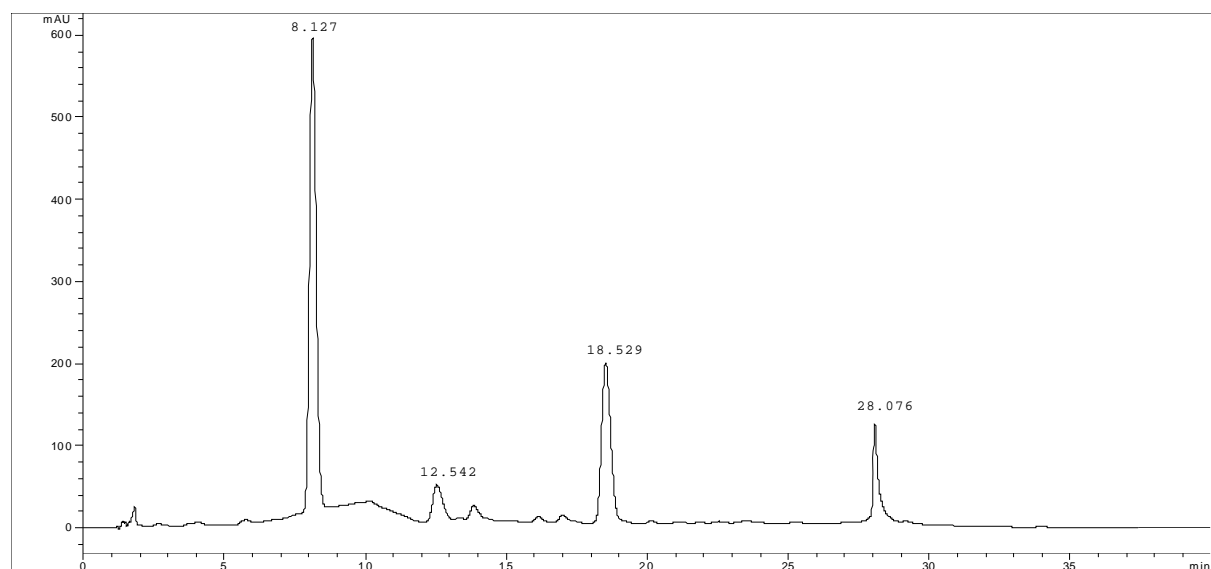


Figure 5.11 HPLC Analysis of Acid Orange 7 Degradation Products after Treatment by *Pleurotus ostreatus* (Fifth Day).

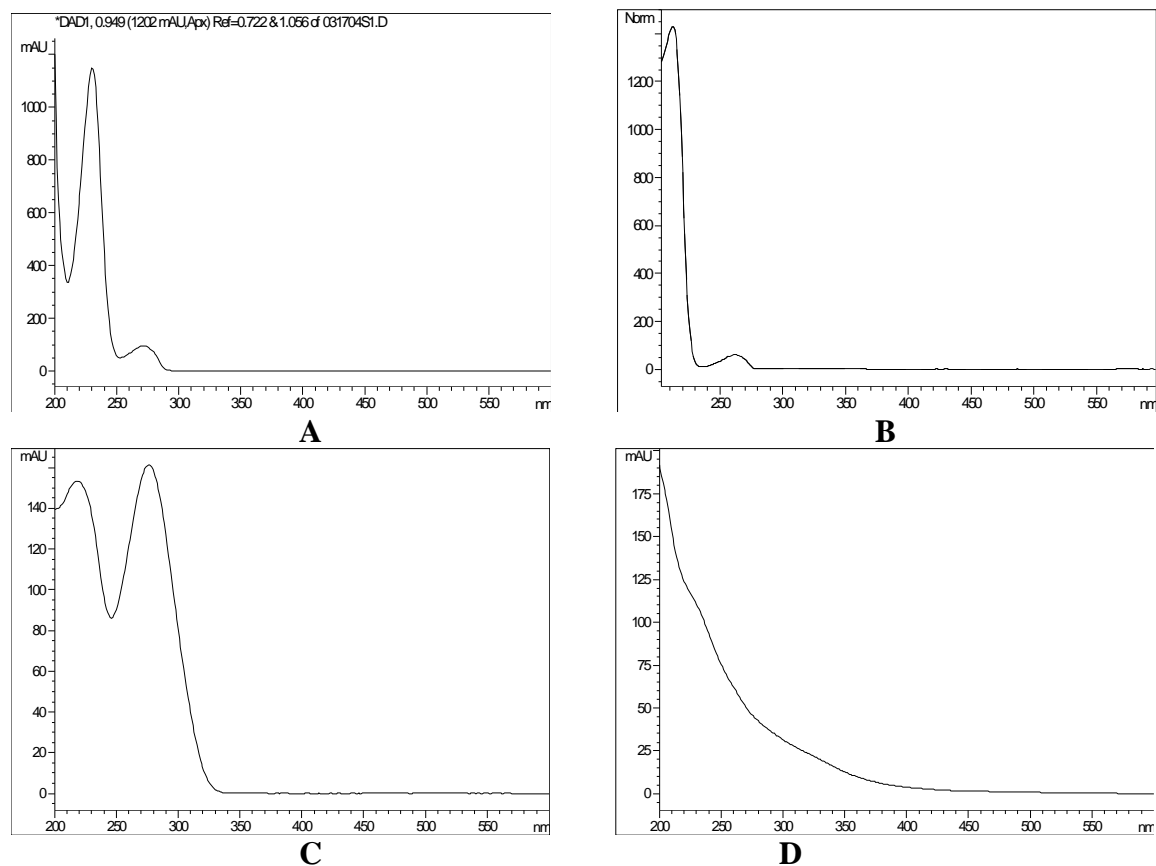


Figure 5.12 UV-Vis Spectra of Acid Orange 7 Degradation Products A: Compound at Retention Time 10.169 min - 4-hydroxybenzenesulfonic acid; B: Compound at Retention Time 12.542 min - Benzenesulfonic acid C: Compound at Retention Time 18.529 min - unknown; D: Compound at Retention Time 28.078 min - Unknown

5.1.5 Other Dyes

The HPLC spectra of degradation products from Acid Orange 12, Food Yellow 3, Acid Red 4, and Acid Red 8 were very complicated. The only degradation product that could be identified was from the Food Yellow 3 degradation solution in the third day. Figure 5.13 shows that the UV spectrum of the degradation product at retention time of 14.596 from Food Yellow 3 is almost the same as the benzenesulfonic acid standard (CAS#: 98-11-3). We confirmed that it is benzenesulfonic acid by comparison with the standard both the retention time and the UV-vis spectrum. Even though HPLC supplied important information which could be used to propose the possible degradation mechanism, most separation peaks could not be assigned due to a lack of standards. In order to further understand the degradation mechanism, capillary electrophoresis combined with electrospray ionization mass spectrometry (CE-ESI-MS) was used to separate and identify degradation products. Mass spectrometry can create important information such as molecular ion and fragmentation ions, and thus more possible degradation products may be identified.

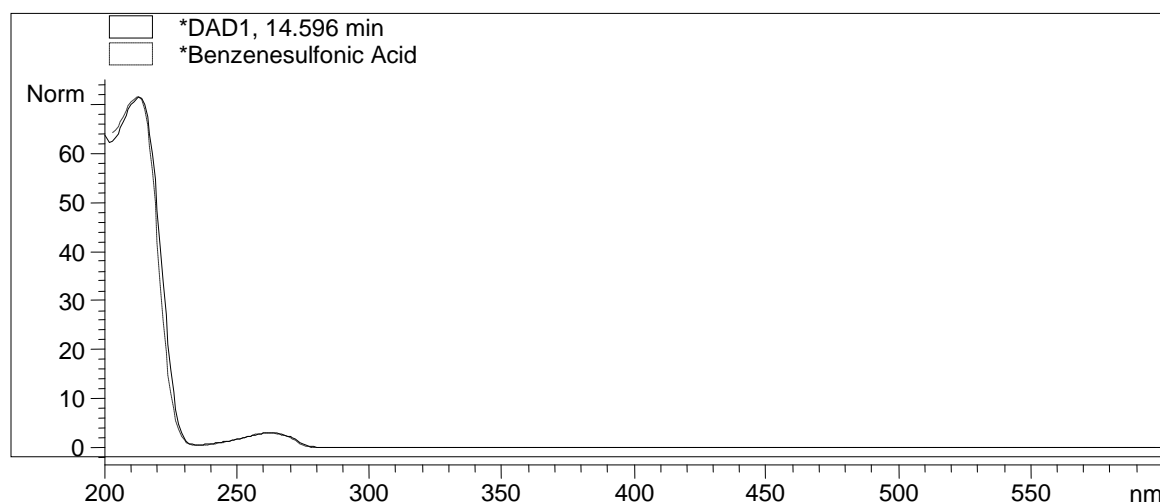


Figure 5.13 Comparing of the UV-Vis Spectrum of the Compound at Retention Time 14.596 min from Food Yellow 3 Degraded by *Pleurotus ostreatus* (Third Day) with that of the Benzenesulfonic Acid Standard

5.2 CE-ESI-MS Analysis of Degradation Products

In order to investigate the degradation products and propose the possible degradation pathway, the separation method employing a mass spectrometer was used in this study. Due to the high polar property of sulphonic groups, capillary electrophoresis linked to an electrospray mass spectrometer is suitable for identifying the water soluble compounds. Figure 5.14 is a CE-ESI-MS electrophorogram of the control sample which contains only Kirk's medium with *Pleurotus ostreatus* (first day). The base peak chromatogram (BPC) shows better peak shape and signal-to-noise ratio than the total ion chromatogram (TIC). There are several major compounds which were separated by CE with retention times of 4.5 min, 6.9 min, and 11.2 min. The peak with retention time of 4.2 min was identified as glucose. In the negative ion mode electrospray spectrum, the $[M-H]^-$ is seen. The ion at m/z 179 in Figure 5.15 is glucose ($C_6H_{12}O_6$) and peaks of m/z 161, 143, 113, 101, 89 are the fragmentation ions of glucose due to loss of H_2O (-18) and C (-12) or CH_2O (-30). The ion at m/z 359 is equal to two molecules of glucose. The compound with retention time of 6.9 min was identified as phosphoric acid and its derivatives, as shown in Figure 5.16. The ion at m/z 97 is phosphoric acid negative ion $[H_2PO_4]^-$ which comes from the culture medium and the highest proportion of the dimer of phosphoric acid $[H_5P_2O_8]^-$ at the peak of m/z 195. The ions at m/z 177 and 159 are $[H_3P_2O_7]^-$ and $[HP_2O_6]^-$, respectively, due to loss of water. The peaks of m/z 293 and 391 are identified as the trimer and tetramer of phosphoric acid. The ions of m/z 321 and m/z 149 are shown at the retention of 11.2 min in Figure 5.17; however, the structure of the compound is not clearly understood. After several days' incubation, the retention times of the molecular peaks were the same as the first day in the culture solution. From the information above, we can exclude the compounds of glucose, phosphoric acid, and the m/z 321 and m/z 149 from the dye degradation solution.

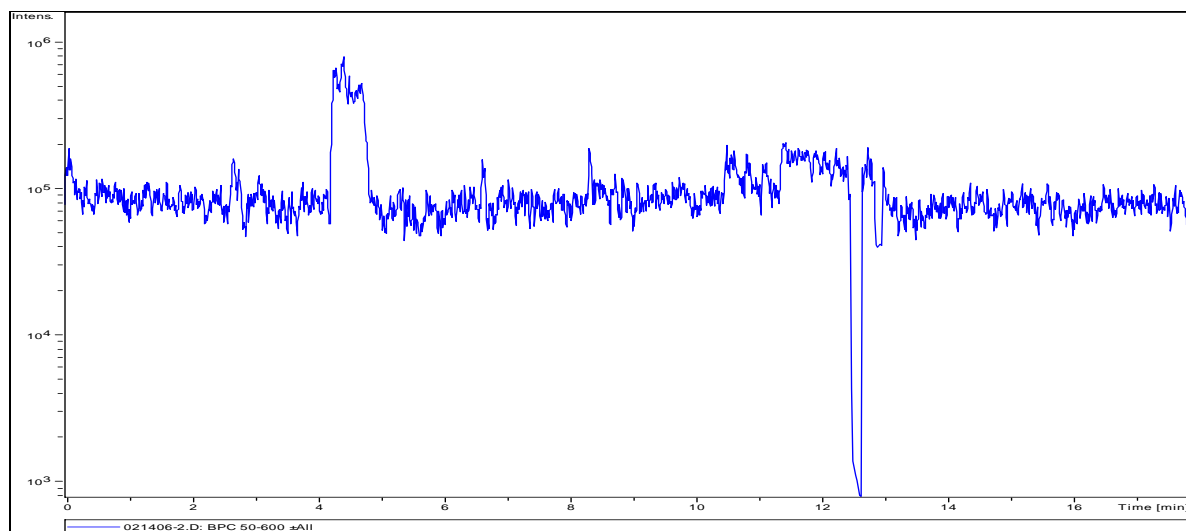


Figure 5.14 CE-ESI-MS Base Peak Chromatogram of Control Sample with only Kirk's Medium and *Pleurotus ostreatus* (First Day).

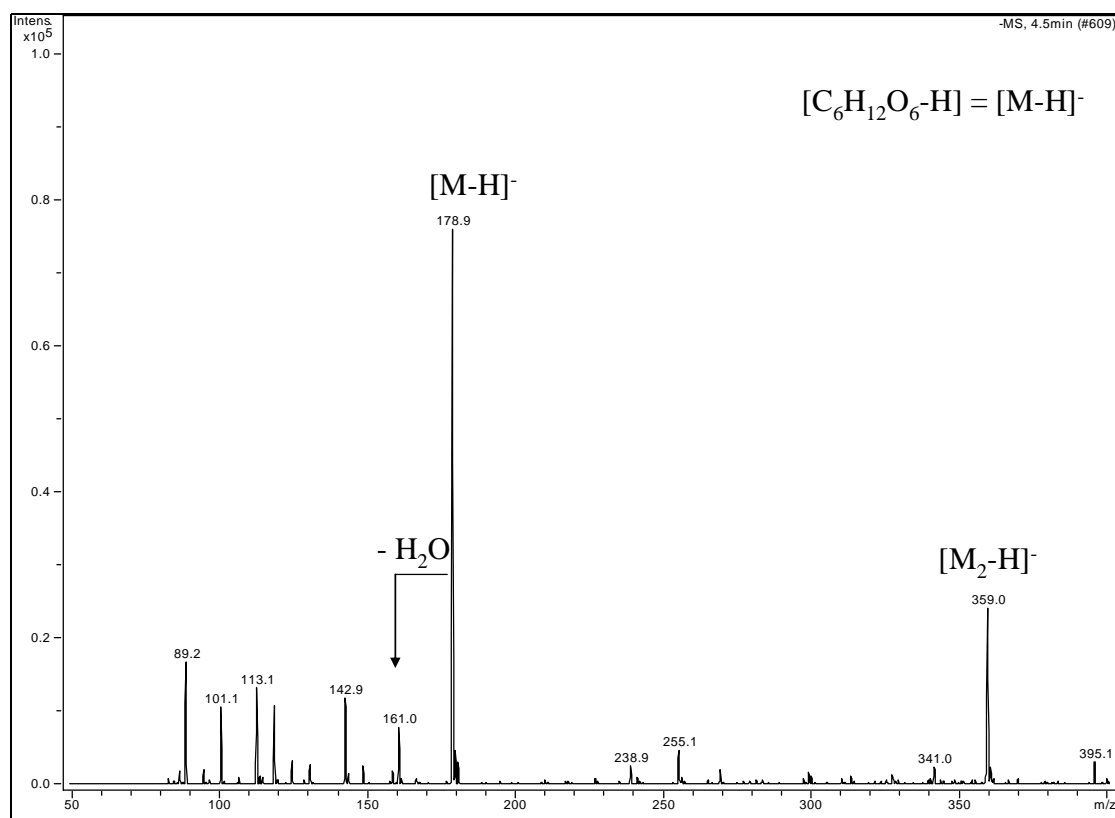


Figure 5.15 Mass Spectrum of Peak with the Retention Time of 4.2 min (Control).

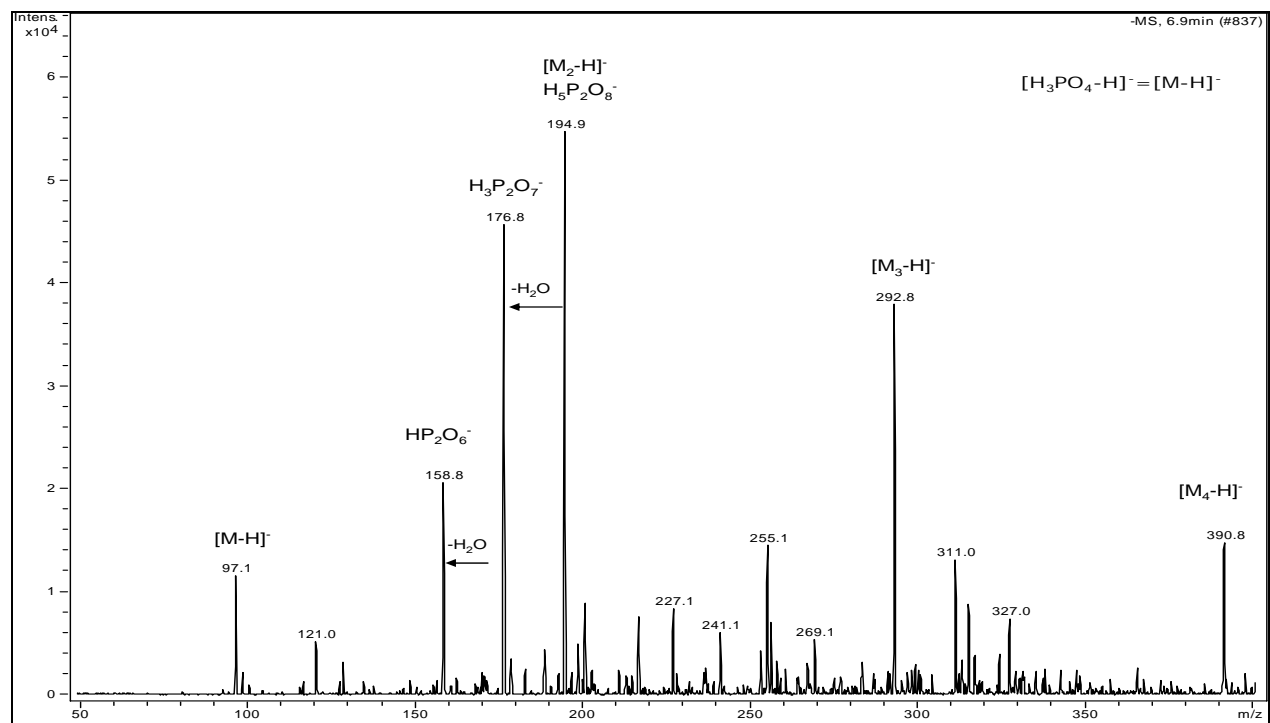


Figure 5.16 Mass Spectrum of Peak with the Retention Time of 6.9 min (Control).

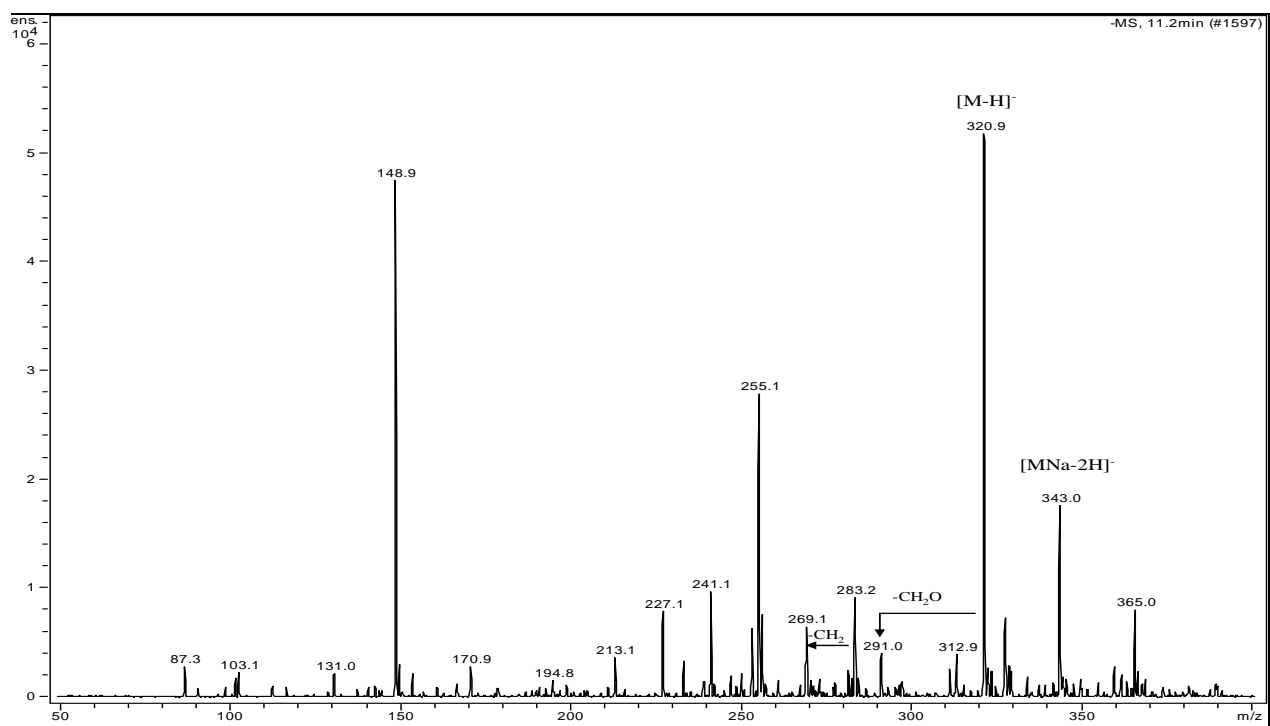


Figure 5.17 Mass Spectrum of Peak with the Retention Time of 11.2 min (Control).

5.2.1 Acid Orange 7

1. Analysis of the Mass Spectrometric Fragmentation of Acid Orange 7

The mass spectrum obtained with the monosulfonated dye Acid Orange 7 exhibited the [M-Na]⁻ peak as the only observed ion (Figure 5.18). Typical fragments, m/z 247, m/z 219, m/z 171, m/z 156, and m/z 107 were observed as a result of fragmentation, as shown in Figure 5.19. The MS^{*n*} fragmentation of ions from m/z 327 is summarized in Table 5.1. The peak at m/z 171 is corresponds to the cleavage of the azo bond. This fragment is an odd electron ion, and its formation from an even electron [M-Na]⁻ ion is due to collision with helium atoms in the ion trap from the ketohydrazone form (B in Scheme 5.1). In the further MS^{*n*} fragmentation spectrum, the loss of 64 Da of m/z 171 leads to the m/z 107 ion. The ion at m/z 156 is identified as benzenesulfonate ion where further fragmentation forms phenol ion due to loss of SO₂. The ion at m/z 247 is formed by loss of SO₂ from dye and the proton rearranges to make a stable structure. The ion at m/z 219 is formed by the MS³ fragmentation of m/z 247 through the loss of CO (28 Da). Richardson (Richardson et. al., 1992) reported that only azo dyes which did not have an *ortho*-hydroxy group and were incapable of forming tautomers lost N₂. The evidence of m/z 219 from m/z 247 shows the five-membered ring structure is the only possible structure. The detailed scheme of fragmentation for Acid Orange 7 is shown in Scheme 5.1.

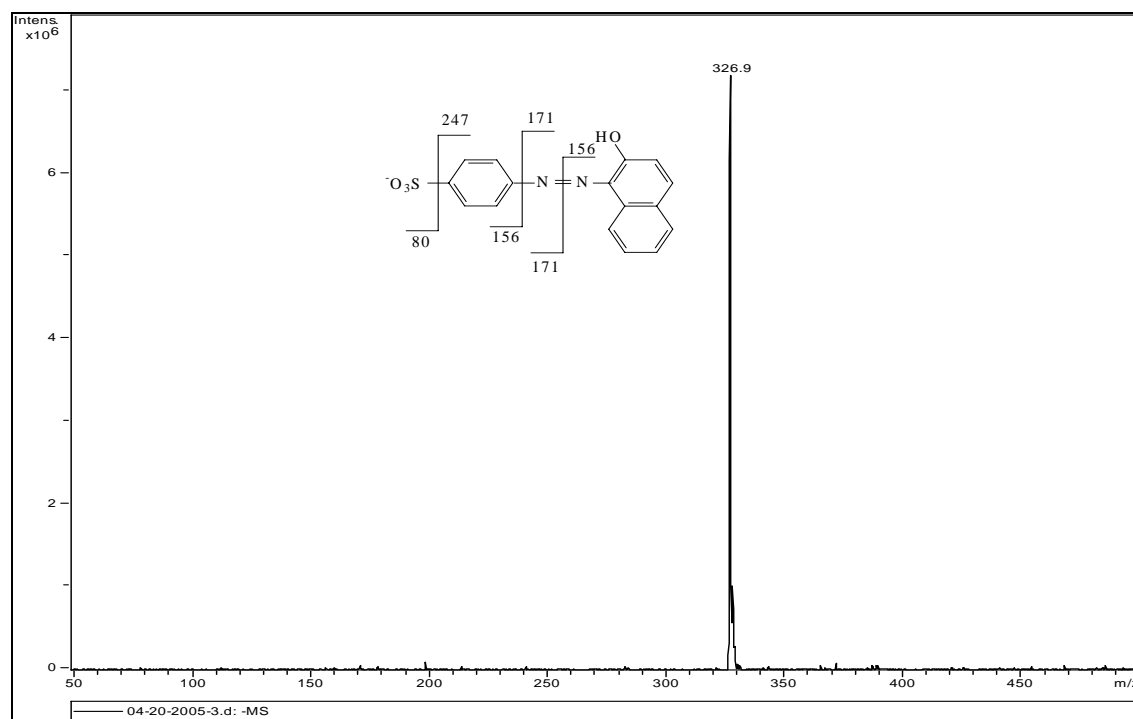


Figure 5.18 Mass Spectrum of Acid Orange 7 in the Negative Mode of ESI-MS

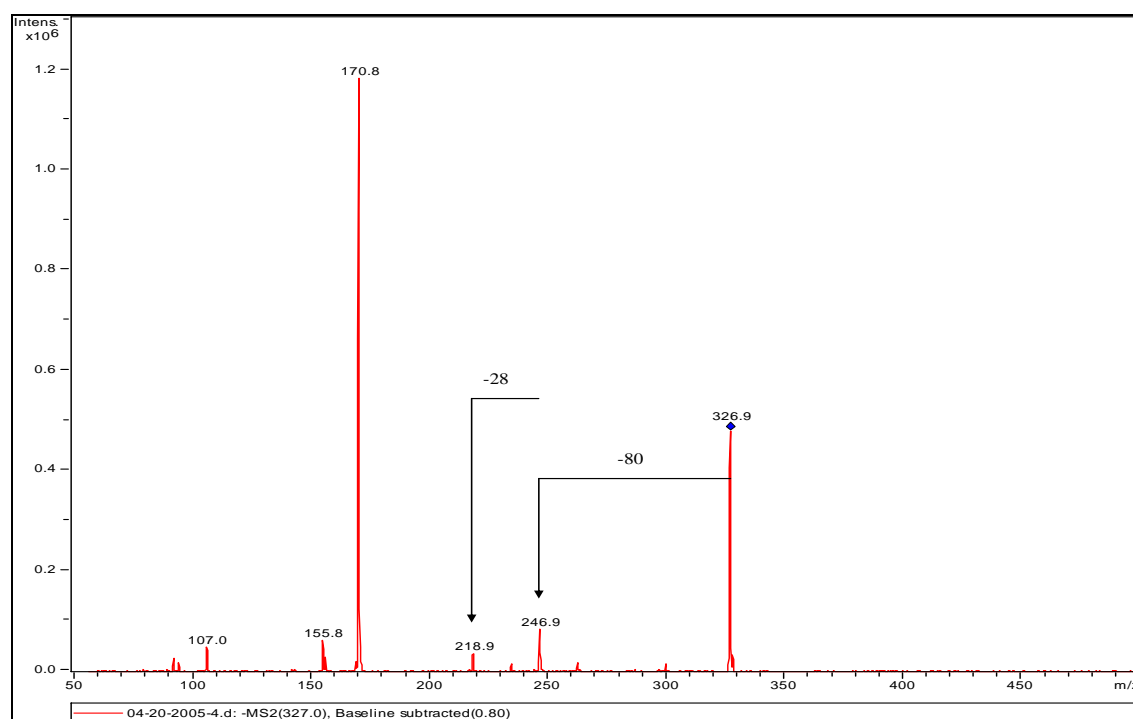
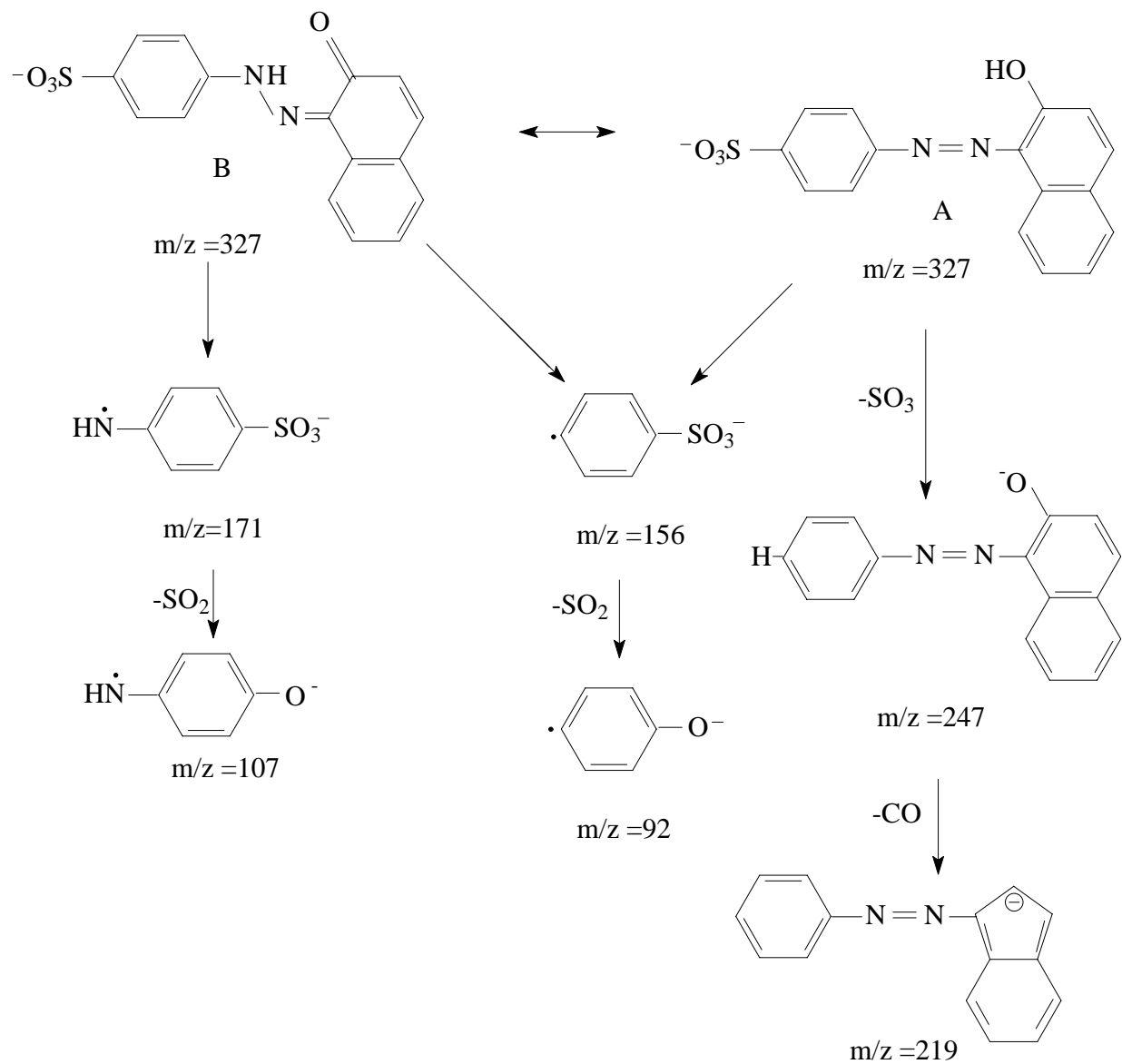


Figure 5.19 The MS^2 Mass Spectrum of MS Fragmentation of Peak at m/z 327 of Acid Orange 7

Table 5.1 The MSⁿ Fragmentation of Ions from *m/z* 327 of Acid Orange 7

Parent ions , <i>m/z</i>	Relative Intensity (%)	Daughter ions, <i>m/z</i>
327	42	247, 219, 171, 156, 107
247	8	219
219	4	N/A
171	100	101
156	6	92
107	5	N/A



Scheme 5.1 Proposed Fragmentation Pattern for Acid Orange 7

2. Identification of Fungal Degradation Products of Acid Orange 7 by CE-MS

The dye Acid Orange 7 was easily separated by capillary electrophoresis in the first two days, and the CE electrophorogram of Acid Orange 7 treated by *Pleurotus ostreatus* showed a large amount of sulphonated anion from the dye itself at m/z 327. In Figure 5. 20, after three days incubation in *Pleurotus ostreatus*, the dye peak totally disappeared from the BPC with two new product peaks (I and II) at migration times of 5.6 min and 6.8 min, suggesting that the structure of dye at m/z 327 was destroyed and degradation products were produced. The corresponding mass spectra of these CE peaks had their base peaks at m/z 157 and m/z 173, respectively, in Figure 5.21 and Figure 5.22. The peak at m/z 156 and m/z 173 were identified as benzenesulfonic acid (CAS #: 98-11-3) and 4-hydroxybenzenesulfonic acid (CAS #: 825-90-1) respectively, by comparison with standard compounds. Their concentrations increased with the extension of fungal incubation and maintained the maximum level on the third day. Benzenesulfonic acid persisted in the dye degradation solution while the 4-hydroxybenzenesulfonic acid vanished after 5 days treatment. Based on the HPLC analysis information of Acid Orange 7, the identification of 1, 2-naphthoquinone, the identification of benzenesulfonic acid and 4-hydroxybenzenesulfonic acid, a possible dye degradation pathway for Acid Orange 7 by *Pleurotus ostreatus* is proposed in Scheme 5.2.

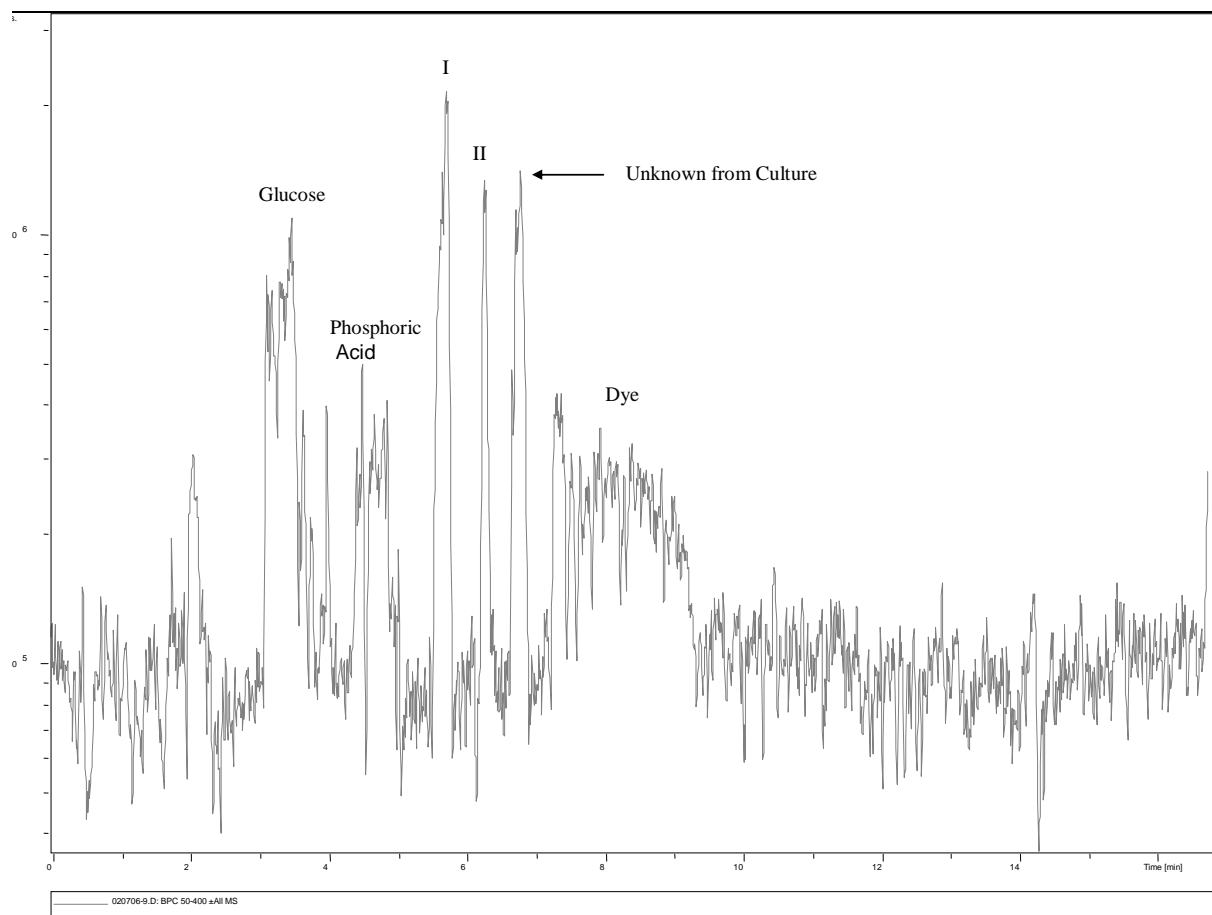


Figure 5.20 CE-ESI-MS Base Peak Chromatogram (BPC) of Acid Orange 7 Treated with *Pleurotus ostreatus* (Third Day).

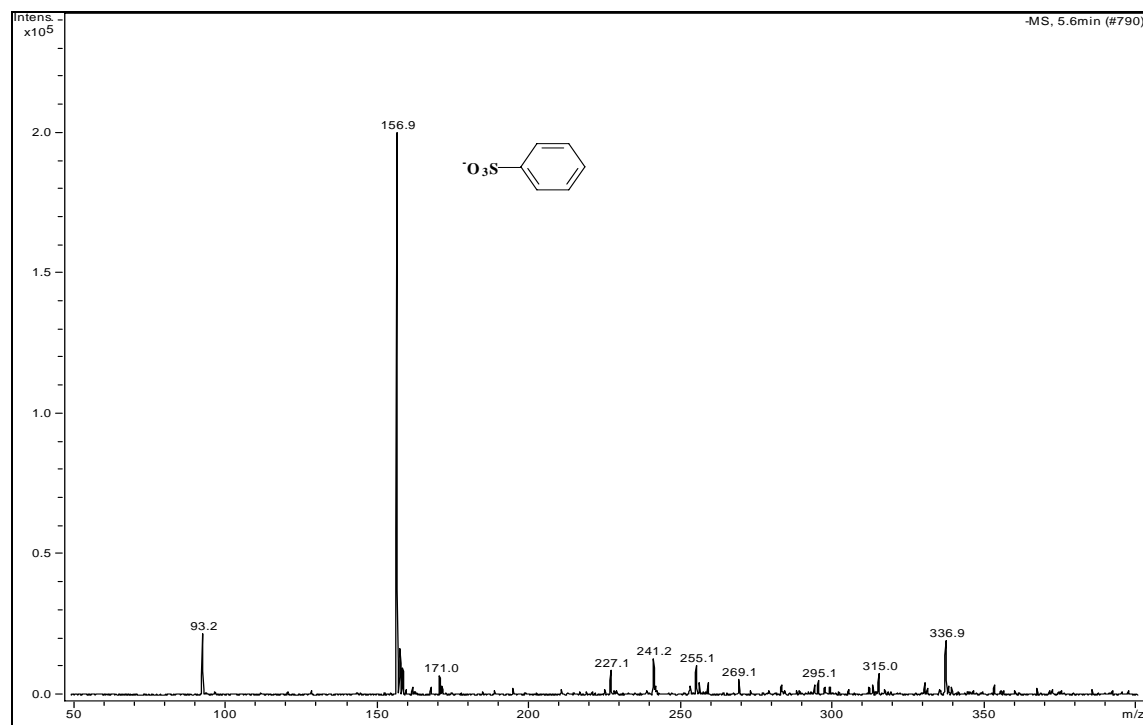


Figure 5.21 Mass Spectrum of Peak with the Retention Time of 5.6 min -Acid Orange 7.

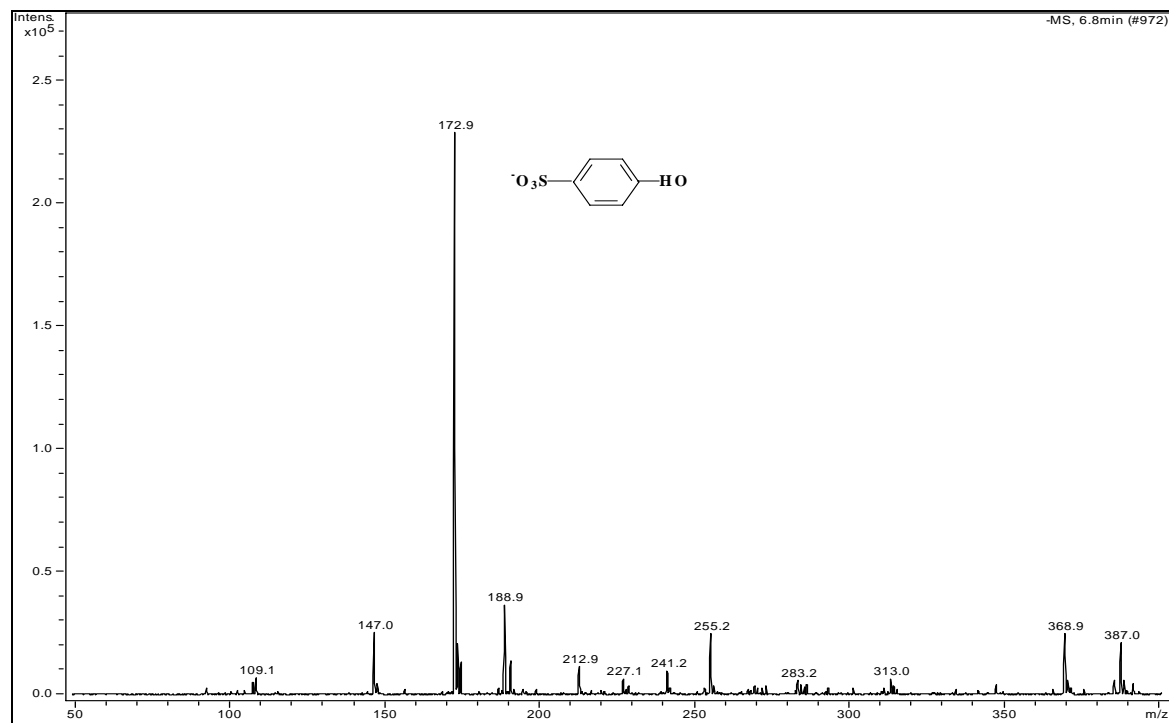
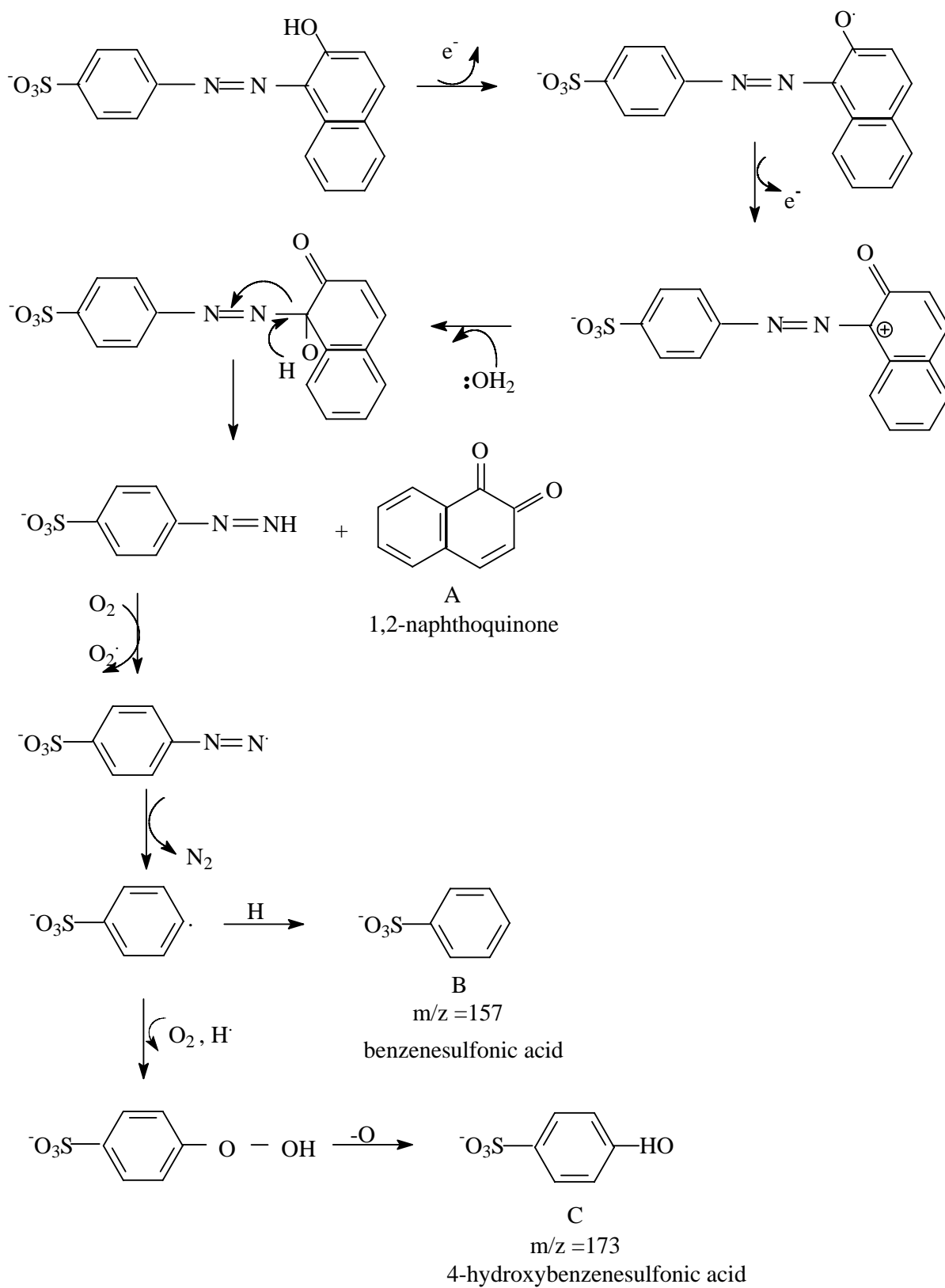


Figure 5.22 Mass Spectrum of Peak with the Retention Time of 6.8 min- Acid Orange 7.



Scheme 5.2 Proposed Mechanism for the Degradation of Acid Orange 7 by *Pleurotus ostreatus*

5.2.2 Acid Orange 8

1. Analysis of the Mass Spectrometric Fragmentation of Acid Orange 8

The mass spectrum obtained for the monosulfonated dye Acid Orange 8 exhibited the [M-Na]⁻ peak as the only observed ion (Figure 5.23, first row). Typical fragments m/z 185, m/z 219, m/z 197, and m/z 261 were observed in the MS² spectrum (Figure 5.23 the second row). The MS^{*n*} fragmentation of ions from m/z 341 is shown in Table 5.2. The formation of m/z 185 is corresponds to the cleavage of the azo bond. This fragment is an odd electron ion, and its formation from an even electron [M-Na]⁻ ion is due to collision with helium atoms in the ion trap. The similar fragmentation pattern has been established by Bruins (Bruins, 1988) for Acid Red 88, another monosulfonated azo dye.

In the further MS³ fragmentation spectrum, the loss of 64 Da of m/z 187 leads to the m/z 121 ion and then to the m/z 107 by loss of a nitrogen atom. The m/z 197 is very interesting where the cleavage of C-N bond is at the naphthalene ring side; furthermore, the active electron deficit nitrogen atom combines with carbon in the methyl group to form a five-membered ring structure. The further loss of 64 Da from m/z 197 forms m/z 133, and shows the presence of the sulphonic group on the compounds of m/z 197.

After careful calculations, a five-membered ring is the only possible structure for m/z 197. Sullivan (Sullivan, et al., 1998) proposed a similar four-membered ring structure when their group studied dye intermediates by ESI-MS and matrix-assisted laser desorption/ionization (MALDI). The ion at m/z 261 is formed by the loss of SO₂ from the dye and further loses an oxygen atom to form m/z 243, and the proton on the *ortho* position rearranged to make a stable structure. The formation of m/z 233 is the MS³ fragmentation of m/z 261 with the loss of CO (28 Da). The details of the fragmentation for Acid Orange 8 are shown in Scheme 5.3.

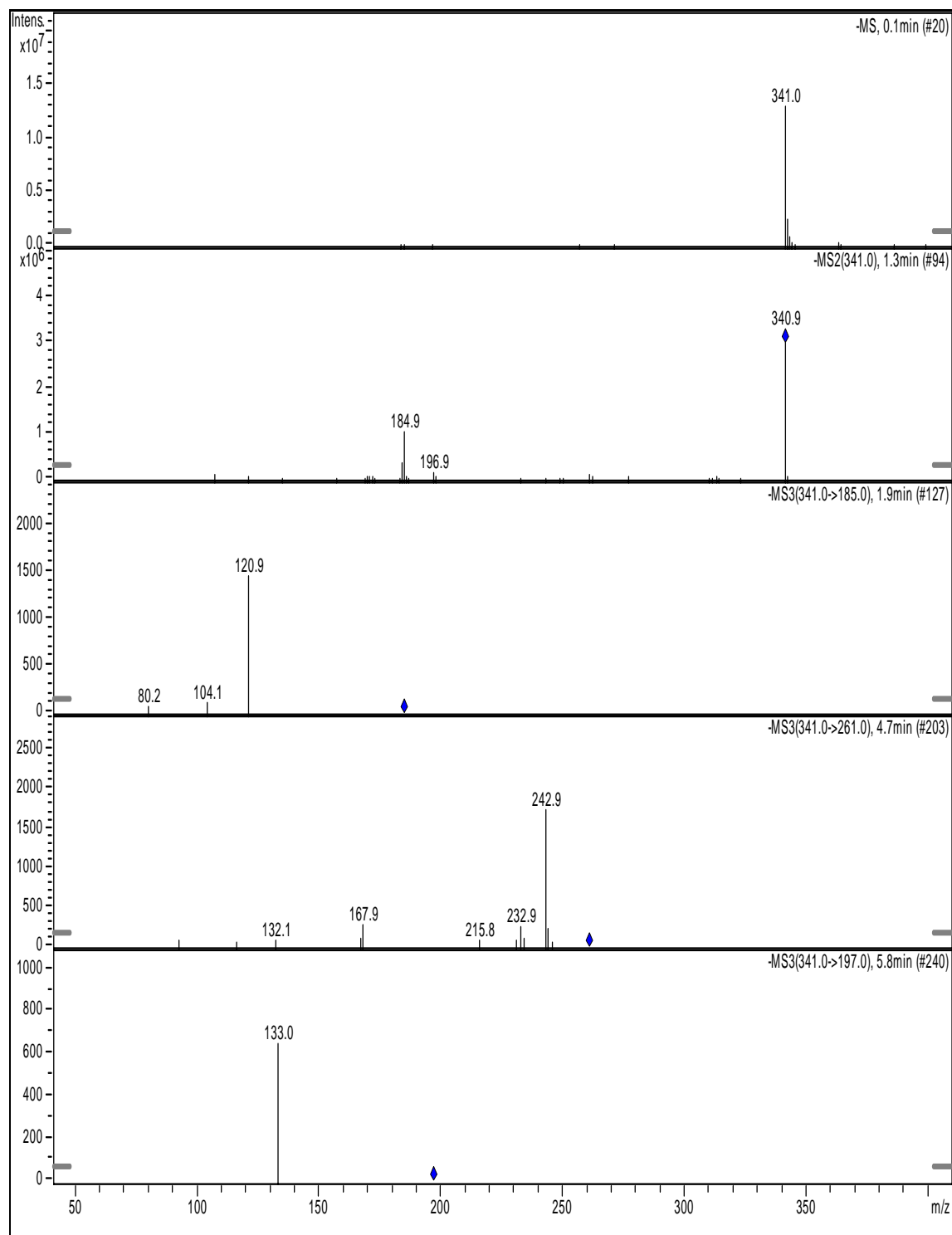
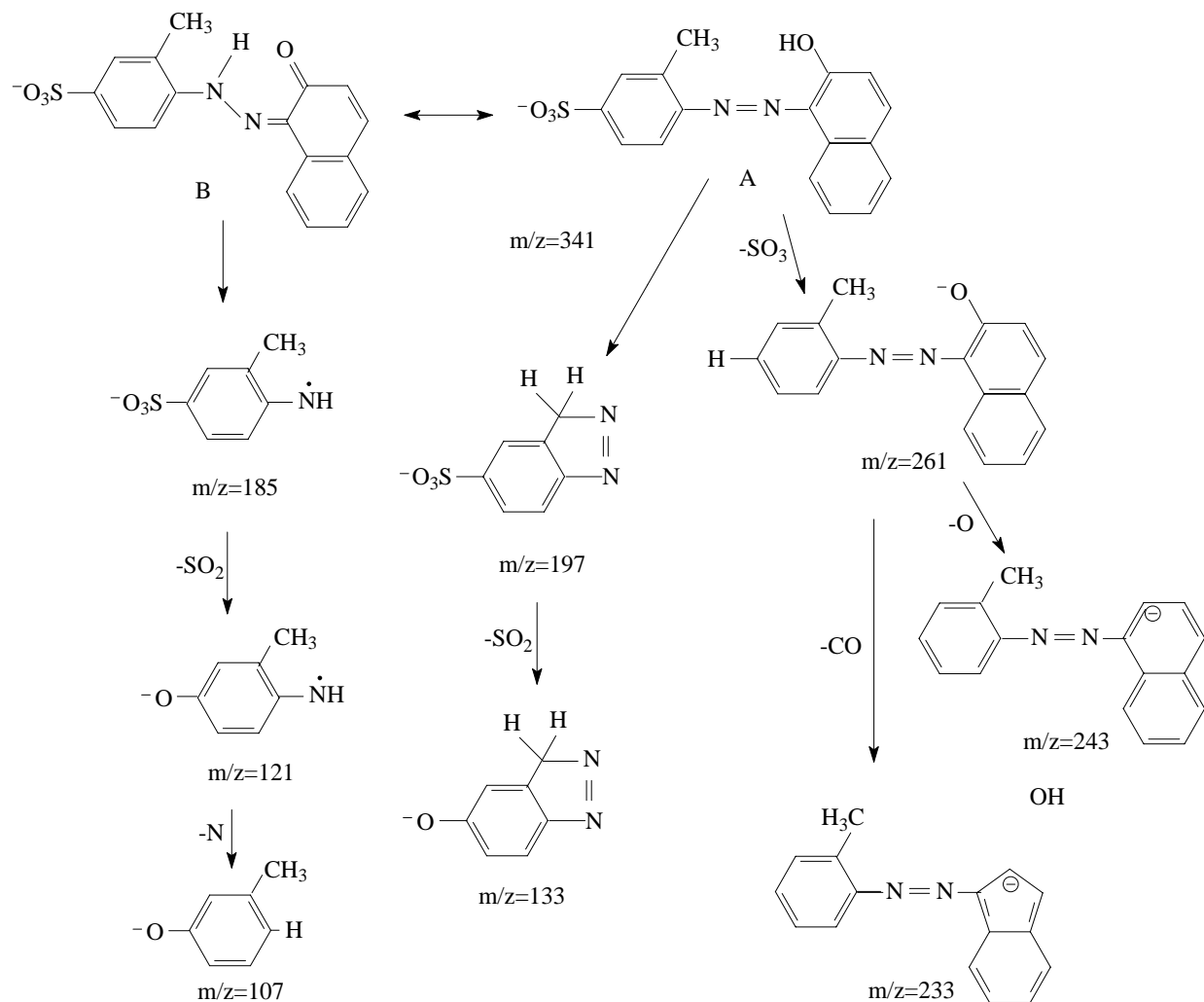


Figure 5.23 The MSⁿ Fragmentation Ions of Peak m/z 341 - Acid Orange 8

Table 5.2 The MSⁿ Fragmentation of Ions from *m/z* 341 of Acid Orange 8

Parent ions , <i>m/z</i>	Relative Intensity (%) in MS ²	Daughter ions, <i>m/z</i>
341	100	261, 232, 197, 185, 121
261	10	243, 233
233	5	N/A
197	24	133
185	70	121, 107
121	5	N/A



Scheme 5.3 Proposed Fragmentation Pattern for Acid Orange 8

2. Identification of Fungal Degradation Products of Acid Orange 8 by CE-MS

Figure 5.24 is a typical electrophorogram of Orange 8 treated by *Pleurotus ostreatus* (fourth day). The Acid Orange 8 peak is identified as the sulphonated anion of the dye itself. The intensity of Acid Orange 8 is strong even after four day's treatment with *Pleurotus ostreatus*. After four days, there are several new product peaks. The intensities of these peaks at 6.8 min and 7.5 min (Figure 5.24) approach a maximum in the fourth. The corresponding mass spectra of these CE peaks have their base peaks at m/z 171 and m/z 187, respectively, in Figures 5.25 and 5.26. The peaks at m/z 171 and m/z 187 are identified as *m*-toluenesulfonic acid (CAS #: 617-97-0) and 4-hydroxy- *m*-toluenesulfonic acid (CAS #: 7134-04-5), respectively. Even though *p*-toluenesulfonic acid is a conventional chemical, its isomer, *m*-toluenesulfonic acid, is not commercially available. Due to the lack of availability of standard compounds, there was no comparison information to confirm the isolated compounds; however, based on the analysis of dye structure, it is very probable that the m/z 170 and m/z 187 are *m*-toluenesulfonic acid and 4-hydroxy- *m*-toluenesulfonic acid. Based on HPLC analysis of Acid Orange 8, the identification of 1, 2-naphthoquinone, and the identification of *m*-toluenesulfonic acid and 4-hydroxy- *m*-toluenesulfonic acid, a possible dye degradation pathway for Acid Orange 8 which is similar to that of Acid Orange 7 by *Pleurotus ostreatus* is proposed in Scheme 5.4.

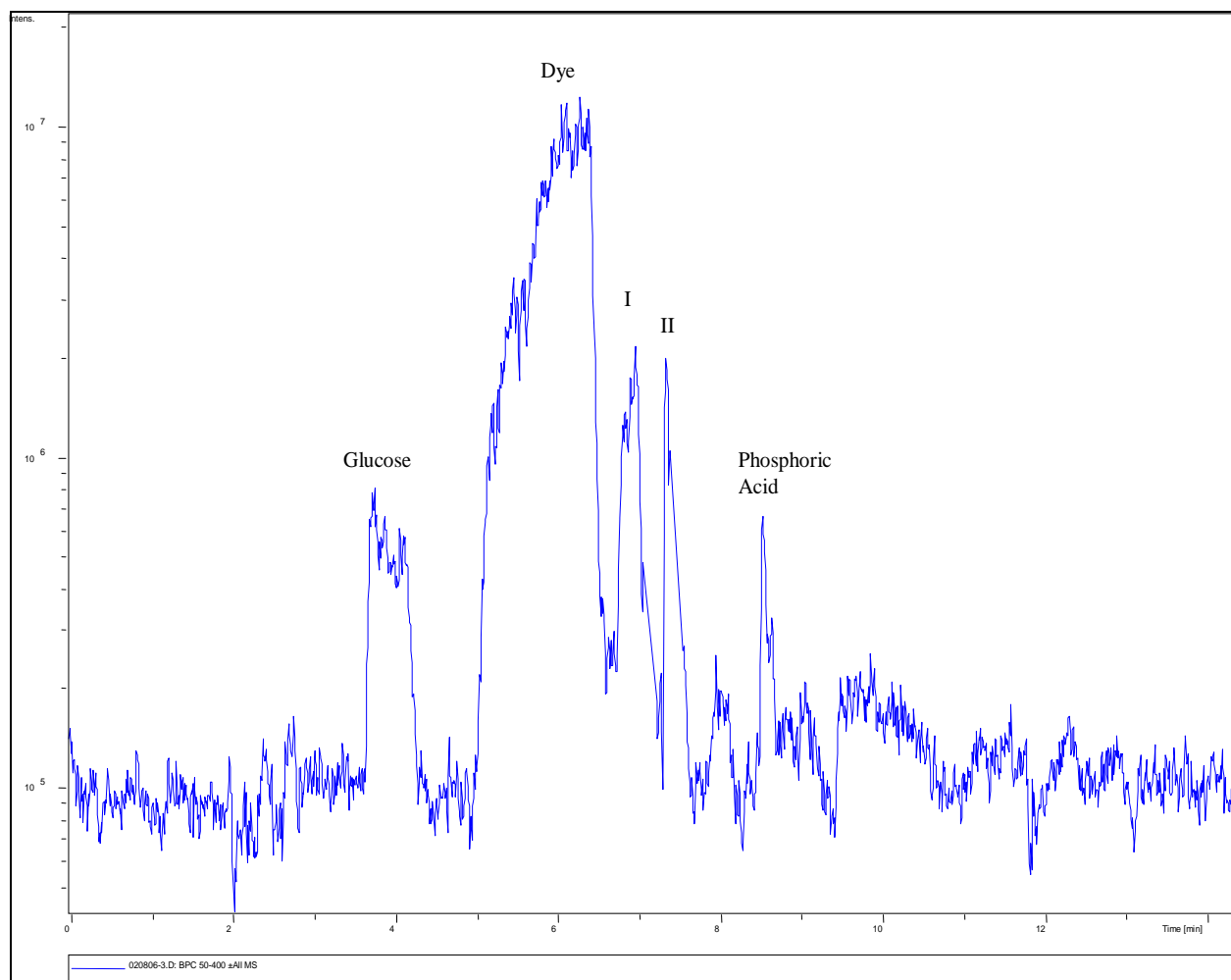


Figure 5.24 CE-ESI-MS Base Peak Chromatogram of Acid Orange 8 Treated with *Pleurotus ostreatus* (Fourth Day).

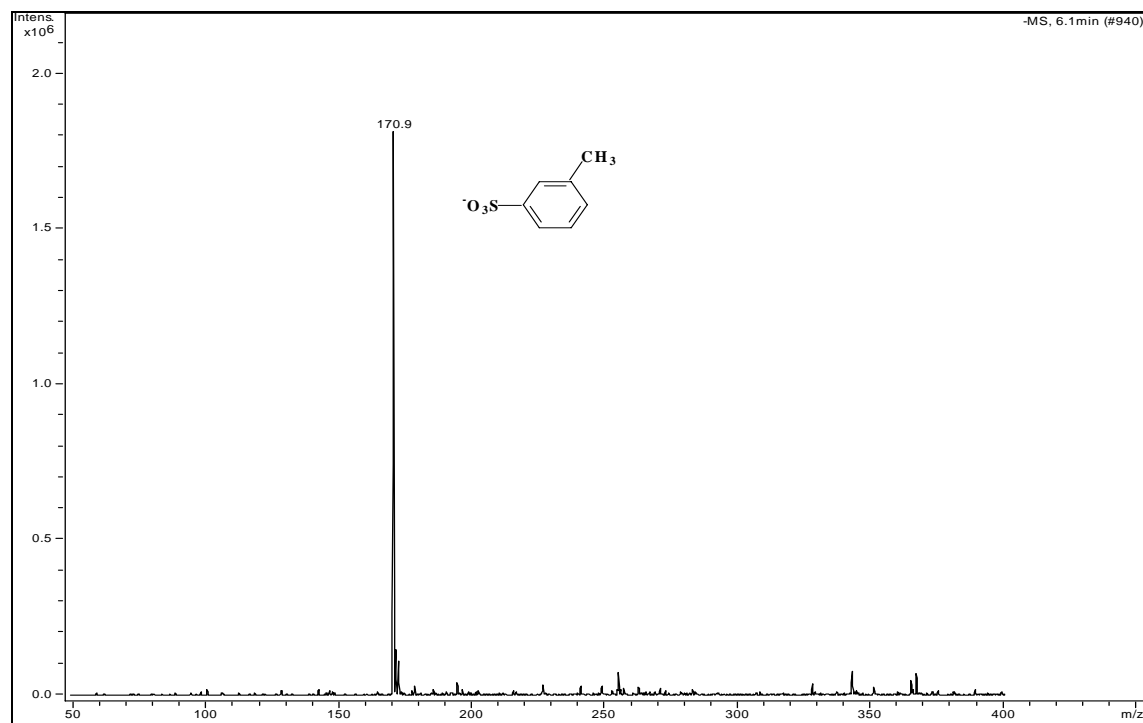


Figure 5.25 Mass Spectrum of Peak with Retention Time of 6.8 min -Acid Orange 8 Treated with *Pleurotus ostreatus*.

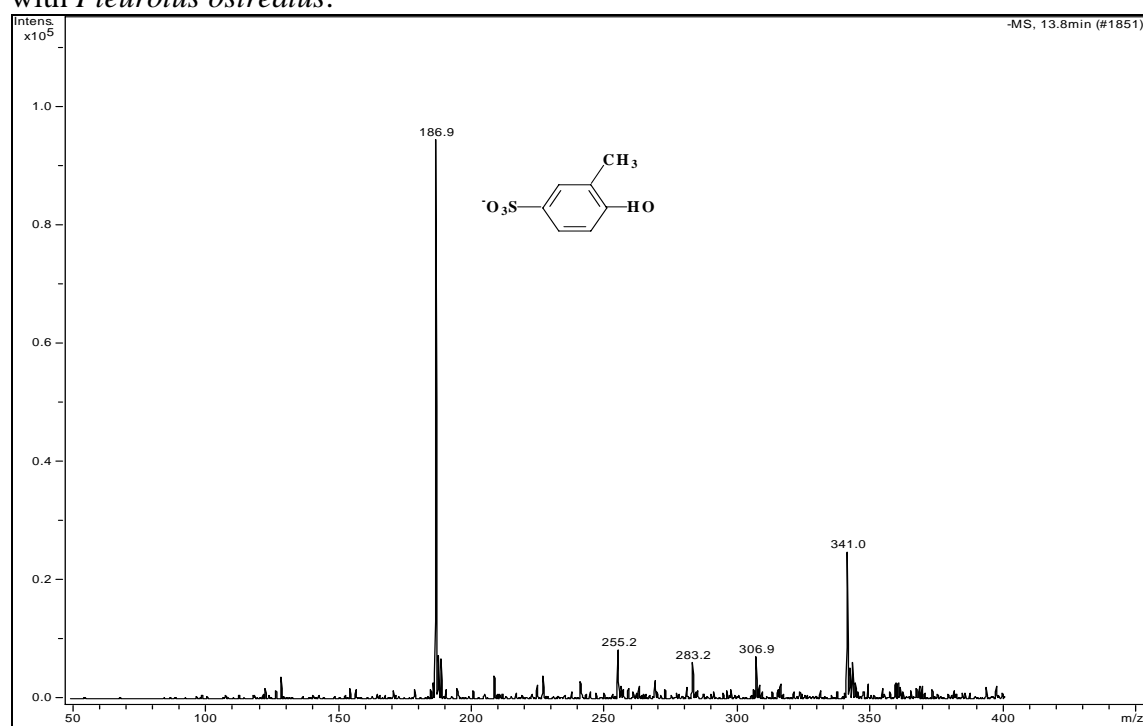
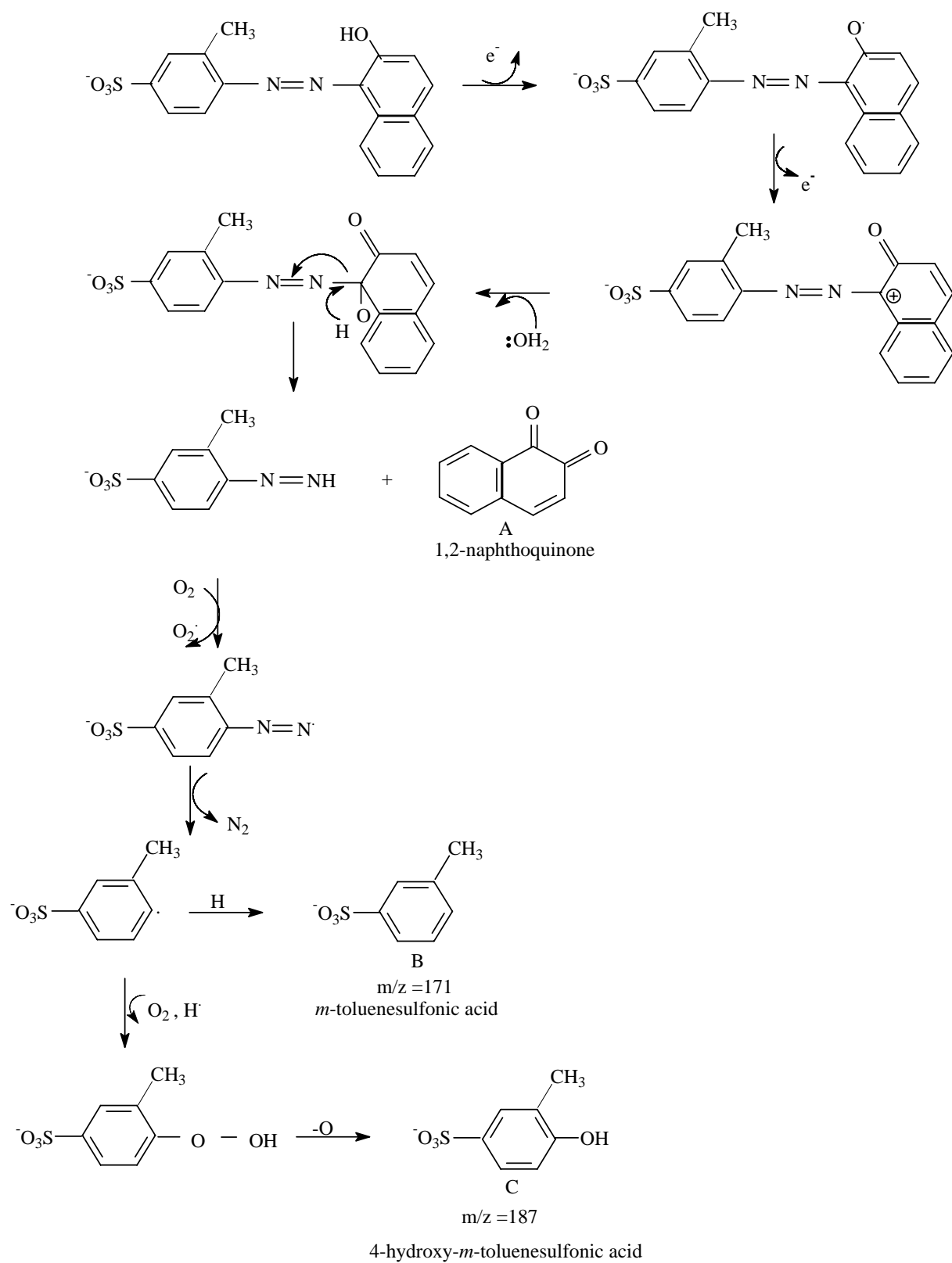


Figure 5.26 Mass Spectrum of Peak with the Retention Time of 7.5 min - Acid Orange 8 Treated with *Pleurotus ostreatus*.



Scheme 5.4 Proposed Mechanism for the Fungal Degradation of Acid Orange 8 by *Pleurotus ostreatus*

5.2.3 Mordant Violet 5

1. Analysis of the Mass Spectrometric Fragmentation of Mordant Violet 5

The structure of this dye has the hydroxyl group is in the *ortho*-position relative to the azo linkage. In this position, hydrogen bonding makes the hydroxyl group a much weaker acid than with *para*-isomer; the *ortho*-isomer is therefore less susceptible to color changes (Zollinger, 1987). Having the hydroxyl group in the *ortho* position also leads to the formation of ketohydrazone tautomers (see Scheme 5.5). While the formation of these tautomers does not affect the mass-to-charge ratio of the molecular anion formed from ESI ionization, it does affect the fragmentation of the azo dyes under collision-induced dissociation condition in the tandem MS/MS. For Mordant Violet 5, which contains two *ortho*- hydroxyl groups, three tautomers can be formed (A, B, C in Scheme 5.5). The MSⁿ fragmentation may supply additional information to further understand the structure of dye and the possible breakdown mechanism.

The mass spectrum of Mordant Violet 5 is shown in Figure 5.27. Because there is only one sulphonic group on the dye molecule, Mordent Violet 5 exhibits the [M-Na]⁻, *m/z* 343 peak as the only observed anion ion in the negative ion ESI mass. The typical fragmentation ions for Mordant Violet 5 are *m/z* 263, *m/z* 186, *m/z* 171, and *m/z* 143 shown in Figure 5.28. The further MSⁿ fragmentation ions of *m/z* 343 are summarized in Table 5.3.

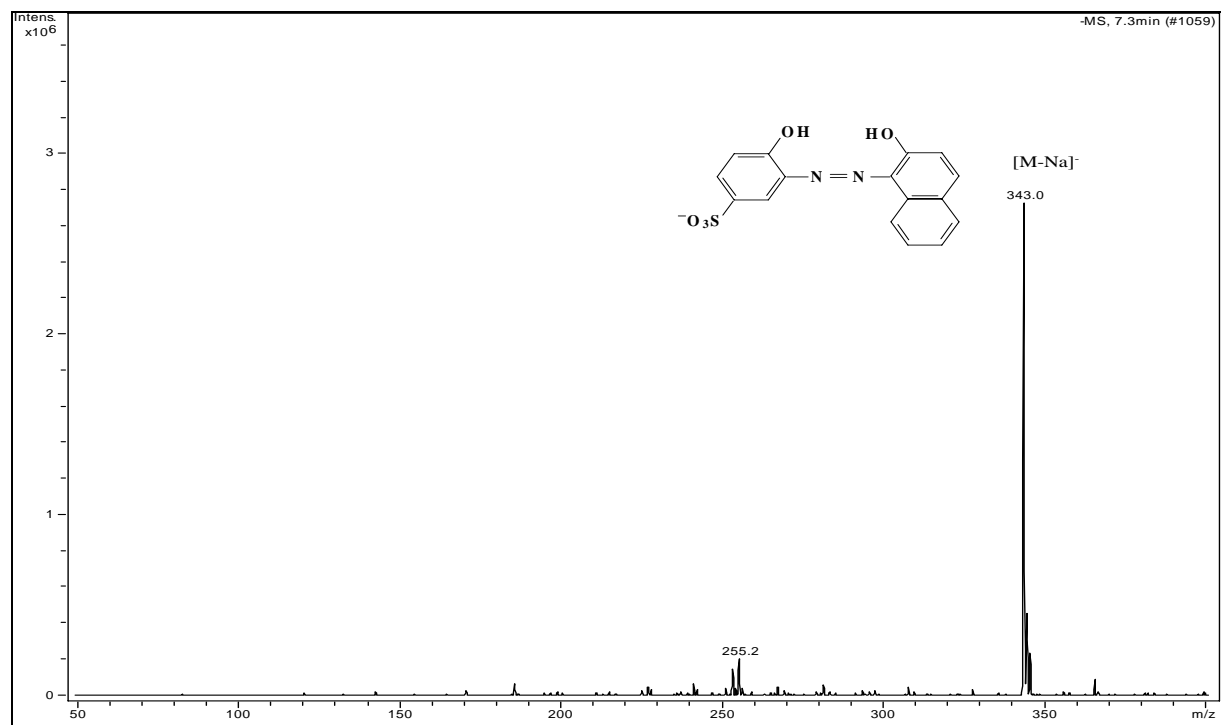


Figure 5.27 The Mass Spectrum of Mordant Violet 5 in the Negative Mode of ESI-MS

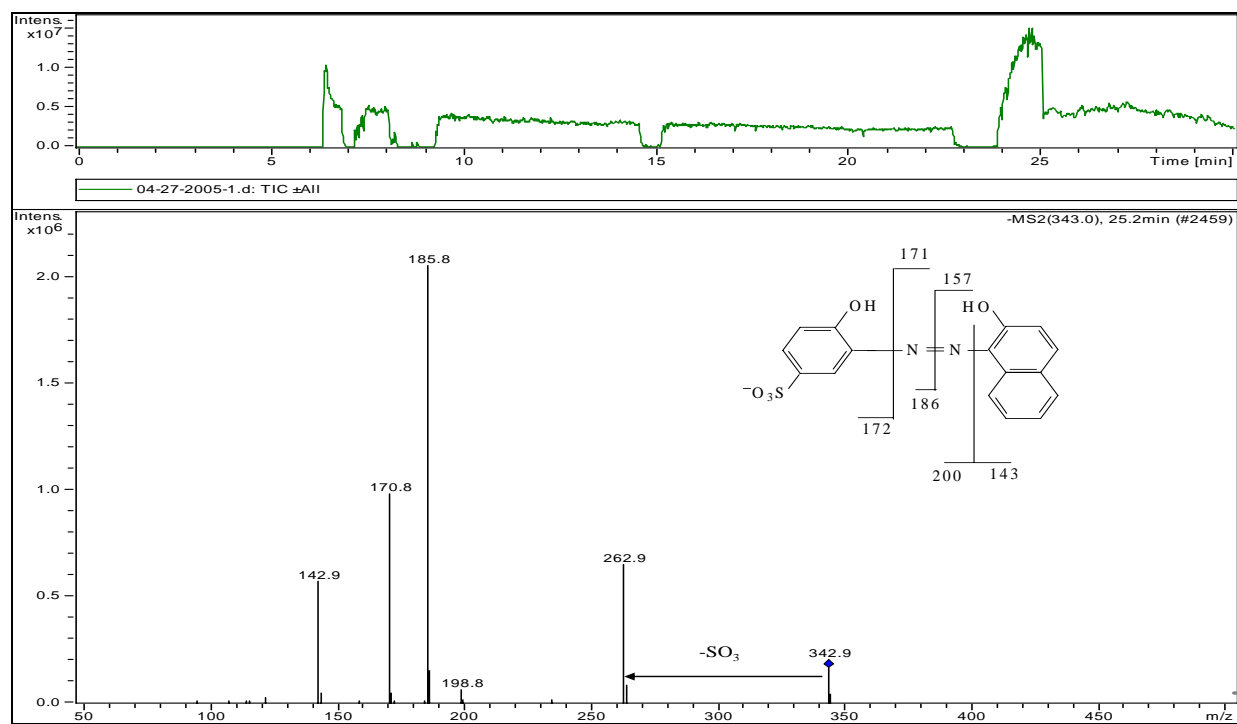


Figure 5.28 The MS^2 Fragmentation Ions of Peak m/z 343, Mordant Violet 5

Table 5.3 MS² Fragmentation of Ions from the Peak m/z 343 of Mordant Violet 5

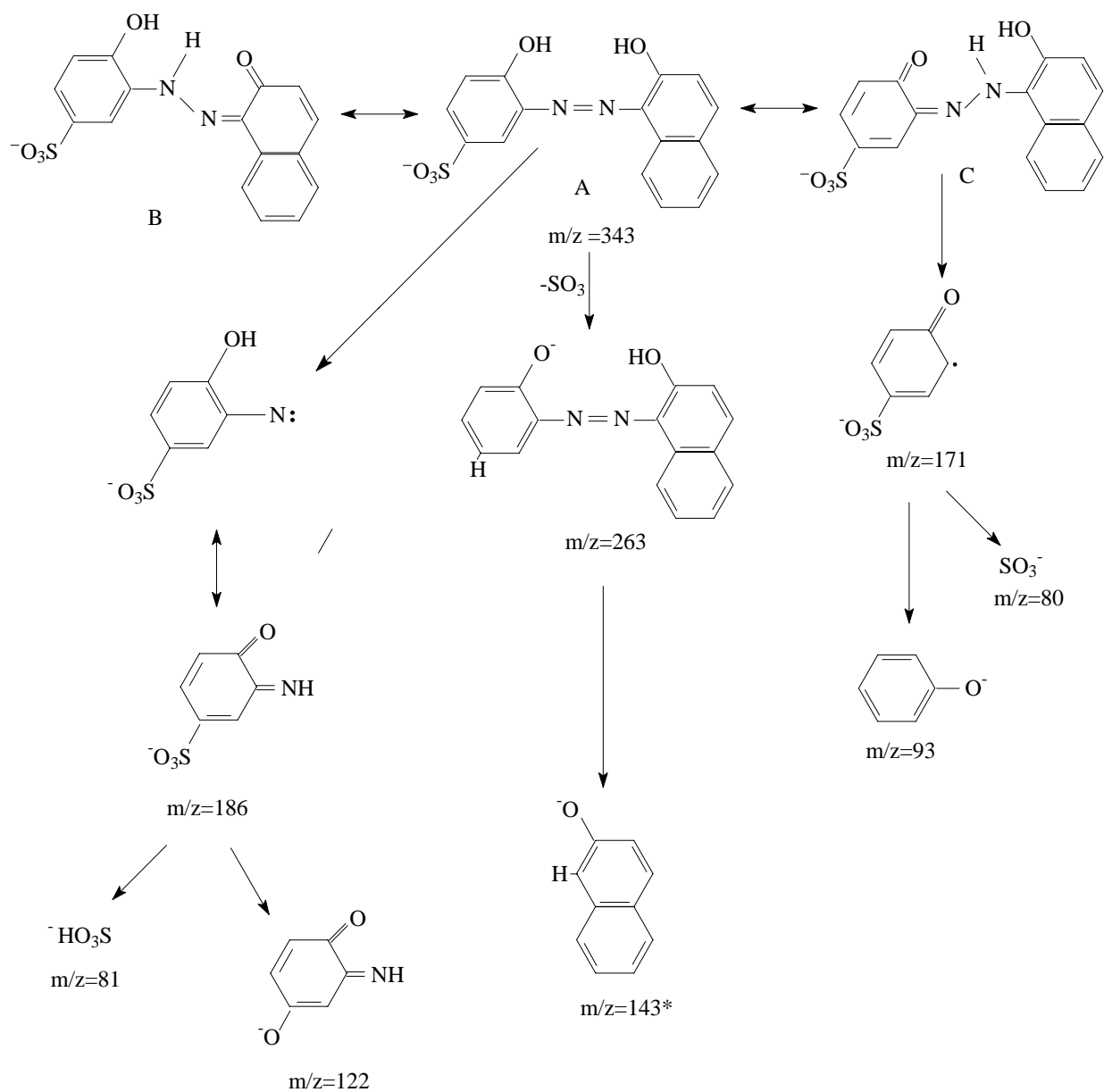
Parent ions m/z	Relative Intensity (%)	Daughter ions, m/z
343	16	263,186,171,143
263	30	143
186	100	122, 81
171	30	93, 80
143	16	80

The loss of SO₃ (80 Da) leads to the m/z 263 ion from m/z 343. The loss of SO₃ during fragmentation in the negative mode can be used as a specific marker for selective monitoring of the presence of a sulphonic group. The MS³ fragmentation of the m/z 263 ion forms m/z 143, which was identified as naphtholate ion by Borgerding (Borgerding, 1994). This is unusual example of an ion formed from the side of the molecule not containing the original charged moiety; however, the m/z 80 is shown in the further fragmentation of m/z 143, suggesting that there is a sulphonic group rather than a naphtholate ion. Furthermore, there isn't any m/z 115, which is usually a typical ion for naphtholate. So the possible structure is still not clearly understood.

The abundant ion at m/z 186 is the result of the cleavage of the azo bond, indicating a fragmentation of the azohydroxy tautomers rather than either of the ketohydrazone forms (B and C in Scheme 5.5) which would give either the m/z 185 or m/z 187 ions. The MS² fragmentation of peak m/z 186 shows a loss of 64 Da to form m/z 122 and an ion corresponding to HSO₃⁻ at m/z 81. The existence of m/z 81 indicates that the proton of the hydroxyl group *meta* to the sulphonates is transferred to the sulphonate. When Borgerding (1994) investigated the

fragmentation of Mordant Violet 5, he made the mistake of locating the sulphonic group on the *para* position of the azo bond rather than the *meta* position, and therefore the formation of a four-membered ring and the resonance stabilized anion structure of m/z 186 he proposed was not established. In fact, due to the position of the sulphonic group at the *meta* position of the azo bond, the assumed four-membered ring structure is unlikely. Another reason that the formation of four-membered ring on the benzene ring is probably not possible is the spatial steric hindrance and the resultant instability. A possible conjugated structure of ion at m/z 186 is proposed in Scheme 5.5.

The ion m/z 171 is from the cleavage of a C-N double bond of a ketohydrazone form, forming a ketene (olefin ketone) structure with a free radical on the adjacent position. The further fragmentation of the m/z 171 ion shows an ion at m/z 93, phenol, and m/z 80 ion, which is an SO_3^- ion, thus showing the evidence of existence of $-\text{SO}_3^-$ group on the benzene ring. Borgerding (Borgerding, 1994) considered the m/z 171 as an epoxide on the *ortho* positions of benzene ring; however, the ring strain of this structure makes formation of this three-membered ring improbable. The complete fragmentation pattern for Mordant Violet 5 is shown in Scheme 5.5.



Scheme 5.5 Proposed Fragmentation Pattern for Mordant Violet 5

* The structure of m/z 143 was proposed by Bogerding (Bogerding, 1994)

2. Identification of Fungal Degradation Products of Mordant Violet 5 by CE-MS

This section examines the separation and identification of fungal dye degradation products with CE-ESI-MS. Figure 5.29 is a typical electrophorogram of Mordant Violet 5 treated by *Pleurotus ostreatus* (first day). Mordant Violet 5 produces a peak at the retention time 7.3 min, easily identified as sulphonated anion of the dye itself (Figure 5.30). The other peak (13 min) was identified as glucose in the culture medium, which we have discussed previously.

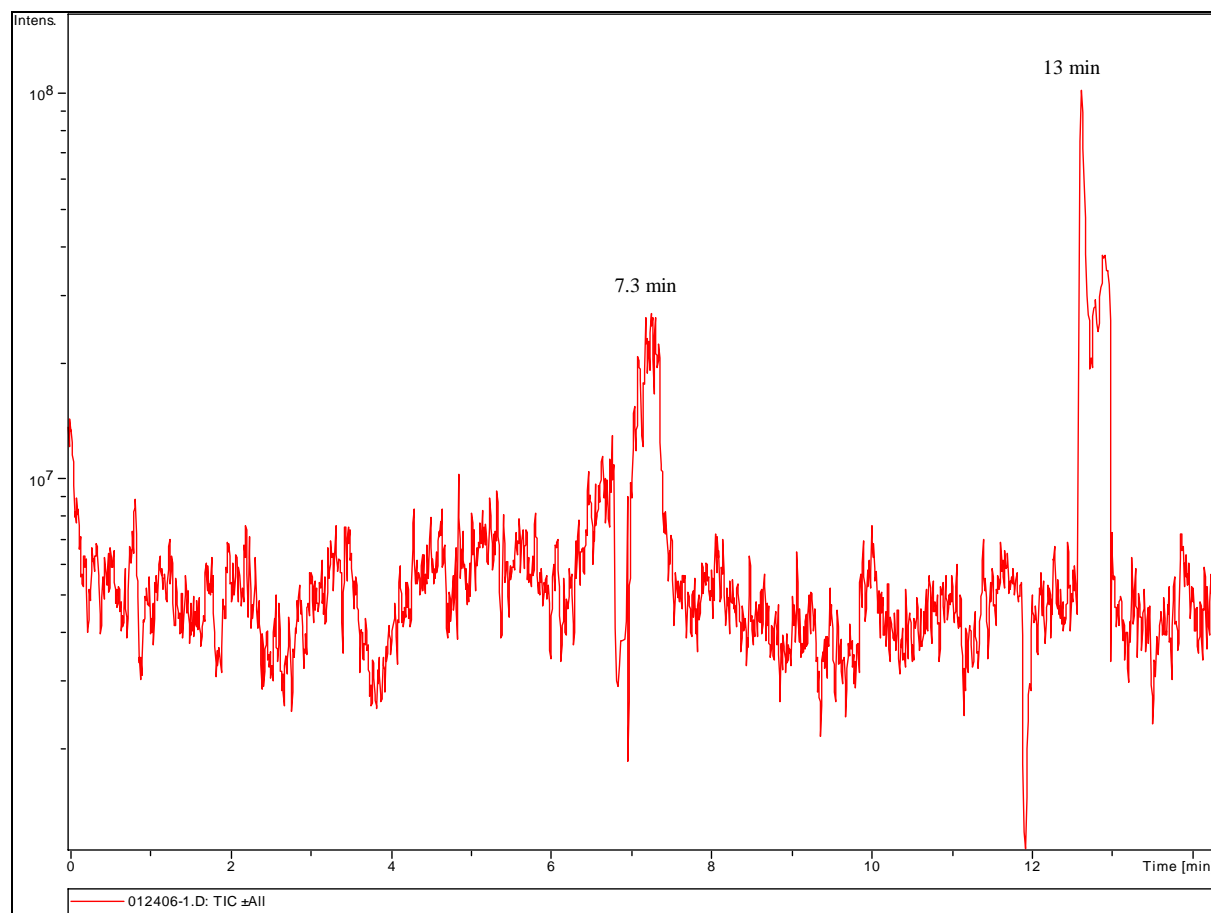


Figure 5.29 CE-ESI-MS Base Peak Chromatogram of Mordant Violet 5 Treated with *Pleurotus ostreatus* (First day).

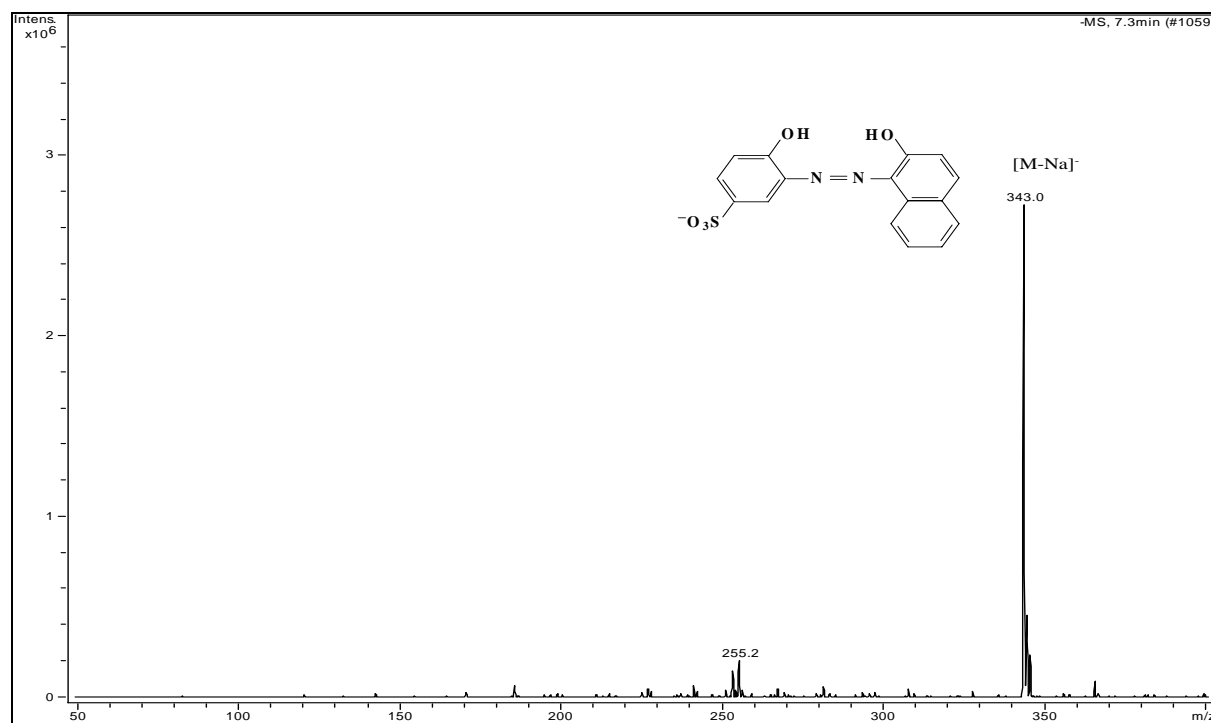


Figure 5.30 The Mass Spectrum of Peak with the Retention Time of 7.3 min of Mordant Violet 5 Treated with *Pleurotus ostreatus* (First Day).

In the second day, the dye peak totally disappeared, with two major new product peaks at migration times of 8.8 min (product I) and 10.4 min (product II), and one minor product at migration time 8.5 min (product III) (Figure 5.31). The corresponding mass spectra of these CE peaks have their base peaks at m/z 329, m/z 173, and m/z 185 respectively.

The peak at m/z 173 (Product II) in Figure 5.32 was identified as 4-hydroxy-benzenesulfonic acid by comparison with the standard compound. Its concentration increased with the extension of the degradation treatment. One very interesting peak (product III) was found at the migration time 8.5 min. The corresponding mass spectrum is shown at m/z 185 in Figure 5.33. The proposed possible structure of the ion at m/z 185 is *p*-diazonium-benzenesulfonic acid ($C_6H_5N_2SO_3^-$, structure shown in Scheme 5.6).

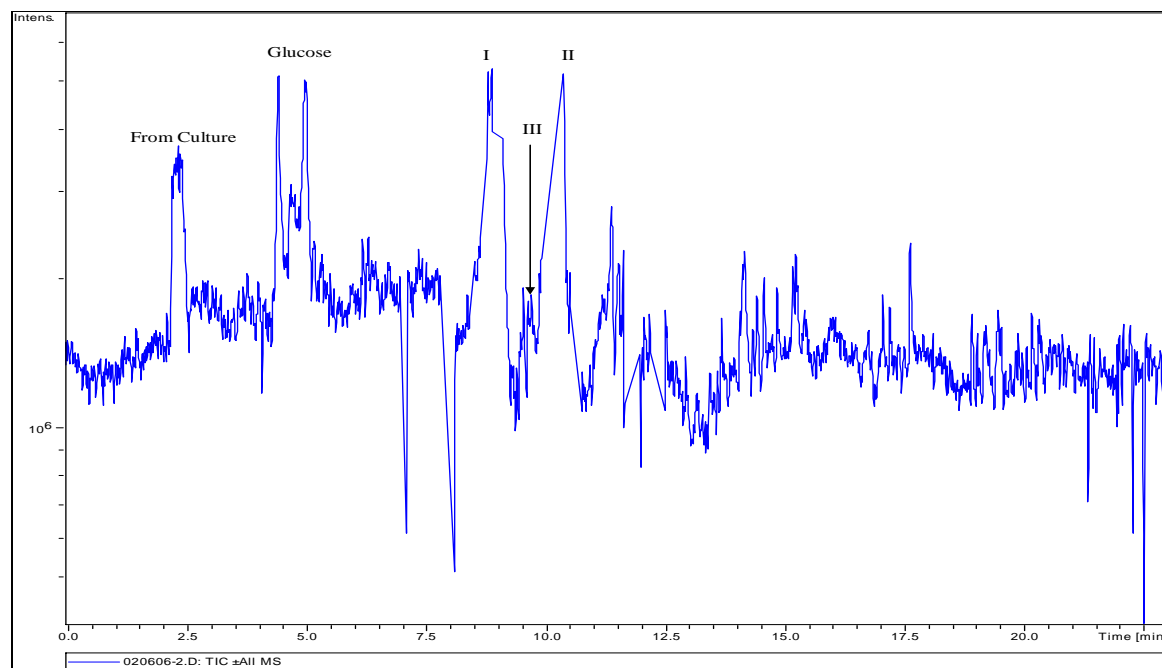


Figure 5.31 CE-ESI-MS Base Peak Chromatogram of Mordant Violet 5 Treated with *Pleurotus ostreatus* (Second Day).

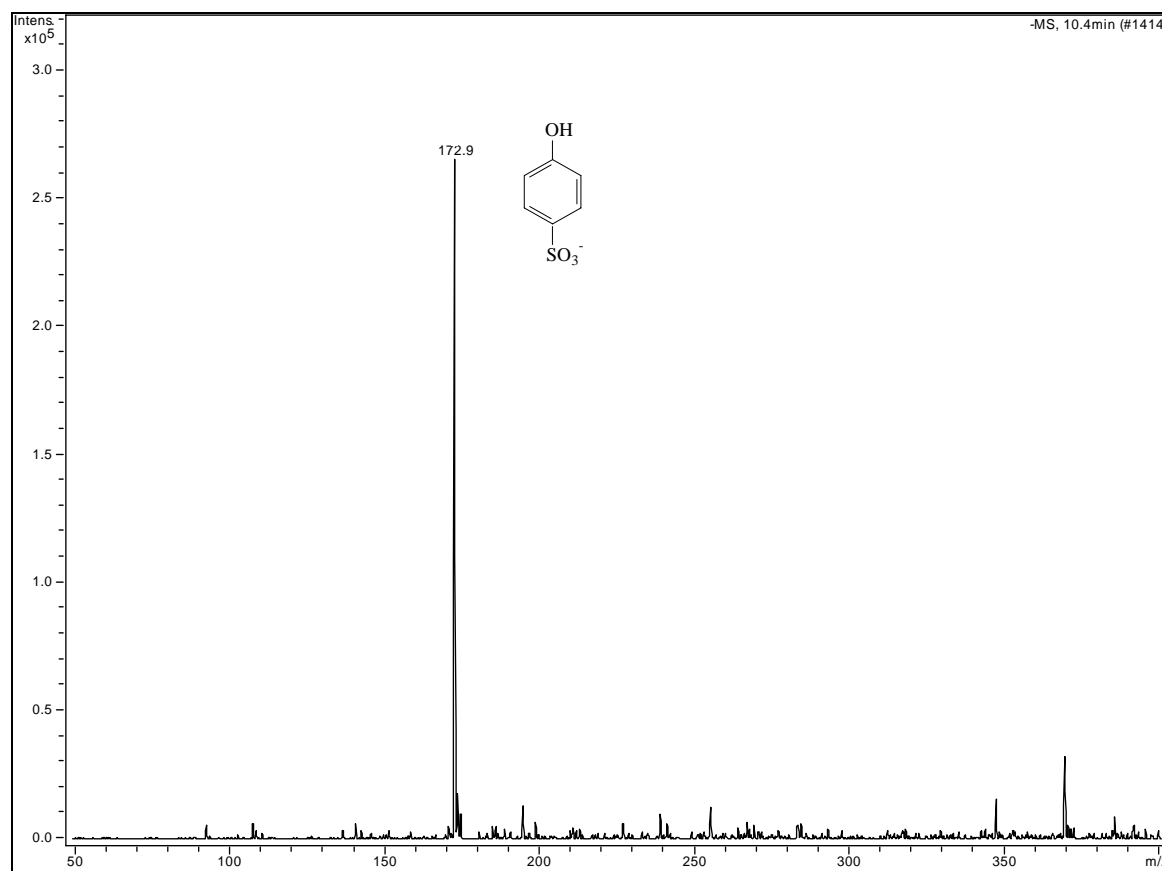


Figure 5.32 Mass Spectrum of Peak with Retention Time of 10.4 min- Product II.

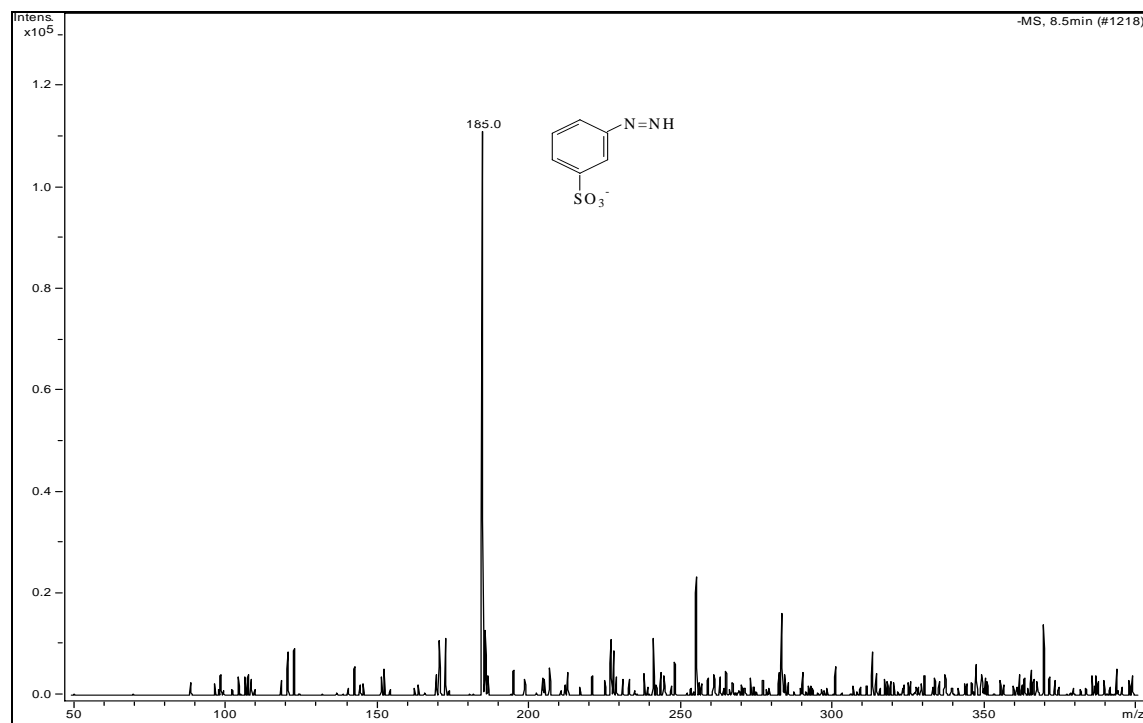


Figure 5.33 Mass Spectrum of Peak with Retention Time of 8.5 min- Product III.

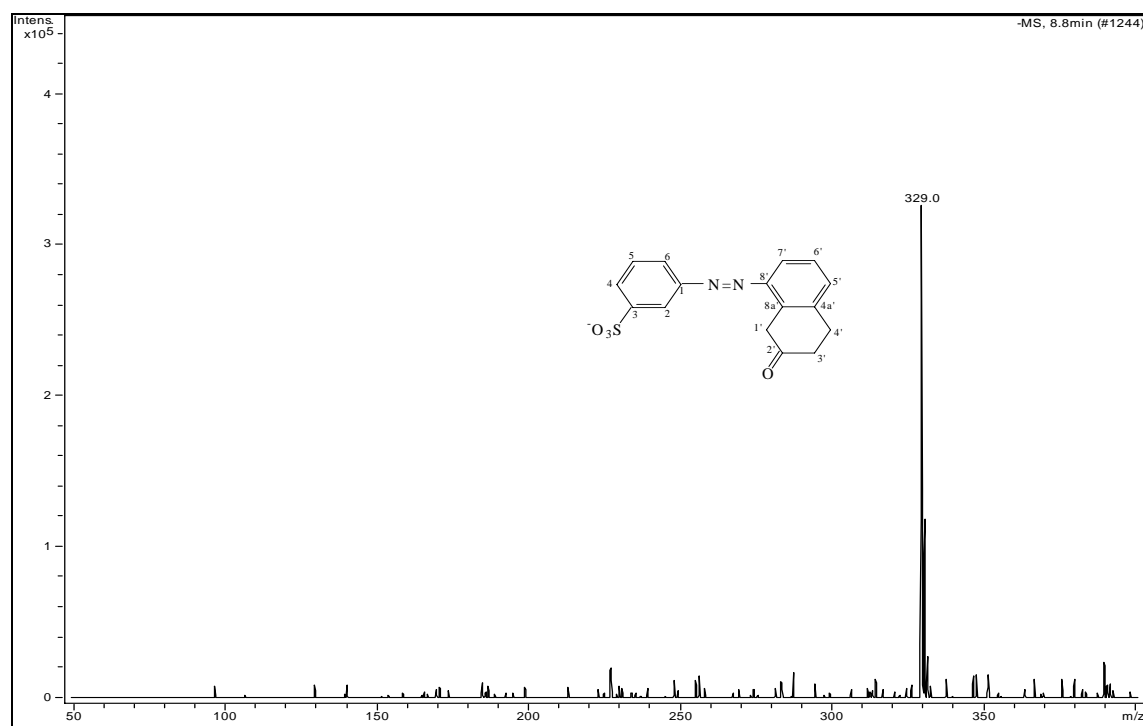


Figure 5.34 Mass Spectrum of Peak with Retention Time of 8.8 min- Product I.

The high intensity ion of m/z 329 (Product I) in Figure 5.34 is curious because there are only 14 Da difference compared to m/z 343 of the dye. This ion started to emerge in the second day and continued to exist until the end of the treatment, suggesting that it had a stable structure. The fragmentation spectrum of m/z 329 is shown in Figure 5.35 and the further MSⁿ fragmentation of ion m/z 329 is summarized in Table 5.4. In Figure 5.35, there is some very important information related to an explanation of the structure. The major fragmentation ions are m/z 301, 249, 221, and 205. More specifically, m/z 301 is formed from m/z 329 by the loss of 28 Da; furthermore, m/z 221 is produced by loss of SO₃ from m/z 301. The ion at m/z 221 is also produced from another routine by loss of SO₃⁻ to form m/z 249 then lose 28 Da again. The ion at m/z 301 loses another 28 Da to form the m/z 273 ion. M/z 221 can also lose another 28 Da to form m/z 193, while m/z 205 is produced by the loss of 44 Da. This could be CO and another O atom or CH₂O from m/z 249. The detailed flow chart of m/z 329 fragmentation is shown in Scheme 5.6.

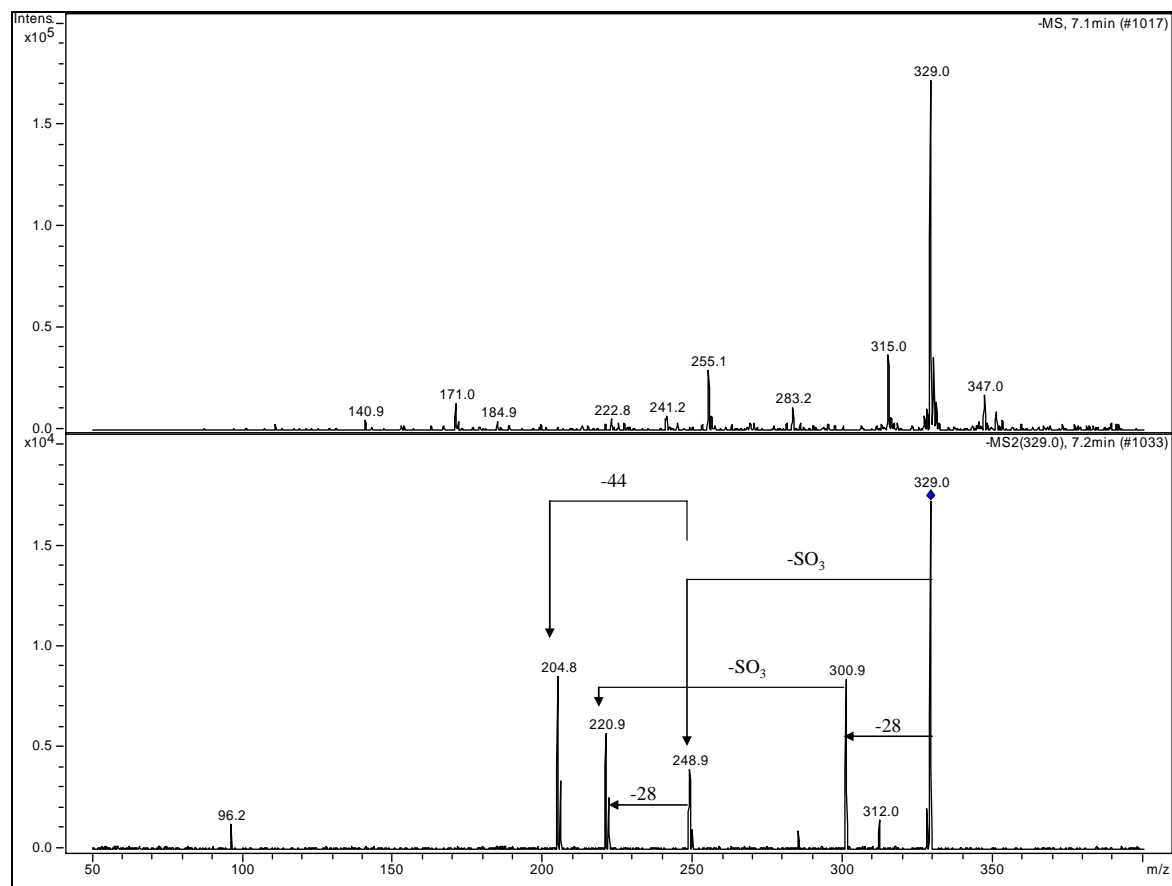


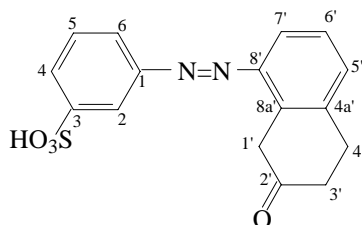
Figure 5.35 The Fragmentation Ions of Peak m/z 329

Table 5.4 The MS² Fragmentation of Ions from m/z 329

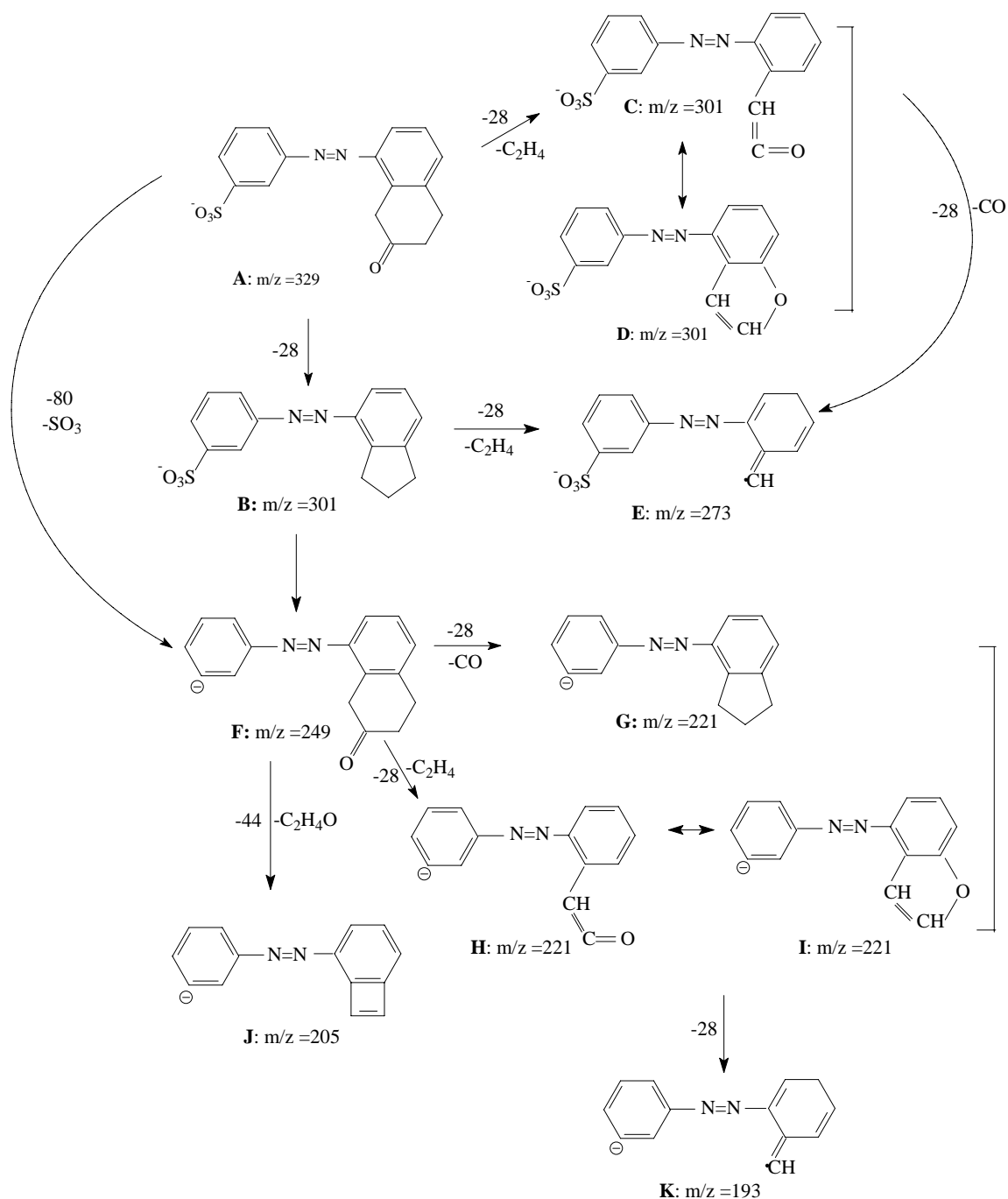
Parent ions , m/z	Relative Intensity (%)	Daughter ions, m/z
329	100	301, 249, 221, 205, 96
301	50	273
249	22	205
221	33	193
205	50	N/A
96	5	N/A

It was surprising that there were no fragmentation peaks in the m/z 100 to 200 range, suggesting that the entire molecular structure is not broken down. It is clear that m/z 329 is capable of losing two 28 Da fragments, which could be CO or $\text{CH}_2\text{-CH}_2$ free radicals. If the structure contained two CO units, the molecular weight would be more than 329, so one CO and one $\text{CH}_2\text{-CH}_2$ free radical in the structure is a possible solution. Because the structure m/z 329 could lose a $\text{CH}_2\text{-CH}_2$ free radical, that is to say, m/z 329 contained a ring structure because there is no any side groups having $\text{CH}_2\text{-CH}_2$ free radical or $\text{-CH}_2\text{=CH}_2\text{-}$. Furthermore, the loss of $\text{CH}_2\text{-CH}_2$ free radicals in the ring means the structure could be cyclohexanone.

Based on the fragmentation pattern, a possible structure of m/z 329 is the compound which has an azo group connecting a benzene ring with a sulphonic group on the *meta* position and another benzene ring fused with a cyclohexanone (Scheme 5.6, compound A). The name of m/z 329 is 3-{1, 8'-azo (2'-oxygen-tetrahydrogen-naphthalene)} benzenesulfonic acid.



In Scheme 5.6, the m/z 329 (compound A) loses one 28 Da to form m/z 301. There are two possibilities to account for 28 Da; one is CO and the other is a $\text{CH}_2\text{-CH}_2$ free radical by cleavage of the cyclic ring. The corresponding structures are compound B, which is formed by the loss of CO, and compound C which is produced by cleavage of the cyclic ring and the loss of a $\text{CH}_2\text{-CH}_2$ free radical. Structure C may be transformed to rearrange to compound D, which is a five-membered ring structure along the benzene ring. Whichever structure of m/z 301 exists, another 28 Da loss results in the formation of m/z 273 (the compound E) which is stable.

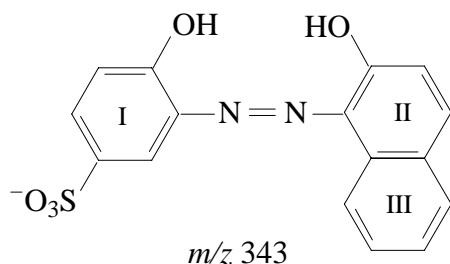


Scheme 5.6 Proposed Fragmentation Pattern for Ion at m/z 329

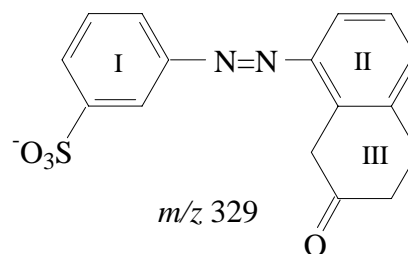
Compound m/z 329 can also lose a SO_3 ion to form m/z 249, compound F, and lose another 28 Da to form m/z 221. There are also two possibilities for the structure of m/z 221, compounds G and H. Compound H may transform to form an isomer compound I. Compound

K is formed by the loss of another 28 Da from m/z 221. Another peak of interest is m/z 205, which comes from m/z 249 (structure F) by loss 44 Da. The possible fragmentation of 44 Da is the loss of a C_2H_2O to form a four-membered ring intermediate (compound J).

We have elucidated the structure of m/z 329, but how it is produced is another question. The original structure of Mordant Violet 5 needs to be investigated carefully.

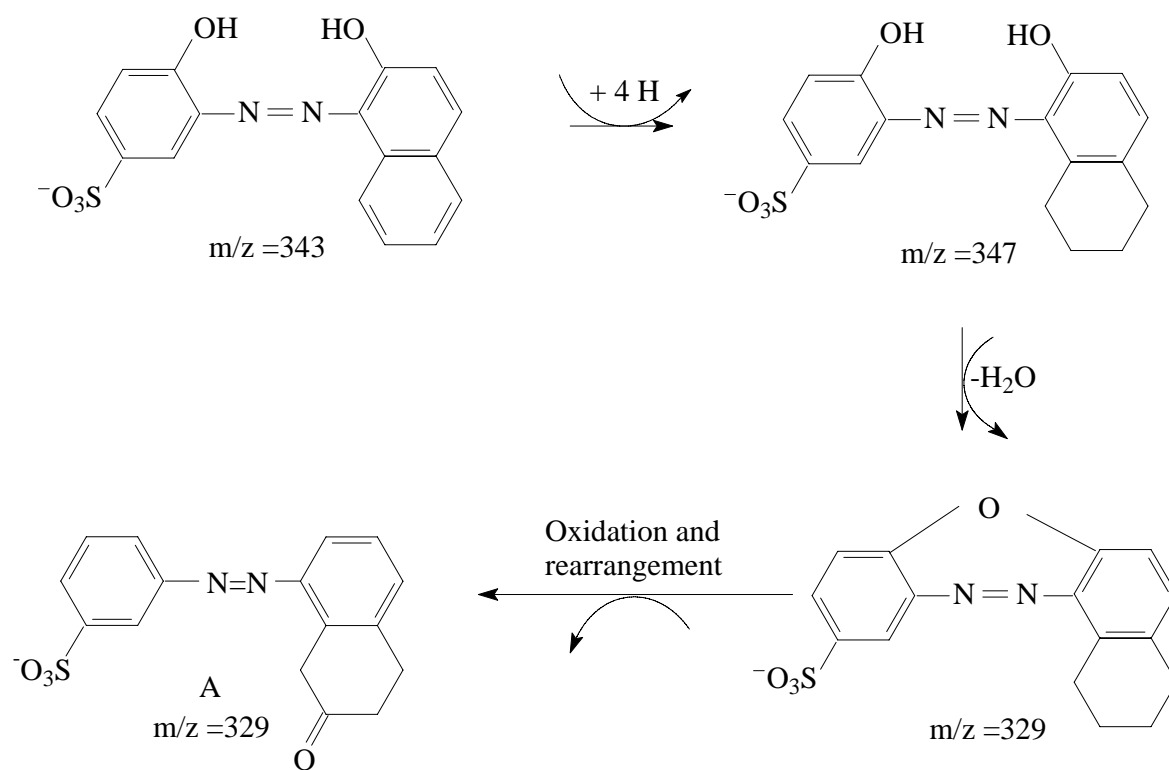


Mordant Violet 5

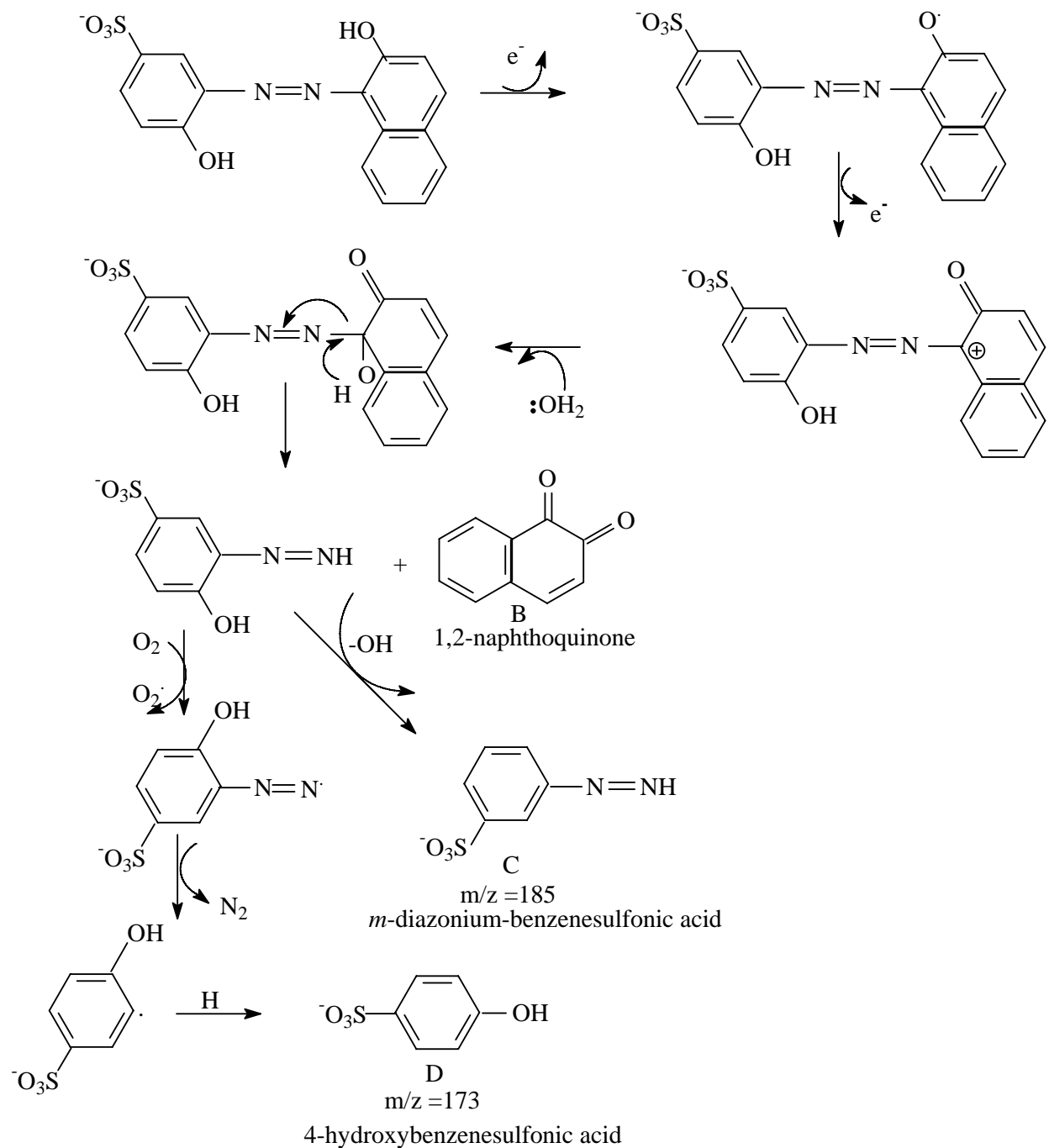


Degradation product m/z 329

There are three benzene rings within the dye structure. The first is the one on the left side which contains a hydroxyl group and a sulphonic group; the second is the one in the naphthalene ring connecting an azo bond and with another hydroxyl group; and the third one is in the naphthalene ring without any functional group. The third ring is the most active one, and can be substituted and reduced by other chemicals under the suitable circumstances. We believe that Mordant Violet 5 is first reduced by adding 4 hydrogen atoms on the third ring to form m/z 347, a 347 m/z can be seen in the top MS spectrum (Figure 5.35). Next step two hydroxyl groups to combine and lose one mole of water to form an ether structure. In addition, through some complicated chemical reactions which may be involve rearrangement and oxidization reactions, the ketone structure of m/z 329 is produced. A possible degradation pathway is generalized in Scheme 5.7. Several other important degradation products of Mordant Violet 5 have been identified by HPLC and CE-ESI-MS, and another degradation pathway which is similar to that Acid Orange 7 and Acid Orange 8 is generalized in Scheme 5.8.



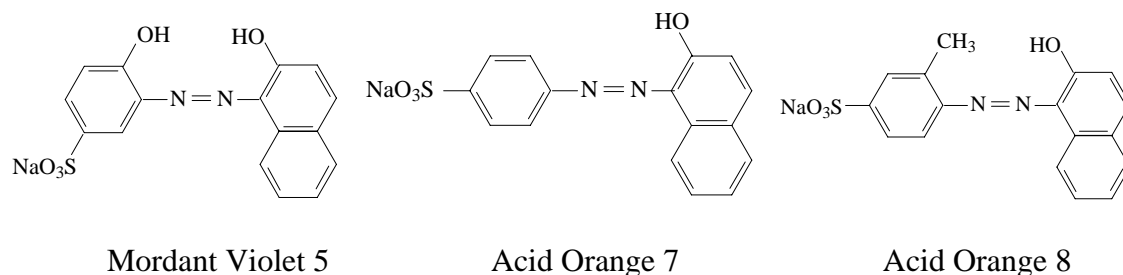
Scheme 5.7 The First Fungal Degradation Pathway Proposed for Mordant Violet 5 by *Pleurotus ostreatus*



Scheme 5.8 The Second Fungal Degradation Pathway Proposed for Mordant Violet 5 by *Pleurotus ostreatus*

5.2.4 Summary of Mass Spectrometric Fragmentation of Mordant Violet 5, Acid Orange 8, and Acid Orange 7

The structures of Mordant Violet 5, Acid Orange 8 and Acid Orange 7 have a naphthalene ring with a hydroxyl group on the *ortho* position beside the azo bond connected to a benzene ring on the another end with a sulphonic group. The difference is that Mordant Violet 5 has another hydroxyl group in the *ortho* position beside the azo bond on the benzene ring while Acid Orange 8 has a methyl and Acid Orange 7 has none at that position.



The difference in functional groups on the benzene ring results in the difference in fragmentation of these three dyes. The symmetrical cleavage of Mordant Violet 5 at the azo bond results in the formation of the most abundant ions at m/z 186 with two free radicals on the nitrogen atom. A possible reason may be the symmetrical influence of the two hydroxyl groups on the *ortho* position on both the benzene and naphthalene rings. Acid Orange 7 and Acid Orange 8 share the same fragmentation pattern, which is the cleavage of the structure at the -N-N- single bond after the formation of ketohydrazone (B in Scheme 5.1 and B in Scheme 5.3), thus producing an odd electron ion. The most abundant peaks of m/z 185 from Acid Orange 8 and m/z 171 from Acid Orange 7 are the evidences to prove this existence. There are also some other differences in the fragmentation patterns among three dyes; however, the amounts of these ions are so small that the patterns related with those ions are not primary patterns.

5.2.5 Summary of the Fungal Degradation Pathway of Mordant Violet 5, Acid Orange 8, and Acid Orange 7

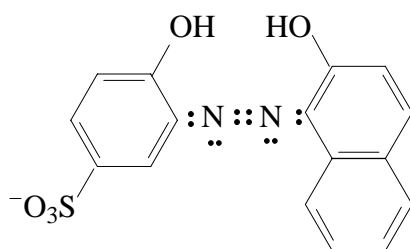
Even though there are two major fragmentation patterns involved in these three dyes, they have a similar major degradation pathway. In addition, Mordant Violet 5 has another degradation pathway.

Acid Orange 7 follows a similar degradation mechanism as Acid Orange 8 and Mordant Violet 5 in which the dye breaks apart at the naphthalene ring side and 1, 2-naphthoquinone is formed by the oxidation reaction. The formation of 1, 2-naphthoquinone may be involved in the enzymatic reaction. The cleavage of these three dyes at the naphthalene ring side also results in the formation of a benzenesulfonic diazonium intermediate or its derivative, further producing benzenesulfonic acid or its derivative by the loss of N_2 . This oxidation reaction involves formation of a peroxide, followed by the loss of an oxygen atom to form an hydroxyl group on the *para* position of benzenesulfonic acid. This degradation pathway is the primary pathway for these three dyes.

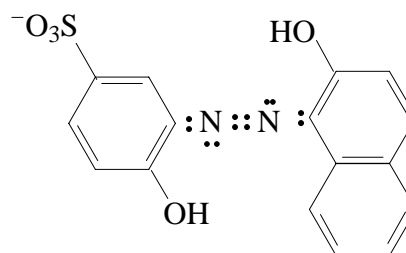
Besides this pathway, Mordant Violet 5 has another degradation mechanism. Mordant Violet 5 is first reduced by adding 4 hydrogen atoms on the third ring to form m/z 347. Then the two hydroxyl groups combine and loose a mole of water to form an ether structure. In addition, through some complicated chemical reactions which may be involve rearrangement and then oxidization, the ketone structure of m/z 329 is produced.

Mordant Violet 5 has two degradation pathways because of its two stereo structures, the *cis* and *trans* stereo-isomers. The *trans*-Mordant Violet 5 structure follows the degradation pathway of reduction, loss of water, then oxidation to form a cyclohexyl keton structure. The *cis*-Mordant Violet 5 follows another degradation pathway which is the same as Acid Orange 8

and Acid Orange 7, that is, cleavage of azo bond at the naphthalene ring side where benzenesulfonic acid and 1, 2-naphthoquinone are formed.



Trans-Mordant Violet 5

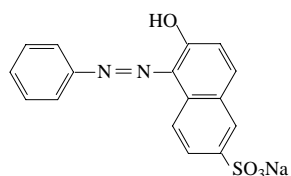


Cis-Mordant Violet 5

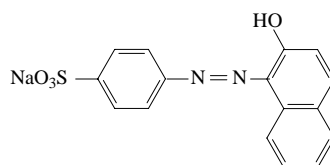
5.2.6 Acid Orange 12

1. Analysis of the Mass Spectrometric Fragmentation of Acid Orange 12

A question remained as to whether a dye which has a sulphonic group on the naphthalene ring follows the same rule for both the mass spectrometric fragmentation pattern and the fungal degradation pathway as do sulphonated azo dyes which have a sulphonic group on the benzene ring.



C.I. Acid Orange 12



C.I. Acid Orange 7

The mass spectrum of Acid Orange 12, which is an isomer of Acid Orange 7, exhibited the [M-Na]- peak m/z 327, as shown in Figure 5.36. The MS^n fragmentation of ions from m/z 341 is shown in Table 5.5. The formation of m/z 235 corresponds to the cleavage of the N-N single bond of the ketohydrazone form. This fragmentation pathway is the same as for Acid Orange 8 and Acid Orange 7. In the further MS^n fragmentation spectrum, the loss of -C=O (28

Da) from m/z 235 leads to the m/z 207 ion, corresponding to $-C=N-$ structure (Scheme 5.9). This pattern was confirmed by Borgerding (1994) by using deuterated ion at m/z 328. This showed ions at m/z 235 and m/z 207, indicating that the proton from the hydroxyl group is not a part of the fragment ions, supporting the structures given in Scheme 5.9. The MS^3 fragmentation of m/z 207 showed several low intensity ions at m/z 181 (loss of $-C=N-$), and m/z 143 (loss of SO_2) that rearranges to form 2-naphthanolate ion, shown by the existence of the characteristic fragmentation ion of m/z 115. The detailed fragmentation pattern of Acid Orange 12 is shown in Scheme 5.9.

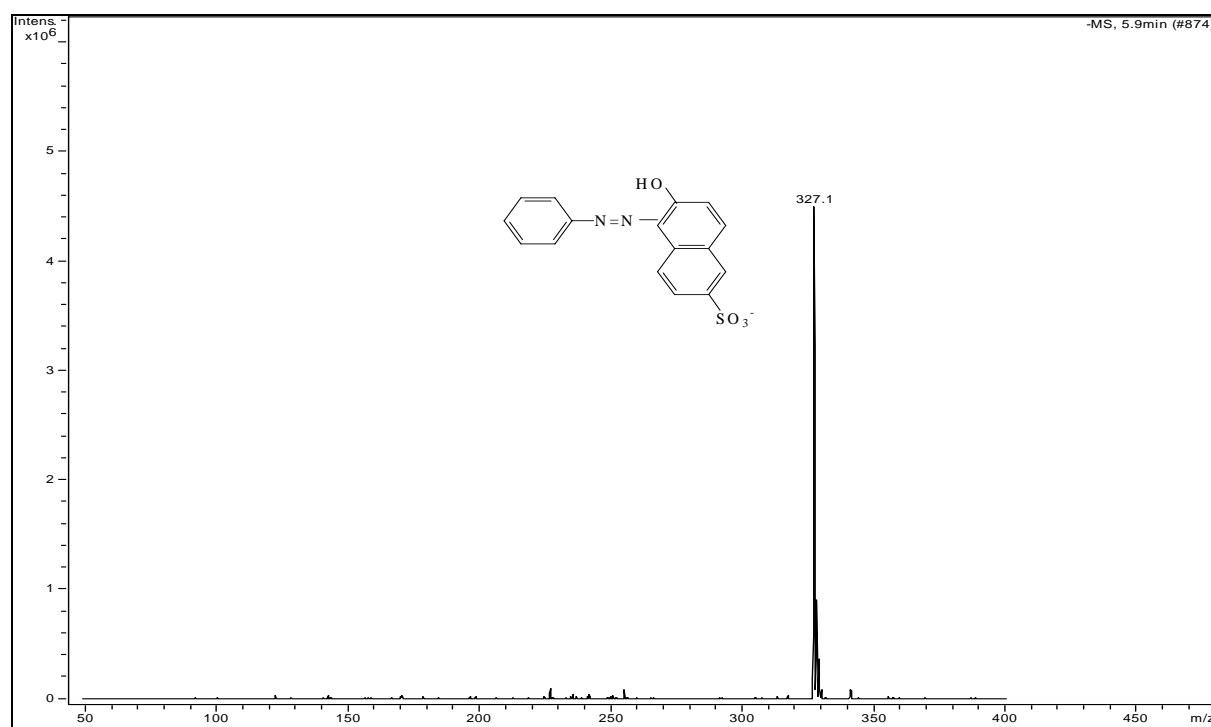


Figure 5.36 Mass Spectrum of Acid Orange 12 in the Negative Mode of ESI-MS

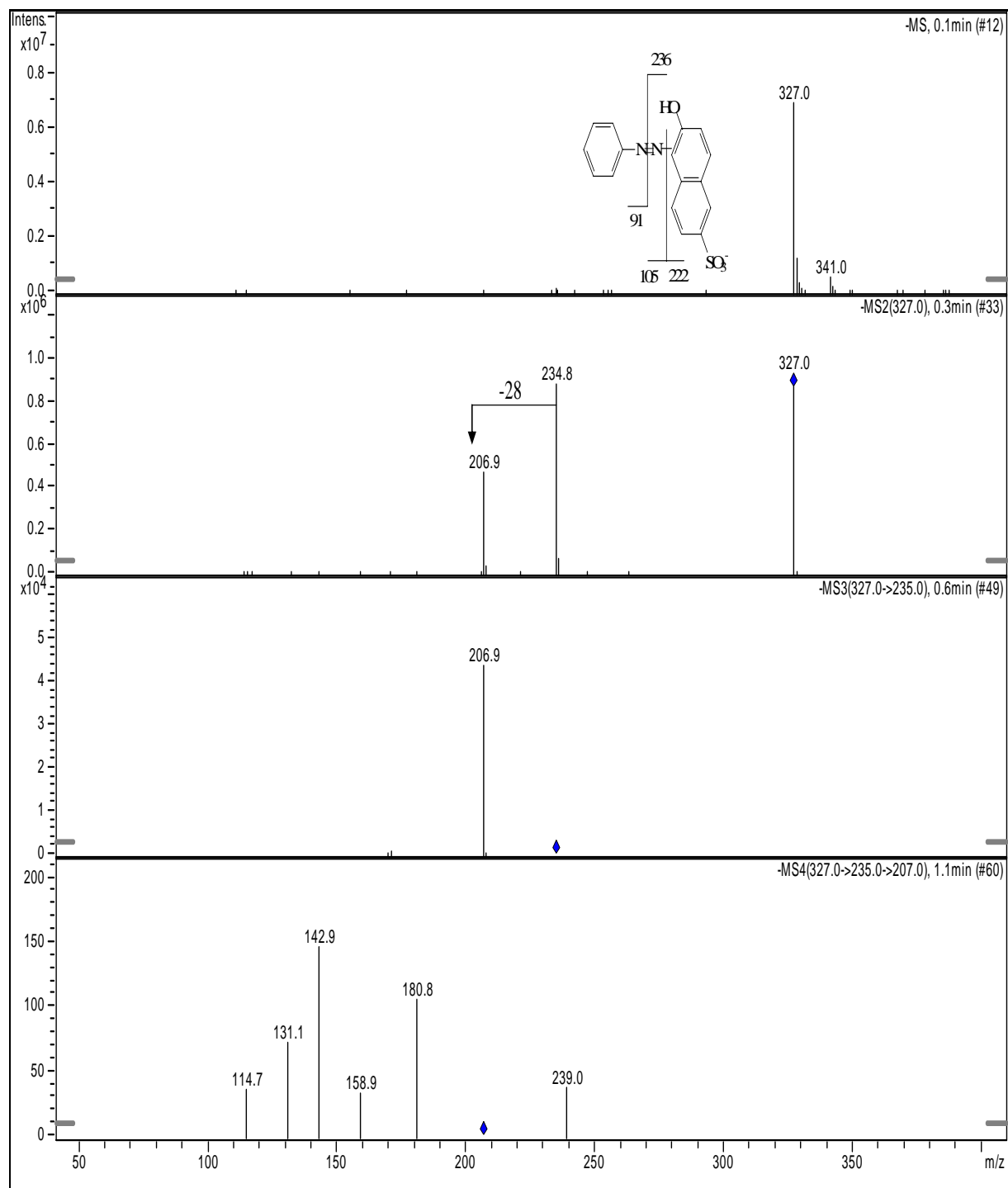
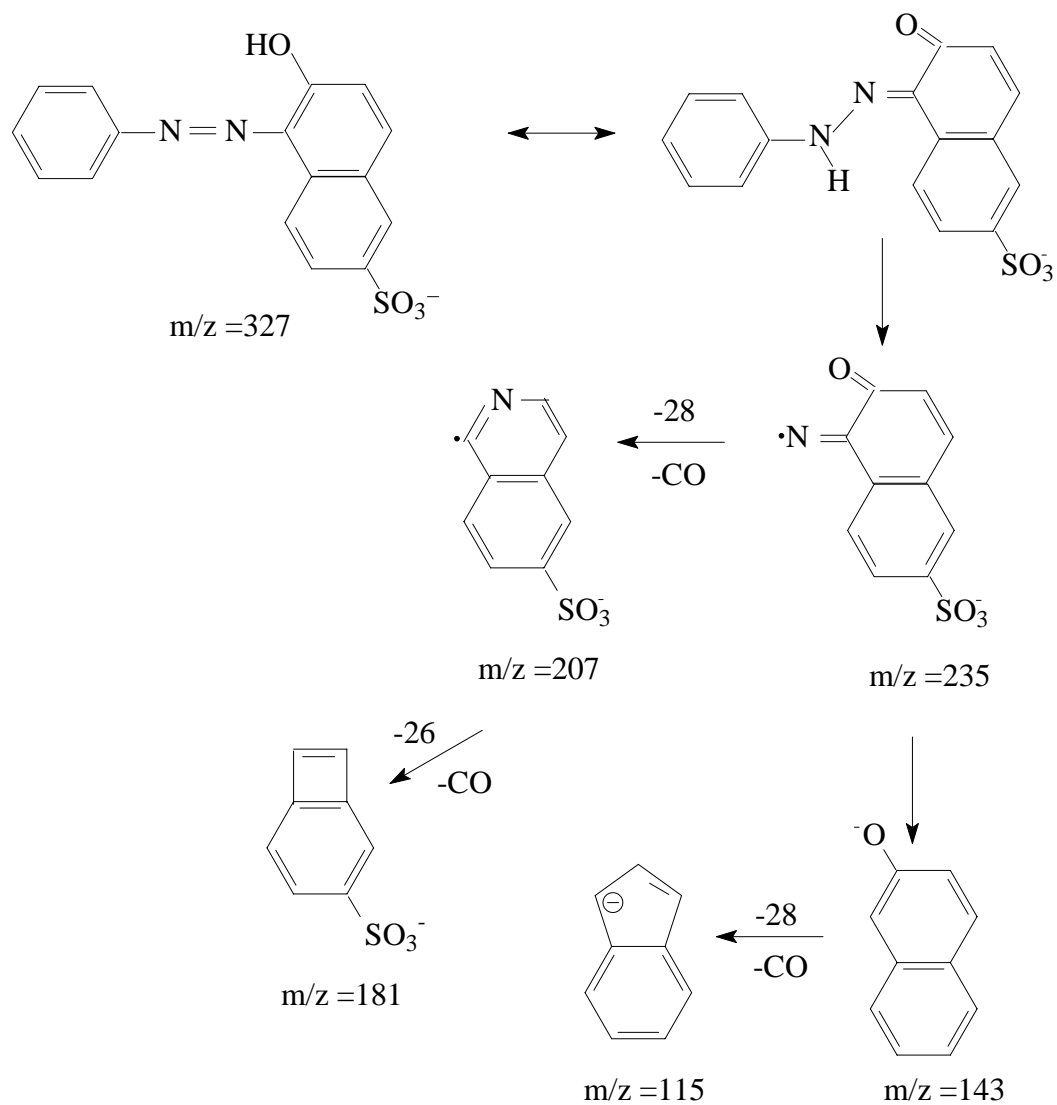


Figure 5.37 MSⁿ Fragmentation Ions of Peak m/z 327 - Acid Orange 12

Table 5.5 The MSⁿ Fragmentation of Ions from *m/z* 327 of Acid Orange 12

Parent ions , <i>m/z</i>	Relative Intensity (%)	Daughter ions, <i>m/z</i>
327	100	235, 207
235	100	207
207	50	181, 159, 143, 131, 115



Scheme 5.9 Proposed Fragmentation Pattern for Acid Orange 12

2. Identification of Fungal Degradation Products of Acid Orange 12 by CE-MS

Figure 5.38 is a typical electrophorogram of Acid Orange 12 treated by *Pleurotus ostreatus* (fourth day). Acid Orange 12 was identified as the sulphonated anion of the dye itself. The intensity of Acid Orange 12 was strong even after four day's treatment. After incubation in *Pleurotus ostreatus* culture for four days, there was a product peak at 25.7 min (Figure 5.38). The corresponding mass spectrum of this peak had its base peak at m/z 299 in Figure 5.39. The m/z 299 ion persisted after its formation in the fourth day. The 28 Da difference is probably a loss of CO from the dye. The MS² fragmentation of m/z 299 shows the m/z 235 ion due to loss of SO₂, and m/z 179 due to loss of a benzene ring and a CO₂. Based on the information above, we infer that the structure of m/z 299 is a five-membered ring whose structure is shown in Scheme 5.10. There is a major peak at m/z 260 in Figure 5.40. Unfortunately, no further structure information has been elucidated because of very short elution time. It was only able to get MS before peak eluted.

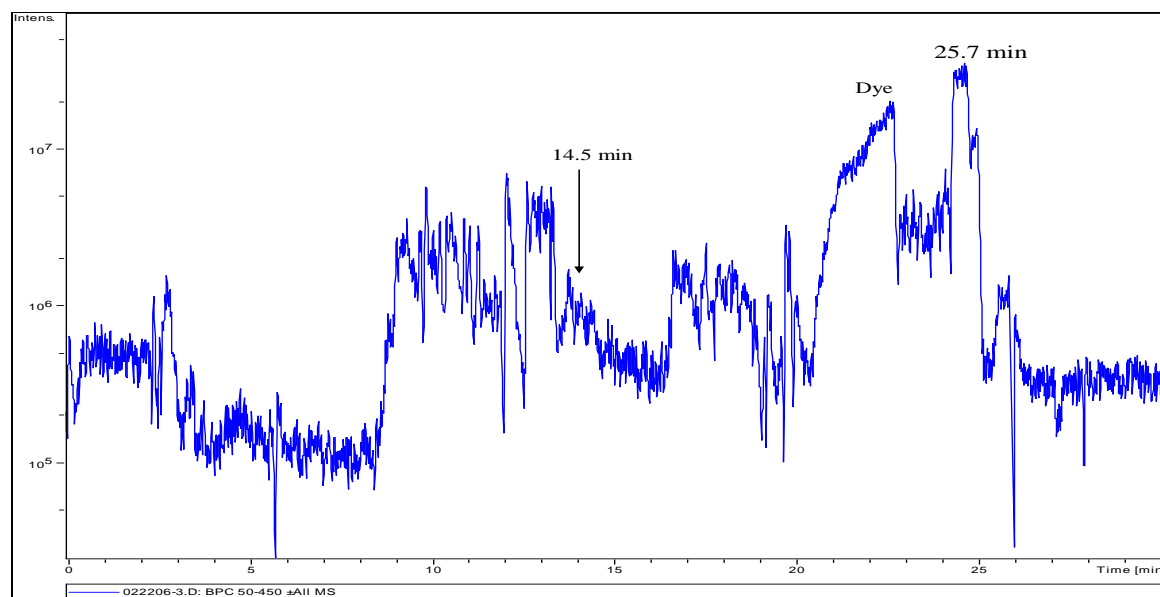


Figure 5.38 CE-ESI-MS Base Peak Chromatogram of Acid Orange 12 Treated by *Pleurotus ostreatus* (Fourth Day)

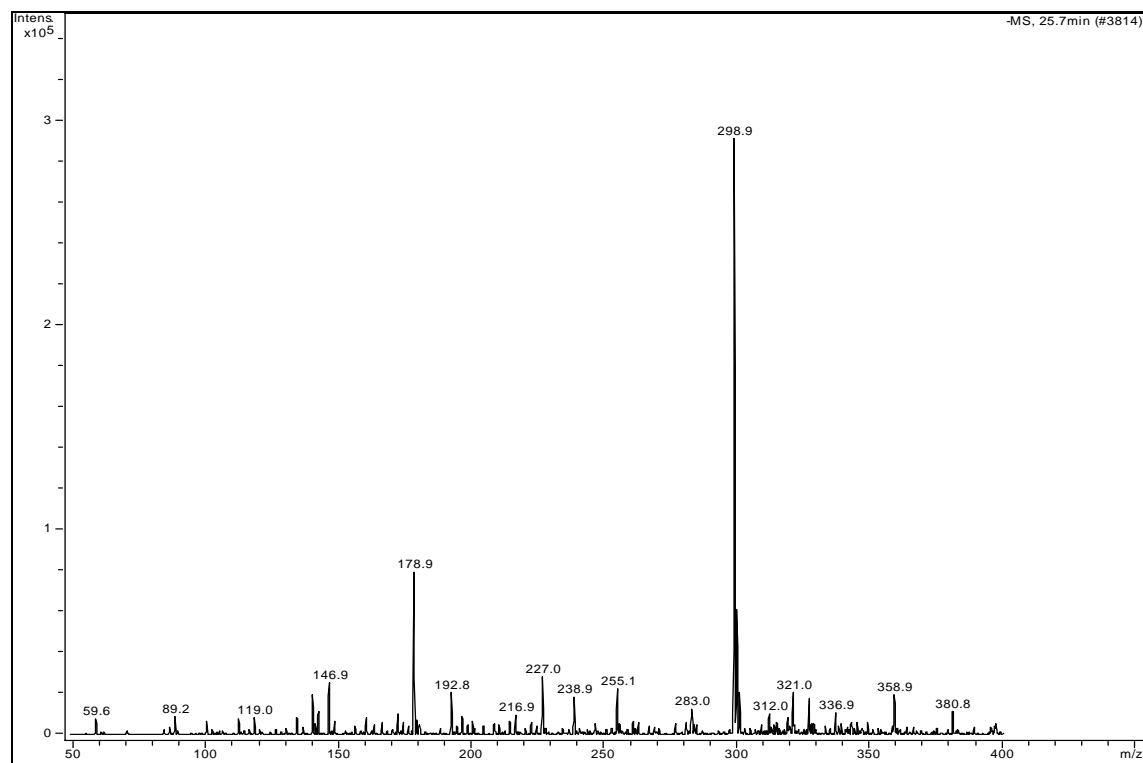


Figure 5.39 Mass Spectrum of Peak with the Retention Time of 25.7 min - Acid Orange 12 Treated by *Pleurotus ostreatus* (Fourth Day).

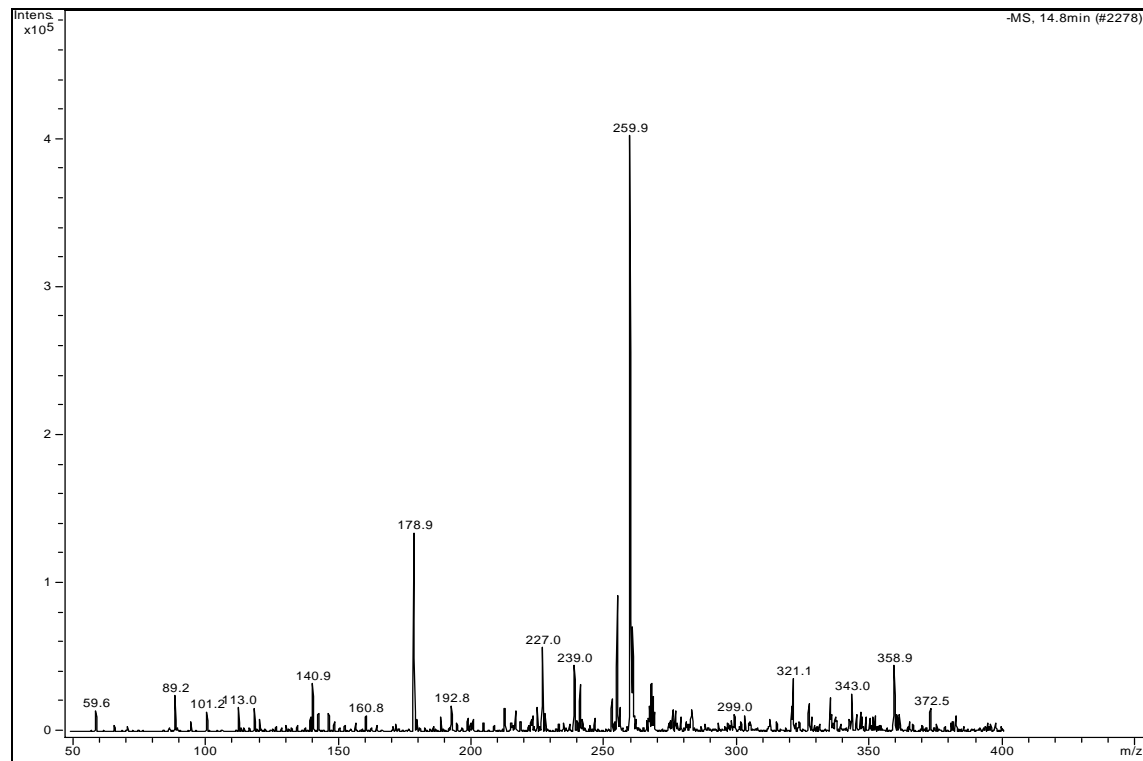
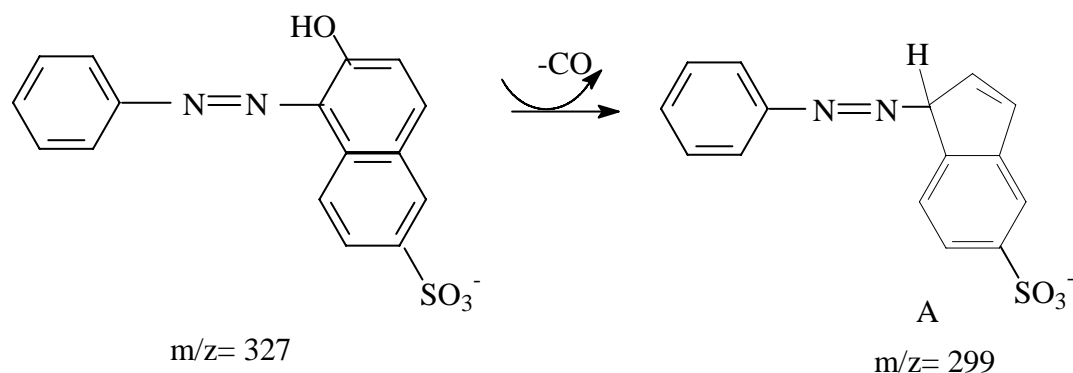


Figure 5.40 Mass Spectrum of Peak with the Retention Time of 14.5 min- Acid Orange 12 Treated by *Pleurotus ostreatus* (Fourth Day).



Scheme 5.10 Proposed Mechanism for the First Step in the Degradation of Acid Orange 12 Treated by *Pleurotus ostreatus*

5.2.7 Food Yellow 3

1. Analysis of the Mass Spectrometric Fragmentation of Food Yellow 3

The structure of Food Yellow 3 incorporates two sulphonic groups, one on each of the units connected by the azo bond. The mass spectra of multi-sulphonated dyes are much more complicated than those of monosulphonated dyes. The mass spectra of disulphonated dyes show de-cationized molecular ions with different charges, e.g. $[\text{M}-\text{Na}]^-$ and $[\text{M}-\text{Na}]^{2-}$. Figure 5. 41 is a typical ESI-MS spectra of the multi-sulphonated dye Food Yellow 3 recorded in the negative mode.

The ions at m/z 429, m/z 407, and m/z 203 are $[\text{M}-\text{Na}]^-$, $[\text{M}-2\text{Na}+\text{H}]^-$, and $[\text{M}-2\text{Na}]^{2-}$, respectively. The other ions (m/z 223, m/z 171, and m/z 142) were identified as 2-naphthanol-6-sulfonic acid, 4-amino-benzensulfonic acid and 2-naphthol, respectively. The MSⁿ fragmentation of Food Yellow 3 is shown in Figure 5.42, while the corresponding fragmentation pattern is shown in Scheme 5.11. Most of these fragmentation ions are also found in the fragmentation pattern of Acid Orange 7 and Acid Orange 12, because the left side of Food Yellow 3 molecule is the same as that of Acid Orange 7, while the right side of Food Yellow 3 is

the same of that of Acid Orange 12. The fragmentation pattern of Food Yellow 3 is the same as Acid Orange 7 and Acid Orange 12.

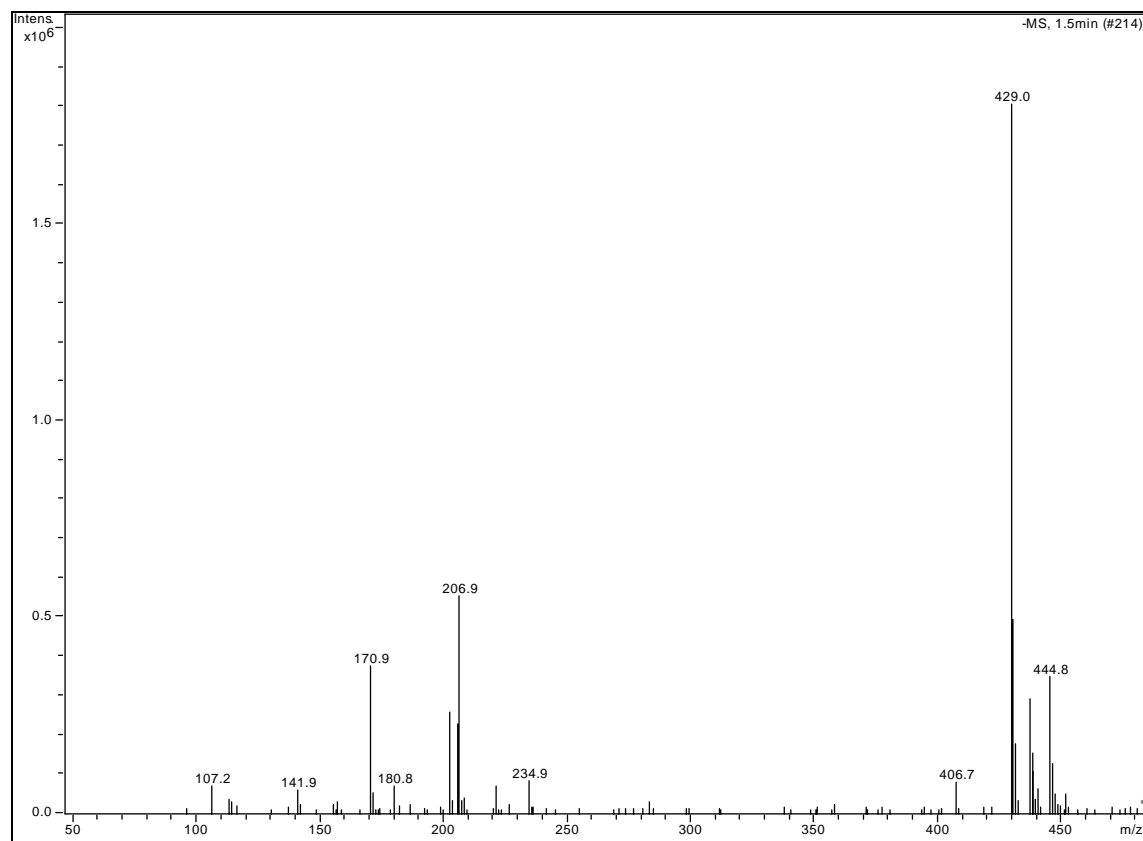
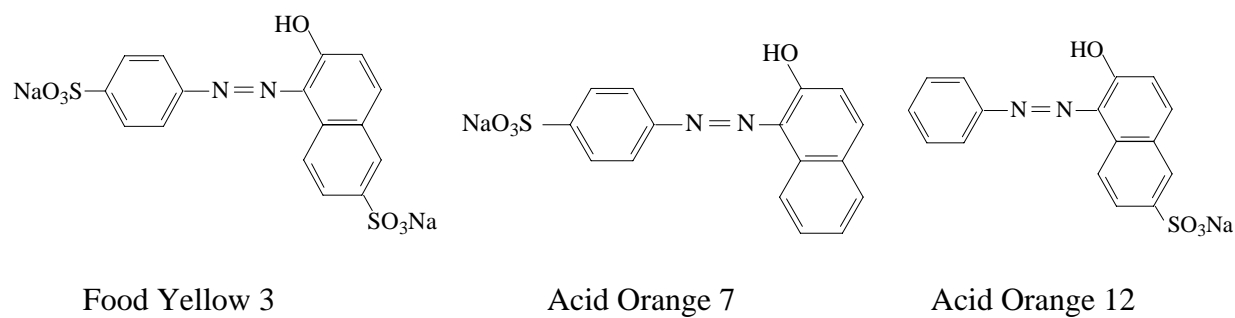


Figure 5.41 ESI-MS Mass Spectrum of Food Yellow 3 in the Negative Mode.

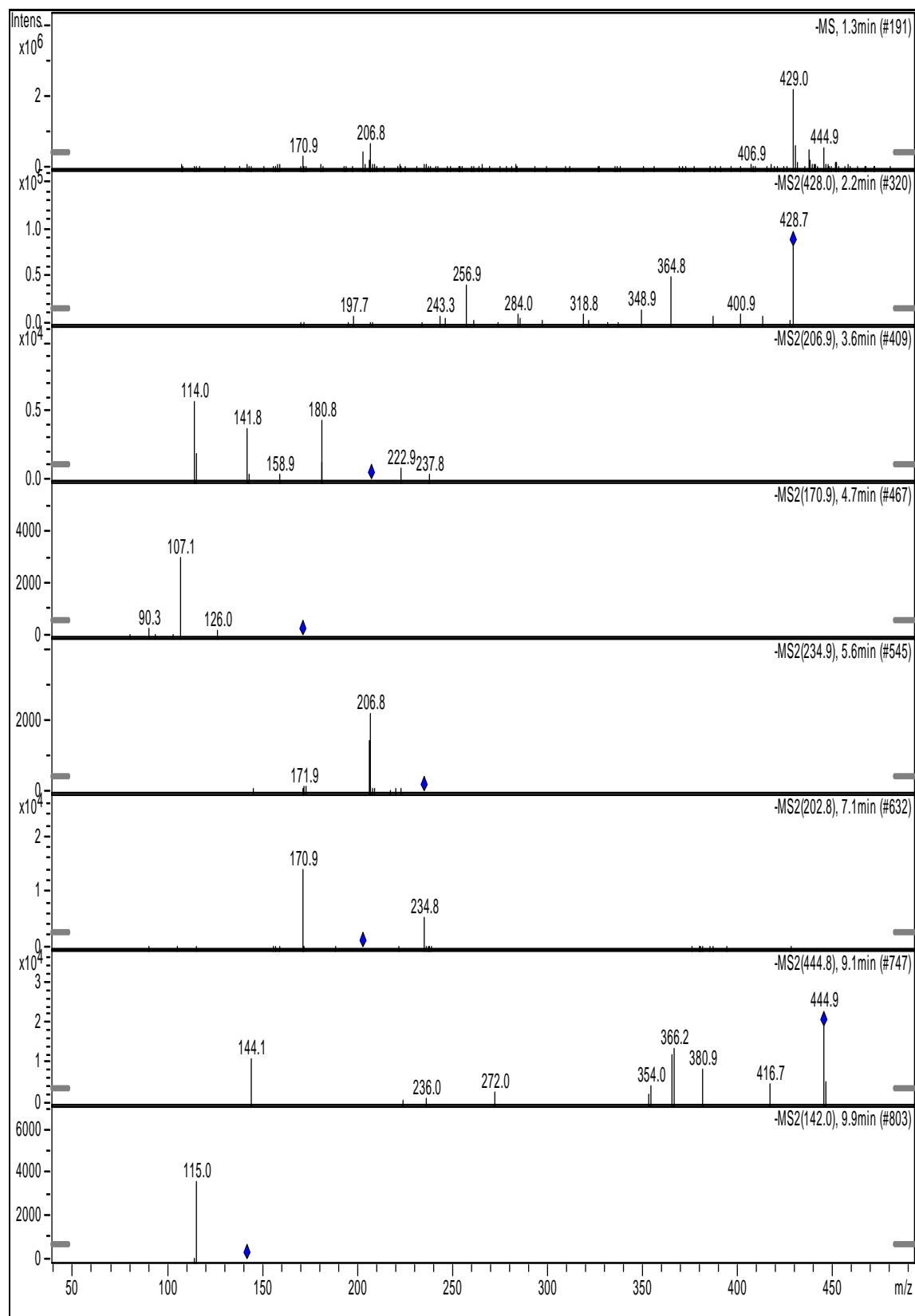
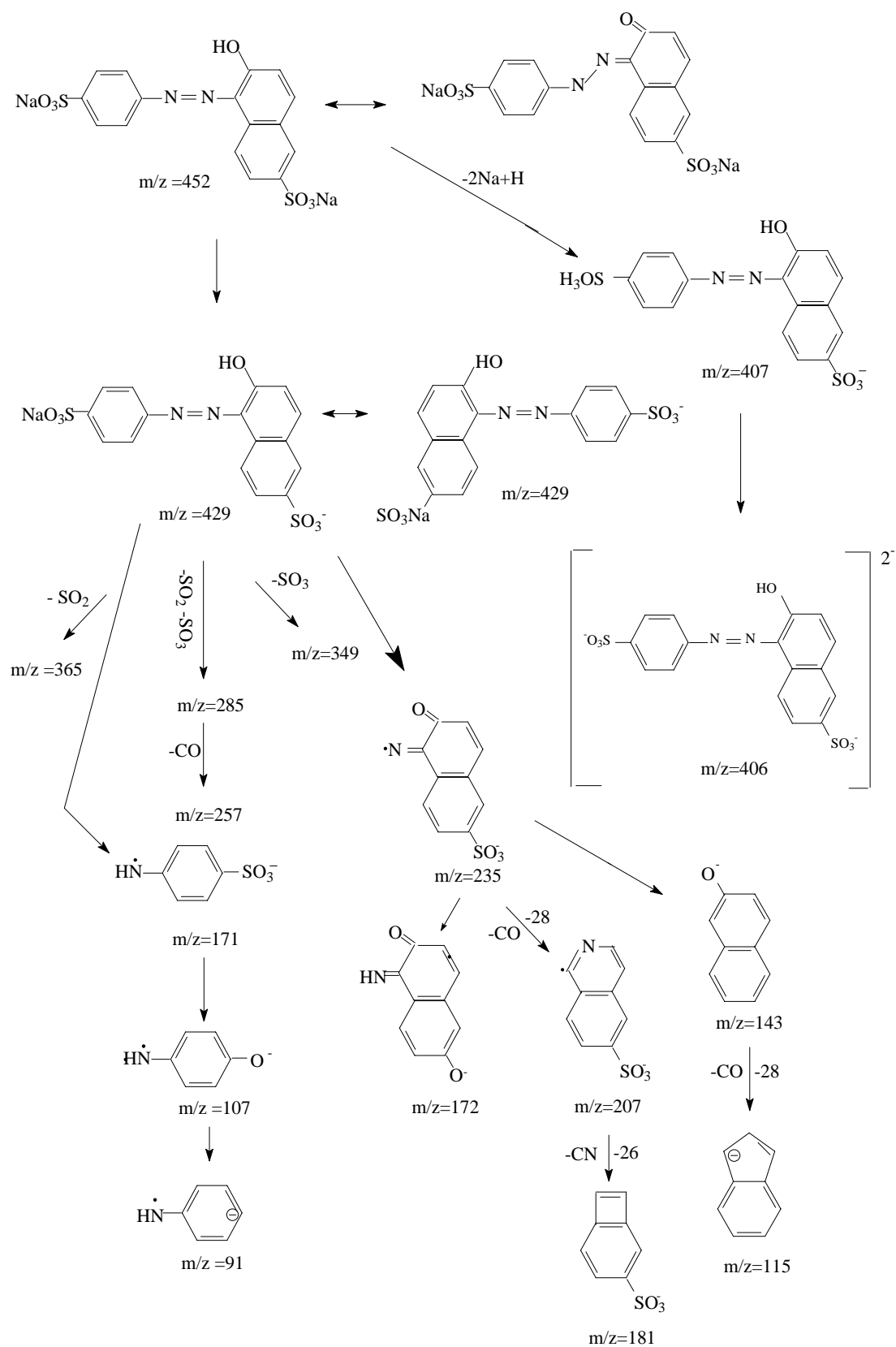


Figure 5.42 MSⁿ Fragmentation Spectrum of Food Yellow 3



Scheme 5.11 Proposed Fragmentation Pattern of Food Yellow 3

2. Identification of Fungal Degradation Products of Food Yellow 3 by CE-MS

After one day incubation in *Pleurotus ostreatus* culture, there were three potential product peaks at migration times of 11.1, 13.6 and 16.1 min (Figure 5.43). The corresponding mass spectra of these CE peaks have their base peaks at m/z 237, m/z 157 and m/z 173 respectively in Figure 5.44, 5.45, and 5.46. The peak at m/z 237 was identified as 1, 2-naphthoquinone-6-sulfonic acid. The existence of 1, 2-naphthoquinone-6-sulfonic acid again shows the degradation pathway of sulphonated azo dyes by cleavage of N-N bond of the ketohydrazone forms. The ions m/z 157 and m/z 173 were identified as benzenesulfonic acid and 4-hydroxybenzenesulfonic acid. The degradation pathway of Food Yellow 3 was the same as Acid Orange 7. After three days incubation in *Pleurotus ostreatus* culture, besides the products we had identified, there was one more product peak at a migration time of 14.7 min (Figure 5.47). The corresponding mass spectrum of this CE peak had its base peak at m/z 245 (Figure 5.48). Since the m/z 245 is a large molecule, it cannot be from the left side of Food Yellow 3. When Storm (2002) studied the ozonation oxidation of naphthalene-1,5-disulfonic acid, several oxidation products were isolated and identified. Among these, 3-sulfonic-phthalic acid was a major product. After referring to other literature and calculating the molecular weight, it was concluded that the structure of m/z 245 was 3-sulfonic-phthalic acid, as shown in Scheme 5.12. The formation of 3-sulfonic-phthalic acid is responsible for the oxidation of 1, 2-naphthoquinone-6-sulfonic acid.

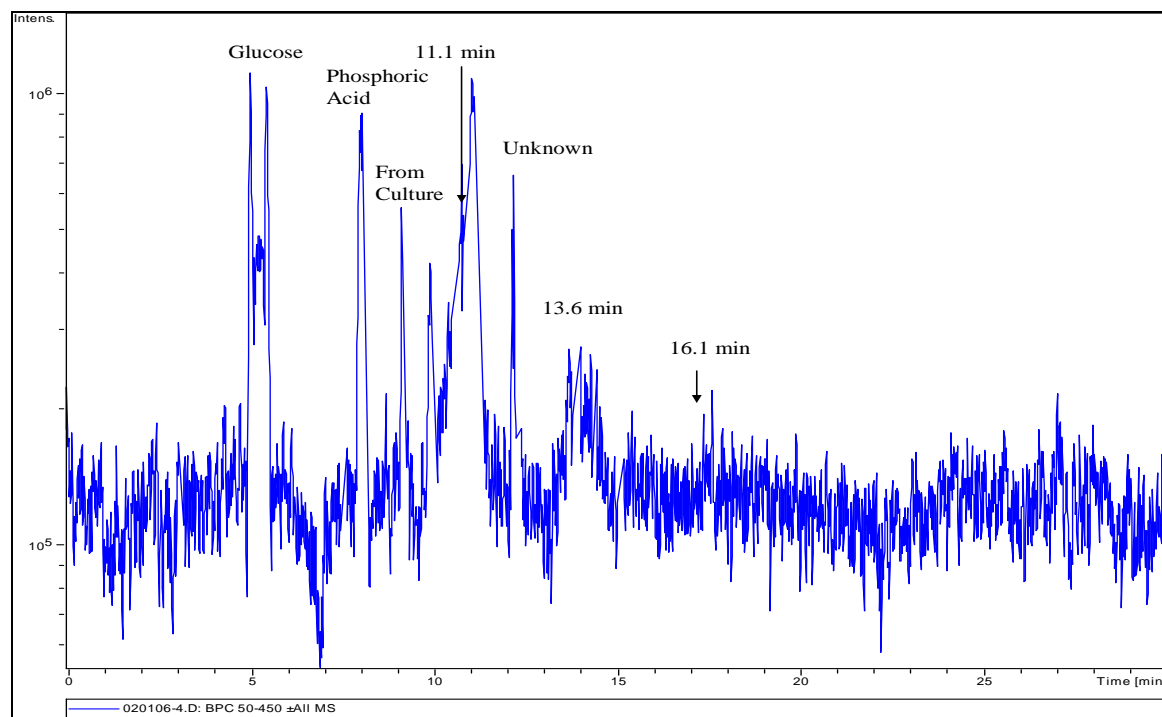


Figure 5.43 CE-ESI-MS Base Peak Chromatogram of Food Yellow 3 Treated by *Pleurotus ostreatus* (First Day)

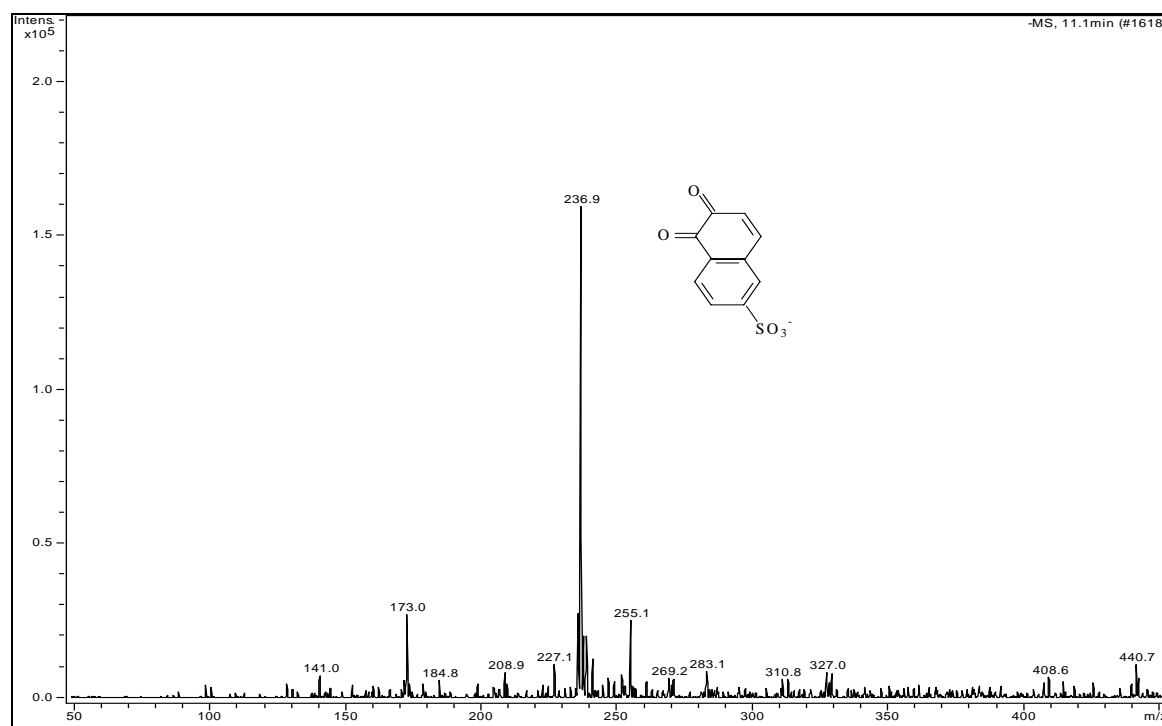


Figure 5.44 Mass Spectrum of Peak with the Retention Time of 11.1 min - Food Yellow 3 Treated by *Pleurotus ostreatus* (First Day).

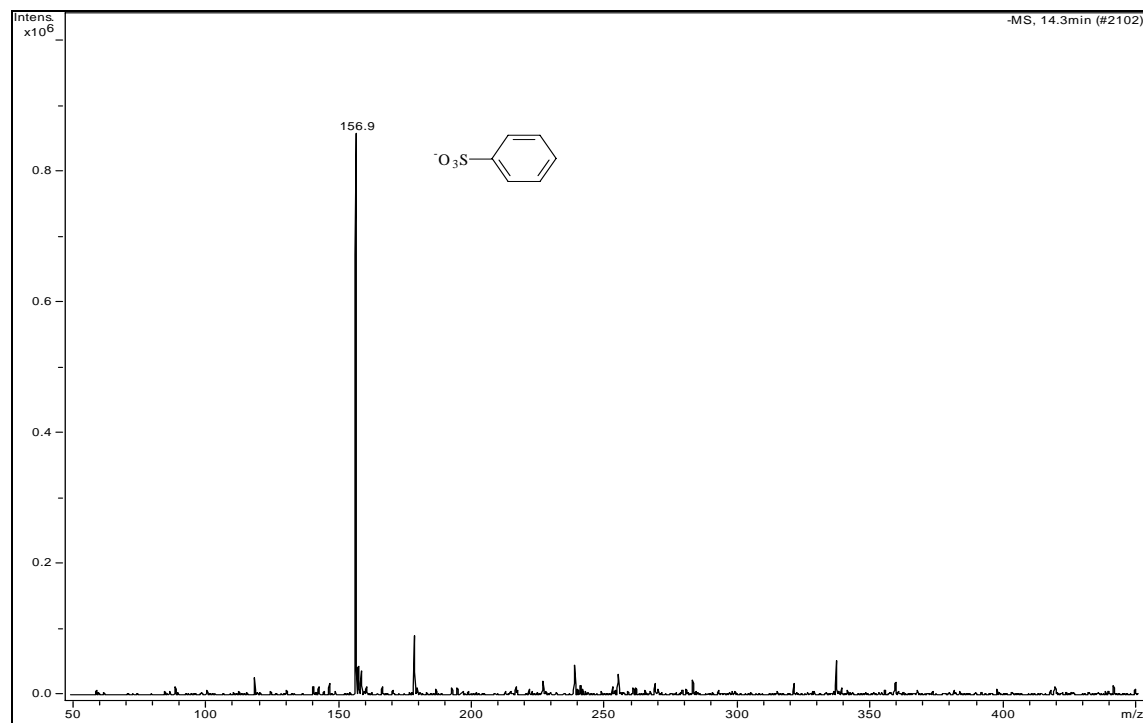


Figure 5.45 Mass Spectrum of Peak with the Retention Time of 13.6 min - Food Yellow 3 Treated by *Pleurotus ostreatus* (First Day)

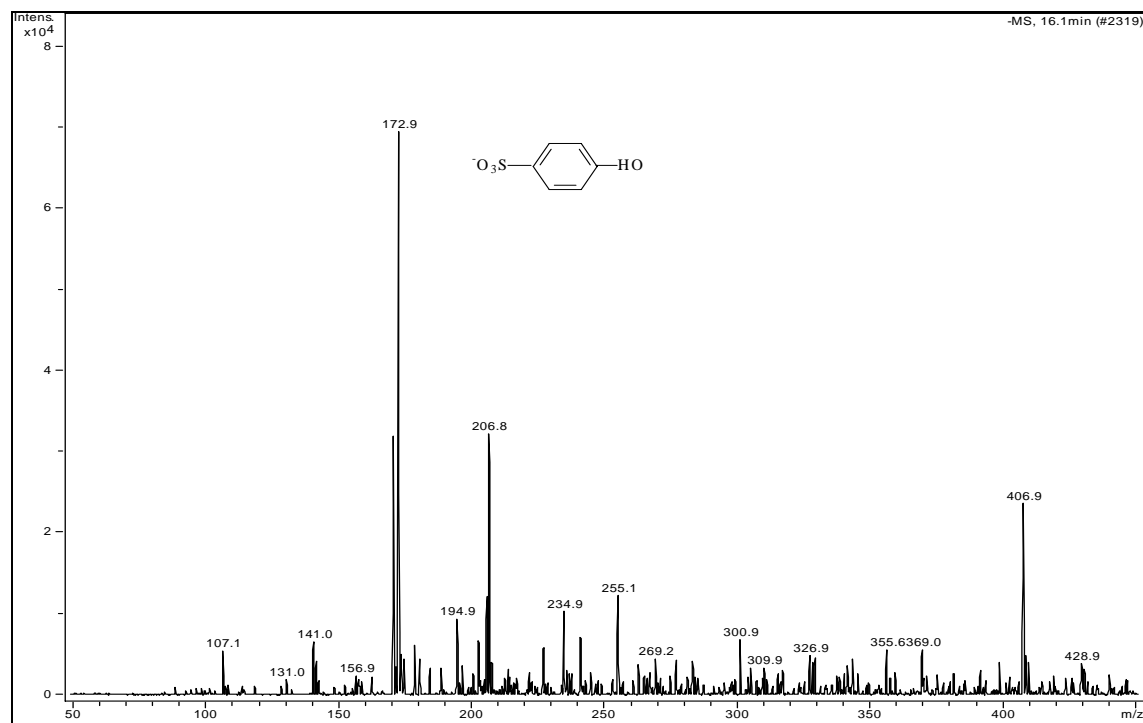


Figure 5.46 Mass Spectrum of Peak with the Retention Time of 16.1 min - Food Yellow 3 Treated by *Pleurotus ostreatus* (First Day).

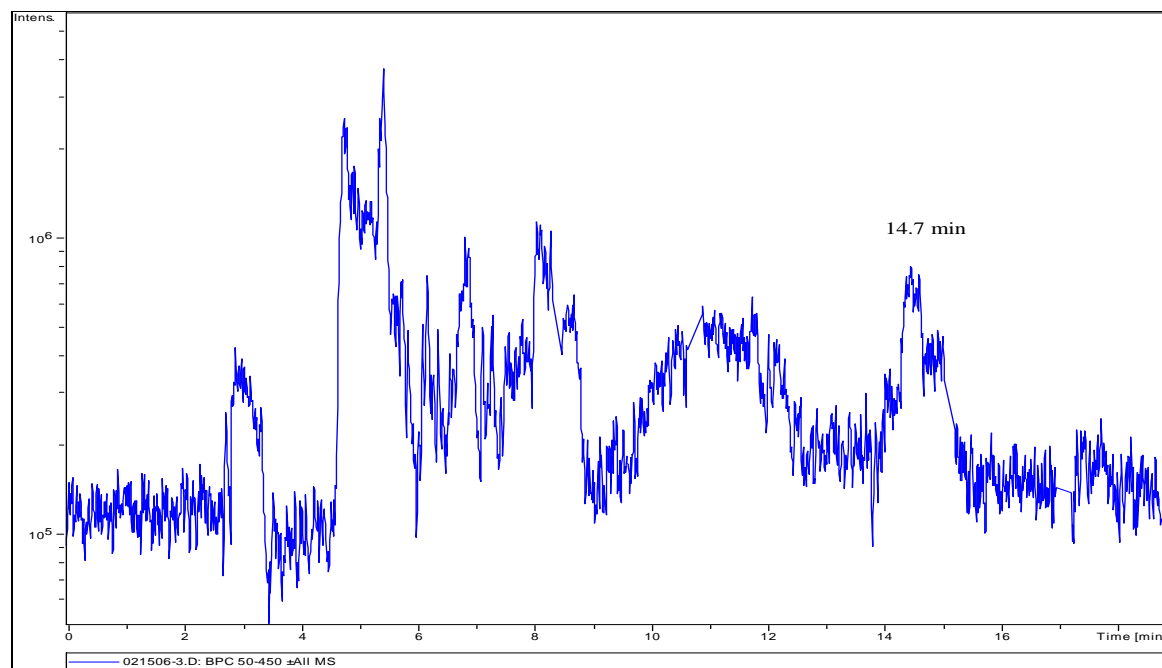


Figure 5.47 CE-ESI-MS Base Peak Chromatogram of Food Yellow 3 Treated by *Pleurotus ostreatus* (Third Day).

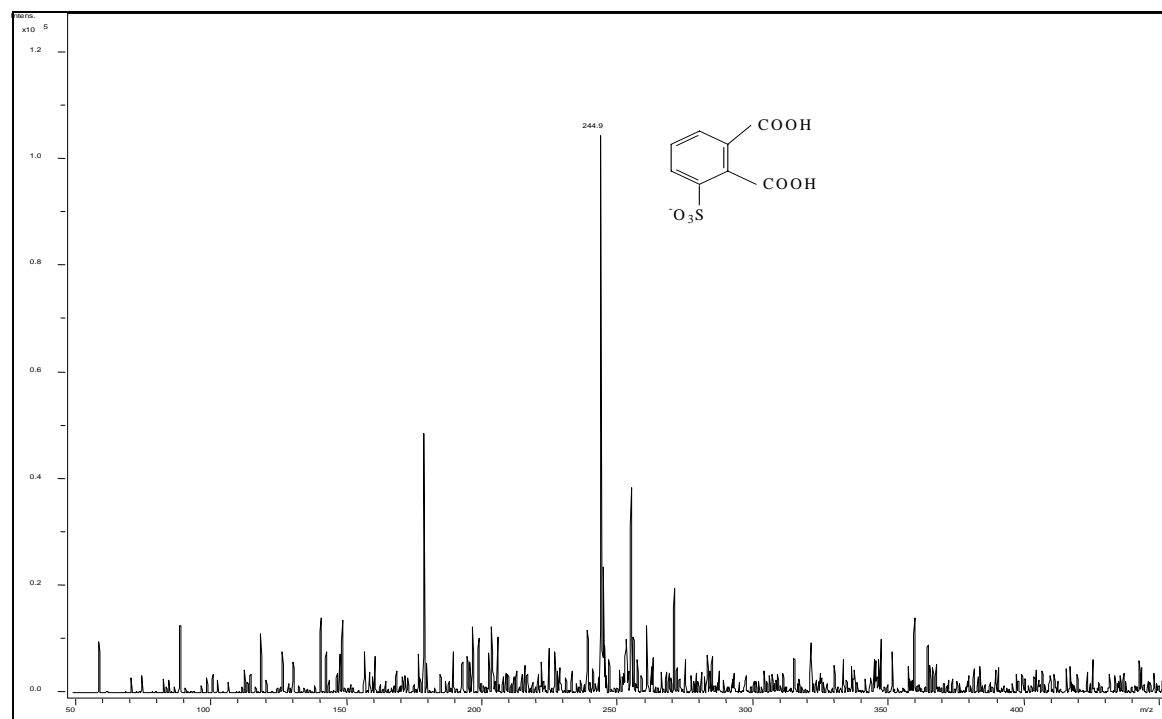
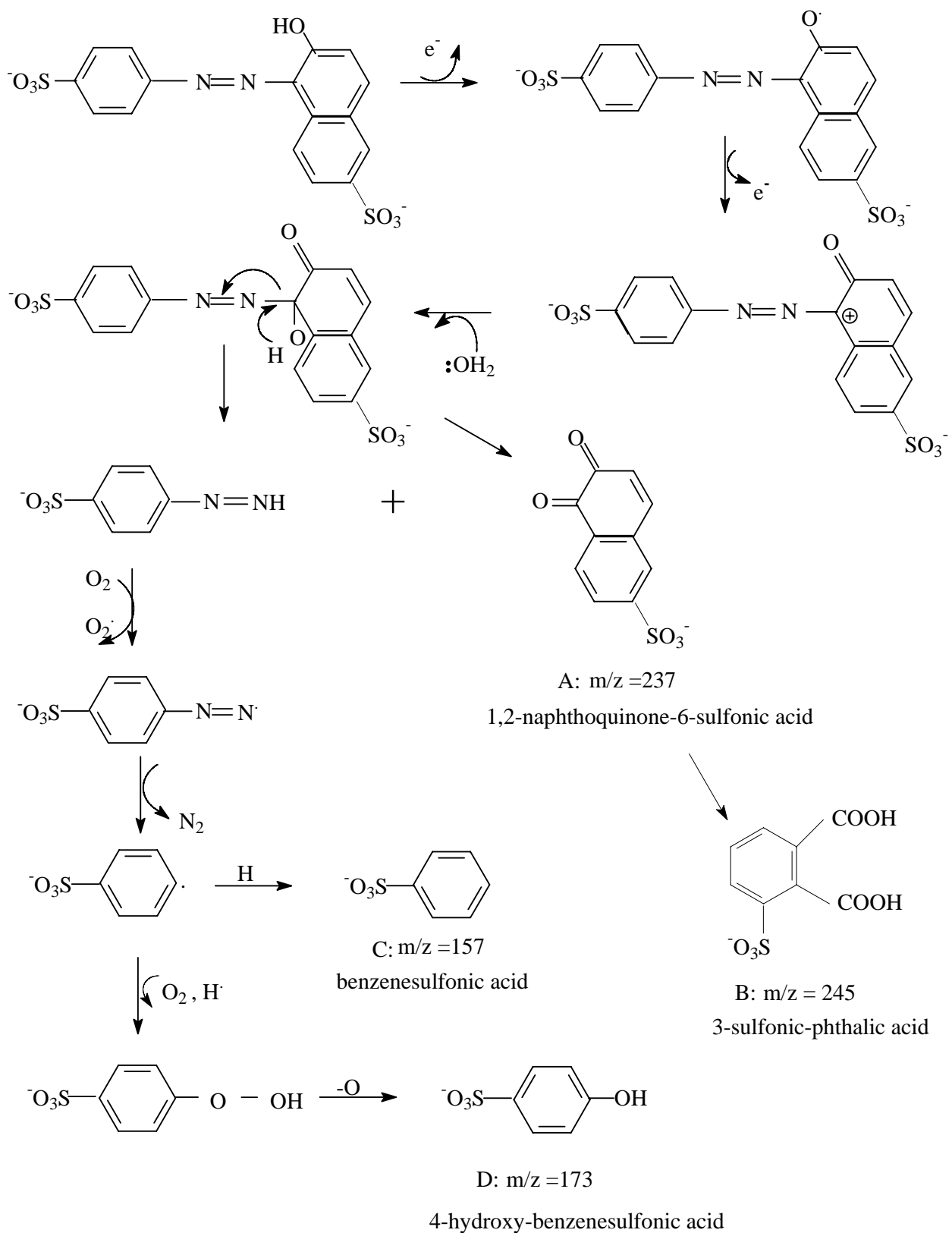
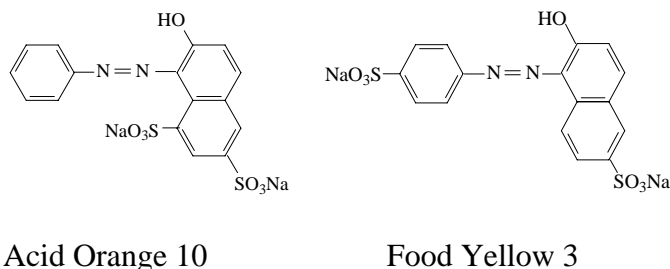


Figure 5.48 Mass Spectrum of Peaks with the Retention Time of 14.7 min - Food Yellow 3 Treated by *Pleurotus ostreatus* (Third Day).



Scheme 5.12 Proposed Mechanism for the Degradation of Food Yellow 3 by *Pleurotus ostreatus*

5.2.8 Acid Orange 10



Acid Orange 10 is an isomer of Food Yellow 3. The mass spectrum of Acid Orange 10 shows $[M-\text{Na}]^-$ and $[M-2\text{Na}+\text{H}]^-$ at m/z 429 and m/z 407 in Figure 5. 49. The MS^n fragmentation of Acid Orange 10 is too complicated to explain at this point (Figure 5.50). The degradation products of Acid Orange 10 treated by white rot fungus are also complicated to explain. The structure of m/z 325 which was found in the third day was identified and shown in Figure 5.51. There is m/z 167 ion in the third day's degradation solution whose structure was not identified (Figure 5.52). So far, the degradation pathway is not clearly understood. However, one thing that is definitely clear is that the Acid Orange 10 degradation pathway differs from any pathways discussed previously in this study.

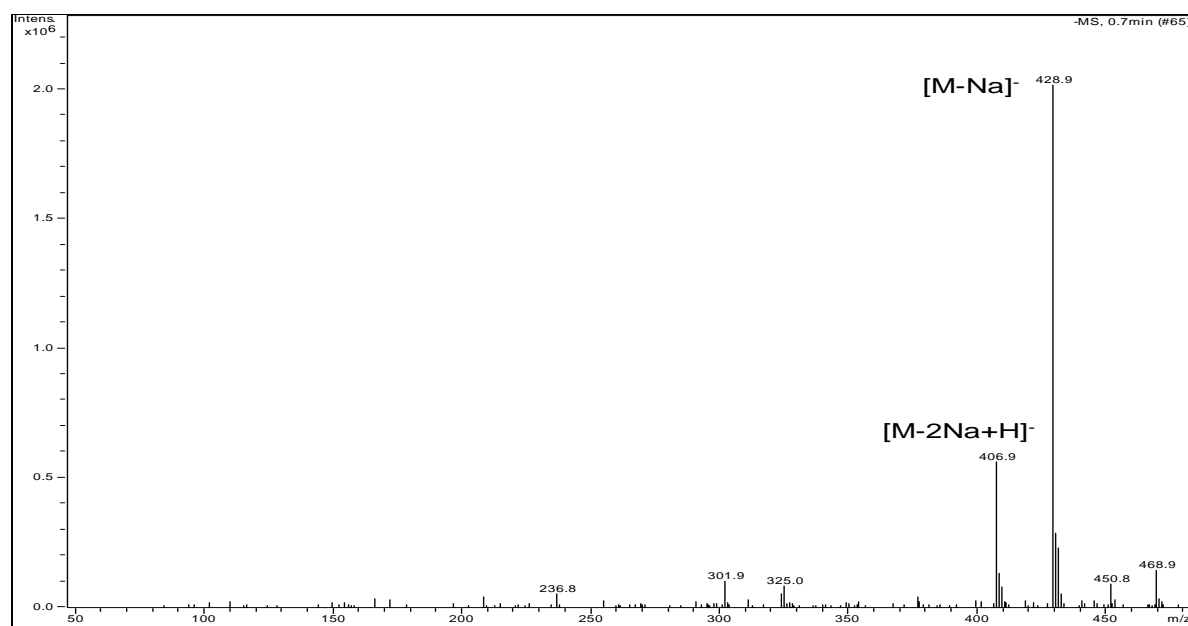


Figure 5.49 ESI-MS Mass Spectrum of Acid Orange 10 in the Negative Mode.

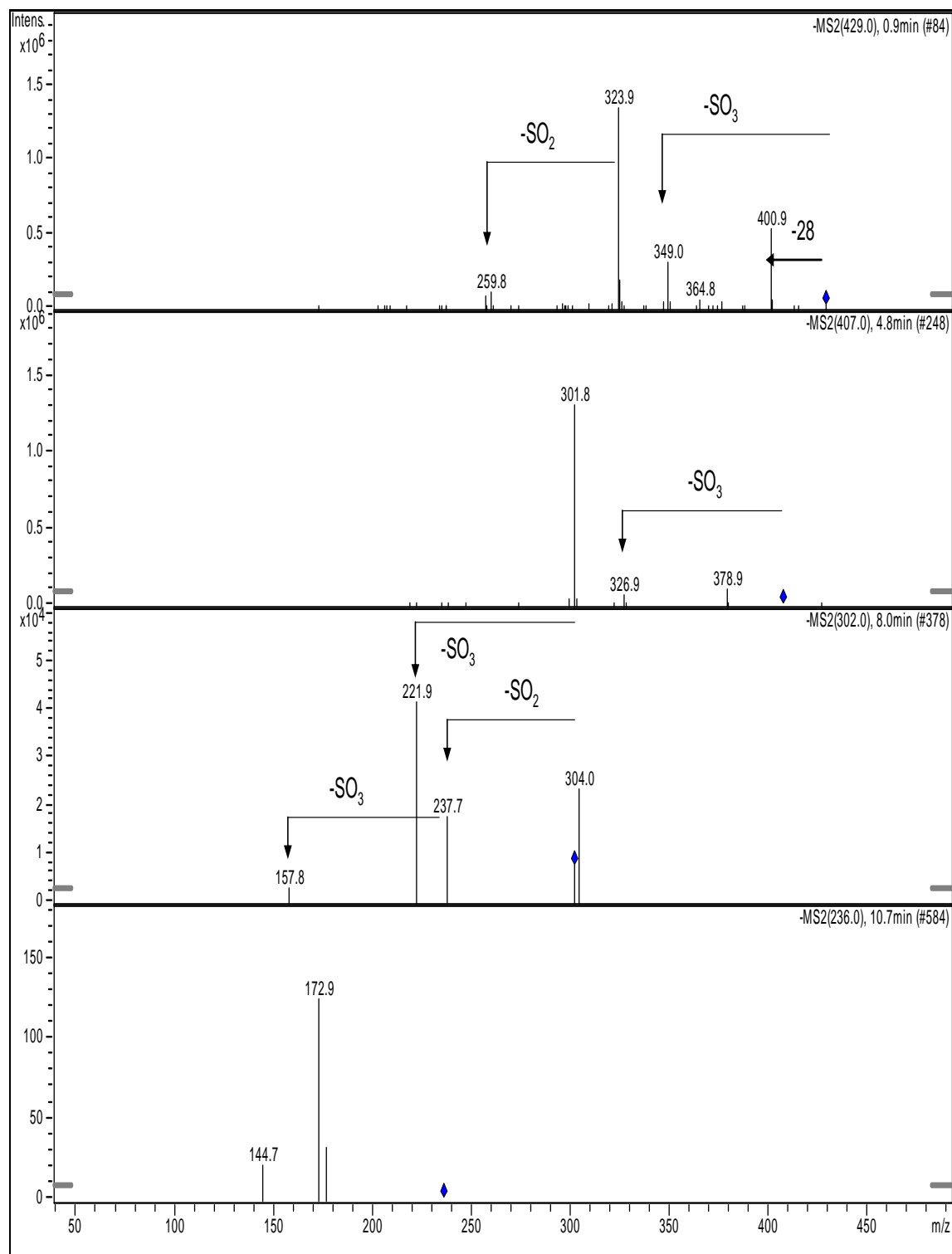


Figure 5.50 MSⁿ Fragmentation Spectrum of Acid Orange 10.

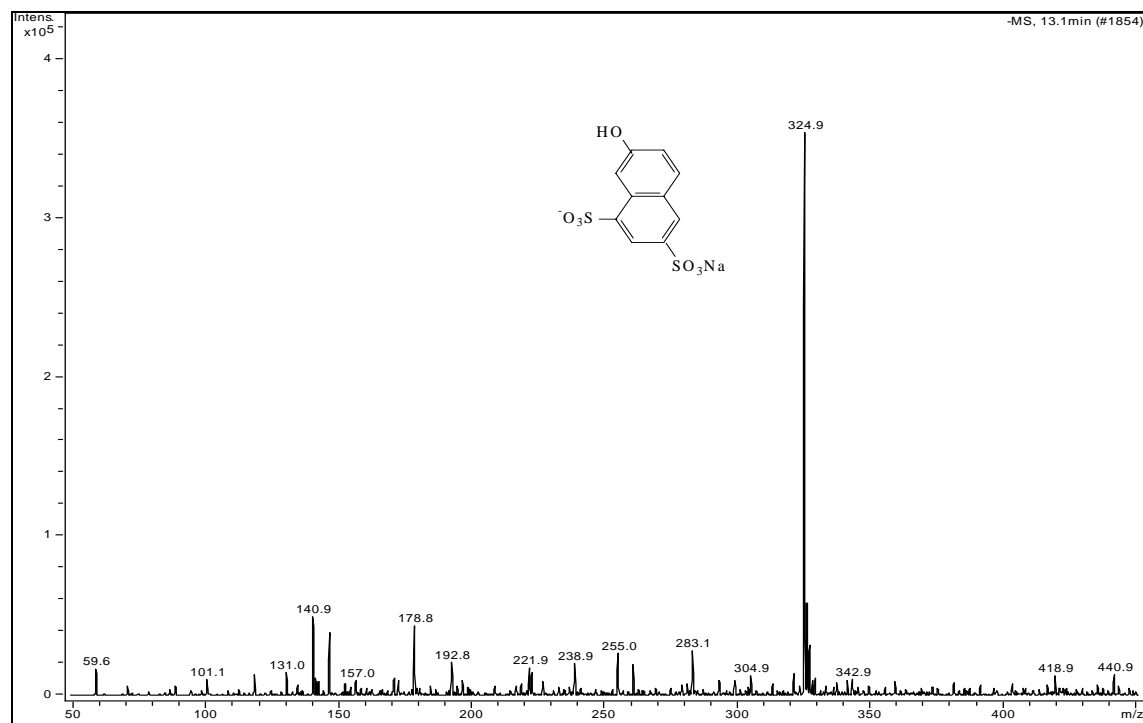


Figure 5.51 Mass Spectrum of Peak with the Retention Time of 13.1 min - Acid Orange 10 Treated by *Pleurotus ostreatus* (Third Day).

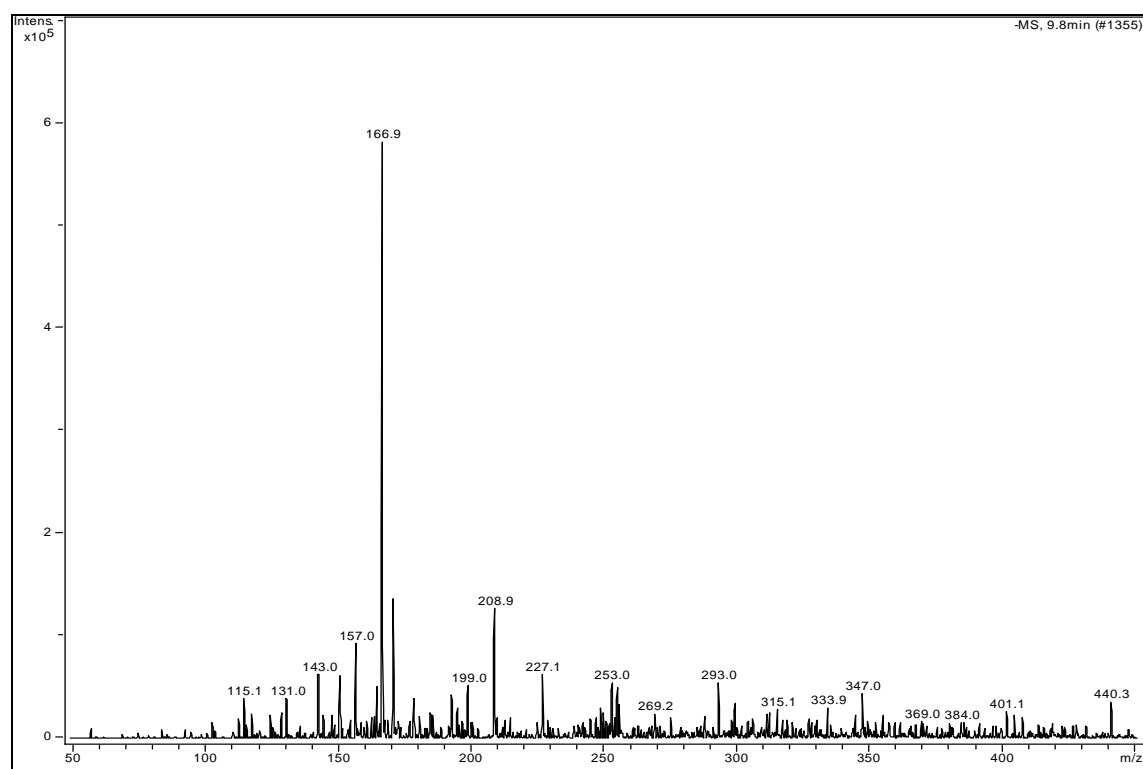
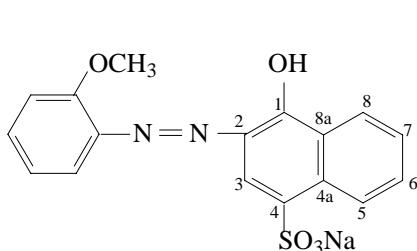


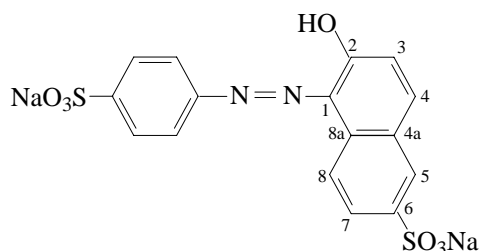
Figure 5.52 Mass Spectrum of Peak with the Retention Time of 9.8 min - Acid Orange 10 Treated by *Pleurotus ostreatus* (Third Day).

5.2.9 Acid Red 4

The azo group of Acid Red 4 is connected to the 2 position of the naphthalene ring while the azo bonds of other dyes we have discussed previously connect at the 1 position of the naphthalene rings.



Acid Red 4



Food Yellow 3

The mass spectrometric fragmentation pattern of Acid Red 4 is also different from the other dyes. The MS fragmentation of Acid Red 4 is shown in Figure 5.53. The m/z 357, [M-Na]⁻ peak is the only observed ion. Typical fragments m/z 342, m/z 277, m/z 171, and m/z 170 are observed as a result of fragmentation. The MSⁿ fragmentation of Ions from m/z 357 is shown in Table 5.6.

The formation of m/z 342 is due to loss of methyl group from the benzene ring. The further fragmentation of ion of m/z 342 results in ions of m/z 278 and 171. The formation of m/z 278 is caused by loss of SO₂, then producing m/z 250 by loss of another CO (28 Da). The further ion from m/z 171 results in m/z 143 by loss of N₂, which is 2-naphthol because of the existence of the characteristic ion of m/z 115 due to loss of CO (28 Da). The formation of the large peak at m/z 277 corresponds to the loss of SO₃ ion from the dye. The further cleavage of azo bond at the benzene ring side results in the formation of m/z 170. The detailed scheme of fragmentation for Acid Red 4 is shown in Scheme 5.13. Since there are so many unknown peaks in the Acid Red 4 degradation products, no further degradation pathway is proposed at this point.

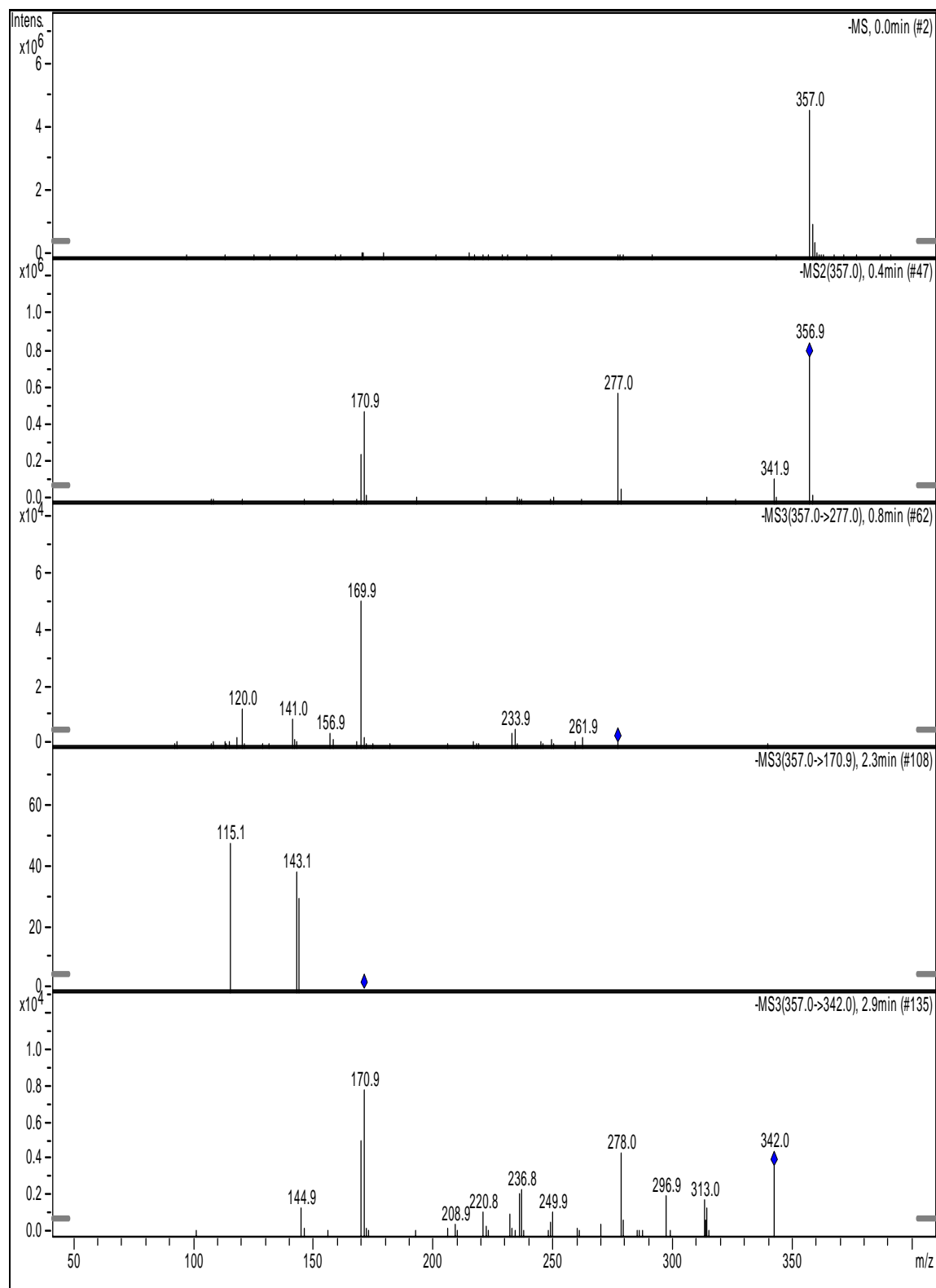
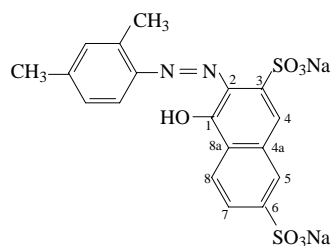


Figure 5.53 The MS^n Fragmentation of Ions from Acid Red 4

Table 5.6 The MSⁿ Fragmentation of Ions from Acid Red 4 at *m/z* 357

Parent ions , <i>m/z</i>	Relative Intensity (%)	Daughter ions, <i>m/z</i>
357	100	342, 277, 171, 170
342	12.5	278, 250, 171
277	62.5	170
171	50	N/A
170	25	143, 115

5.2.10 Acid Red 8



Acid Red 8

The structure of Acid Red 8 is also different from the other dyes. The azo group of Acid Red 8 is connected to the 2 position of the naphthalene ring. Figure 5.54 is a typical ESI-MS spectra of the multi-sulphonated dye Acid Red 8 recorded in the negative mode. The ions at m/z 457, m/z 435, and m/z 217 are $[M-Na]^-$, $[M-2Na+H]^-$, and $[M-2Na]^{2-}$, respectively. The MSⁿ fragmentation of Acid Red 8 is shown in Figure 5.55, while the corresponding fragmentation pattern is shown in Scheme 5.14.

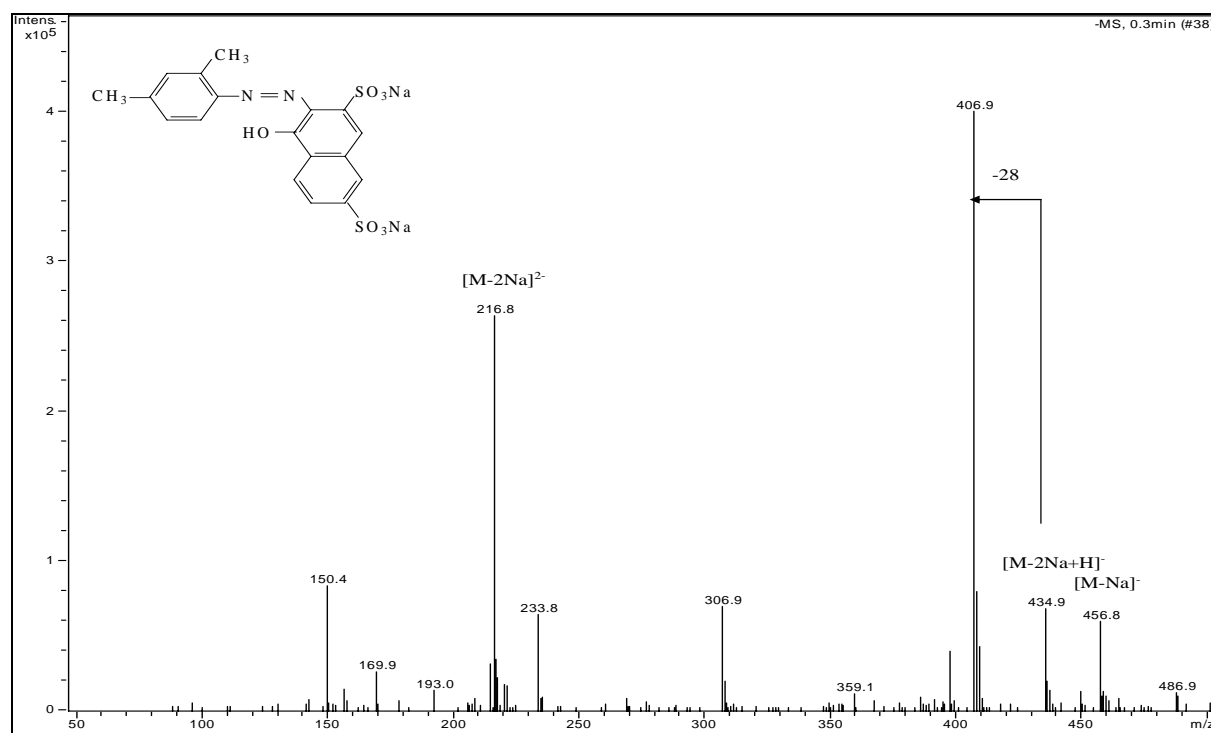


Figure 5.54 ESI-MS Mass Spectrum of Acid Red 8 in the Negative Mode.

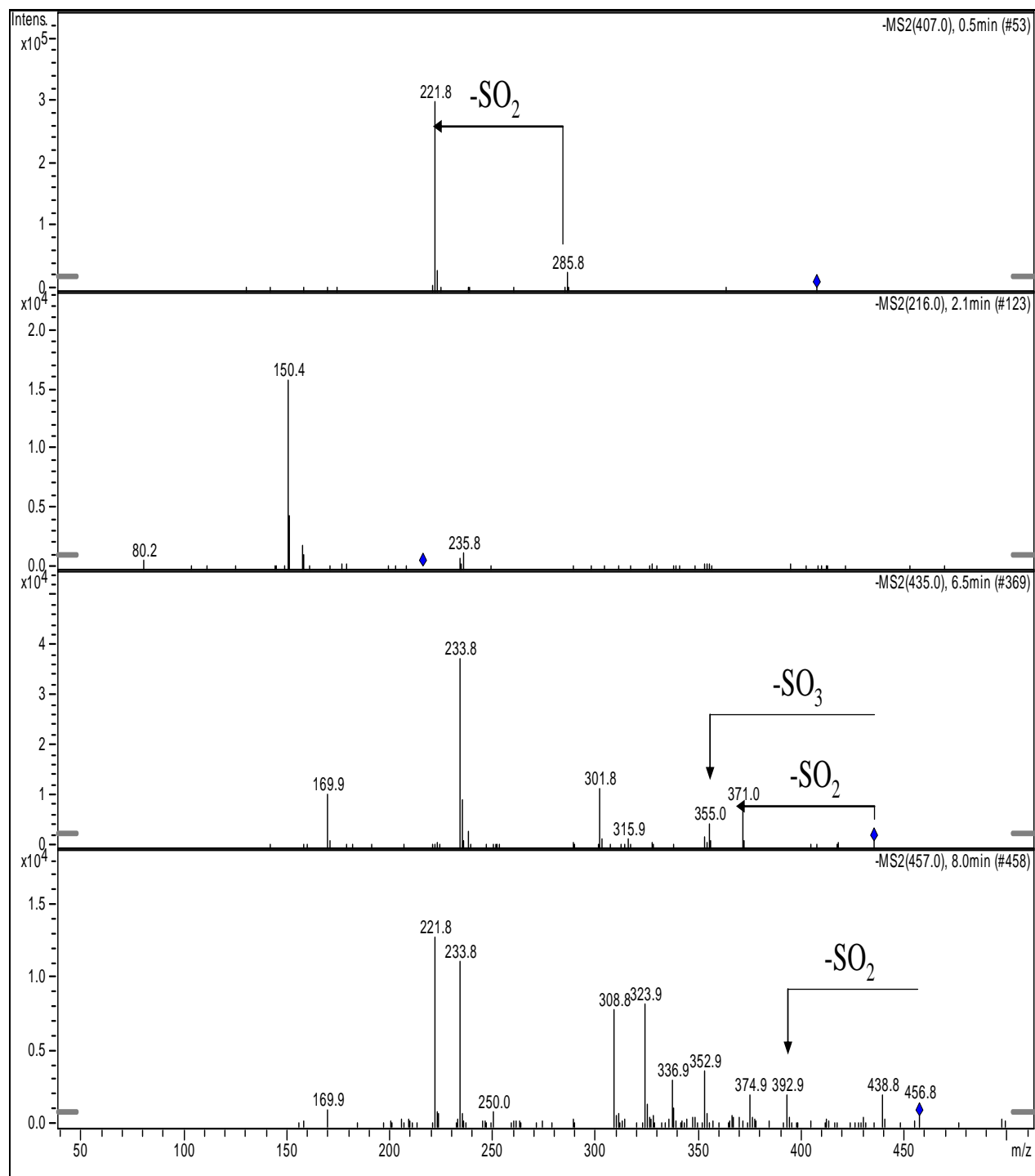
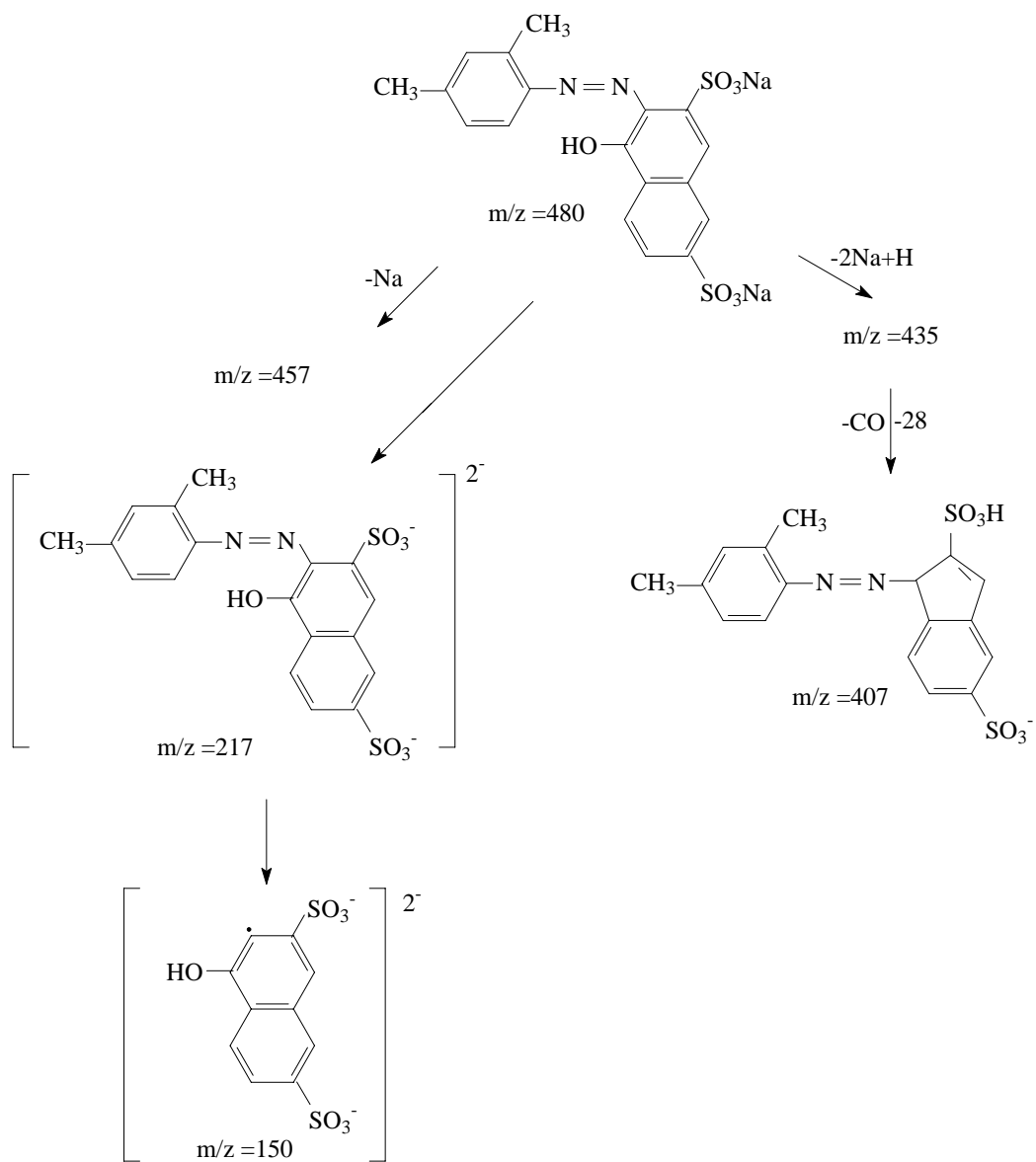


Figure 5.55 MSⁿ Fragmentation of Ions from Acid Red 8



Scheme 5.14 Proposed Fragmentation Pattern for Acid Red 8

The degradation products of Acid Red 8 treated by white rot fungus are also complicated to explain. There is m/z 423 ion in the second day's degradation solution whose structures was not identified (Figure 5.56). So far, the degradation pathway is not clearly understood. Further work may examine the influence of the multifunctional groups of azo dyes as well as the position of azo bond on the naphthalene ring of the dyes treated by the white rot fungus *Pleurotus ostreatus*.

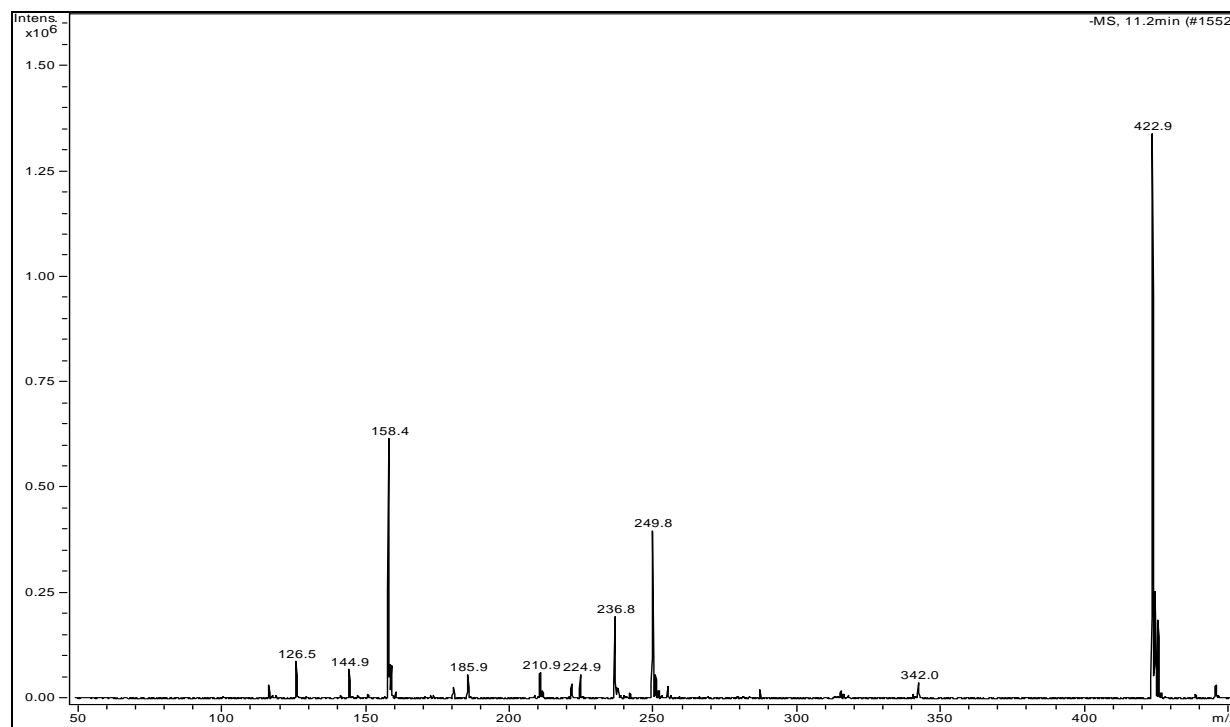
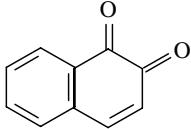
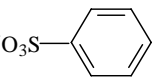
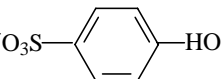
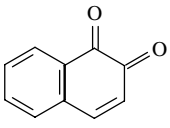
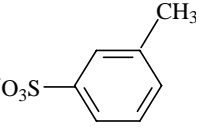
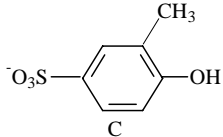
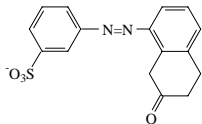
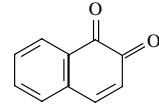
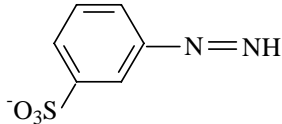
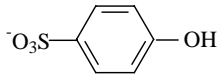
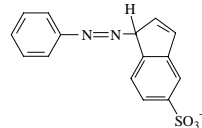


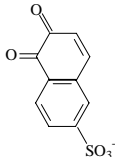
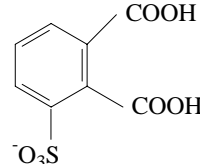
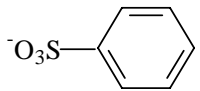
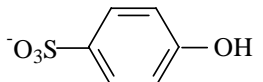
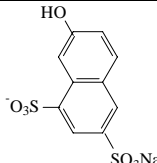
Figure 5.56 Mass Spectrum of Peak with the Retention Time of 11.2 min - Acid Red 8 Treated by *Pleurotus ostreatus* (Second Day).

After treatment by the white rot *Pleurotus ostreatus*, all eight sulphonated phenylazonaphthol dyes in this study were degraded in some extent. Several important degradation products were isolated and identified. The structures and confirmation information are summarized and shown in Table 5.7.

Table 5.7 The Confirmation Information of Possible Degradation Products for The Phenylazonaphthol Azo Dyes

Degradation Compounds		Hypothesized		Standard	Annotation
		M.W.	Structure		
From Acid Orange 7 (Scheme 5.2)	A		1,2-naphthoquinone 	Confirmed by comparisons of both the retention time and UV-vis spectrum by HPLC.	This product was found and reported in literature in degradation of a similar dye structure (Chivukula, 1995a).
	B	158	benzenesulfonic acid 	Confirmed by comparison of both molecular weight and its fragmentation pattern by MS.	The structure was published in the related literature (Zhao, 2005).
	C	174	4-hydroxy-benesulfonic acid 	Confirmed by comparison of both molecular weight and its fragmentation pattern by MS.	The structure was published in the related literature (Zhao, 2005).
From Acid Orange 8 (Scheme 5.4)	A		1,2-naphthoquinone 	Confirmed by comparisons of both the retention time and UV-vis spectrum by HPLC.	This product was found and reported in literature in degradation of a similar dye structure (Chivukula, 1995a).
	B	171	m-toluenesulfonic acid 		Confirmed by molecular weight. Same degradation mechanism as Acid Orange 7.

	C	187	4-hydroxy-m-toluenesulfonic acid 		Confirmed by molecular weight. Same degradation mechanism as Acid Orange 7.
From Mordant Violet 5 (Scheme 5.7 and Scheme 5.8)	A	329	3-{1, 8'-azo (2'-oxygen-tetrahydrogen-naphthalene)} benzenesulfonic acid 		Confirmed by molecular weight. The fragmentation pattern can explain the structure very well.
	B		1,2-naphthoquinone 	Confirmed by comparisons of both the retention time and UV-vis spectrum by HPLC.	This product was found and reported in literature in degradation of a similar dye structure (Chivukula, 1995a).
	C	185	p-diazonium-benzenesulfonic acid 		Confirmed by molecular weight.
	D	173	4-hydroxy-benzenesulfonic acid 	Confirmed by comparison of both molecular weight and its fragmentation pattern by MS.	The structure was published in the related literature (Zhao, 2005).
From Acid Orange 12 (Scheme 5.10)	A	299			Confirmed by molecular weight.

From Food Yellow 3 (Scheme 5.12)	A	237	1,2-naphthoquinone-6-sulfonic acid 		Confirmed by molecular weight. Same degradation mechanism as Acid Orange 7 and Acid Orange 8.
	B	245	3-sulfonic-phthalic acid 		Confirmed by molecular weight. The structure was published in the related literature in degradation of a similar dye structure (Storm, 2002).
	C	157	benzenesulfonic acid 	Confirmed by comparison of both molecular weight and its fragmentation pattern by MS.	The structure was published in the related literature (Zhao, 2005).
	D	173	4-hydroxy-benzenesulfonic acid 	Confirmed by comparison of both molecular weight and its fragmentation pattern by MS.	The structure was published in the related literature (Zhao, 2005).
From Acid Orange 10 (Figure 5.51)	A	325			Confirmed by molecular weight.

CHAPTER 6

CONCLUSIONS

6.1 Conclusions

After treatment by the white rot *Pleurotus ostreatus*, all eight sulphonated phenylazonaphthol dyes in this study were decolorized. This work shows that decolorization of sulphonated phenylazonaphthol dyes for industrial waste effluents is possible under integrated aerobic conditions if the optimum conditions for fungus growth are available. This study shows that practical application of the decolorization method is feasible, though optimum conditions of pH, temperature and agitation will need to be determined at the industry site, and taking into account the dye mixture operated on.

This research studied the decolorization of sulphonated phenylazonaphthol dyes treated by the white rot fungus *Pleurotus ostreatus* and investigated the degradation mechanism. The key findings from this research are generalized as following.

1. The white rot fungus *Pleurotus ostreatus* is capable of decolorizing water soluble sulphonated azo dyes.
2. Because of the different molecular structures of the dyes, the decolorization efficiency ranged from 70 percent to 90 percent after 7 days treatment. Dyes with electron withdrawing group(s) on the benzene ring degraded quickly and had relatively high decolorization. Dyes with electron donating group(s) on the benzene ring had relatively

- lower decolorization. Dyes without functional group(s) on the benzene ring had relatively high decolorization even though they were less affected in the first three days.
3. Not only the total solubility of dyes but also the difference in solubility parameters of molecular units connected by the azo bonds affects the decolorization. The more similar the solubility of the units connected by the azo bonds, the better the decolorization. The active center of the enzyme can attack the azo bond completely.
 4. Both manganese peroxidase (MnP) and laccase were detected in the culture system. The positive lignin peroxidase (LiP) activity was possibly due to the existence of veratryl alcohol oxidase (VAO) and the interference from laccase in the *Pleurotus ostreatus* cultures.
 5. High performance liquid chromatography (HPLC) and capillary electrophoresis - electrospray ion trap mass spectrometry (CE-ESI-MS), and UV-Visible spectrophotometry, were used in the analytical investigation. Corresponding methods which are suitable for fungal degradation analysis have been developed.
 6. The MS/MS fragmentation technique was used to analyze how the dye molecules might break down. The fragmentation patterns of dyes including Mordant Violet 5, Acid Orange 8, Acid Orange 7, Acid Orange 12, Food Yellow 3 and Acid Red 4 were clearly explained.
 7. Due to the complicated nature of the fragmentation patterns, the breakdown of multisulphonated dyes such as Acid Orange 10 and Acid Red 8 could not be completely generalized at this point.
 8. Mordant Violet 5 had two degradation pathways when degraded by *Pleurotus ostreatus*.

- a. The first degradation pathway for Mordant Violet 5 was for *trans* structure. Mordant Violet 5 was first reduced by adding four hydrogen atoms on the third ring to form *m/z* 347. Then the two closely located hydroxyl groups combined and lost a mole of water to form an ether structure. In addition, through some complicated chemical reactions, which may involve rearrangement and then oxidization, the ketone structure of *m/z* 329 was produced.
- The second degradation pathway involved breakdown at the naphthalene ring side of the molecule with formation of 1, 2-naphthoquinone. The cleavage of dyes at the naphthalene ring side also resulted in the formation of a benzenesulfonic diazonium intermediate or its derivative, producing benzenesulfonic acid or its derivative by loss of N₂. The *cis*-Mordant Violet 5 followed this pathway.
9. Acid Orange 8 and Acid Orange 7 had the same degradation mechanism as the first degradation mechanism for Mordant Violet 5, that is cleavage of azo bond at the naphthalene ring side where benzenesulfonic acid and 1,2-naphthoquinone are formed.
10. The degradation pathway of Food Yellow 3 was the same as Acid Orange 7. The only difference was the formation of 3-sulfonic-phthalic acid which resulted from oxidation of 1, 2-naphthoquinone-6-sulfonic acid.
11. The degradation pathway of Acid Orange 10 was not defined. But, it is clear that the Acid Orange 10 degradation pathway was different from other pathways discussed.
12. No fragmentation pattern and degradation pathway were elucidated for Acid Red 8.

6.2 Future Work

There is still research needed to fully understand the biodegradation mechanism used by white rot fungi to degrade textile dyes. Some other work recommended is as follows:

1. Other conditions for CE should be investigated to determine if better separation could lead to more detection of possible degradation products.
2. Isotopic labeled techniques should be used for specific atoms in the molecular structure to assist in explaining the mechanisms.
3. Even though manganese peroxidase (MnP) and laccase are detected in our system, exactly which enzymes are responsible for the decolorization is still not understood and the function of enzymes may be the next research direction.
4. Other factors that may influence degradation such as mediators and the presence of other molecules should be investigated.
5. Assessment of toxicity of organic pollutants after biodegradation will be studied. It has been demonstrated that some products accumulate after decolorization of azo dyes by white rot fungi. The biotransformation products that resist further degradation may be toxic or genotoxic. Thus, the toxicity of dyes after fungal degradation should be assayed. The relationship between the structures of parent pollutants and toxicity after treatment should be studied, and methods to detoxify the toxic products are needed.

REFERENCES

- Agematu, H., Shibamoto, N., Nishida, H., Okamoto, R., Shin, T. and Murao, S., Oxidative decarboxylation of 4-hydroxymandelic acid and 2-(4-hydroxyphenyl)glycine by laccase from *Trachyderma tsunodae* and *Myrothecium verrucaria*. *Bioscience, Biotechnology, and Biochemistry*, 57, 1877-1881, 1993.
- Akthar, M., Blanchette, R. A. and Kirk, T. K., Fungal delignification and biomechanical pulping of wood. Berlin: Springer, 1997.
- Altenbach, B. and Giger, W., Determination of benzene- and naphthalenesulfonates in wastewater by solid-phase extraction with graphitized carbon black and ion-pair liquid chromatography with UV detection. *Analytical Chemistry*, 67, 2325-2333, 1995.
- Baiocchi, C., Brussino, M. C., Pramauro, E., Prevot, A. B., Palmisano, L., Marci, G., Characterization of methyl orange and its photocatalytic degradation products by HPLC/UV-VIS diode array and atmospheric pressure ionization quadrupole ion trap mass spectrometry. *International Journal of Mass Spectrometry*, 214, 247-256, 2002.
- Banat, I.M., Nigam, P., Singh, D., and Marchant, R., Microbial decolorization of textile-dye-containing effluents: a review. *Bioresource Technology*, 58, 217-227, 1996.
- Banat, I.M., McMullan, G., Meehan, C., Kirby, N., Nigam, P., Smyth, W.F., and Marchant, R., Microbial decolorization of textile dyes present in textile industries effluent. In: *Proceedings of the Industrial Waste Technical Conference*, Indianapolis, USA, 1-16, 1999.
- Bear, G.R., Surfactant characterization by reversed-phase ion pair chromatography. *Journal of Chromatography*, 371, 387-402, 1986.
- Benedek, K. and Guttman, A., High performance capillary electrophoresis: an overview. In *HPLC: practical and industrial application*. J. K. Swadesh, Ed., CRC press, Boca Raton, FL, 2001.
- Borgerding, A.J., and Hites, R.A., Effect of tautomerization on the fast-atom bombardment tandem mass spectra of azo dyes. *Journal of American Society for Mass Spectrometry*, 407-415, 1994.
- Bradford, M.M., A rapid and sensitive for the quantitation of microgram quantities of protein utilizing the principle of protein-dye binding. *Analytical Biochemistry*, 72, 248-254, 1976.

Bruise, A.P., Weidol, L.O.G., Henion, J.D., and Budde, W.L., Determination of sulfonated azo dyes by liquid chromatography/atmospheric pressure ionization mass spectrometry. *Analytical Chemistry*, 59, 2647-2652, 1987.

Cao, H., Decolorization of textiles dyes by white rot fungi. Ph. D dissertation, University of Georgia, 2000.

Carliell, C. M., Barclay, S. J., Shaw, C., Wheatley, A. D., Buckley, and C. A., The effect of salts used in textile dyeing on microbial decolorization of a reactive azo dye. *Environmental Technology*, 19, 1133-1137, 1998.

Camp, S.R., and Sturrock, P.E., The identification of the derivatives of C.I. Reactive Blue 19 in textile wastewater. *Water Resources*, 24, 1275-1281, 1990.

Capalash, N., and Sharma, P., Biodegradation of textile azo dyes by *Phanerochaete chrysosporium* for potential application in azo dye degradation and decolorization in wastewater. *World Journal of Microbiology & Biotechnology*, 8, 309-312, 1992.

Chivukula, M., J. T. Sparado, and V. Renganathan, Lignin peroxidase-catalyzed oxidation of sulfonated azo dyes generates novel sulfophenyl hydroperoxides. *Biochemistry*, 34, 7765-7772, 1995a.

Chivukula, M. and V. Renganathan, Phenolic azo dye oxidation by laccase from *Pyricularia oryzae*. *Applied and Environmental Microbiology*, 61(12), 4374-4377, 1995b.

Chung K.T., Fluk G.E. and Andrews A.E., Mutagenicity testing of some commonly used dyes. *Applied and Environmental Microbiology*, 42, 641-648, 1981.

Chung K.T. and Cerniglia C.E., Mutagenicity of azo dyes: Structure-activity relationships. *Mutation Research*, 277, 201-220, 1992.

Conneely, A., Smyth, W. F., and McMullan, G., Metabolism of the phthalocyanine textile dye Remazol Turquoise Blue by *Phanerochaete chrysosporium*. *FEMS Microbiology Letters*, 179, 333-337, 1999.

Cripps, C., Bumpus J., and Aust, S., Biodegradation of azo and heterocyclic dyes by *Phanerochaete chrysosporium*. *Applied and Environmental Microbiology*, 56, 1114-1118, 1990.

Donlon, B.A., Razo-Flores, E., Luijten, M., Swarts, H., Lettinga, G. and Field, J.A., Detoxification and partial mineralization of the azo dye mordant orange 1 in a continuous upflow anaerobic sludge-blanket reactor. *Applied Microbiology and Biotechnology*, 47, 83-90, 1997

Easton, J.R., The dye maker's view. In: *Colour in dyehouse effluent*, Cooper P., Society of dyers and colourists, Nottingham, 9-22, 1995

- Eichlerova, I., Homolka, L., Lisa, L., and Nerud, F., Orange G and Remazol Brilliant Blue R decolorization by white rot fungi *Dichomitus squalens*, *Ischnoderma resinsum* and *Pleurotus calypttratus*. Chemosphere, 60, 398-404, 2005.
- Fenn, J. B., Mann, M., Meng, C.K., and Wong, S.F., Whitehouse, G.M., Electrospray ionization for mass spectrometry of large biomolecules. Science, 246, 64-71, 1989.
- Fedors, R.F., Method for estimating both the solubility parameters and molar volumes of liquids. Polymer Engineering and Science, 14, 147-154, 1974.
- Fu, Y., and Viraraghavan, T., Fungal decolorization of dye wastewaters: a review. Bioresource Technology, 79, 251-262, 2001.
- Glenn, J. K. and Gold, M. H., Purification and characterization of an extracellular Mn(II)-dependent peroxidase from the lignin-degrading basidiomycete, *Phanerochaete chrysosporium*. Archives of Biochemistry and Biophysics, 242, 329-341. 1985.
- Gahr, F., Hermanutz, F. and Opperman, W., Ozonation – an important technique to comply with new German law for textile wastewater treatment. Water science and technology, 30, 255–263, 1994.
- Goszczynski, S., Paszczynski, A., Pasti-Grigsby, M.B., Crawford, R.L., New pathway for degradation of sulfonated azo dyes by microbial peroxidases of *Phanerochaete chrysosporium* and *Streptomyces chromofuscus*. Journal of Bacteriology, 176, 1339-1347, 1994.
- Grover, I.S., Kaur A. and Mahajan R.K., Mutagenicity of some dye effluents. National Academy Science Letters of India, 19, 149-158, 1996.
- Ha, H.C., Honda, Y., Watanabe, T., and Kuwahara, M., Production of manganese peroxidase by pellet culture of the lignin-degrading basidiomycete, *Pleurotus ostreatus*. Applied Microbiology and Biotechnology, 55, 704–711, 2001.
- Hatakka, A., Lignin-modifying enzymes from selected white-rot fungi: production and role in lignin degradation. FEMS Microbiology Reviews, 13, 125-135, 1994.
- Hofrichter, M., Ziegenhagen, D., Vares, T., Friedrich, M., Jager, M. G., Fritsche, W. and Hatakka, A., Oxidative decomposition of malonic acid as basis for the action of manganese peroxidase in the absence of hydrogen peroxide. FEBS Letters, 434, 362-366, 1998.
- Hofrichter, M., Vares T., Kalsi M., Galkin S., Scheibner K., and Fritsche W., Production of manganese peroxidase and organic acids and mineralization of ^{14}C -labelled lignin (^{14}C -DHP) during solid-state fermentation of wheat straw with the white rot fungus *Nematoloma frowardii*. Applied Environmental Microbiology, 65, 1864–1870, 1999.
- Hosono, M., Arai, H., Aizawa, M., Yamamoto, I., Shimizu, K. and Sugiyama, M., Decoloration and degradation of azo dye in aqueous solution of supersaturated with oxygen by irradiation of high-energy electron beams. Applied Radiation and Isotopes, 44, 1199–1203, 1993.

Jandera, P., Churacek, J., and Taraba, B., Comparison of retention behaviour of aromatic sulphonic acids in reversed-phase systems with mobile phases containing ion-pairing ions and in systems with solutions of inorganic salts as the mobile phases. *Journal of Chromatography*, 262, 121-140, 1983.

Juang, R.S., Tseng, R.L., Wu, F.C. and Lin, S.J., Use of chitin and chitosan in lobster shell wastes for colour removal from aqueous solutions. *Journal of Environmental Science. Health A*, 31, 325-338, 1996

Kang, S., Shin, K., Han, Y., Youn, H., and Yung, C., Purification and characterisation of an extracellular peroxidase from white-rot fungus *Pleurotus ostreatus*, *Biochimica et Biophysica Acta (BBA) – Protein. Structure and Molecular Enzymology*, 1163 (2), 158-164, 1993.

Kersten, P. J. and Kirk, T. K., Involvement of a new enzyme, glyoxal oxidase, in extracellular H₂O₂ production by *Phanerochaete chrysosporium*. *Journal of bacteriology*, 169, 2195-2201, 1987.

Kirk, T. K. and Farrell, R. L., Enzymatic “combustion”: the microbial degradation of lignin. *Annual Review of Microbiology*, 41, 465-505, 1987.

Kirby, D.P., Thorne, J.M., Gotzinger, W.K. and Karger, B.L., A CE/MS interface for stable, low-flow operation. *Analytical Chemistry*, 68, 4451-4457, 1996.

Kofujita, H., Ohta, T., Asada, Y., and Kuwahara, M., Alkyl-aryl cleavage of phenolic β -O-4 lignin substructure model compound by Mn(II)-peroxidase isolated from *Pleurotus ostreatus*. *Mokuzai Gakkaishi*, 37, 555-561, 1991.

Knapp, J. S., Zhang, F., and Tapley, K., Decolourisation of Orange II by a wood-rotting fungus. *Journal of Chemical Technology & Biotechnology*, 69, 289-296, 1997.

Lange, F.T., Wenz, M. and Brauch, H.-J., Trace-level determination of aromatic sulfonates in water by on-line ion-pair extraction/ion-pair chromatography and their behavior in the aquatic environment. *Journal of High Resolution Chromatography*, 18, 243-252, 1995.

Leonowicz, A., Edgehill, R. U. and Bollag, J.-M., The effect of pH on the transformation of syringic and vanillic acids by the laccases of *Rhizoctonia praticola* and *Trametes versicolor*. *Archives of microbiology*, 137, 89-96, 1984.

Leonowicz, A., Cho, N., Luterek, J., and Wilkolazka, A., Fungal laccase: properties and activity on lignin. *Journal of Basic Microbiology*, 41, 185-227, 2001

Lobos, S., Larrain, J., Salas, L., Cullen, D. and Vicuna, R., Isoenzymes of manganese-dependent peroxidase and laccase produced by the lignin-degrading basidiomycete *Ceriporiopsis subvermispora*. *Microbiology*, 140, 2691-2698, 1994.

Lu, W., Study of the degradation of azo dyes by the white rot fungus *Pleurotus ostreatus*, Ph. D dissertation, University of Georgia, 2006.

Marshall, A. G., Milestones in Fourier transform ion cyclotron resonance mass spectrometry technique development. *International Journal of Mass Spectrometry*, 200, 331-356, 2000.

Martinez, M. J., et al., Purification and catalytic properties of two manganese-peroxidases isoenzymes from *Pleurotus eryngii*. *European Journal of Biochemistry*, 237, 424-432, 1996.

Martins M. A. M., Ferreira, I. C., Santos, I. M., Queiroz, M. J., and Lima N., Biodegradation of bioaccessible textile azo dyes by *Phanerochaete chrysosporium*. *Journal of Biotechnology*, 89 (2-3), 91-98, 2001.

Martins, M. A. M., Queiroz, M. J., Silvestre, A. J. D., and Lima N., Relationship of chemical structures of textile dyes on the pre-adaptation medium and the potentialities of their biodegradation by *Phanerochaete chrysosporium*. *Research in Microbiology*, 153 (6), 361-368, 2002.

Martins, M. A. M., Lima N., Silvestre, A. J. D., and Queiroz, M. J., Comparative studies of fungal degradation of single or mixed bioaccessible reactive azo dyes. *Chemosphere*, 52, 967-973, 2003.

Mester, T. and Tien, M. Oxidation mechanism of ligninolytic enzymes involved in the degradation of environmental pollutants. *International Biodeterioration & Biodegradation*, 46, 51-59, 2000.

Mishra, G. and Tripathy, M., A critical review of the treatments for decolourization of textile effluent. *Colourage*, 40, 35-38, 1993

Mock, W.I., Cucurbituril. *Topics in Current Chemistry*, 175, 1-24, 1995

Nachiyar, C. V. and Rajkumar, G. S., Degradation of a tannery and textile dye, Navitan Fast Blue S5R by *Pseudomonas aeruginosa*. *World Journal of Microbiology & Biotechnology*, 19, 609-614, 2003.

Nasser, N.M. and El-Geundi, M., Comparative cost of colour removal from textile effluents using natural adsorbents. *Journal of Chemical Technology and Biotechnology*, 50, 257-264, 1991.

Olivares, J.A., Nguyen, N.T., Yonker, C. R. and Smith, R. D., On-line mass spectrometric detection for capillary zone electrophoresis. *Analytical Chemistry*, 59, 1230 – 1232, 1987.

O'Neill, C., Hawkes, F.R., Hawkes, D.L., Lourenco, N.D., Pinheiro, H.M. and Delee, W., Colour in textile effluents – sources, measurement, discharge consents and simulation: a review. *Journal of Chemical Technology and Biotechnology*, 74, 1009-1018, 1999.

Pak, D., and Chang, W., Decolorizaion of dye wastewater with low temperature catalytic oxidation. *Water Science and Technology*, 40, 115-121, 1999.

Paszczynski, A., Huynh, V.B. and Crawford, R. C., Comparison of ligninase-1 and peroxidase-M2 from the white rot fungus *Phanerochaete chrysosporium*. *Archives of biochemistry and biophysics*, 244, 750-765, 1986.

Paszczynski, A. and Crawford, R.L., Degradation of azo compounds by ligninase from *Phanerochaete chrysosporium*: involvement of veratryl alcohol. *Biochemical and Biophysical Research Communications*, 178, 1056-1063, 1991.

Peralto-Zamora, P., Kunz, A., Gomez de Morales, S., Pelegri, R., de Capos Moleiro, P., Reyes, J. and Duran, N., Degradation of reactive dyes I. A comparative study of ozonation, enzymatic and photochemical processes. *Chemosphere* 38, 835–852, 1999.

Perkins, J. R. and Tomer, K. B., Capillary electrophoresis/electrospray mass spectrometry using a high-performance magnetic sector mass spectrometer. *Analytical Chemistry*, 66, 2835-40, 1994.

Pielesz, A., Baranowska, I., Rybak, A., and Wlochowicz, A., Detection and determination of aromatic amines as products of reductive splitting from selected azo dyes. *Ecotoxicology and Environmental Safety*, 53, 42-47, 2002.

Plum, A., Braun, G., and Rehorek, A., Process monitoring of anaerobic azo dye degradation by high-performance liquid chromatography-diode array detection continuously coupled to membrane filtration sampling modules. *Journal of Chromatography, A*, 987, 395-402, 2003.

Potthast, A., Rosenau, T., Chen, C.-L. and Gratzl, J. S., Selective enzymatic oxidation of aromatic methyl groups to aldehydes. *Journal of Organic Chemistry*, 60, 4320-4321, 1995.

Raghavacharya, C., Colour removal from industrial effluents – a comparative review of available technologies. *Chemical Engineering World*, 32, 53–54, 1997.

Rao, K.L.L.N., Krishnaiah, K. and Ashutush, Colour removal from a dyestuff industry effluent using activated carbon. *Indian journal of chemical technology*, 1, 3–19, 1994.

Reemtsma, T. and Jekel, M., Analysis of sulphonated polyphenols, synthetic tanning agents in heavily polluted tannery wastewaters. *Journal of Chromatography, A*, 660, 199-204, 1994.

Reichstein, T. , Foreword. In *Chromatography*, 5th edition, Fundamentals and applications of chromatography and related differential migration methods. E. Heftmann, Ed. Elsevier, New York, NY, 1992.

Richardson, S, McGuire,J., Thruston., A., and Baughman,G., *Organic Mass Spectrometry*, 27, 289-296, 1992.

Righetti, P. G., Electrophoresis. In Chromatography, 5th edition, Fundamentals and applications of chromatography and related differential migration methods. E. Heftmann, Ed. Elsevier, New York, NY, 1992.

Riu, J., Schonsee, I., Barcelo, D., and Rafols, C., Determination of sulfonated azo dyes in water and wastewater. Trends in Analytical Chemistry, 16, 405-419, 1997.

Robinson, T., McMullan, G., Marchant, Roger, and Nigam, P., Remediation of dyes in textiles effluent: a critical review on current treatment technologies with a proposed alternatives. Bioresource Technology, 77, 247-255, 2001.

Rosenkranz, H.S. and Klopman, G., Structural basis of the mutagenicity of phenylazoaniline dyes. Mutation Research, 221, 217-234, 1989.

Rosenkranz, H.S. and Klopman, G., Structural basis of the mutagenicity of 1-amino-2-naphthol-based azo dyes. Mutagenesis, 5, 137-146, 1990

Sannia, G., Limongi, P., Cocca, E., Buonocore, F, Nitti G. and Giardina, P., Purification and characterization of a veratryl alcohol oxidase enzyme from the lignin degrading basidiomycete *Pleurotus ostreatus*. Biochimica et Biophysica Acta (BBA) - General Subjects, 1073, 114-119, 1991.

Schmitt-Kopplin, P. and Frommberger, M., Capillary electrophoresis – mass spectrometry: 15 years of developments and applications. Electrophoresis, 24, 3837-3867, 2003.

Severs, J. C., Hofstadler, S. A., Zhao, Z., Senh, R. T., and Smith, R. D., The interface of capillary electrophoresis with high performance fourier transform ion cyclotron resonance mass spectrometry for biomolecule characterization. Electrophoresis, 17, 1808-1817, 1996.

Slokar, Y.M. and Le Marechal, A.M., Methods of decoloration of textile wastewaters. Dyes and Pigments, 37, 335–356, 1997.

Shin, K., Oh, I., and Kim, C., Production and purification of Remazol Brilliant Blue R decolorizing peroxidase from the culture filtrate of *Pleurotus ostreatus*, Applied Environmental Microbiology, 63, 1744-1748, 1997.

Smith, R. D., Barinaga, C. J., and Udseth, H. R., Improved electrospray ionization interface for capillary zone electrophoresis-mass spectrometry. Analytical Chemistry, 60, 1948-1952, 1988.

Soares, G. M. B., Amorim, M. T. P., Hrdina, R., and Costa-Ferreira, M., Studies on the biotransformation of novel disazo dyes by laccase. Process Biochemistry, 37, 581-587, 2002.

Spadaro, J. T.; Gold, M. H. and Renganathan, V., Degradation of azo dyes by the lignin-degrading fungus *Phanerochaete chrysosporium*. Applied Environmental Microbiology, 58, 2397-2401, 1992.

Spadaro, J.T., and Renganathan, V., Peroxidase-catalyzed oxidation of azo dyes: mechanism of Disperse Yellow 3 degradation. *Archives of Biochemistry and Biophysics*, 312, 301-307, 1994

Spector, T., Refinement of the coomassie blue method of protein quantitation. A simple and linear spectrophotometric assay for less than or equal to 0.5 to 50 microgram of protein. *Analytical Biochemistry*, 86, 142-147, 1978.

Sullivan, A.G., Garner, R., and Gaskell, S., Structure analysis of sulfonated monoazo dyestuff intermediates by electrospray tandem mass spectrometry and matrix-assisted laser desorption/ionization post-source decay mass spectrometry. *Rapid Communications in Mass Spectrometry*, 12, 1207-1215, 1998.

Sugiura, T., and M. C. Whiting., The identification of azo dyes. Part 3. Methylation of sulfonate groups and mass spectrometry. *Journal of Chemical Research*, 2426-2441, 1980.

Swamy, J.; Ramsay, J. A. The evaluation of white rot fungi in the decoloration of textile dyes. *Enzyme and Microbial Technology*, 24, 130-137, 1999.

Tan, N.C.G., Integrated and sequential anaerobic/aerobic biodegradation of azo dyes. Doctoral Thesis. Wageningen University. Wageningen, The Netherlands, 2001.

Taylor, P.W. and Nickless, G., Paired-ion high-performance liquid chromatography of partially biodegraded linear alkylbenzenesulphonate. *Journal of Chromatography A*. 178, 259-269, 1979.

Takeda, S., Tanaka, Y., Nishimura, Y., Yamane, M., Siroma, Z., and Wakida, S., Analysis of dyestuff degradation products by capillary electrophoresis. *Journal of Chromatography A*, 853, 503-509, 1999.

Tien, M., and Kirk, T. K., Lignin-degrading enzyme from the Hymenomycete *Phanerochaete chrysosporium* Burds. *Science*, 221, 661-663, 1983.

Tien, M., Kirk, T. K., Bull, C. and Fee, J. A., Steady-state and transient-state kinetic studies on the oxidation of 3,4-dimethoxybenzyl alcohol catalyzed by the ligninase of *Phanerochaete chrysosporium* Burds. *The Journal of Biological Chemistry*, 261, 1687-1693, 1986.

Urzua, U., Kersten, P. J. and Vicuna, R., Manganese peroxidase-dependent oxidation of glyoxylic and oxalic acids synthesized by *Ceriporiopsis subvermispota* produces extracellular hydrogen peroxide. *Applied Environmental Microbiology*, 64, 68-73, 1998.

Vaidya, A.A., and Datye, K.V., Environmental pollution during chemical processing of synthetic fibers. *Colourage* 14, 3-10, 1982.

Verhaert, P., Uttenweiler-Joseph, S., Vries, M., Loboda, A., Ens, W., and Standing, K. G., Matrix-assisted laser desorption/ionization quadrupole time-of-flight mass spectrometry: an elegant tool for peptidomics. *Proteomics*, 1, 118-131, 2001.

Vinodgopal, K. and Peller, J., Hydroxyl radical-mediated advanced oxidation processes for textile dyes: A comparison of the radiolytic and sonolytic degradation of the monoazo dye Acid Orange 7. *Research on Chemical Intermediates*, 29, 307-316, 2003.

Vyas, B.R.M., and Molitoris, H.P., Involvement of an extracellular H_2O_2 -dependent ligninolytic activity of the white rot fungi *Pleurotus ostreatus* in the decolorization of Remazol Brilliant Blue R. *Applied Environmental Microbiology*, 3919-3927, 1995.

Wang, L. and Tsai, S., Simultaneous determination of oxidative hair dye p-phenylenediamine and its metabolites in human and rabbit biological fluids. *Analytical Biochemistry*, 312, 201-207, 2003.

Wariishi, H.; Valli, K.; Renganathan, V.; and Gold, M.H., Thiol-mediated oxidation of nonphenolic lignin model compounds by manganese peroxidase of *Phanerochaete chrysosporium*. *The Journal of Biological Chemistry*, 264, 14185-14191, 1989.

Wariishi, H., Valli, K. and Gold, M. H., Manganese(II) oxidation by manganese peroxidase from the basidiomycete *Phanerochaete chrysosporium*. Kinetic mechanism and role of chelators. *The Journal of Biological Chemistry*, 267, 23688-23695, 1992.

Wariishi, H., Akileswaran, L. and Gold, M. H., Manganese peroxidase from the basidiomycete *Phanerochaete chrysosporium*: spectral characterization of the oxidized states and the catalytic cycle. *Biochemistry*, 27, 5365-5370, 1998.

Wesenberg, D., White rot fungi and their enzymes for treatment of industrial dye effluents. *Biotechnology Advances*, 22, 161-187, 2003.

Wey, A.B. and Thormann, W., Capillary electrophoresis and capillary electrophoresis – ion trap multiple stage mass spectrometry for the differentiation and identification of oxycodone and its major metabolites in human urine. *Journal of Chromatography B*, 770, 191-205, 2002.

Xu, Y. and Lebrun, R.E., Treatment of textile dye plant effluent by nanofiltration membrane. *Separation science and technology*, 34, 2501–2519, 1999.

Yang, Y., Wyatt II, D.T. and Bahorsky, M., Decolorization of dyes using UV/ H_2O_2 photochemical oxidation. *Textile Chemist & Colorist*, 30, 27–35, 1998.

Zapanta, L. S. and Tien, M., The roles of veratryl alcohol and oxalate in fungal lignin degradation. *Journal of Biotechnology*, 53, 93-102, 1997.

Zhao, X., Chemical analysis of fungal degradation of azo dyes. Ph. D dissertation, University of Georgia, 2004.

Zhao, X., Lu, Y., and Hardin, I.R., Determination of biodegradation products from sulfonated dyes by *Pleurotus ostreatus* using capillary electrophoresis coupled with mass spectrometry. *Biotechnology Letters*, 27, 69–72, 2005.

Zerbinati, O., Ostacoli, G., Gastaldi, D., and Zelano, V., Determination and identification by high-performance liquid chromatography and spectrofluorimetry of twenty-three aromatic sulphonates in natural waters. *Journal of Chromatography A*, 640, 231-240, 1993

Zollinger, H., *Color Chemistry: Synthesis, properties, and applications of organic dyes and pigments*, New York, 1987.